

CONFIDENTIAL

This document contains confidential information which is proprietary to Conoco Norway Inc. or others. Such information is not to be used or disclosed outside of the Conoco affiliated companies except as Conoco Norway Inc. authorizes in writing and as is permitted by an agreement with

SANDIA dated 30.07.84

TENSION PILE STUDY

CNRD 13-2

VOLUME III

**FINAL REPORT ON SMALL
DIAMETER PILE SEGMENT TESTS**

Report Number 82-200-03

Report

to

CONOCO NORWAY, INC.

Through

DET NORSKE VERITAS

Oslo, Norway

By

THE EARTH TECHNOLOGY CORPORATION

Houston, Texas

June, 1983

3535 Briarpark Drive, Suite 100, Houston, Texas 77042
Telephone: (713) 974-1555

June 6, 1983
Project No. 82-200

Det Norske Veritas
Veritasveien 1
N-1322 Hovik
Oslo, Norway

Attn: Mr. Tore J. Kvalstad

**TENSION PILE STUDY
CNRD 13-2
Volume III
Final Report on Small-Diameter Pile Segment Tests**

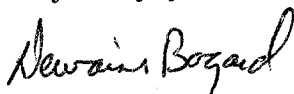
Gentlemen:

In accordance with the contract between The Earth Technology Corporation and Det Norske Veritas, submitted herein is our final report concerning Conoco Norway Subproject CNRD 13-2 of the Tension Pile Study. The information and analysis reported in this Volume III report were derived from all tasks associated with the small-diameter segment tests.

Results of this program will also be incorporated into the large-diameter instrumented pile program, CNRD 13-3, now in progress, to accomplish the overall goals of obtaining a better understanding of pile-soil interaction and developing guidelines and recommendations for the foundation design for TLP structures.

We have thoroughly enjoyed participating in this phase of the project and look forward to continuing the Tension Pile Study.

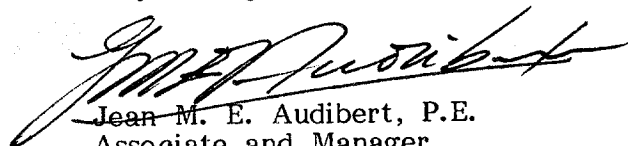
Very truly yours,



Dewaine Bogard
Project Engineer



Thomas K. Hamilton, P.E.
Project Engineer



Jean M. E. Audibert, P.E.
Associate and Manager
The Earth Technology Corporation
Gulf States Region

JDB/TKH/JMEA:cla
Rev:HM
Enclosure

TABLE OF CONTENTS

	<u>Page</u>
TRANSMITTAL LETTER	ii
PREFACE	ix
EXECUTIVE SUMMARY	x
1.0 INTRODUCTION	1
1.1 Purpose of Study	1
1.2 Previous Reports	1
1.2.1 Planning Study	1
1.2.2 Site Characterization Study	2
1.2.3 Pile Segment Test Plan	3
1.3 Final Report	3
1.4 Continuing Work	4
2.0 TEST SITE CHARACTERIZATION PROGRAM	5
2.1 Test Site Selection	5
2.2 Detailed Site Investigation	5
2.2.1 General	5
2.2.2 Field Operations	6
2.2.3 Laboratory Testing	7
2.2.4 Site Characterization	8
2.2.5 Conventional Axial Pile Design Analysis	9
3.0 SMALL-DIAMETER PILE SEGMENT TEST SYSTEM	11
3.1 General	11
3.2 Design of Pile Segment Device	11
3.3 Data Acquisition System	12
3.4 Equipment Calibration	13
3.5 Loading System	14
3.6 Proof Tests	14

TABLE OF CONTENTS (continued)

	<u>Page</u>
4.0 OFFSHORE FIELD TESTING PROGRAM	15
4.1 General.	15
4.2 Test Set-Up	15
4.3 Instrument Installation	16
4.4 Testing Program.	18
5.0 IN SITU TESTING CONDITIONS	19
5.1 Pressure Histories.	19
5.2 Estimated and Measured In Situ Stress Conditions	19
5.3 In Situ Shear Strength	21
6.0 RESULTS OF SMALL-SEGMENT TESTS	22
6.1 Test Types and Purposes	22
6.1.1 Types of Tests	22
6.1.2 Immediate Tests	22
6.1.3 Short-Term Tests.	23
6.1.4 Long-Term Tests	23
6.1.5 Short-Term Small-Displacement Tests	23
6.1.6 Progressively Increasing Load Controlled Tests	23
6.1.7 Retests After Additional Consolidation.	24
6.2 Results of Type I Tests	24
6.2.1 Immediate Tests	24
6.2.2 Short-Term Large-Displacement Tests	25
6.2.3 Long-Term Large-Displacement Tests	25
6.2.4 Summary of Type I Tests	26
6.3 Results of Type II Tests	27
6.3.1 Short-Term Small-Displacement Tests	27
6.3.2 Progressively Increasing Load Controlled Test.	28
6.3.3 Retests After Additional Consolidation.	29

TABLE OF CONTENTS (continued)

	<u>Page</u>
7.0 ANALYSIS OF TEST DATA	30
7.1 General.	30
7.2 Time Histories During Testing.	30
7.2.1 Immediate Test at 63.4 m (208 ft)	30
7.2.2 Long-Term Test at 63.4 m (208 ft)	31
7.2.3 Time Histories at 45.1 m (148 ft)	32
7.3 Stress Paths	33
7.3.1 General	33
7.3.2 Pressure Responses from Varying Loading Patterns	34
7.3.3 Composite Stress Paths	35
7.4 T-Z Curves.	36
7.5 Summary of Results.	36
 8.0 CONTINUING WORK	 39

REFERENCES

TABLES

ILLUSTRATIONS

APPENDIX

LIST OF TABLES

Table No.

- | | |
|---|---|
| 1 | Results of Immediate Tests (Type I) |
| 2 | Results of Short-Term Large-Displacement Tests (Type I) |
| 3 | Results of Long-Term Large-Displacement Tests (Type I) |
| 4 | Comparison of Type I and Type II Short-Term Tests |
| 5 | Comparison of Type I and Type II Long-Term Tests |

ILLUSTRATIONS

	<u>Plate No.</u>
General Location Map	1
Maximum Past Pressure Versus Penetration	2
Comparison of Undrained Shear Strength Profiles	3
Vertical Pressure Distribution	4
Pile Design Data	5
Diagram of Small-Diameter Pile Segment	6
Final Assembly of Small-Diameter Pile Segment	7
Details of Small-Diameter Pile Segment	8
Data Acquisition Building	9
Calibration Frame Assembled	10
Calibration of Small-Diameter Pile Segment	11
Schematic Diagram of Testing Arrangement for 3-Inch Diameter Segment Tests	12
Field Preparations	13, 14 and 16
Deck Layout	15
Installation of Instrument	17 and 18
Load Testing	19
Conoco Small Tool Program	20
Summary of Tests Performed	21
Pore Pressure History	
Depth = 17.7 m (58 ft)	22
Depth = 45.1 m (148 ft)	23
Depth = 54.3 m (178 ft)	24
Depth = 63.4 m (208 ft)	25
In Situ Vertical Stress Conditions	26
K_0 Versus Penetration	27
Revised Estimates for Undrained Shear Strength	28
Peak Friction (f_{max}) Versus Depth for Type I Tests	29
Comparison of Estimated Undrained Shear Strength to Peak Friction From Type I Tests	30

ILLUSTRATIONS (continued)

	<u>Plate No.</u>
Comparison of Long-Term Test Results and Analytical Pile Capacity Predictions	31
Comparison of Minimum and Maximum Friction, Type I Tests	32
Comparison of Minimum (Degraded) Friction to Undrained Shear Strength Estimated Using SHANSEP Procedures	32A
Shear During Test; Hole 1 at 208 ft (Immediate)	33
Pressure During Test; Hole 1 at 208 ft (Immediate)	34 and 35
Shear During Test; Hole 1 at 208 ft	36 and 39
Pressure During Test; Hole 1 at 208 ft	37, 38; 40, 41
Shear During Test; Hole 1 at 148 ft (Immediate)	42
Pressure During Test; Hole 1 at 148 ft (Immediate)	43 and 44
Shear During Test; Hle 1 at 148 ft	45
Pressure During Test; Hole 1 at 148 ft	46 and 47
Stress Paths, 208 ft Depth	48
Stress Paths - Hole 1, 63.4 m (208 ft) Immediate and Long-Term (Type I) Test	49
Stress Paths - Hole 3, 63.4 m (208 ft) Immediate and Short-Term Small-Displacement (Type II) Test	50
Stress Paths - Hole 3, 54.3 m (178 ft) Immediate and Short-Term Progressively Increasing Load Controlled (Type II) Test	51
Stress Path Comparison of Undisturbed, Load Controlled and Siplacement Controlled Tests (Stratum III)	52
Stress Paths - Composite of Tests Performed in Stratum I, 17.7 m (58 ft)	53
Stress Paths - Composite of Tests Performed in Stratum II, 45.1 m (148 ft)	54
Stress Paths - Composite of Tests Performed in Stratum III, 54.3 m (178 ft) and 63.4 m (208 ft)	55
T-Z Curves for Long-Term Test at 45.1 m (148 ft)	56
T-Z Curves for Long-Term Test at 63.4 m (208 ft)	57

PREFACE

This final report concludes CNRD 13-2. The project reported herein is part of a larger project sponsored by Conoco to develop a better understanding of the pile-soil interaction associated with foundation piles for a tension leg platform.

The work reported was performed by The Earth Technology Corporation, acting as a designated subcontractor to Det Norske Veritas. The project team was composed of the following staff members:

- Hudson Matlock, Vice President of Research and Development, provided overall technical direction of the project.
- Tom Hamilton was responsible for project planning, administrative matters and the production of this report.
- Dewaine Bogard was responsible for the development of the small-diameter pile segments and the performance of the field testing program.
- Ronald Boggess and Neil Dwyer assembled the data acquisition system.
- Lino Cheang assisted in data reduction during and after the field tests.
- Leon Holloway, assisted by Fleet Brown, supervised the field operations.
- Jean Audibert, Manager of the Houston office, provided project guidance and report review.

Special thanks go to Tore Kvalstad and Kjell Hauge of Det Norske Veritas and Messrs. Jack H. C. Chan, Jeff Mueller and George Santos of Conoco for their support. We would also like to thank Mr. Alan Young and the McClelland Engineers, Inc. field crews for a job well done and Mr. Bryan Fisher of Small Systems Solutions, Inc., who developed the data acquisition software for this project. Kjell Karlsrud of NGI and Lars Grande from the University of Trondheim observed portions of the offshore test.

EXECUTIVE SUMMARY

Conoco is sponsoring a research program to improve the understanding of pile-soil interaction resulting from static and cyclic tensile loading that will be produced by a deep-water Tension Leg Platform (TLP). The goal of the program is to develop design procedures and recommendations for pile foundations for this type structure.

The project planning was authorized under a separate authorization, CNRD 13-1. The results of this work were two technical reports, one by Det Norske Veritas and one by The Earth Technology Corporation.

These reports outlined a three-part experimental program consisting of 1) a laboratory model pile test program in Norway; 2) a field testing program on small diameter model pile segments in the Gulf of Mexico; and 3) a field testing program on a large diameter instrumented pile at the same offshore site as the small diameter tests. Veritas was to conduct the laboratory study with The Earth Technology Corporation performing the two field test programs.

This report is The Earth Technology Corporation's final report for Subproject CNRD 13-2. The work reported includes 1) producing a site characterization study; 2) developing small-diameter pile segment instruments and related data acquisition and loading equipment and 3) performing field tests and reporting the data.

The site characterization study was completed in April, 1982. The results were reported in The Earth Technology Corporation's CNRD 13-2 Volume I report. In general, the site selected for field tests consists of underconsolidated to normally consolidated clay, typical for this region of the Gulf of Mexico. The characterization study included in situ testing using cone penetrometer and wireline vane shear as well as a comprehensive suite of laboratory tests. The result was a comprehensive set of soil parameters which could be used to develop pile capacity predictions based on any of the normally used criteria and most of the newer effective stress concepts.

Four small-diameter pile segment tools were developed to be used in the field testing program. Each has the capability of measuring shear transfer, axial displacement, total lateral pressure and pore water pressure. A specially designed data acquisition system, including hardware and software, was developed to handle the data recording and processing needs. The entire system, including the loading mechanism, was proof-tested on land at two different locations to insure proper operation and crew familiarity with the equipment.

The offshore field tests were performed in late November and early December, 1982. Testing was done in three test holes at three or four test levels in each hole. A final test plan for the work was submitted in August, 1982, and was designated as Volume II of the CNRD 13-2 project. This report outlined the field testing program which consisted of the following:

1. Immediate (after driving) tests,
2. Short-term tests,
3. Long-term tests,
4. Load controlled progressively increasing cyclic tension tests.
5. Two-way (tension-compression) small-displacement cyclic tests.
6. Retests on pile segments after additional consolidation had been allowed following large-displacement cycling.

The test program was performed with no major difficulties or malfunctions. The results are reported in this final report, CNRD 13-2, Volume III. The results of the tests indicate the following:

1. For long and short-term load tests on previously untested pile segments, the measured maximum friction was in all cases greater than the undisturbed shear strengths from both the field and laboratory soil testing programs.

2. The minimum friction measured after large displacement cycling was approximately equivalent to the average undrained shear strength estimated using SHANSEP procedures (Ladd, et al, 1977).
3. Large-displacement cycling resulted in a reduction in pile friction of 50% in Stratum I and 33% in Strata II and III from the maximum friction on previously untested pile segments.
4. The majority of the loss in friction from large-displacement cycling occurred in the first cycle.
5. In almost all cases, a significant drop in effective pressure was observed between the first and second tension cycle to failure (following the compression cycle to failure).
6. After the drop in effective pressure noted above, subsequent cycles produced a reduction in pile friction with no further significant change in effective pressure at failure.
7. After consolidation and first cycle loading to failure in tension, subsequent cycles showed increasing effective pressure during plastic slip with no increase in pile friction.
8. Load-controlled one-directional cycling resulted in the same maximum frictional capability as first cycle loading to failure. Small-displacement two-way cycling, with increasing displacement ranges, produced a maximum friction value approximately equal to the degraded friction from large-displacement cycling.
9. Shear transfer-displacement (t-z) curves became elastic-plastic after large displacement cycling.
10. Initial slip occurred at displacements ranging from 0.46 mm to 0.91 mm, which are equivalent to 0.6 to 1.2 percent of the pile diameter.

The results of this program will be used to further develop the plans for the large diameter instrumented pile test. Also, the data will be backfitted using the CASH computer program which is being developed to better understand the pile-soil interaction mechanism. Comparisons of this information with that from the laboratory work and the subsequent large-diameter tests should provide a wealth of information for the development of design guidelines for tension leg platforms in clay.

1.0 INTRODUCTION

1.1 Purpose of Study

Conoco is currently constructing the first tension leg platform (TLP) for the Hutton Field in the North Sea. The TLP concept is considered to be a feasible solution for other deepwater locations, including the Gulf of Mexico. However, in order to increase the economic feasibility of this type structure, a better understanding of the pile-soil interaction is needed. Since TLP foundations are subjected to continuous cyclic loads in tension, careful study of cyclic behavior is a requirement. The degradation of frictional capacity under this type loading has been observed in laboratory tests (Holmquist and Matlock, 1975; Bogard and Matlock, 1979), but the mechanics are not well understood, particularly under in situ conditions. To address this poorly understood phenomenon, Conoco authorized Det Norske Veritas and The Earth Technology Corporation, as a designated subcontractor, to conduct a study with the objective of improving the technology relating to TLP foundations. Specific emphasis was placed on soil conditions found in the Gulf of Mexico.

1.2 Previous Reports

1.2.1 Planning Study

The initial phase of the project was a planning study conducted during the summer of 1981 under authorization from Conoco Norway. The final products of this study (CNRD 13-1) were two technical reports which outlined a comprehensive plan for the research work. The reports are as follows:

1. Veritas Report No. 81-0587: Tension Pile Planning Study, Subproject CNRD 13-1 Final Report, August, 1981.
2. Final Technical Report, Subproject CNRD 13-1, Report No. 81-204, The Earth Technology Corporation, August, 1981.

The studies resulted in a recommendation to perform a three-phase program. One phase was to be a laboratory model study on 2.54 cm (1.0 in.) diameter instrumented model piles. This work was to be conducted in a specially constructed triaxial cell equipped with a loading mechanism which would allow the model pile to be subjected to varying degrees of tension and compression cycling.

The second phase included in situ load tests on 7.62 cm (3.0 in.) diameter instrumented model pile segments. The site was planned to be at a platform offshore Louisiana near the Mississippi River delta. Soil conditions at this site were believed to be similar to those at prospective deepwater TLP sites in the Gulf of Mexico.

The third phase of the plan was to include a pile load test on an instrumented 76.2 cm (30.0 in.) diameter pile at the same site as the instrumented segment tests.

Veritas was to be primarily responsible for conducting the laboratory test program while The Earth Technology Corporation was assigned responsibility for the two in situ test programs, including interpretation of soil conditions at the site and analysis of test results.

1.2.2 Site Characterization Study

The first two phases of the project, the laboratory tests and the instrumented segment tests, began in November, 1981, as Conoco Norway subproject CNRD 13-2. Two reports have been issued by The Earth Technology Corporation prior to this final report.

The first report provided documentation of the site selected for the small pile segment and instrumented pile testing. This report was entitled:

Tension Pile Study, Volume I, Site Investigation and Soil Characterization Study at Block 58 West Delta Area, Gulf of Mexico, April, 1982.

The contents included the following information:

- Reasons for selection of the site
- Description of the detailed field investigation which included in situ cone penetrometer and vane shear tests
- Results of a comprehensive laboratory testing program
- Site characterization
- Analysis of pile capacity based on conventional and new methodologies

1.2.3 Pile Segment Test Plan

The second report issued by The Earth Technology Corporation under CNRD 13-2 was entitled:

Tension Pile Study, Volume II, Plan for Performing Small-Diameter Pile Segment Tests, August, 1982.

This report presented a description of the instruments and data acquisition systems to be used, and a detailed field operations plan.

1.3 Final Report

This report is the final technical report to be issued under CNRD 13-2. Included are sections which describe the test instruments, the test system, the performance of the field tests, and presentation and analysis of the test results. Subsequent reports will be issued under CNRD 13-3.

1.4 Continuing Work

The Earth Technology Corporation is presently conducting the third phase of the program outlined in the 1981 Planning Report. This third phase will include the following:

- A load testing program on a large-diameter instrumented pile
- An additional series of small diameter-pile segment tests
- Continued theory development and correlation with test results
- Guidelines for TLP foundation design in clay

The results of the test programs developed by Veritas and The Earth Technology Corporation are expected to significantly increase the understanding of foundation requirements for Tension Leg Platforms.

2.0 TEST SITE CHARACTERIZATION PROGRAM

2.1 Test Site Selection

A search for a suitable test site was performed as part of the initial planning study and was reported in detail in The Earth Technology Corporation's "Final Technical Report, Subproject CNRD 13-1", submitted in August, 1981. The general site requirements were as follows:

1. Test stratum homogeneity
2. Soil type and stress history
3. Stratum thickness
4. Operational considerations

The site selected was located in Block 58, West Delta Area of the Gulf of Mexico. The general location is shown on Plate 1. From preliminary assessments, it was determined that, of several candidate sites, soil conditions at this location were most likely to resemble those at potential deep water TLP sites in the Gulf of Mexico. An added advantage was the availability of an existing platform at the location which could be used as a test structure for the small-diameter segment tests as well as the subsequent large pile test.

2.2 Detailed Site Investigation

2.2.1 General

In November, 1981, a detailed site investigation was performed near structure "A" in West Delta Block 58 to verify the suitability of the site and to obtain the information needed to fully characterize the existing soil conditions.

The investigation consisted of three separate borings in which the following were accomplished:

1. Cone penetrometer tests from 3.7 m (12 ft) to 77.1 m (253 ft) below the seafloor
2. In situ vane shear tests at intervals of 3.05 m (10 ft.) from 6.1 m (20 ft.) to 74.4 m (244 ft.) below the seafloor
3. Push samples from the seafloor to 73.2 m (240 ft.) below the seafloor to be used in an extensive laboratory testing program.

Details of the site investigation, laboratory testing, and data interpretation programs were presented in The Earth Technology Corporation's "Tension Pile Study, Volume I, Site Investigation and Soil Characterization Study at Block 58, West Delta Area, Gulf of Mexico", dated April, 1982. A summary of this study is presented in the following sections.

2.2.2 Field Operations

The geotechnical field program was conducted over a nine-day period beginning on November 4, 1981. The site investigation was planned and supervised by The Earth Technology Corporation, Inc. with the field work contracted by Conoco to McClelland Engineers, Inc.

Operations were performed from the M/V R.L. Perkins. Drilling and sampling was accomplished using a skid-mounted Failing 2000 rotary drilling rig operating through a centerwell in the deck of the vessel. The borings were drilled using 115 mm (4-1/2 in) IF drill pipe. A motion compensation system was used to control vertical motion of the drill string during sampling and in situ testing.

In situ tests were also performed through the drillstring using wireline operated tools. Continuous cone penetrometer tests (CPT) were accomplished using the "Swordfish" system. In situ remote vane shear tests were also performed.

2.2.3 Laboratory Testing

An extensive laboratory testing program was conducted on soil samples recovered from the field investigation. The purposes of the program were to fully document the site and to develop the soil parameters required to compare future small and large-diameter test results to various pile capacity design methods.

Laboratory tests were performed at the following laboratories:

1. The Earth Technology Corporation, Long Beach, California
2. McClelland Engineers, Inc., Houston, Texas
3. Det Norske Veritas, Oslo, Norway
4. Norwegian Institute of Technology, Trondheim, Norway
5. Norwegian Geotechnical Institute, Oslo, Norway

The results of the programs conducted by The Earth Technology Corporation and McClelland were discussed in The Earth Technology Corporation's CNRD 13-2, Volume I report and are summarized in the following paragraphs.

The laboratory programs consisted of classification, physical property and strength tests. Classification tests included

- (1) natural moisture content
- (2) unit weight
- (3) specific gravity
- (4) Atterberg limits
- (5) hydrometer tests.

Physical property tests included stress history evaluation based on the results of one-dimensional consolidation tests and K_0 triaxial consolidation data.

The strength testing program ranged from simple tests to the very sophisticated. Included were

- (1) miniature vane shear
- (2) unconfined compression
- (3) unconsolidated-undrained triaxial
- (4) isotropically consolidated-undrained triaxial
- (5) anisotropically (K_0) consolidated-undrained triaxial
- (6) anisotropically (K_0) consolidated-undrained direct simple shear

2.2.4 Site Characterization

From the results of the field and laboratory testing programs, the subsurface conditions in Block 58, West Delta Area were classified as follows:

<u>Stratum</u>	<u>Depth, m(ft)</u> <u>Below the Seafloor</u>		<u>Soil Description</u>
	<u>From</u>	<u>To</u>	
I	0 (0)	- 24.4 - 80.0)	Very soft to soft olive gray clay with silt pockets and partings.
II	24.4 (80.0)	- 48.8 - 160.0)	Soft to stiff gray silty clay.
III	48.8 (160.0)	- 77.1 - 253.0)	Stiff to very stiff gray clay with shell fragments.
IV	77.1 (253.0)	- Termination* - Termination*)	Gray fine sand.

* Termination depths in the three boreholes ranged from 73.2m (240 ft.) to 77.4m (254 ft.) below the seafloor.

Further analysis of the test results indicated that the soil is underconsolidated. This was expected since the geologic history of the Mississippi River delta indicates a period of rapid deposition for this portion of the Gulf of Mexico. The release of dissolved gases from the samples after recovery could have resulted in the sample disturbance which, in turn, could have masked true stress history conditions. However, we believe that very good samples were obtained. This is evidenced by the comparison of estimated and measured pressures discussed later in this report.

The estimated maximum past pressure of soils at the West Delta site are shown on Plate 2. This profile was based on results of consolidation tests and from empirical correlations with liquidity indices. Taking these in situ stress conditions, together with the results of normalized laboratory tests, inferred in situ shear strength profiles were developed and are shown on Plate 3.

2.2.5 Conventional Axial Pile Design Analysis

In order to compare results from future small and large-diameter in situ pile tests to conventional pile design, pile capacities were developed using the results of the site characterization study and commonly used axial capacity calculation methods. Methods considered were:

- (1) API RP 2A (1981)
- (2) Lambda (Vijayvergiya and Focht, 1972)
- (3) Effective Stress β (Burland, 1973)
- (4) Simplified General Effective Stress (Esrig and Kirby, 1979)

The vertical pressure distribution as a function of depth to be used with the effective stress methods is given on Plate 4. The resulting unit skin friction values using both total and effective stress concepts were calculated and are shown on Plate 5. Comparisons of these values with those actually measured in the field during the small-diameter segment tests will be given and discussed in later portions of this report.

It should be realized that all of the above pile capacity computation methods address only static axial capacity. The primary purpose of this CNRD project is to better understand the pile-soil response of piles loaded cyclically in tension. The test results included in the remainder of this report, along with the laboratory tests by Veritas and the large-diameter pile test by the The Earth Technology Corporation, are expected to increase this understanding.

3.0 SMALL DIAMETER PILE SEGMENT TEST SYSTEM

3.1 General

After completion of the test site verification and characterization studies, efforts were concentrated on designing the small-diameter test segment instruments and the associated loading and data acquisition systems. The small-diameter pile segment instrument was a new design of an in situ tool used previously by The Earth Technology Corporation for a similar type test program. A new load testing system also had to be developed which would allow precise control of displacement during test performance. Detailed descriptions of the instruments and test system were given in The Earth Technology Corporation's report "Tension Pile Study, Volume II, Plan for Performing Offshore Small-Diameter Pile Segment Tests", dated August, 1982. A summary is provided in the following sections.

3.2 Design of Pile Segment Device

Four small-diameter instrumented pile segment tools were constructed for use in the program. Each instrument is 7.62 cm (3.00 in.) in diameter. The total length of the tool is 430 cm (169.0 in.), including a thin-walled cutting shoe to simulate an open-ended pile. Optionally, the instrument can be driven closed-end to simulate a plugged pile.

Each instrument is capable of measuring shear transfer, displacement of the instrument relative to the soil at test depth, total lateral pressure and pore water pressure. A diagram of the instrument is shown on Plate 6. Photographs on Plate 7 show the final assembly of the tools in our Houston, Texas laboratory (top photo) and the exit point for cables awaiting final wiring of the underwater cable connector (bottom photo).

Shear transfer is measured by taking the difference in load on two cross-sections of the instrument. The cross-sections are 77.6 cm (30.6 in.) apart, a length chosen to give an external surface area of 0.186 sq m (2.0 sq ft) between the load measurement points. The strain gage bridge is sensitive only to axial soil resistance applied between the load cell locations. Common axial loads, transverse bending loads, and temperature are self-cancelling.

Displacement relative to the soil at test depth is measured using a DC-operated LVDT (linear variable differential transformer). This is accomplished by designing the instrument so that the upper section, including the load cells, can move axially with respect to the lower section which includes the cutting shoe. The total allowable movement is 2.54 cm (1.0 in.). The LVDT core is fixed to the lower cutting shoe section; the LVDT housing is fixed to the upper instrument section. This lower assembly is shown at the top of Plate 8.

Total lateral pressure and pore water pressure are measured at a point mid-way between the two axial load cells. Total pressure is measured by weighing the force exerted on a small load cell which projects through the wall of the pile segment. The active face is shaped to conform to the outside surface of the tool, thus avoiding disruptions of radial pressure near the transducer. Pore water pressure is measured using a commercially-available diaphragm-type transducer mounted in a cylindrical housing. The active face, located next to the total pressure gage, is separated from the soil by a porous carborundum filter also shaped to conform to the instrument exterior surface. A photograph of the total pressure and pore pressure transducer housing is shown at the bottom of Plate 8.

3.3 Data Acquisition System

The data acquisition system is built around a high-level language programmable computer system. The Digital Equipment Corporation MINC-23 computer was

combined with FORTRAN data acquisition programs to allow real time data collection and test control. Incoming signals are digitized by a HP-3497A scanner digitizer. This system can scan up to 100 channels and provide high resolution A/D conversion of strain gage level signals without the need of analog amplification.

Data collected is stored immediately as raw voltages on a floppy disc and printed in engineering units on a printer. Selected variables can be displayed, at the operator's discretion, on a digital plotter to aid in visualization. Analog plotting of data is also performed to visually monitor test progress. Data stored on disc are transferred to a 9-track tape at a time convenient to the test operator. This provides a permanent, transportable record for future processing and analysis.

The entire data acquisition system is housed in a waterproof, air-conditioned portable building. Photographs of the interior of the building with the data acquisition system installed are shown on Plate 9.

3.4 Equipment Calibration

Each component of the four small-diameter pile segment tools was calibrated in The Earth Technology Corporation's Houston laboratory prior to deployment offshore. Total pressure transducers were calibrated from parallel measurements of water pressure from the precalibrated pore pressure transducers. These total pressure calibrations were further verified with a series of dead weight loadings.

The shear transfer load cells were calibrated using a special calibration frame and the hydraulic ram and pump system used for loading in the field tests. A diagram of the calibration frame is shown on Plate 10; photographs taken while the load cell calibration was in progress are shown on Plate 11.

3.5 Loading System

The hydraulic loading system consists of a load frame plate, a removable upper frame, a "through-hole" hydraulic jack, an electric pump, and associated fittings, valves and hardware. The 1,335 kN (150-ton) double-acting jack has a 30.5 cm (12 in.) stroke. Electrically actuated control valves allow remote operations of the system from the data acquisition building. This system can be controlled either by manual switches or by computer control, at the option of the test operator. A schematic of the testing apparatus is shown on Plate 12. More detailed descriptions of system operation are given in a subsequent section.

3.6 Proof Tests

The entire small-diameter pile segment test system was fully proof tested on land prior to mobilization offshore. Sample test programs were performed at Sabine Pass, Texas and near New Orleans, Louisiana. During these tests, all aspects of the equipment and equipment operation system were exercised. In addition, the two onshore tests allowed for training of the test crew to insure optimum performance during the offshore test program.

4.0 OFFSHORE FIELD TESTING PROGRAM

4.1 General

The offshore field testing program using the small-diameter pile segment instruments was conducted at the West Delta 58A platform during late November and early December, 1982. A total of ten installations were made in three separate boreholes. In all, thirty-three loading sequences were performed. These included tests over time periods ranging from a few minutes to 144 hours after installation. Open-ended and full displacement pile segment tests were performed. One-directional, progressively increasing loadings were applied as well as large displacement two-directional loadings. This section describes the method for testing and the type of tests performed. Following sections discuss results of the testing program.

4.2 Test Set-up

Equipment used to perform the testing program included (1) four small-diameter pile segment instruments; (2) the test system and related data acquisition equipment; (3) a mobile drilling rig with pipe, drillrod and support tools; and (4) a self-propelled, self-elevating barge which provided a crane and also served as housing for the test personnel.

The jack-up barge was used to transport a portion of the equipment offshore. After unloading, it was positioned alongside the West Delta 58A platform and was used for food, lodging, communications and other logistical needs for the duration of the test program.

Prior to mobilizing to the offshore platform, 32.4 cm (12 3/4 in.) casing was installed from the platform deck to a level approximately 9 m (30 ft) below the mudline for each of the three test holes. The purpose of the casing was

to insulate the test instruments from wave and current action. A relief hole was drilled in the casing at approximately 3.0 m (10 ft) above the water level in order to lower the water level in the casing from deck height to the hole elevation, a difference of about 11.6 m (38 ft). This reduced the possibility of hydraulic fracturing of soft soils near the seafloor.

After the casing was set and cut-off at deck level, the lower load frame plates were installed and welded to the platform (see Plates 13 and 14). Skid beams for the drill rig were aligned parallel to the three test holes to allow movement of the rig from one hole to another.

The drilling rig and drilling crew were provided by McClelland Engineers, Inc. The rig was a Failing 1500 skid-mounted unit. Approximately 275 m (900 ft) of 115 mm (4-1/2 in) IF drill pipe and the same amount of N-rod was also provided by McClelland.

Prior to mobilizing, the N-rod (90 m for each borehole) was pre-strung with the instrument cable to facilitate lowering and retrieving the instruments. Special racks were constructed by The Earth Technology Corporation personnel to aid in drill rod and cable handling (see Plate 14, lower photo).

The data acquisition building was located directly in front of the three test holes to allow clear visual contact with the operations. Instrument cables were routed to minimize the possibility of damage during pipe handling. A lay-out of the test set-up is shown on Plate 15.

4.3 Instrument Installation

The procedure used to install each instrument was identical for each borehole and each test level. This procedure was preplanned to make optimum use of the time available offshore. The installation sequence used was essentially the

same as shown pictorially in Ertec's CNRD 13-2, Volume II report. The steps are described briefly below:

1. Pre-check and prepare instrument and data system.
2. Advance boring to pre-determined depth.
3. Lower instrument with N-rod through the drill pipe until the instrument reaches the bottom of the test hole.
4. Assemble test frame and place hydraulic jack in position.
5. Place casing hammer and drive the small-diameter pile segment to the pre-calculated test depth.
6. Perform initial (as-driven) load test.
7. Allow at rest consolidation to proceed until desired time for load test sequence.

Photographs showing preparation of the instrument and installation are shown on Plates 16 through 19.

Digital data logging began just prior to instrument insertion into the drill pipe and continued, uninterrupted, until the tool was removed and on the platform deck. Time intervals for sampling were determined by the needs of each test. For example, during the consolidation phase, sample rates which geometrically increased from 30 seconds to a maximum of two hours were used.

4.4 Testing Program

Primary testing was performed at three different depths in three separate boreholes. A fourth level was also tested in the third borehole. The three primary depths were selected to represent the three major strata identified in the site characterization study. A chart showing the test hole number, test type, and elevations where the various tests were performed is shown on Plate 20.

Test Hole No. 1 was dedicated to long-term (approximately 72 hour) tests. Hole No. 2 was used for short-term (approximately 8 hour) tests although several long-term tests were included at the deepest depth. Test Hole No. 3 was used for a variety of tests including 1) short-term, large displacement, 2) short-term, progressive one way cycling and 3) long-term tests after previously performed large displacement cycling. Load tests immediately after driving were performed in all test holes at all elevations. Except for one load-controlled test, performed in Test Hole No. 3 at 54.3 m (178 ft), all tests were displacement controlled.

A summary of all test performed with approximate times after insertion is shown on Plate 21. Where f_{max} and f_{min} are both shown, full reversal of loading direction was included in the test program, thereby allowing frictional degradation under large strain cycling.

5.0 IN SITU TESTING CONDITIONS

5.1 Pressure Histories

Radial total pressure, σ_r , and pore pressure, u , were measured and recorded for each instrument from the beginning of installation until instrument recovery. Thus, pressure changes were monitored during the quiescent periods of consolidation as well as during the testing phases.

Plates 22 through 25 show the pore pressure histories for all instruments at the four depths tested. These plates primarily display pore pressure versus time, on a logarithmic scale, during non-testing periods. The time periods when testing was in progress are shown as broken lines. Also, it should be noted that in Hole No. 1 at the 17.7 m (58 ft) depth, the pore pressure increased for a period of time beginning at about 2,100 minutes. It was later determined that this was due to drilling disturbance in Hole No. 2, about 12 feet away. In all subsequent drilling operations, no weight material was used, and such pressure increases were not observed.

Computer plots of the pressure histories for various tests are given in the Illustrations and Appendix sections of this report. These consist of one plot showing total radial pressure and pore pressure versus time and one plot showing effective radial pressure versus time. In these graphs, time is plotted on an arithmetic scale.

5.2 Estimated and Measured In Situ Stress Conditions

From results of the site investigation and subsequent laboratory testing programs, the in situ stress conditions were estimated prior to performing the field pile segment testing program. This estimate was shown in the site charac

terization report and was also reproduced for this report (see Plate 2). Pressure information obtained from the pile segment testing program was used to revise the previous estimated state of stress, as shown on Plate 26.

The original estimates for total and effective vertical pressures and pore water pressure are shown as dashed lines. Measured pore pressures, u , based on the seventy-two hour tests at the three primary test elevations, are shown as triangles. Also shown are measured radial total pressures, σ_r , (open squares) and radial effective pressure, σ'_r , (open circles) determined from subtracting u from σ_r .

The previous estimates of the in situ state-of-stress were expressed in terms of vertical stress conditions. Therefore, to compare "measured" to "estimated" conditions, it was necessary to convert the measured radial pressures to corresponding vertical pressures. This was accomplished by using the relationship

$$\sigma'_v = \sigma'_r / K_0 \text{ ----- (1)}$$

where σ'_r equals σ_r (measured) minus u (measured) and K_0 equals the values shown on Plate 27 derived from laboratory tests and reported in the site characterization study. Total vertical pressure, σ_v , could also be inferred by adding the measured u to σ'_v . These new estimates of the vertical soil pressures, σ_v and σ'_v , calculated in the manner explained are shown on Plate 26 as solid squares and circles, respectively.

The solid lines show revised estimates for in situ vertical stress conditions. As can be seen, the original estimates for effective pressure were very close to the revised curve through the first two strata, 0 to 48.8 m (0 to 160 ft). In the deepest test stratum, the in situ effective stress inferred from the measured radial and pore pressures was higher than had been estimated previously.

5.3 In Situ Shear Strength

The interpreted shear strength profile based on laboratory undrained tests remains unchanged from that given in the earlier report. However, the profile based on effective stress parameters, normalized soil behavior (Ladd et al, 1977), required change since the values for σ'_v changed, as previously discussed. This is particularly evident from 48.8 to 77.1 m (160 to 253 ft) where the estimated in situ range of shear strength is considerably higher than that given previously. Plate 28 shows this revised profile. These new values for shear strength will be used in all subsequent comparisons of pile friction and shear strength.

6.0 RESULTS OF SMALL-SEGMENT TESTS

6.1 Test Types and Purposes

6.1.1 Types of Tests

The testing program was developed to examine soil-pile behavior during the various phases in the "life" of a TLP foundation. The tests which were deemed relevant to the study included the following:

- a. Immediate (after driving) tests, Type I
- b. Short-term, large-displacement tests, Type I
- c. Long-term, large-displacement tests, Type I
- d. Short-term, small-displacement tests, Type II
- e. Progressively increasing load controlled tests, Type II
- f. Retests performed after full-reversed cycling and some amount of additional consolidation, Type II

The immediate and short- and long-term large-displacement tests have been designated as Type I tests, where loading to failure was accomplished prior to any other disturbance, with the exception of installation. The small-displacement tests, load controlled tests, and retests have been designated Type II tests. Subsequent paragraphs discuss the purpose of the different types of tests.

6.1.2 Immediate Tests

Immediate (after driving) tests were performed after the installation of each instrument at each level. The purpose of these tests was to determine the skin friction immediately after driving. For normally consolidated soils, the frictional capability at this period in time should be the lowest since remolding has occurred and pore pressures are elevated due to cavity expansion during driving. The test arrangement was such that these tests were performed within minutes after completion of driving.

6.1.3 Short-Term Tests

Short-term, large-displacement tests were performed at three elevations in Test Hole No. 2 and at one elevation in Test Hole No. 3. These tests, performed approximately eight hours after installation, were to determine maximum and minimum values for shear transfer after an intermediate amount of consolidation had occurred. This information, along with immediate and long-term results, allow a curve showing increase in pile friction with time to be constructed. A relationship of this type is important since the construction of a TLP may not allow time for full consolidation of large-diameter piles prior to applying loads to the foundation.

6.1.4 Long-Term Tests

Long-term, large-displacement tests were performed at three-elevations in Test Hole No. 1. For these tests, the instrument was left undisturbed for a nominal seventy-two hour period after installation and immediate testing. Therefore, advanced consolidation had occurred prior to testing. The purpose of these tests was to determine the maximum and minimum (degraded) frictional resistance available after a time period corresponding to possibly several years after the installation of a prototype TLP foundation pile.

6.1.5 Short-Term Small-Displacement Tests

Tests with progressively increasing displacement were performed at two elevations in Test Hole No. 3. The purpose of these tests was to determine if the small-displacements experienced by a TLP foundation during normal environmental conditions have an effect on the ultimate frictional capability (maximum and minimum) which may be encountered during larger displacement cycling from storm loading.

6.1.6 Progressively Increasing Load Controlled Tests

One short-term load controlled test was performed in Test Hole No. 3. This test

test was performed using one-way tension only cycling. The purpose was to investigate the differences, if any, between one and two-directional cycling.

6.1.7 Retest After Additional Consolidation

Six retests were performed in Test Hole Nos. 2 and 3. These tests were performed at times ranging from twenty to one hundred forty-four hours after installation and after at least one full-displacement cyclic test had been performed. The purpose of the tests was to investigate the "healing" effect after soil degradation. This test simulates a pile which had at some time in the past experienced extreme storm loading. For most of the tests, data was also recorded during "pullout" of the instrument.

6.2 Results of Type I Tests

6.2.1 Immediate Tests

Immediate tests were performed following the installation of each instrument. In most cases, the test began within ten minutes after completion of driving. Each test consisted of loading the segment to failure in tension followed by one compression cycle to failure. Each instrument was then positioned to approximately mid-range of the displacement measuring device prior to beginning the consolidation phase.

Results of each immediate test are given in the Appendix. These typically consist of one or more of the following plots:

- a. Shear Transfer versus Axial Displacement (t-z)
- b. Total Pressure versus Axial Displacement ($\sigma_r - z$)
- c. Pore Pressure versus Axial Displacement (u-z)
- d. Effective Pressure versus Axial Displacement ($\sigma'_r - z$)

In all, ten immediate tests were performed. Results are tabulated on Table 1. Shown additionally are undrained shear strengths based on laboratory tests on undisturbed samples (see Plate 5). The ratio of the average peak friction during

initial loading to the undrained shear strength averaged 0.76 for three of the four depths tested. This ratio for the uppermost test depth, 17.7 m (58.0 ft), was 0.54.

6.2.2 Short-Term, Large Displacement Tests

A series of tests were performed on a portion of the instruments after approximately eight hours of undisturbed consolidation. Tension loading to failure followed by large-displacement cycling was conducted at 17.7, 45.1 and 63.4 m (58.0, 148.0 and 208.0 ft) in Test Hole No. 2 and at 45.1 m (148.0 ft.) in Test Hole No. 3.

Results of these tests are shown on Table 2, together with the ratios of the maximum and minimum values of friction to interpreted shear strength based on the various laboratory tests on undisturbed samples (left side of Plate 5). For both maximum and minimum friction values, the ratio f/S_u increases with depth. Selected computer plots of shear transfer, total pressure, pore pressure, and effective pressure versus axial displacement are given in the Appendix.

6.2.3 Long-Term, Large-Displacement Tests

All three tests performed in Test Hole No. 1 were long-term, large-displacement tests. After installation and immediate testing, each instrument was allowed to consolidate, undisturbed, for approximately seventy-two hours. At the end of this period, each small pile segment instrument was loaded to failure in tension and then cycled in tension and compression until a minimum friction value was obtained. This normally consisted of approximately ten cycles.

The results of these tests are shown on Table 3 along with comparisons to shear strength such as those given for the immediate and short-term tests. The ratio, f_{\max}/S_u , was approximately 1.05 for the top two strata. This ratio was much higher, 1.60, at the deepest test level. The ratio of minimum friction to shear strength increased with depth as in the short-term Type I tests. Graphic displays for these test are also given in the Appendix.

6.2.4 Summary of Type I Tests

A summary of peak measured friction, f_{\max} , versus depth below the seafloor for all Type I tests is shown on Plate 29. For the immediate tests, the f_{\max} profile begins at zero and linearly increases through the upper two strata to approximately 26.3 kPa (0.55 ksf) at 48.8 m (160 ft). At the beginning of Stratum III, the rate of increase of f_{\max} with depth increases; the extrapolated value for f_{\max} at the bottom of Stratum III is 35.9 kPa (0.75 ksf).

For the long-term Type I tests, the same trend appears. However, the seafloor intercept for f_{\max} is approximately 8.1 kPa (0.17 ksf). Also the rate of increase in f_{\max} with depth is higher than for the immediate tests below 48.8 m (160 ft).

As would be expected, the magnitude of f_{\max} for the short-term Type I tests is between those measured immediately after driving and after a long period of consolidation in Strata I and III. However, in Stratum II, the extrapolated profiles for f_{\max} from the short- and long-term tests coincide. This indicates that the time for complete pile "set-up" is much shorter in this stratum. Since the soil in Stratum II has a lower plasticity and higher coefficient of consolidation than Stratum I or III, a faster set-up period would be expected.

A comparison of estimated undrained shear strength versus peak friction from the various Type I tests is shown on Plate 30. For Stratum I and II, the magnitude of the measured friction from the long-term tests is slightly higher than the interpreted shear strength profile from the site characterization report. The magnitude of the measured friction from the short-term tests is slightly lower than the interpreted curve in Stratum I and is higher, coinciding with the long-term tests, in Stratum II. The slope of both the short and long-term f_{\max} curves is almost identical to that of the interpreted shear strength line.

Below 48.8 m (160.0 ft), the interpreted undrained shear strength is substantially less than measured peak friction from both the short and long-term tests. Also, as shown on Plate 30 in the shaded section, the range of shear strength predicted from normalized soil behavior relationships (Ladd et al, 1977) are also significantly lower than the measured f_{\max} from the long-term tests.

Plate 31 is a reproduction of pile capacity analyses from the site characterization report. However, included are results from the three long-term Type I tests. It can be easily seen that the measured f_{\max} values are substantially higher than the unit skin friction derived from any of the currently used pile capacity prediction methods. A comparison of maximum and minimum (degraded) friction from Type I tests is shown on Plate 32. There were no significant differences in the degraded frictional resistance which resulted from continued large-displacement cycling following long and short-term tests at this site. Therefore, the minimum friction, f_{\min} , profile is a single line, as shown.

The profile originates at zero and linearly increases to 23.9 KPa (0.50 ksf) at 48.8 m (160 ft). At this point, the interface with Stratum III, the rate of change with depth of the frictional resistance profile increases to an extrapolated value of 95.8 kpa (2.0 ksf) at 77.1 m (253 ft). In Stratum I and Stratum II, the profile roughly corresponds to f_{\max} for the immediate tests. In Stratum III, f_{\min} is greater than f_{\max} for the immediate tests. One interesting observation, though possibly coincidental, is that the minimum friction line follows the mean value of shear strength predicted by the normalized soil behavior relationship, as shown on Plate 32A. In other words, for this location, the following equation applies:

$$f_{\min} = 0.23 \sigma'_v \text{ ----- (2)}$$

where σ'_v is obtained from the in situ vertical stress conditions estimated from field measurements, as shown on Plate 26.

6.3 Results of Type II Tests

6.3.1 Short-Term Small-Displacement Tests

A short-term, small displacement test was performed at 17.7 m (58.0 ft) in Test Hole No. 3. An immediate test was run on the instrument after installation; undisturbed consolidation was then allowed for approximately eight hours before testing began. Cycling in both tension and compression was initiated by loading in tension to a displacement of 0.127 mm (0.005 in), unloading, and reloading in

compression to the same displacement. After about five cycles, the displacement was increased by ± 0.127 mm (± 0.005 in) to ± 0.254 mm (± 0.010 in).

This procedure was continued until displacement reached ± 0.762 mm (± 0.030 in), the point at which time failure occurred. The instrument was then cycled ± 1.27 mm (± 0.050 in) to obtain maximum degradation of frictional resistance.

A similar test was performed at 63.4 m (208 ft), except the load was controlled instead of the displacement for the first series of cycles. Afterwards, displacement control was used similar to that employed for the test at 17.7 m (58.0 ft). Increasing displacement intervals of ± 0.05 mm (± 0.002 in) were used until failure occurred as cycling between -0.61 mm and $+0.51$ mm (-0.024 and $+0.020$ in) was attempted. This is shown as the initial portion of the curve on Plate A-56. At this time, cycling continued at ± 1.27 mm (± 0.050 in) to obtain the minimum friction.

Both the peak and minimum friction values obtained at the 17.7 m (58.0 ft) depth during this test were higher than those obtained from the Type I short-term test at the corresponding depth. At 63.4 m (208.0 ft), f_{\max} was lower and f_{\min} was higher than those recorded during the short-term Type I tests at the same depth. Results of both short-term, small-displacement tests are given on Table 4. Computer plots can be found in the Appendix.

6.3.2 Progressively Increasing Load Controlled Test

A one-directional load controlled test was performed at 58.4 m (178.0 ft). The test began after an eight-hour consolidation period following the immediate test.

To begin the test, the pile segment was loaded in tension to 26.3 kPa (0.55 ksf), which was estimated to be 50% of failure, based on the results of tests in Test Hole No. 2. Cycling at $\pm 5\%$ (45 to 55%) about the tension bias was then performed for 20 cycles. At this time the load levels were increased by $\pm 5\%$ to cycle between 40% and 60% of the estimated failure load.

The load range was progressively increased as follows: 30% to 70%; 20% to 80%; 14% to 86%; 5% to 95%; and -5% to 105%. At 105%, failure began to

occur as permanent displacement was observed. On the subsequent cycle, failure occurred at a lower value of friction. Large-displacement, two-directional cycling was then performed to obtain f_{\min} .

The initial failure from one-directional tension cycling occurred at 67.03 kPa (1.40 ksf). On the following cycle, failure occurred at approximately 57.5 kPa (1.20 ksf). Minimum friction, f_{\min} , from two-way cycling was 38.30 kPa (0.80 ksf). Results of this test are shown on Table 4. Plots are given in the Appendix.

6.3.3 Retests After Additional Consolidation

At some of the test levels in Test Hole Nos. 2 and 3, the instruments were left in place after the specified tests were completed. Additional large-displacement tests were performed in these cases after additional time was allowed for consolidation. Five retests were performed at the following elevations and times after installation:

- a. 45.1 m (148.0 ft) - 20 hrs; 44 hrs.
- b. 54.3 m (178.0 ft) - 20 hrs.
- c. 63.4 m (208.0 ft) - 70 hrs; 144 hrs.

Results of the five retests are given in Table 5, with the plots of the digital data in the Appendix. The results suggest that, at the 63.4 m (208.0 ft) depth, the losses in resistance due to cyclic loading are recoverable. Partial recovery was also observed at the shallower test depths; however, the length of time between tests was insufficient to allow any definite conclusions to be reached.

The recovery in soil resistance with time after cyclic loading will be further explored during the upcoming offshore test program.

7.0 ANALYSIS OF TEST DATA

7.1 General

Computer plots for various tests are shown in the Appendix. These plots show shear transfer (pile friction), total and effective lateral pressure, and pore water pressure as functions of displacement. During the cyclic tests, data samples were obtained at discrete intervals of load or displacement between preset control points. Data outside the limits, or values prior to the first interval after reversal, were not recorded by the digital system; thus, the digital plots of data as a function of displacement appear truncated near each control point. Continuous analog (x-y) records of shear and displacement were taken, and will be supplemented by the digital records in determining the t-z relationships.

The data acquisition system used for this study also allowed cross-plotting of the primary parameters measured against each other and as a function of time. Two very informative cross-plotting techniques used to examine the data were 1) shear transfer and lateral pressures versus time and 2) shear transfer versus effective pressure. The latter produced "stress path" plots similar to those which are constructed from triaxial and direct or simple shear test results.

7.2 Time Histories During Testing

7.2.1 Immediate Test at 63.4 m (208 ft)

A time history of shear versus elapsed time for the immediate test in Test Hole No. 1 at 63.4 m (208 ft) is shown on Plate 33. The event (tension failure, slip, etc.) which is occurring is shown on the right hand side of the page and corresponds to the number labels on the plot. The total lateral pressure and pore water pressure which were measured during the same period of time are shown on Plate 34. A slight drop in total pressure is seen until initial failure occurs. This is followed by a gradual increase in total pressure with a minor perturbation occurring during unloading in tension.

Changes in pore pressure during the test are much more dramatic. A substantial drop in pressure is seen at initial failure in tension. The pore pressure remains

depressed during continuous slip. Upon unloading and reloading in compression, the pore pressure increases to near its original level, peaks at compression failure, and then drops again during compression slip. The same pattern occurs during the second tension cycle.

Effective pressure versus time is shown on Plate 35. Since the variations in total pressure with time were small compared to the pore pressure changes, the effective pressure plot is very nearly a mirror image of the pore pressure-time diagram. It is interesting to note that the peak friction in tension occurred at the lowest value for effective stress in the first cycle. Subsequent peaks in compression and tension also occurred at low effective pressure values. Another observation is that, for this immediate test, the effective stress tends to increase during continued slip in either tension or compression with no corresponding change in friction.

7.2.2 Long-Term Test at 63.4 m (208 ft)

Time histories for the long-term test in Test Hole No. 1 at 63.4 m (208 ft) are shown on Plates 36 through 38. Nine tension-compression cycles are shown from 0 to approximately 0.70 hours of elapsed time. The remainder of the plot is the "pull-out" of the instrument. Examination of this data reveals that after the first two complete cycles the results become very repeatable.

In order to more closely examine the results, the scale was expanded to include only the first 0.3 hours of the test. The various events in the loading history are shown in the same manner as for the immediate tests. Shear transfer versus time for the first three and one-half cycles are shown on Plate 39. The corresponding total lateral pressure and pore water pressure is shown on Plate 40. After a slight increase during the first loading, the total pressure remains fairly constant except during unloading in tension and reloading in compression. The lowest total pressure occurs at "zero load" (Point No. 3), just prior to applying a compression load.

As with the immediate test, the pore water pressure fluctuations are more dramatic and essentially mirror the effective pressures shown on Plate 41.

Contrary to the immediate test, the effective pressure during the long-term test (in the same test hole at the same depth) increased during the first loading cycle to failure. At failure and during tension slip, the effective pressure dropped, also contrary to the immediate test. However, after the initial tension failure in the long term test, the pressure responses were very similar to the immediate test. That is, the effective pressure dropped during unloading in tension and reloading in compression, reached a minimum at compression failure, and increased during compression slip. Also, like the immediate test, during tension cycles subsequent to the first cycle, a decrease in pressure is seen during reloading in tension followed by a depression at tension failure and a gradual increase in effective pressure during tension slip with no change in friction.

It must be noted that the data gathered was digital data and that the plotting routine employed simply constructed straight lines between each consecutive data point. Because of the sampling intervals selected, some unavoidable gap in data occurred. Examples are shown as dashed lines in Plates 39 through 41.

Similar gaps in data occur in other plots of digital data, particularly in the shear transfer-displacement curves in the Appendix where truncation occurs at the displacement limits. However, for convenience, dashed lines were provided only in the examples noted above.

7.2.3 Time Histories at 45.1 m (148 ft)

Time histories for Tests Hole one at 45.1 m (148 ft) are shown on Plate 42 through 47. The first three plates are for the immediate test; the last three show the long-term Type I test. The same numbers used previously to denote events are used in these graphs.

A comparison of effective pressure versus time for the immediate (as driven) tests at the two different elevations and two different soils show remarkable similarities. Both indicate a drop in effective pressure at tension failure followed by a rise in effective pressure during slip. Also, in both cases the pressure drops during loading in compression. At compression failure, however, there is a difference between the soils at the two depths. Effective pressure

is at a minimum when slip begins at the 63.4 m (208 ft) depth, (Point 4), and then increases with continued compression slip to Point 5. At the 45.1 m (148 ft) depth, the effective pressure reaches a minimum just as failure begins and has reached a maximum by the time full slip in compression has been reached. The pressure responses during the second tension cycle of both immediate tests are similar.

A comparison of lateral pressures from the first long-term test tension cycles at 45.1 m (148 ft) and 63.4 m (208 ft) shows quite a difference in pressure response. The effective pressure at failure during the 45.1 m (148 ft) test shown on Plate 47 was much lower than the pressure at the beginning of the test. The same failure point (Point 1) at 63.4 m (208 ft) on Plate 41 indicated a slight increase in effective pressure had occurred.

However, after the initial tension failure, the patterns of effective pressure response at the two elevations become quite similar. In fact, the only major difference is during compression failure where the minimum value for effective pressure is reached as slip begins and is increasing by the time the end of slip is achieved. This was the same difference noted in the comparison of immediate tests at the two depths.

7.3 Stress Paths

7.3.1 General

The most familiar, and likely the most meaningful, method for examining the test data is by use of stress path plots. For these analyses, the shear transfer, or "pile friction", is plotted against effective pressure. The initial point on each diagram is the pressure at which the load test began. Then, as load is applied the corresponding values for friction, f , and radial effective stress, σ'_r , develop a "stress path" to failure.

Diagrams of this kind were initially plotted using the computer, as shown on Plate 48 for the 63.4 m (208 ft) depth in Test Hole No. 1. However, due to the numerous data points, with many of these coinciding with each other, manual plotting of key points only was determined to provide the clearest graphical display.

7.3.2 Pressure Responses From Varying Loading Patterns

Three very distinctive type loading patterns were applied to the small diameter pile segments during the testing program. These patterns were as follows:

1. Continuous loading to failure,
2. Small displacement (two-way) cycling, and
3. Progressively increasing load controlled (one-way) cycling.

At the conclusion of each of these tests, large displacement cycling was conducted to fully degrade the soil. Stress paths for these tests are shown on Plates 49 through 51. In addition, the immediate (as driven) tests are shown.

The immediate and long-term (Type I) tests performed at 63.4 m (208 ft) are shown on Plate 49. The open triangle shows the conditions prior to beginning the test. The solid squares indicate the peak value for friction measured during the cycle indicated. The minimum, or residual, conditions measured at the end of tension slip is shown as a solid circle. Note that the effective stress at the end of slip following the ninth cycle was higher than the effective pressure at failure during the ninth cycle.

Compression cycles are not shown on Plate 49. However, the second cycle tension peak shown occurred after one complete compression cycle to failure. It should be noted that after the first compression cycle, and during reloading in tension, there was a reduction in effective stress of approximately 25% of the effective stress during the first tension cycle to failure. Subsequent cycles produced only small fluctuations in effective stress at failure.

Plate 50 shows the stress path produced by increasing small-displacement (two way) cyclic testing. Although many cycles were performed, only conditions after selected cycles in the displacement ranges shown were plotted. As can be seen, the initial effective stress, prior to testing, gradually decreased with increasing values for displacement. Failure occurred at approximately 85% of the pre-test consolidation pressure.

The results of the one-way progressively increasing load-controlled test is shown on Plate 51. As in the previous test, only conditions during selected cycles are shown. From this test, it appears that with only one-way slip, the initial effective stress decreases only slightly until loads nearing failure are reached. This test was performed at 54.3 m (178 ft) whereas the two previous tests were at 63.4 m (208 ft). However, all three tests were in the same soil type and all three were in Stratum III of the soil profile.

To observe the results in a more meaningful manner, the results of the three tests were normalized with respect to their initial consolidation pressure, σ'_{rc} . A plot of normalized friction, f/σ'_{rc} , versus normalized radial effective stress, σ'_r/σ'_{rc} , is shown on Plate 52.

Based on normalized results, the peak friction for the undisturbed and one-way load controlled tests were very close to the same. However, the peak friction obtained from two-way small-displacement cycling was much lower. In fact, it was very near the values obtained after large-displacement cycling in all three tests.

7.3.3 Composite Stress Paths

Stress path analyses were performed for the various tests in each stratum (See Plates 53 through 55). The purpose was to investigate the soil-pile properties much in the same way triaxial stress-path data is analyzed. No interpretations of properties were made since there were a limited number of tests in each stratum. However, from the results produced from these tests, similarities and trends were evident.

For most cases, there was a distinct effective pressure drop associated with the degradation of friction from the first to second cycle. This pressure drop would help explain the reduction in frictional capability from an effective stress basis. However, subsequent cycling (after the second cycle), typically shows a reduction in the measured friction with no associated reduction in effective pressure. In fact, with continued slip, there is an increase in effective pressure concurrent with a slight drop in measured friction.

Construction of failure envelopes would indicate that the behavior of the soil is not totally a function of the effective pressure acting normal to the pile surface. There apparently is an intercept, similar to a "cohesion intercept", which, combined with the pressure-friction angle component, accounts for the total measured friction.

7.4 T-Z Curves

An important aspect of the program is the development of shear transfer-displacement (t-z) curves for input into soil-pile modelling systems such as the DRIVE 10 computer program (Matlock and Foo, 1979). Various computer plots of t-z curves are shown in the Appendix. Two curves, for the long-term tests at 45.1 m (148 ft) and 63.4 m (208 ft), are shown in detail on Plates 56 and 57, respectively.

For both cases, the t-z curves become more elastic-plastic after continued cycling. At the 45.1 m (148 ft) level, initial failure during the first cycle occurred at approximately 0.9 mm (0.036 in.) of displacement. At the 63.4 m (208 ft) elevation, failure occurred at 0.46 mm (0.018 in) of movement. This corresponds to 1.2% and 0.6% respectively, of the pile diameter of 76 mm (3.0 in). After continued cycling, failure occurred at approximately 0.5 mm (0.02 in), or 0.66 % of the pile diameter for both cases. Since only one pile diameter was used for this study, the validity of constructing t-z curves with displacement scaled to pile diameter was not investigated. However, a comparison of the small-diameter segment test results to the large-diameter instrumented pile test results should prove beneficial in evaluating this scale effect.

7.5 Summary of Results

A large amount of information was gathered during the small diameter pile segment test program. Many correlations and comparisons are possible due

to the good quality of the data taken. Some general observations from the test program are listed below:

1. For long and short-term load tests on previously untested pile segments, the measured maximum friction was in all cases greater than the undisturbed shear strengths from either the field or laboratory soil testing program.
2. The minimum friction measured after large displacement cycling was approximately equivalent to the average undrained shear strength estimated using SHANSEP procedures (Ladd, et al, 1977).
3. Large-displacement cycling resulted in a reduction in pile friction of 50% in Stratum I and 33% in Strata II and III from the maximum friction on previously untested piles.
4. The majority of the loss in friction from large-displacement cycling occurred in the first cycle.
5. In almost all cases, a significant drop in effective pressure was observed between the first and second tension cycle to failure (following the compression cycle to failure).
6. After the drop in effective pressure noted above, subsequent cycles produced a reduction in pile friction with no further significant change in effective pressure at failure.
7. After consolidation and first cycle loading to failure in tension, subsequent cycles showed increasing effective pressure during plastic slip with no increase in pile friction.
8. Load-controlled one-directional cycling resulted in the same maximum frictional capability as first cycle loading to failure. Small-displacement two-way cycling, with increasing displacement

ranges, produced a maximum friction value approximately equal to the degraded friction from multiple cycle loading to failure.

9. Shear transfer-displacement (t-z) curves became elastic plastic from large displacement cycling.
10. Initial slip occurred at displacements ranging from 0.46 mm to 0.91 mm, which are equivalent to 0.6 to 1.2 percent of the pile diameter.

8.0 CONTINUING WORK

At the present time, work is continuing on the development of plans and hardware for a large-diameter instrumental pile to be tested at the same offshore site where the small-segment tests were performed.

Results from the tests reported in this document are vital to the development of the test program for the large-diameter pile. Currently, results from the small-diameter test are being back-fitted using the analytical tool, the CASH program, which has been under development to assist in explaining the pile-soil interaction phenomenon. In addition, the test data from the small-diameter tests will be used as input into the DRIVE program (Matlock and Foo, 1979) in an effort to model large-pile behavior based on small-diameter test results.

At the conclusion of all field and laboratory work, the test results will be used to develop design guidelines for TLP foundations in clay.

REFERENCES

REFERENCES

- American Petroleum Institute, Recommended Practice for Planning, Designing and Constructing Fixed Offshore Platforms, API RP 2A, Twelfth Edition, 1981.
- Bogard, D., and Matlock, H., "A Model Study of Axially Loaded Pile Segments, Including Pore Pressure Measurements", Report to the American Petroleum Institute, University of Texas, May, 1979.
- Burland, J. B., "Shaft Friction of Piles in Clay, A Simple Fundamental Approach", *Ground Engineering*, Vol. 6, No. 3, 1973.
- Det Norske Veritas, "Tension Pile Planning Study, Subproject CNRD 13-1 Final Report", Report to Conoco Norway, Inc., Report No. 81-0587, August, 1981.
- Earth Technology Corporation, "Final Technical Report, Subproject CNRD 13-1", Report to Conoco Norway, Inc. through Det Norske Veritas, Report No. 81-204, August, 1981.
- Earth Technology Corporation, "Tension Pile Study, Volume I, Site Investigation and Soil Characterization Study at Block 58 West Delta Area, Gulf of Mexico", Report to Conoco Norway, Inc. through Det Norske Veritas, Report No. 82-200-1, April, 1982.
- Earth Technology Corporation, "Tension Pile Study, CNRD 13-2, Volume II, Plan for Performing Offshore Small Diameter Pile Segment Tests", Report to Conoco Norway, Inc. through Det Norske Veritas, Report No. 82-200-2, August, 1982.
- Esrig, M. I., and Kirby, R. C., "Advances in General Effective Stress Methods for the Prediction of Axial Capacity for Driven Piles in Clay", Proceedings, OTC 3406, 11th Annual Offshore Technology Conference, Houston, Texas, April 30 thru May 3, 1979.

Holmquist, D. V., and Matlock, H., "Resistance-Displacement Relationships for Axially Loaded Piles in Soft Clay", Proceedings, 7th Annual Offshore Technology Conference, Houston, Texas, OTC 2474, May, 1975.

Ladd, C. C., Foote, R., Ishihava, K., Poulos, H. G., and Schollosser, F., "Stress-Deformation and Strength Characteristics", State-of-the-Art Report, Session I, 9th International Conference on Soil Mechanics and Foundation Engineering, Tokyo, Vol. 2, pp. 421-494, 1977.

Matlock, H., and Foo, S. H. C., "Axial Analysis of Piles Using a Hysteretic and Degrading Soil Model," Proceedings of the International Conference on Numerical Methods in Offshore Pilings, ICE, London, May, 1979.

Vijayvergiya, V. N., and Focht, J. A. Jr., "A New Way to Predict the Capacity of Piles in Clay", Proceedings, 4th Annual Offshore Technology Conference, Houston, Texas, Vol. II, 1972.

TABLES

TABLE 1
RESULTS OF IMMEDIATE TESTS (TYPE I)

Depth M (Ft)	Peak Friction, f_{max} , KPa (KSF)			f_{max} (average) KPa (KSF)	S_u KPa (KSF)	$\frac{f_{max}}{S_u}$
	Hole No. 1	Hole No. 2	Hole No. 3			
17.7 (58.0)	9.10 (P) (0.19)	7.66 (P) (0.16)	12.93 (P) (0.27)	9.90 (0.21)	18.20 (0.38)	0.54
45.1 (148.0)	29.69 (0.62)	25.86 (P) (0.54)	24.42 (0.51)	26.65 (0.56)	33.50 (0.70)	0.80
54.3 (178.0)	-	-	34.47 (0.72)	34.47 (0.72)	45.50 (0.95)	0.76
63.4 (208.0)	39.26 (0.82)	52.19 (1.09)	43.57 (0.91)	45.01 (0.94)	62.20 (1.30)	0.72

NOTE: (P) Designates instruments were installed as fully-plugged piles.
All others were driven open-ended.

TABLE 2
RESULTS OF SHORT-TERM LARGE-DISPLACEMENT TESTS (TYPE I)

Depth M (Ft)	Hole No. 2		Hole No. 3		Average		S _u KPa (KSF)	f _{max} S _u (average) (average)	f _{min} S _u (average) (average)
	f _{max} KPa (KSF)	f _{min} KPa (KSF)	f _{max} KPa (KSF)	f _{min} KPa (KSF)	f _{max} KPa (KSF)	f _{min} KPa (KSF)			
17.7 (58.0)	14.36 (P) (0.30)	8.62 (P) (0.18)	-	-	14.36 (0.30)	8.62 (0.18)	18.20 (0.38)	0.79	0.47
45.1 (148.0)	38.78 (0.81)	26.81 (0.56)	32.56 (P) (0.68)	20.11 (P) (0.42)	35.91 (0.75)	23.46 (0.49)	33.50 (0.70)	1.07	0.70
63.4 (208.0)	78.52 (1.64)	57.46 (1.20)	-	-	78.52 (1.64)	57.46 (1.20)	62.20 (1.30)	1.26	0.92

NOTE: (P) Designates instruments were installed as fully-plugged piles.
All others were driven open-ended.

TABLE 3
RESULTS OF LONG-TERM LARGE-DISPLACEMENT TESTS (TYPE I)

Depth M (Ft)	Hole No. 1		S _u KPa (KSF)	$\frac{f_{max}}{S_u}$	$\frac{f_{min}}{S_u}$
	f _{max} KPa (KSF)	f _{min} KPa (KSF)			
17.7 (58.0)	19.15 (P) (0.40)	7.66 (P) (0.16)	18.20 (0.38)	1.05	0.42
45.1 (148.0)	34.95 (0.73)	22.50 (0.47)	33.50 (0.70)	1.04	0.67
63.4 (208.0)	99.59 (2.08)	64.64 (1.35)	62.20 (1.30)	1.60	1.04

NOTE: (P) Designates instruments were installed as fully-plugged piles.
All others were driven open-ended.

TABLE 4
COMPARISON OF TYPE I AND TYPE II SHORT-TERM TESTS

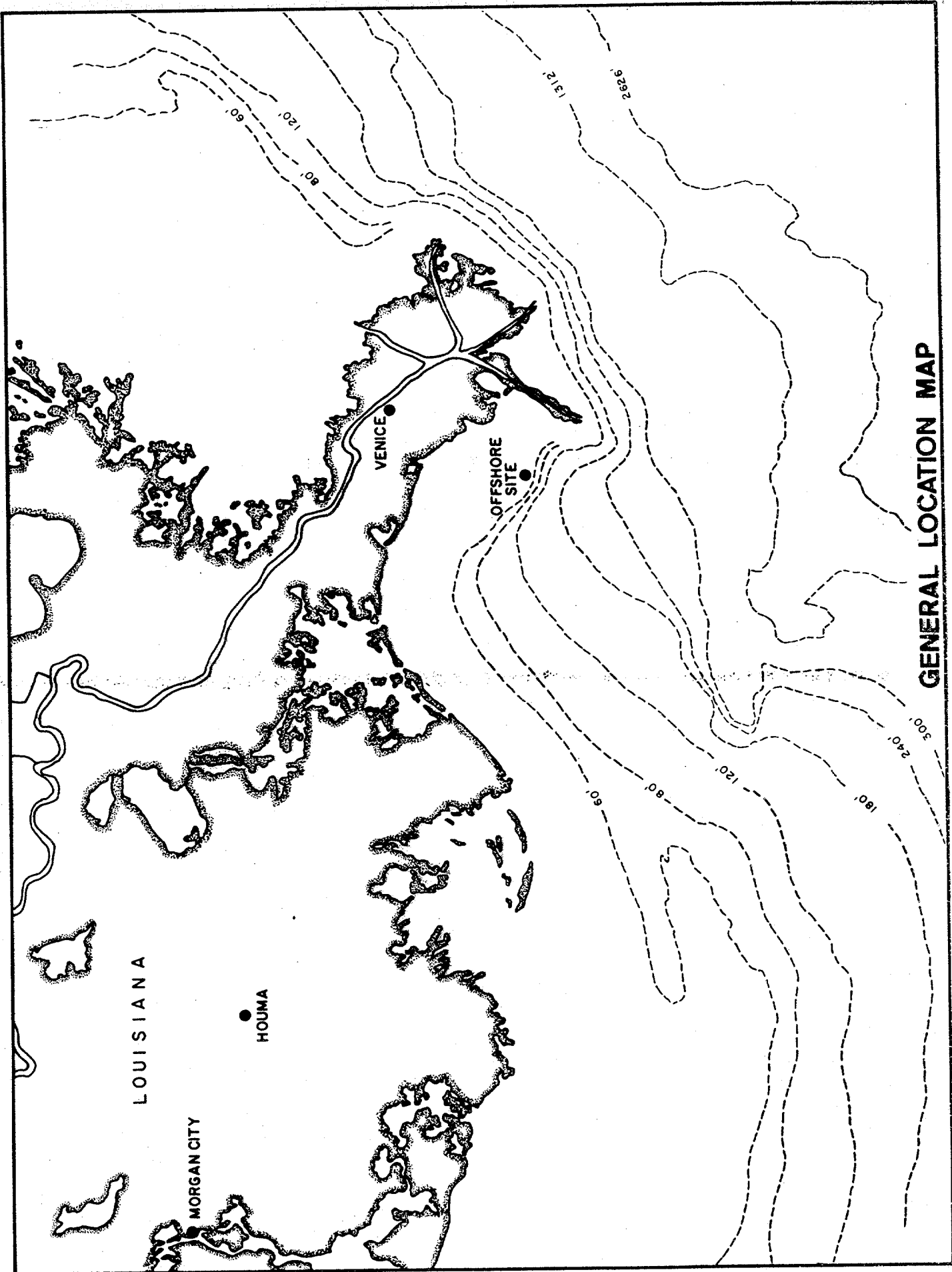
Depth M (Ft)	Type Test	Hole No. 2		Hole No. 3		$\frac{f_{\max} \text{ (Type I)}}{f_{\max} \text{ (Type II)}}$	$\frac{f_{\min} \text{ (Type I)}}{f_{\min} \text{ (Type II)}}$
		f_{\max} KPa (KSF)	f_{\min} KPa (KSF)	f_{\max} KPa (KSF)	f_{\min} KPa (KSF)		
17.7 (58.0)	Type I	14.36 (0.30)	8.62 (0.18)	-	-	0.68	0.51
	Type II (Small Disp.)	-	-	21.07 (0.44)	16.76 (0.35)	-	-
45.1 (148.0)	Type I	38.78 (0.81)	26.81 (0.56)	32.56 (0.68)	20.11 (0.42)	-	-
54.3 (178.0)	Type II (One-way Tension)	-	-	68.95 (1.44)	43.09 (0.90)	-	-
63.4 (208.0)	Type I	78.52 (1.64)	57.46 (1.20)	-	-	0.99	0.75
	Type II (Small Disp.)	-	-	69.43 (1.45)	57.46 (1.20)	-	-

TABLE 5

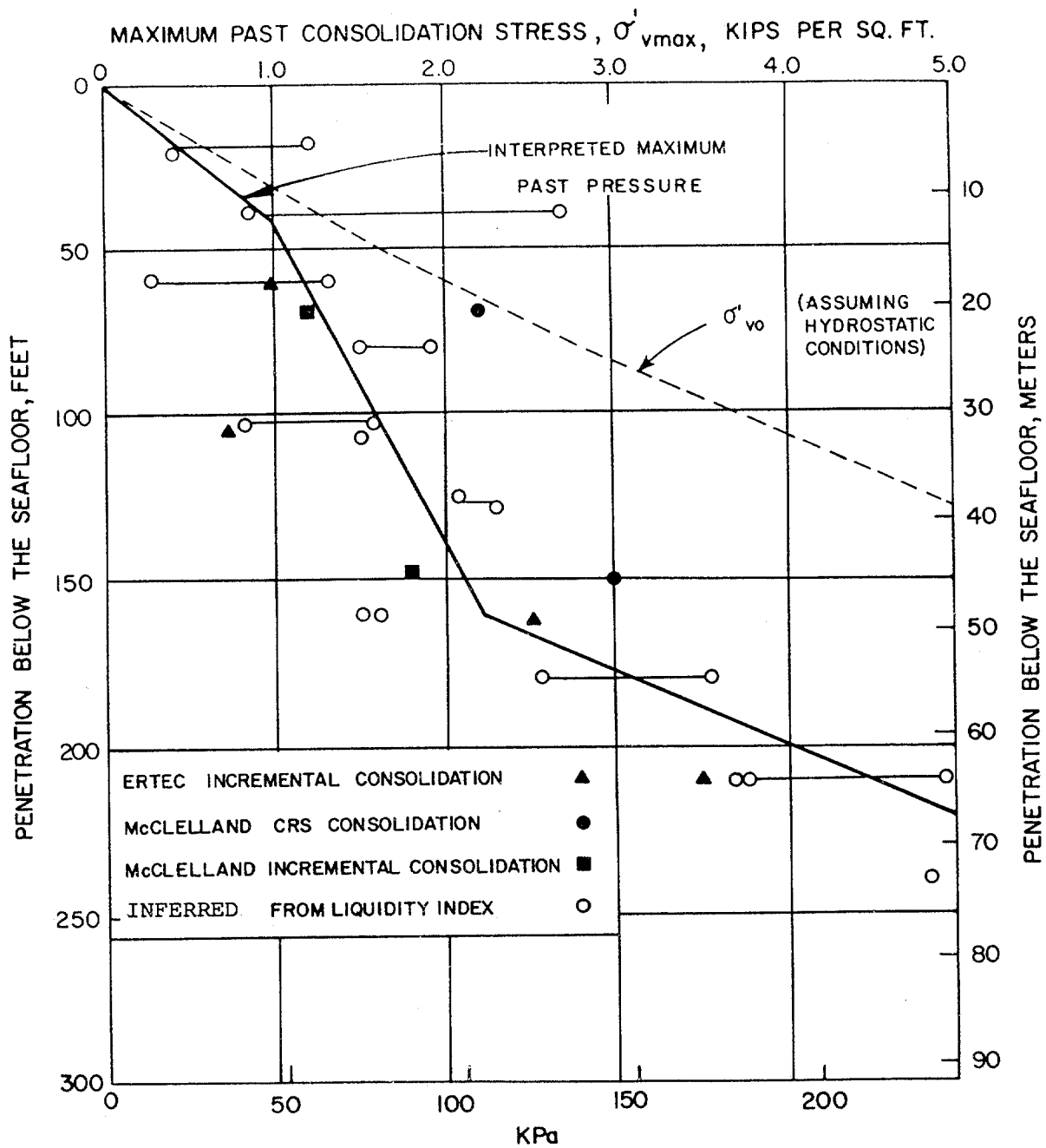
COMPARISON OF TYPE I AND TYPE II LONG-TERM TESTS

Depth M (Ft)	Type Test	Hole No. 1 (Type I)		Hole No. 2 (Type II)		Hole No. 3 (Type II)		$\frac{f_{\max, \text{Type I}}}{f_{\max, \text{Type II}}}$	$\frac{f_{\min, \text{Type I}}}{f_{\min, \text{Type II}}}$
		f_{\max} KPa (KSF)	f_{\min} KPa (KSF)	f_{\max} KPa (KSF)	f_{\min} KPa (KSF)	f_{\max} KPa (KSF)	f_{\min} KPa (KSF)		
45.1 (148.0)	Type I (72-hrs)	34.95 (0.73)	22.50 (0.47)	-	-	-	-	-	-
	Type II (20-hrs)	-	-	-	-	36.87 (0.77)	23.94 (0.50)	0.95	0.94
54.3 (178.0)	Type II (44-hrs)	-	-	-	-	28.73 (0.60)	21.55 (0.45)	1.22	1.04
	Type II (20-hrs)	-	-	-	-	67.03 (1.40)	38.30 (0.80)	-	-
63.4 (208.0)	Type I (72-hrs)	99.59 (2.08)	64.64 (1.35)	-	-	-	-	-	-
	Type II (70-hrs)	-	-	114.93 (2.39)	81.40 1.70	-	-	0.87	0.79
	Type II (144-hrs)	-	-	98.63 (2.06)	77.57 (1.62)	-	-	1.01	0.83

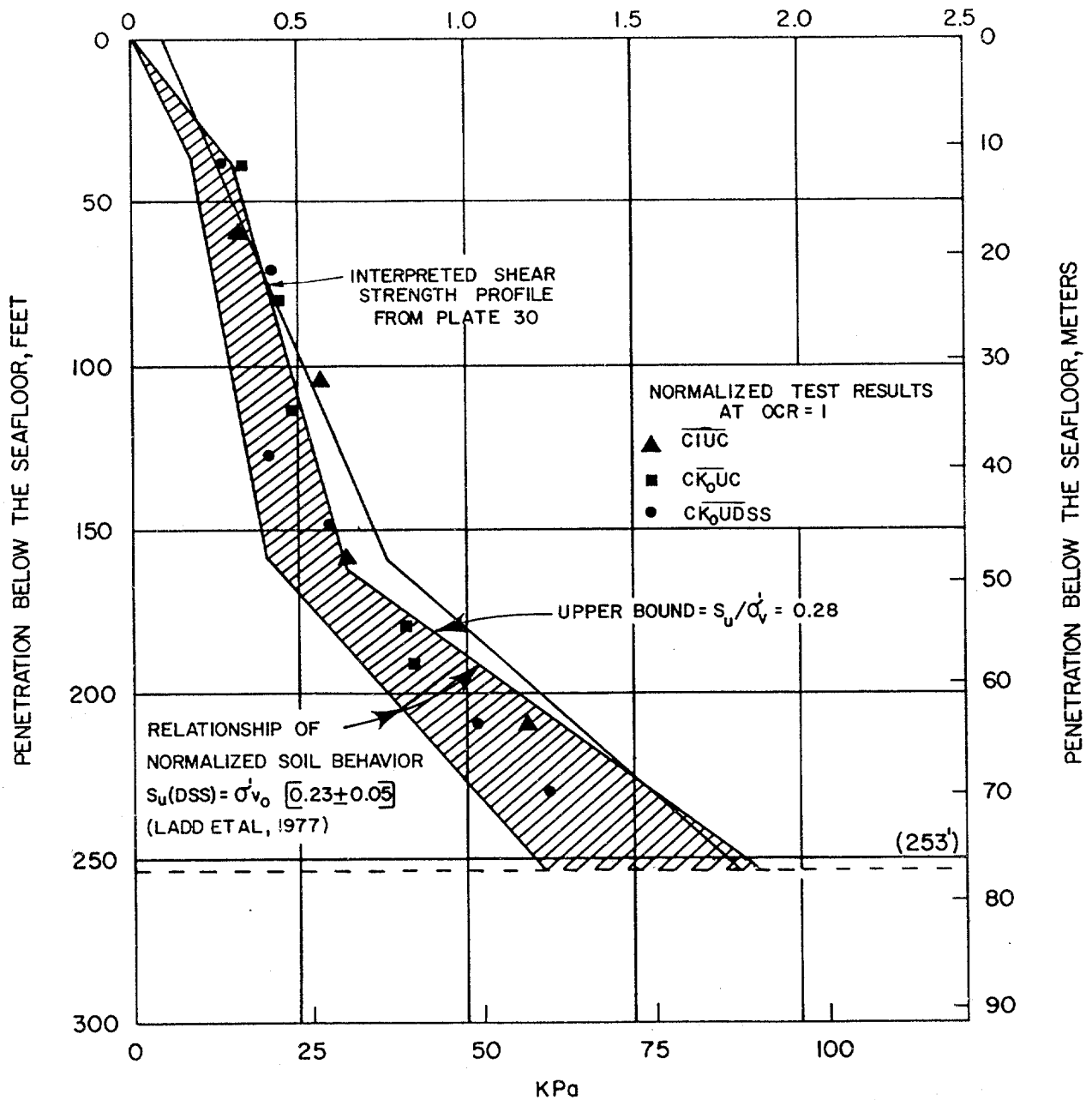
ILLUSTRATIONS



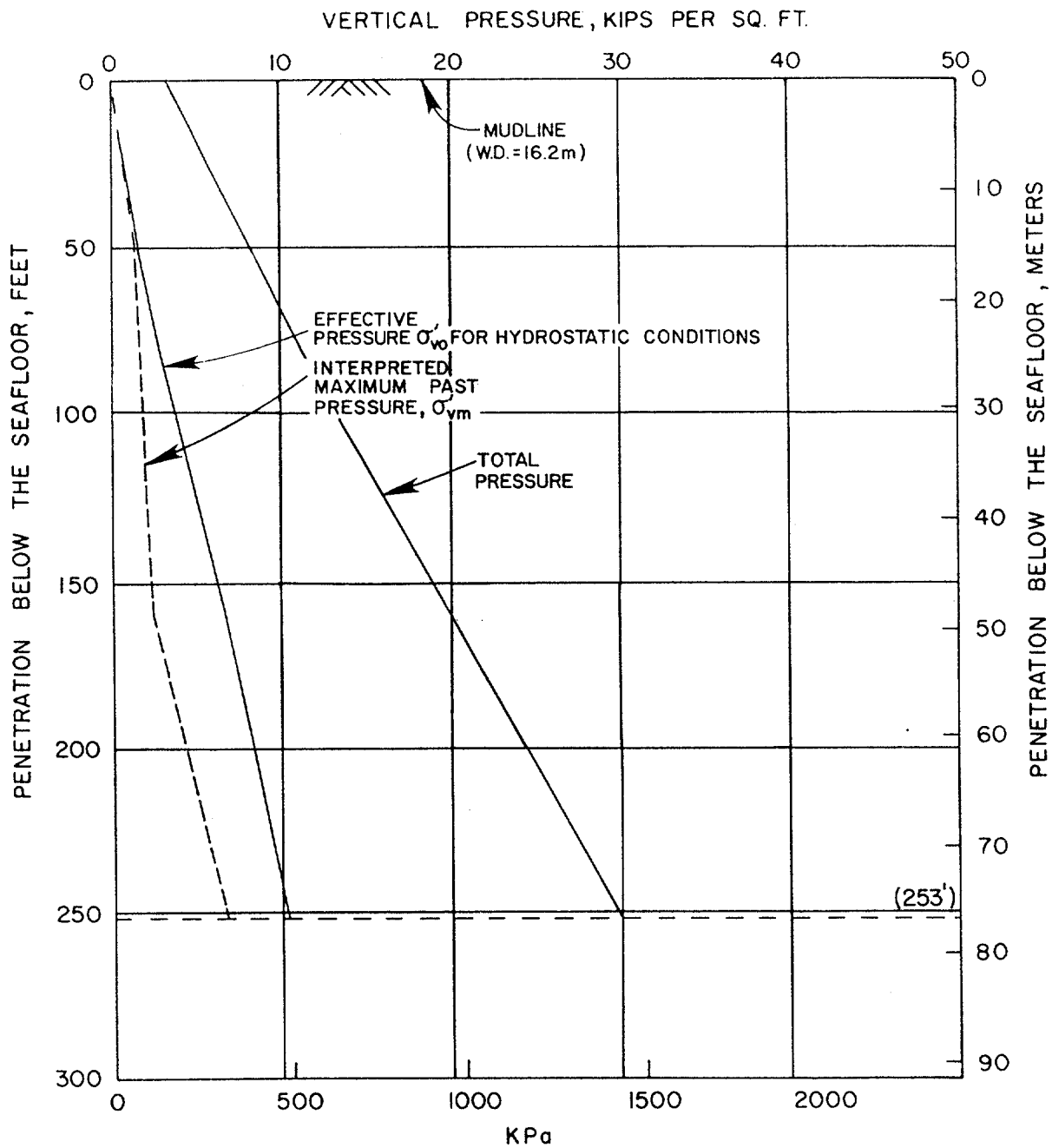
GENERAL LOCATION MAP



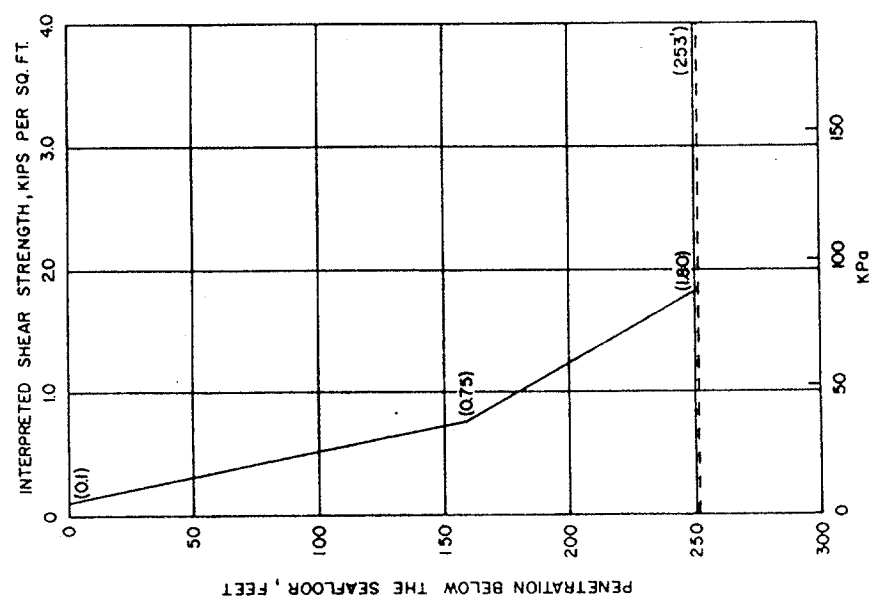
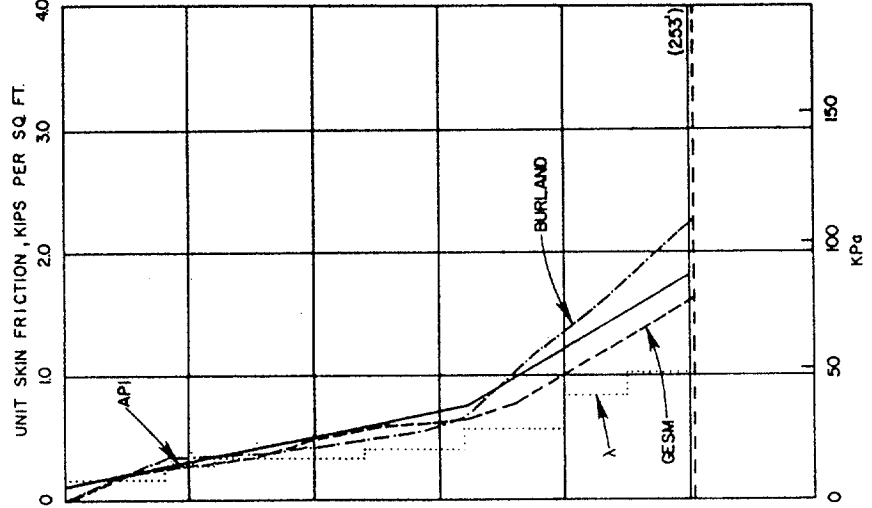
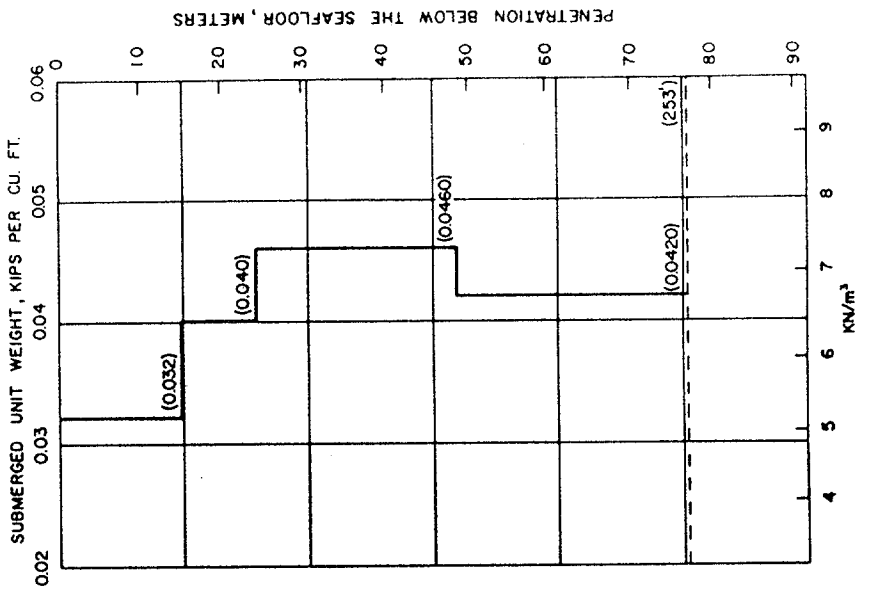
UNDRAINED SHEAR STRENGTH, KIPS PER SQ. FT.



COMPARISON OF UNDRAINED SHEAR STRENGTH PROFILES



VERTICAL PRESSURE DISTRIBUTION



PILE DESIGN DATA
 BLOCK 58, WEST DELTA AREA
 GULF OF MEXICO

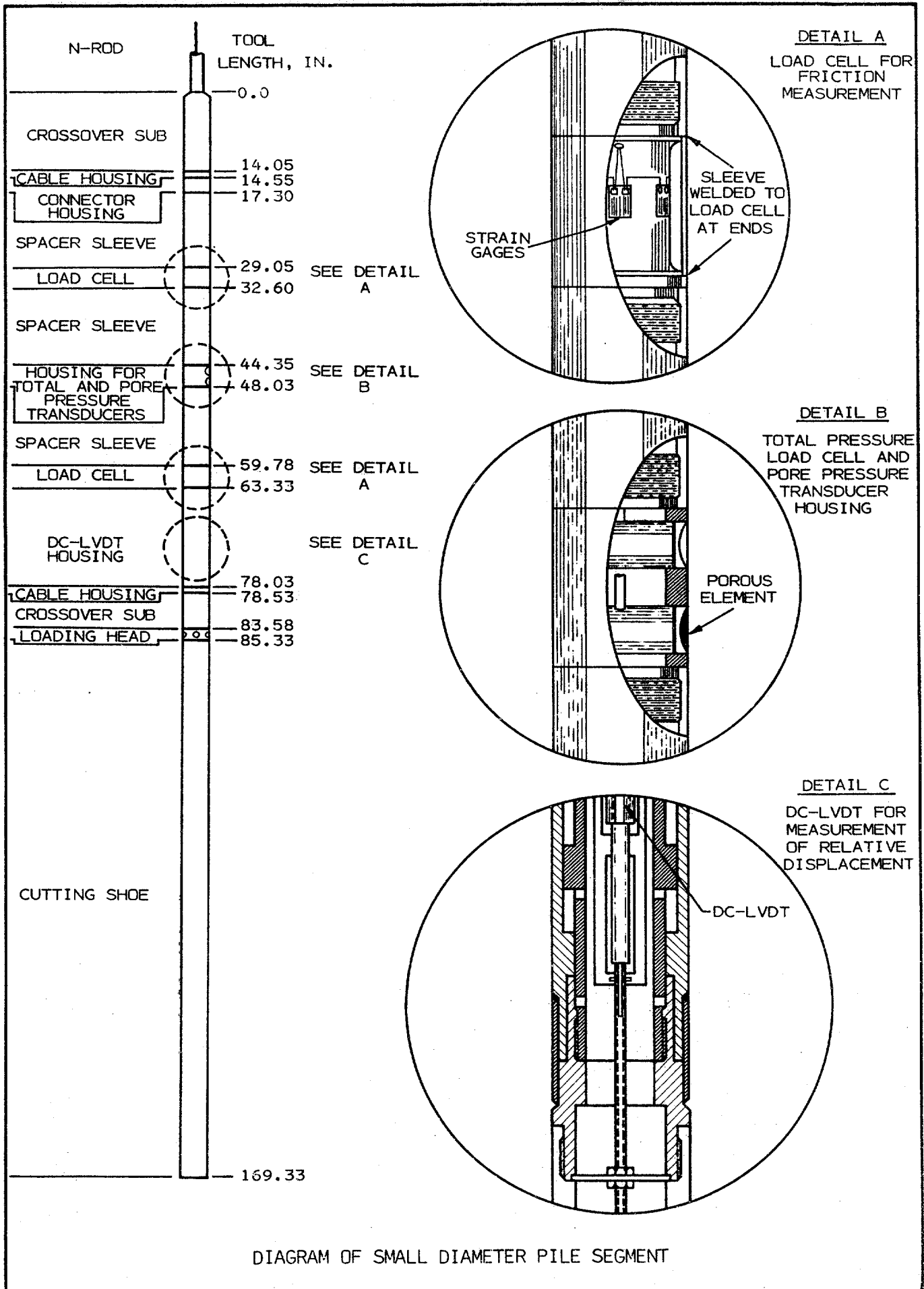
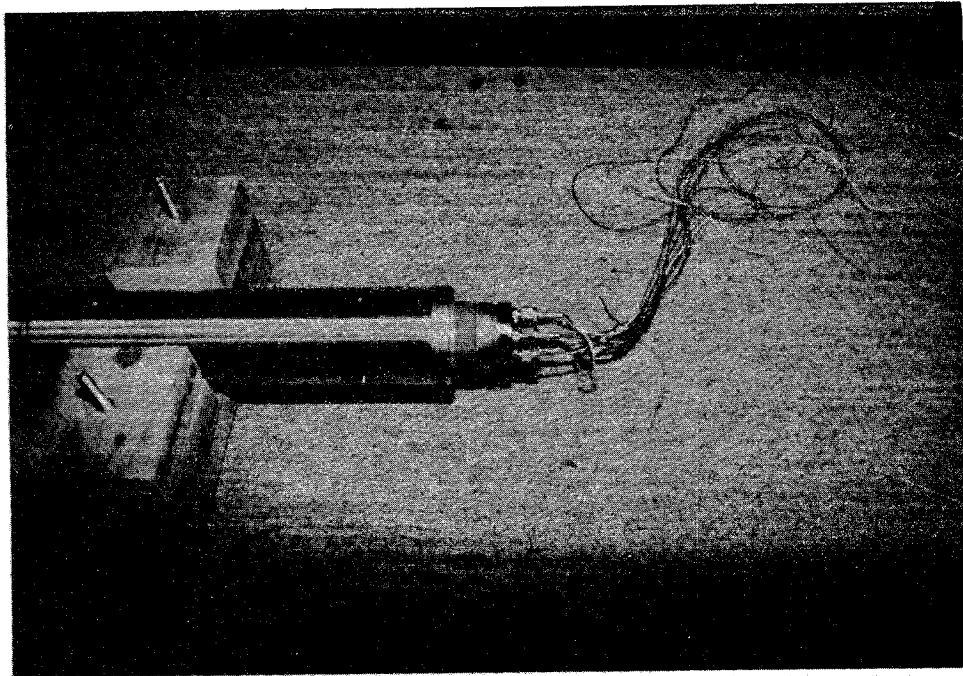


DIAGRAM OF SMALL DIAMETER PILE SEGMENT

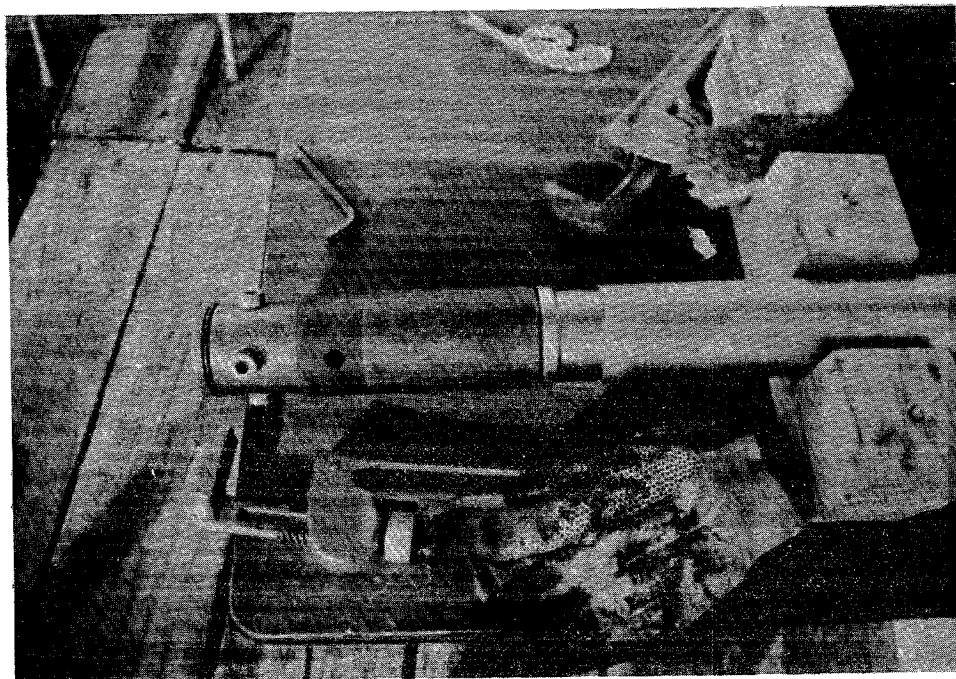


FINAL ASSEMBLY OF SMALL DIAMETER INSTRUMENTED
PILE SEGMENT

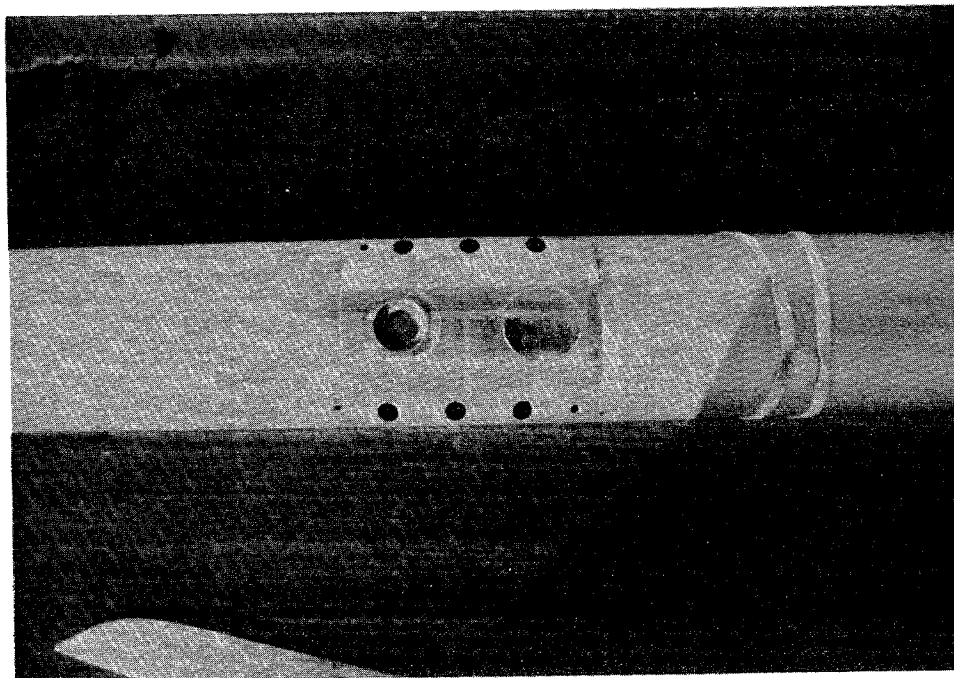


PILE SEGMENT ASSEMBLED AWAITING WIRING OF UNDERWATER
CABLE CONNECTOR

FINAL ASSEMBLY OF SMALL-DIAMETER PILE SEGMENT

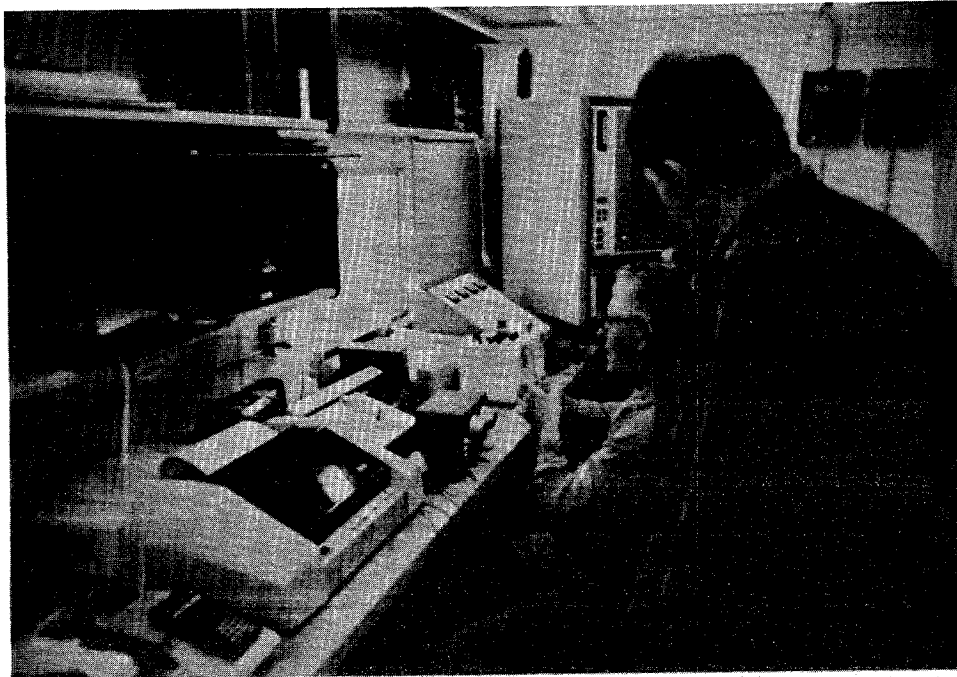


LOWER ASSEMBLY SHOWING CUTTING SHOE ADAPTOR HEAD
AND DC-LVDT SLIP CONNECTION

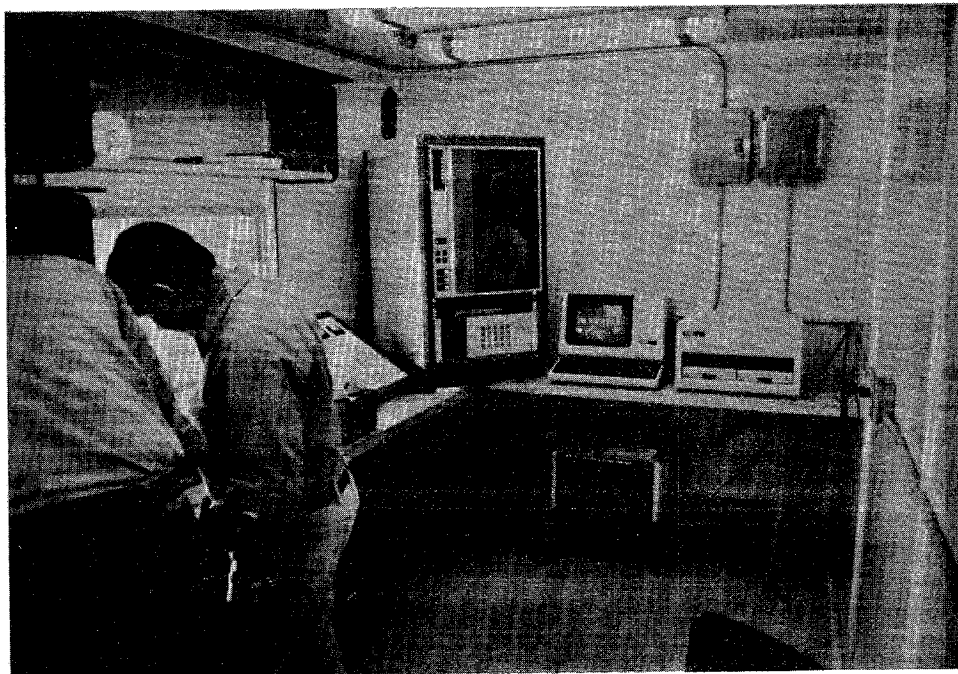


TOTAL PRESSURE AND PORE PRESSURE TRANSDUCER HOUSING

DETAILS OF SMALL-DIAMETER PILE SEGMENT

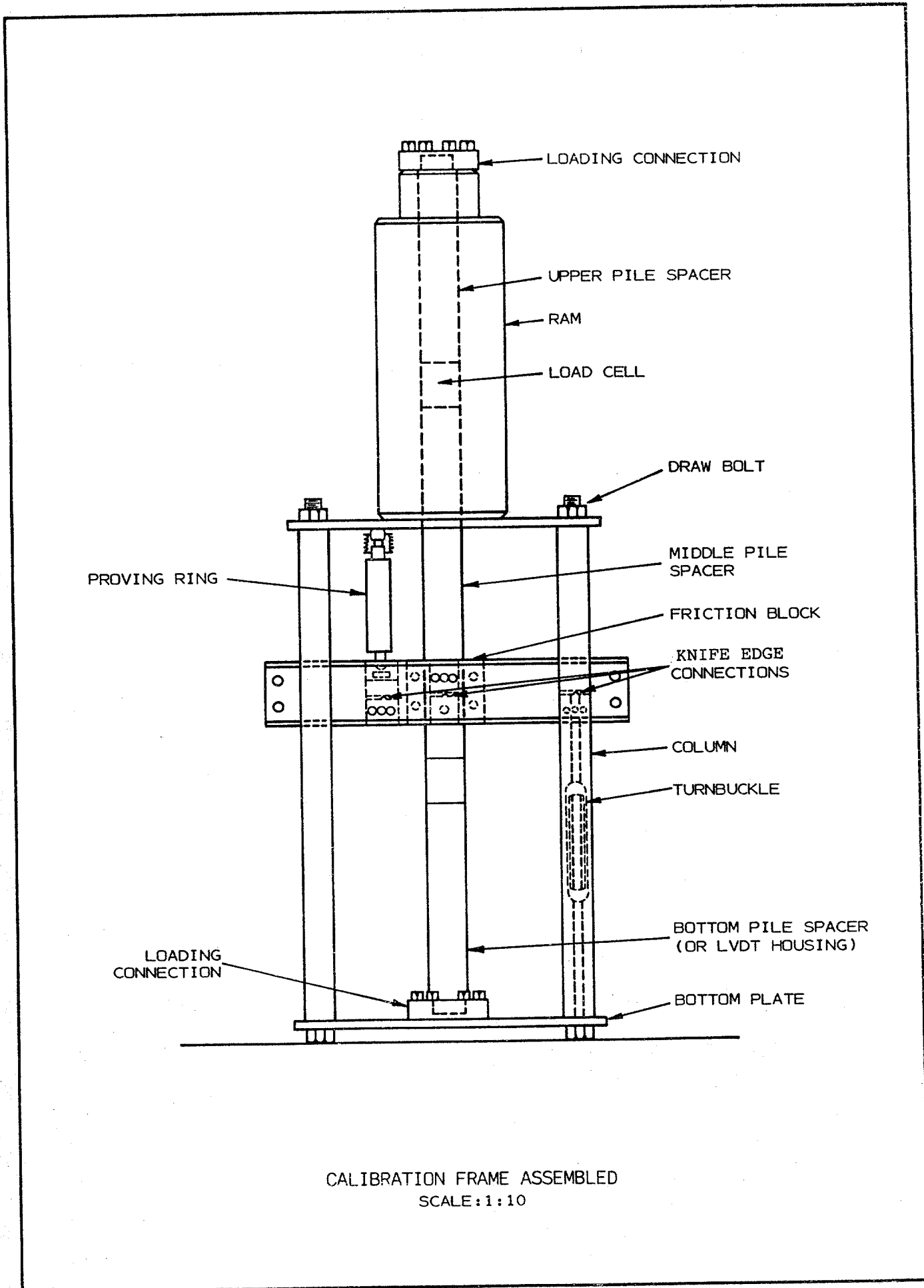


DATA ACQUISITION BUILDING SHOWING ANALOG AND DIGITAL PLOTTERS WITH HIGH SPEED PRINTER



DATA ACQUISITION BUILDING SHOWING 9-TRACK TAPE DRIVE SIGNAL CONDITIONER, CRT CONSOLE AND FLOPPY DISK DRIVE

DATA ACQUISITION BUILDING



LOADING CONNECTION

UPPER PILE SPACER

RAM

LOAD CELL

DRAW BOLT

PROVING RING

MIDDLE PILE SPACER

FRICTION BLOCK

KNIFE EDGE CONNECTIONS

COLUMN

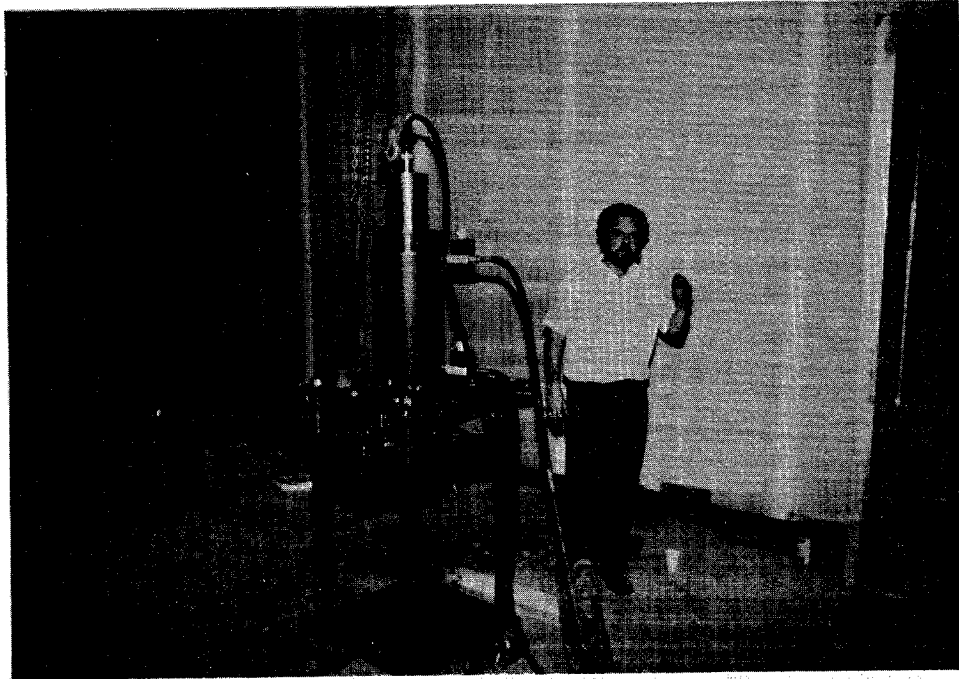
TURNBUCKLE

BOTTOM PILE SPACER (OR LVDT HOUSING)

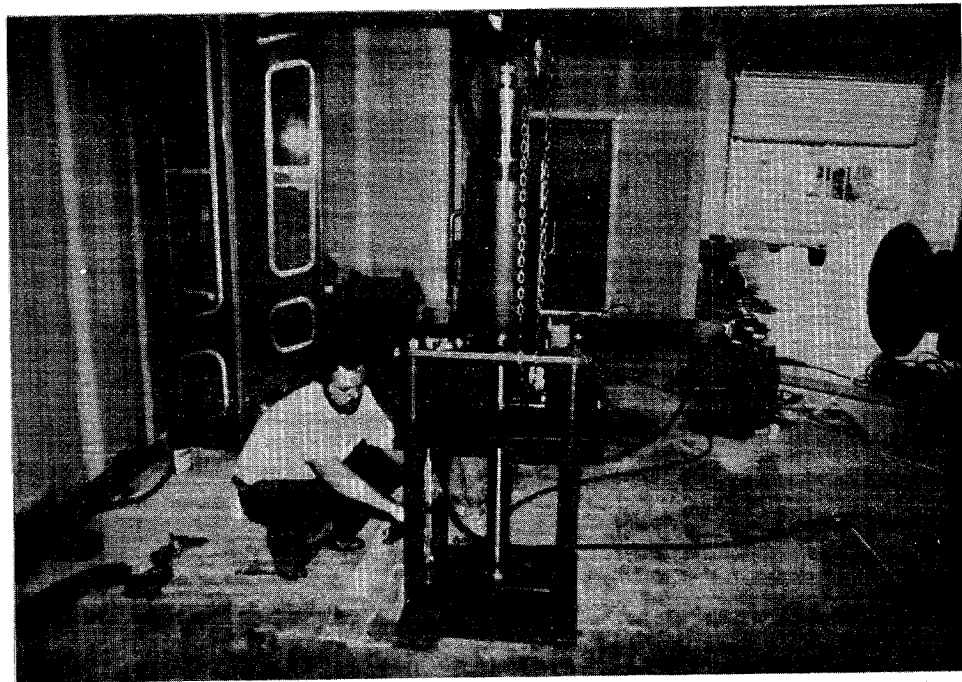
LOADING CONNECTION

BOTTOM PLATE

CALIBRATION FRAME ASSEMBLED
SCALE: 1:10

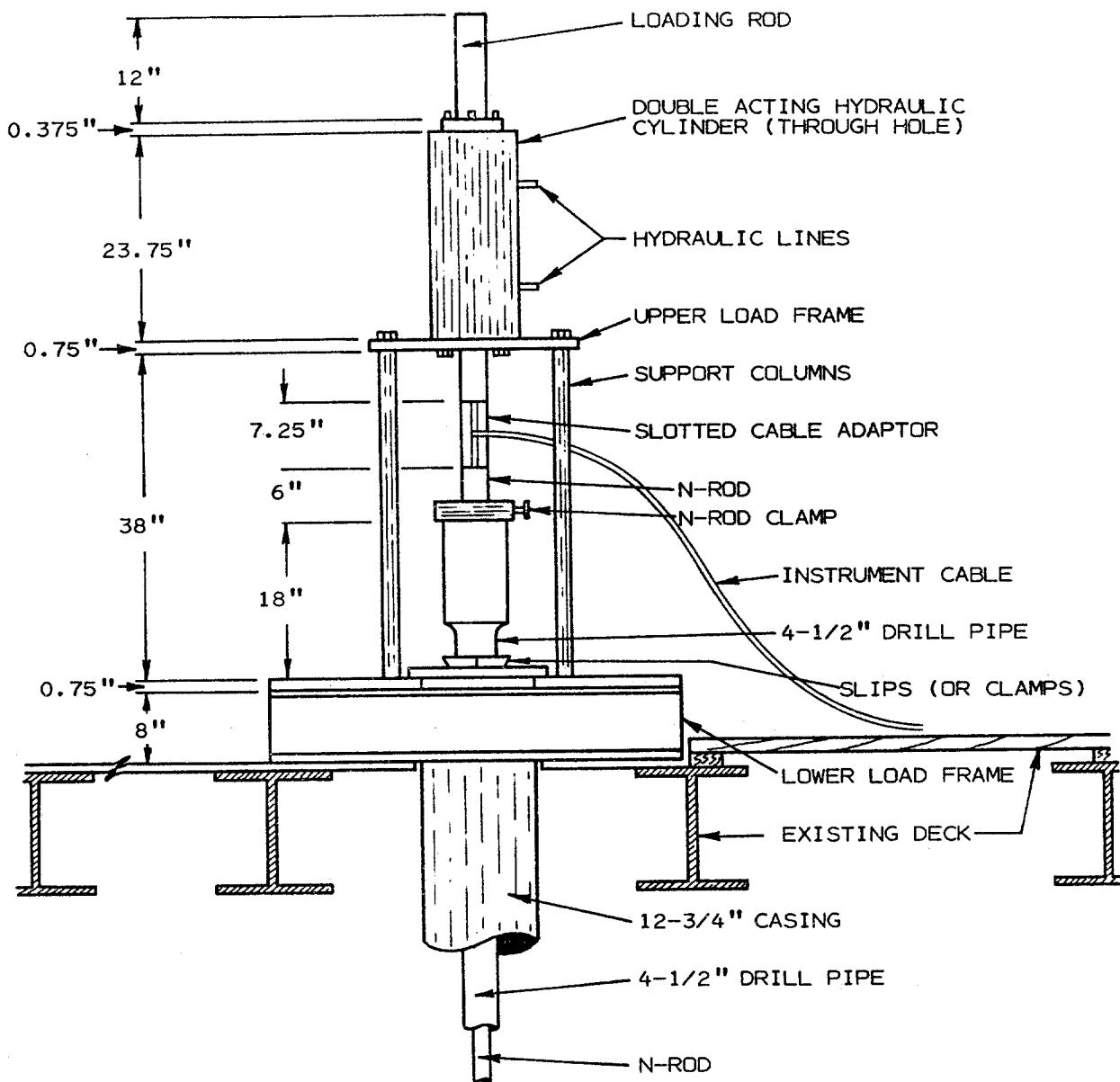


CALIBRATION OF SMALL DIAMETER PILE SEGMENT

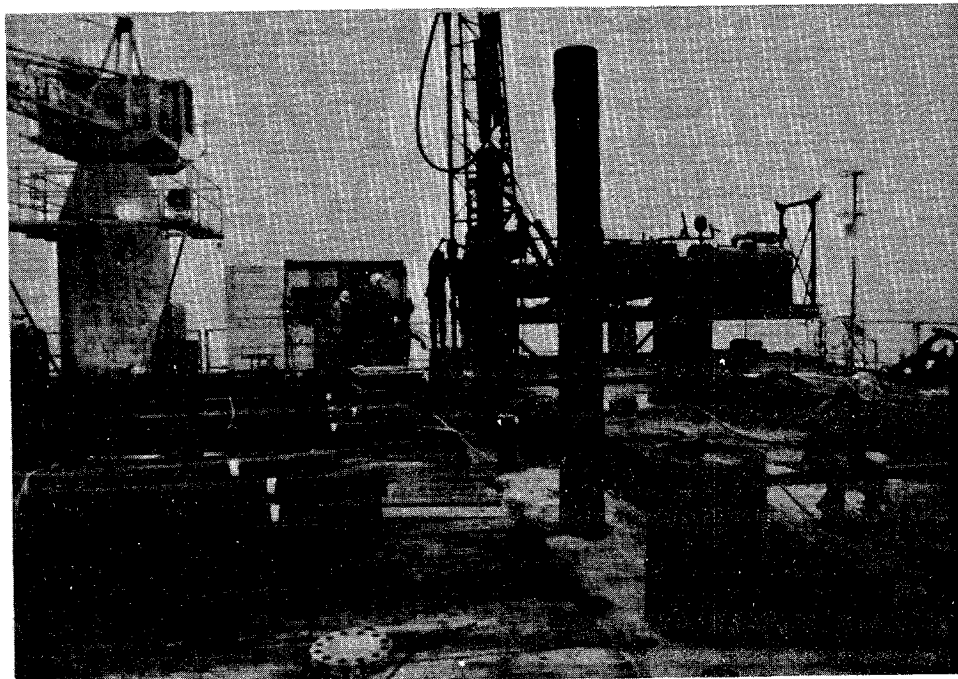


FINAL ADJUSTMENTS TO THE LOADING FRAME PRIOR
TO CALIBRATION

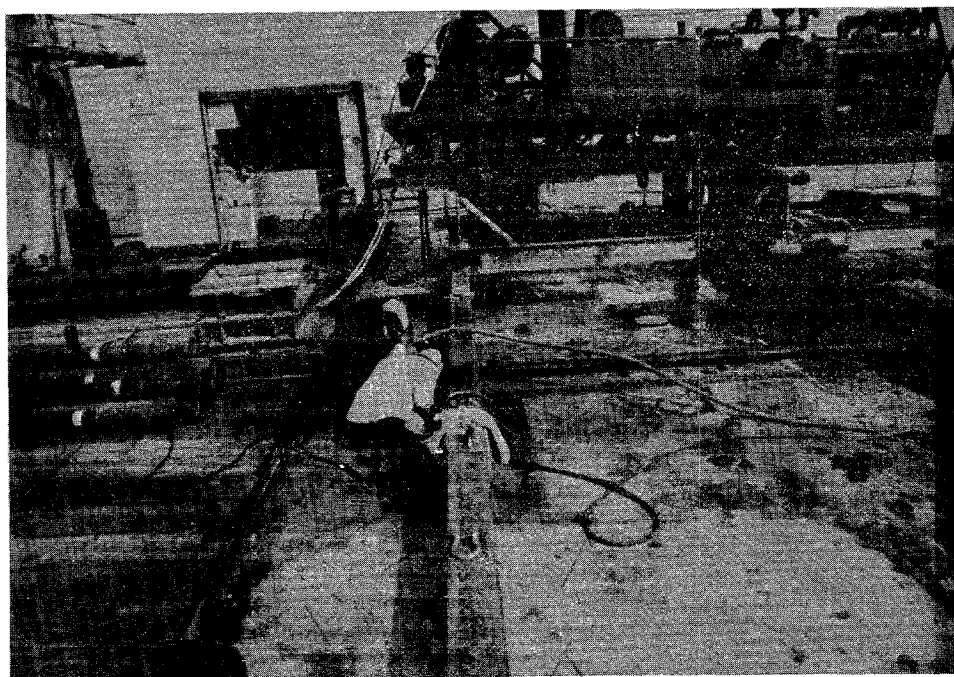
CALIBRATION OF SMALL-DIAMETER PILE



SCHMATIC DIAGRAM OF TESTING ARRANGEMENT
FOR 3-INCH DIAMETER PILE SEGMENT TESTS

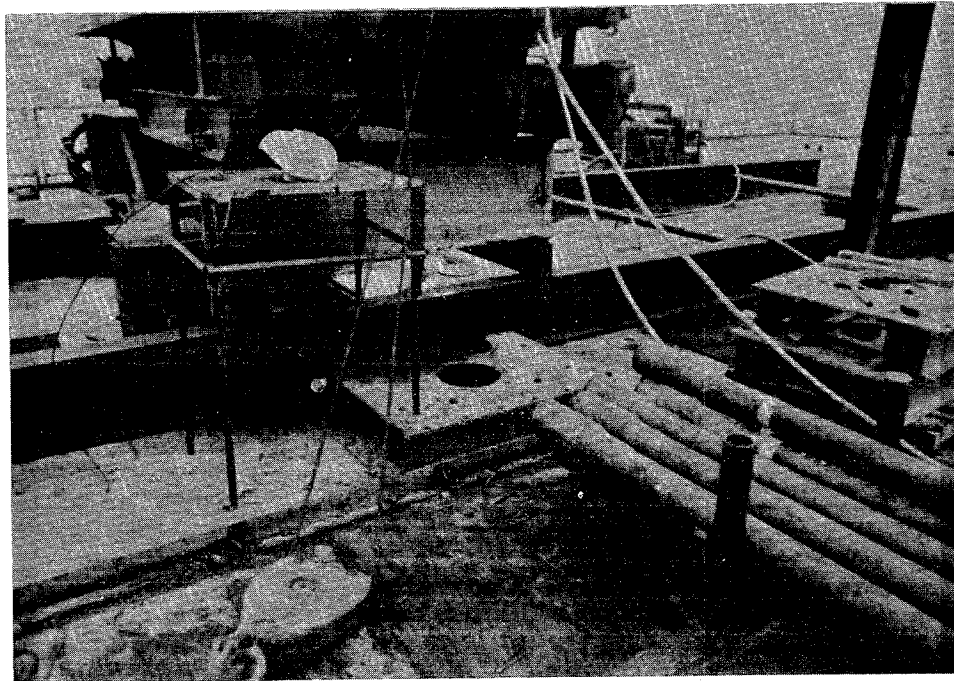


MOBILIZATION OF EQUIPMENT AND INSTALLATION OF CASING

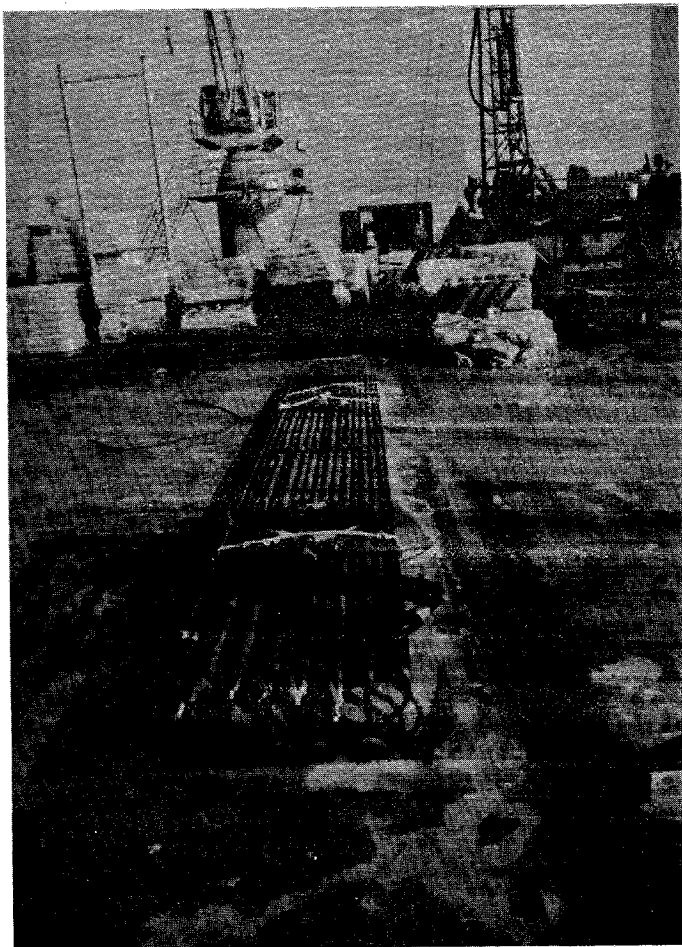


FINAL INSTALLATION OF DECK FIXTURES

FIELD PREPARATIONS

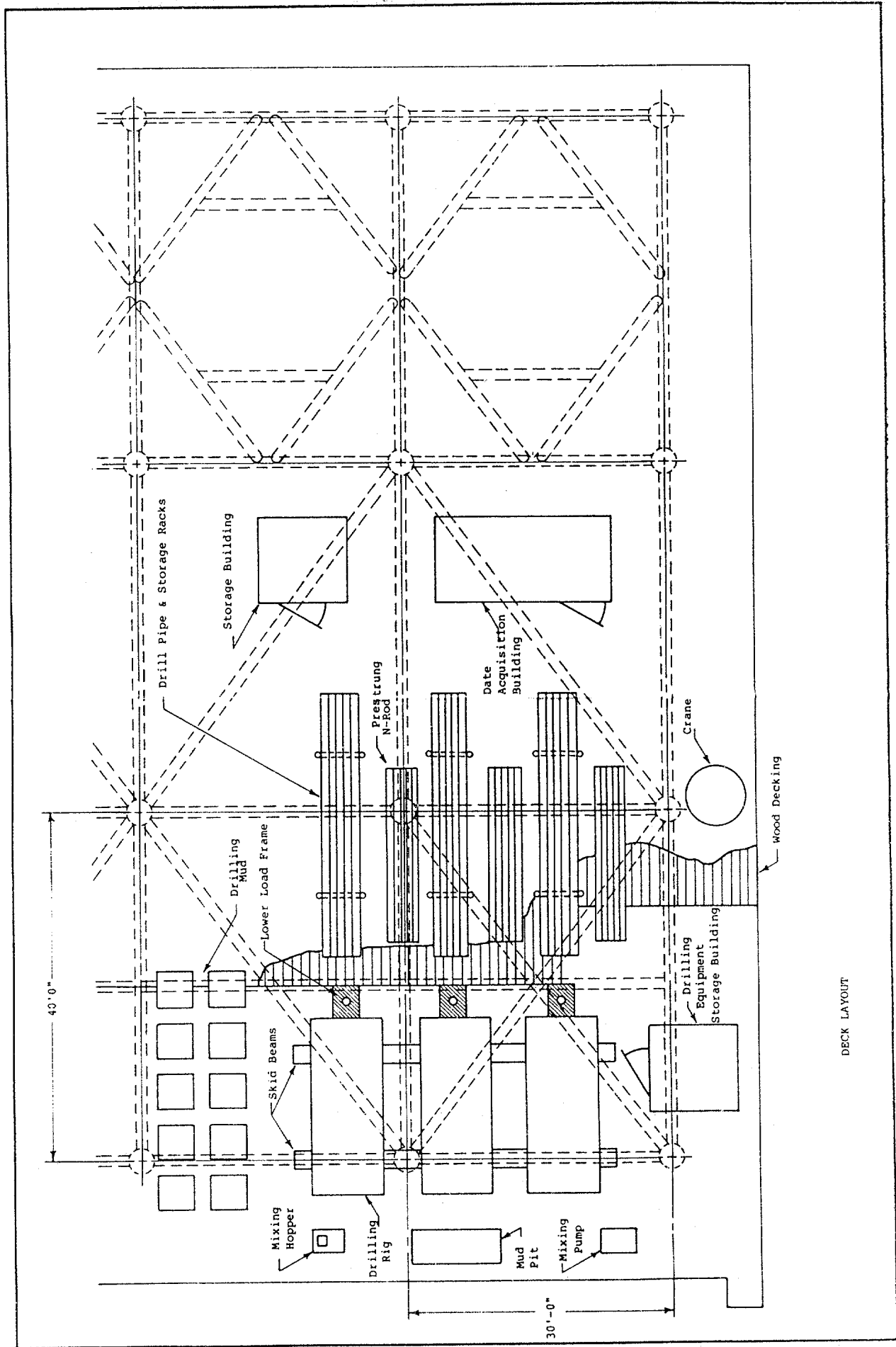


DECK MOUNTED LOWER LOADING FRAME

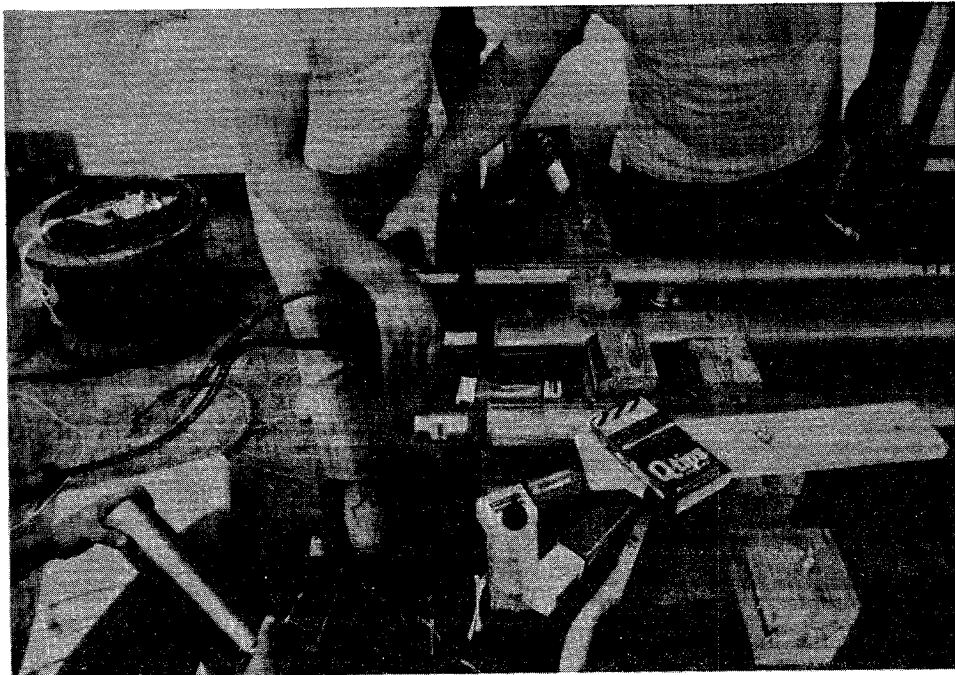


DRILL RODS WITH PRE-STRUNG
INSTRUMENT CABLE

FIELD PREPARATIONS



DECK LAYOUT

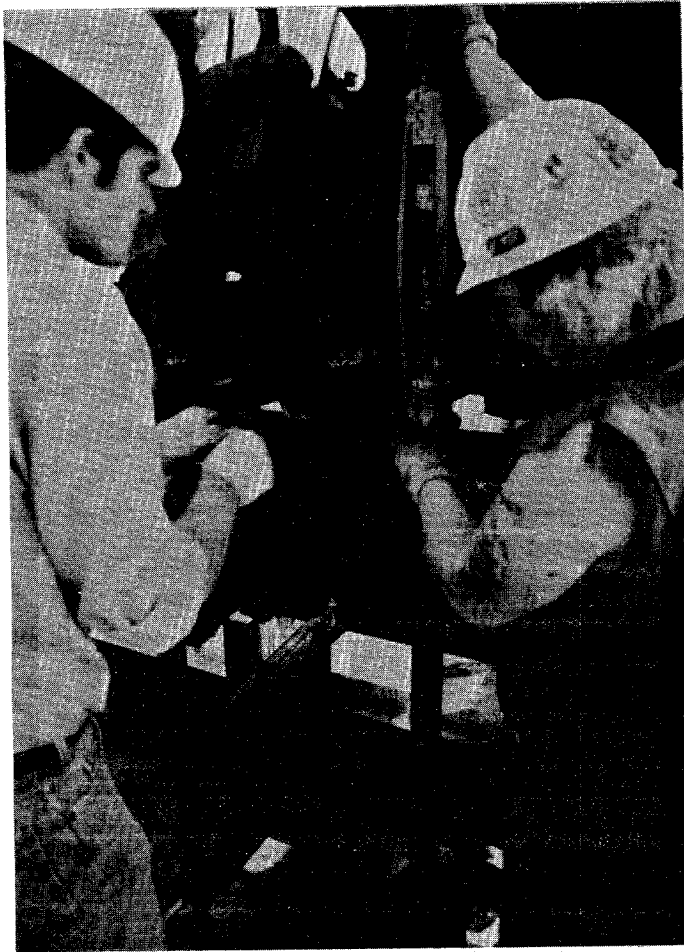


ATTACHING INSTRUMENT CABLES TO THE MODEL
PILE SEGMENTS

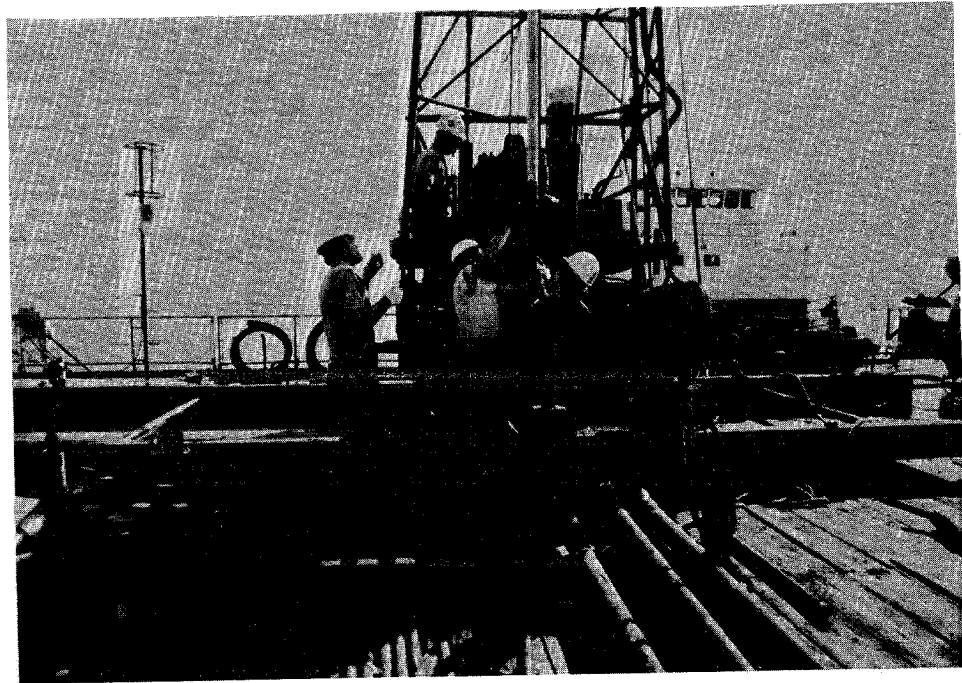


SATURATING POROUS STONE FOR PORE PRESSURE TRANSDUCER
PRIOR TO INSTALLATION OF INSTRUMENT INTO THE DRILL PIPE

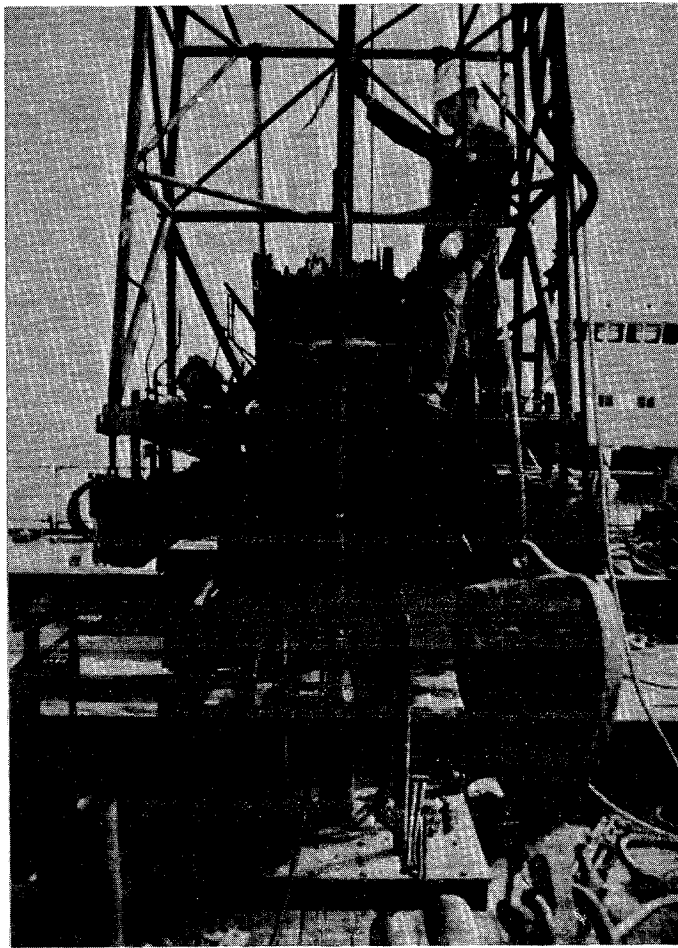
FIELD PREPARATIONS



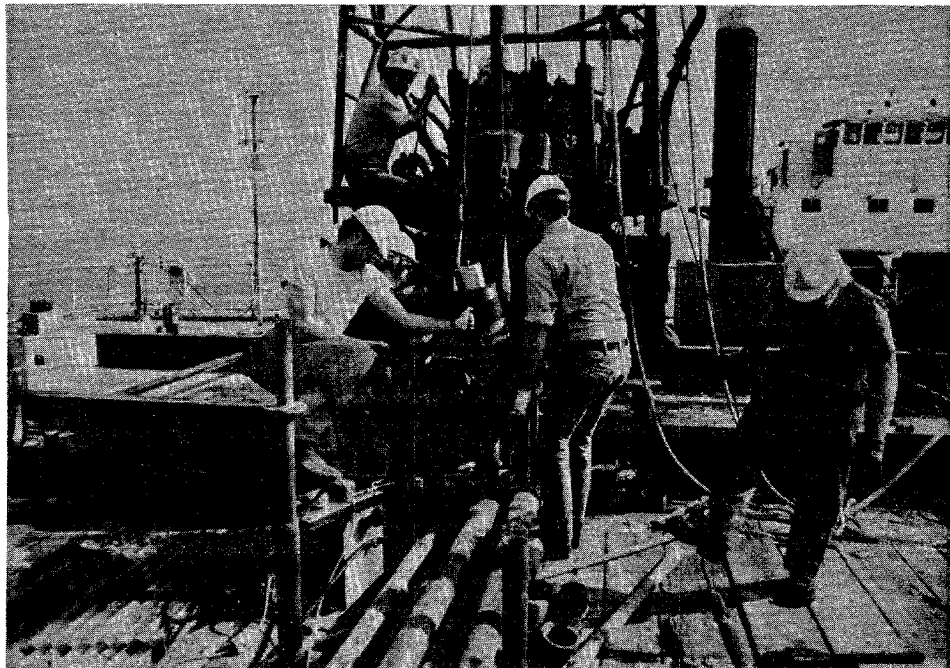
ATTACHING ROD CENTRALIZERS



ATTACHING PILE CUTTING SHOE
INSTALLATION OF INSTRUMENT

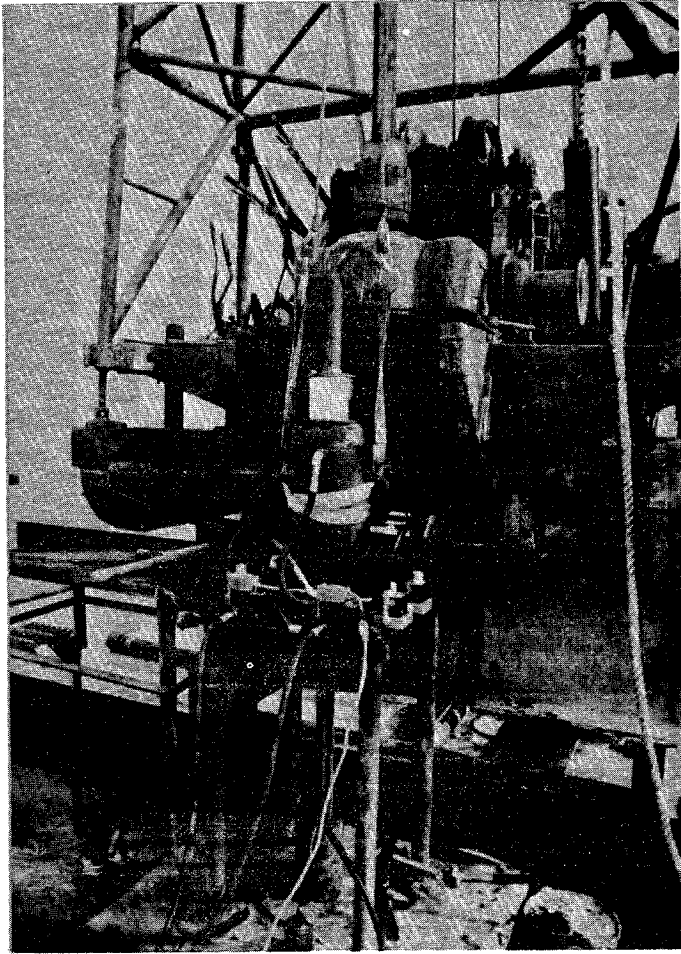


DRILL ROD ASSEMBLY
WITH SLOTTED CABLE
ADAPTOR AWAITING
HAMMER FOR DRIVING
INSTRUMENT

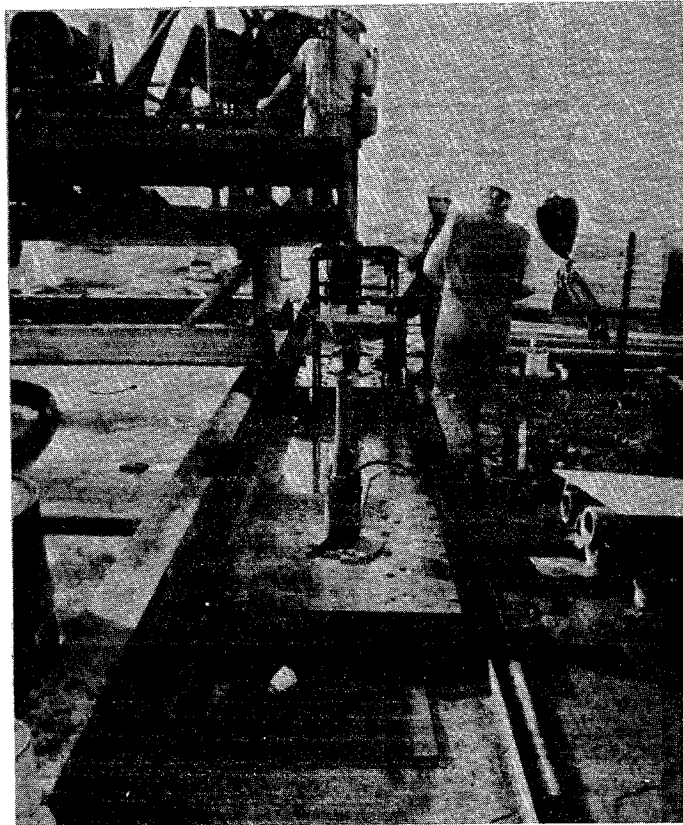


POSITIONING CENTERHOLE HYDRAULIC RAM AND POWER PACK

INSTALLATION OF INSTRUMENT



COMPLETED ASSEMBLY
READY FOR LOAD TEST



DRILLING SECOND
HOLE WHILE FIRST
PILE SEGMENT
CONSOLIDATES

LOAD TESTING

HOLE 1

2

3

DEPTH
0

Mudline

-58

-148

-178

-208

Large Displ - Long Time
Fully Plugged

Large Displ - Short Time
Fully Plugged

Small Displ - Short Time
Fully Plugged

Large Displ - Long Time
Open End

Large Displ - Short Time
Fully Plugged

Large Displ - Short Time
Open End

Large Displ - Long Time
Open End

Large Displ - Short-Long-Long
Open End

One-Way Tension - Short Time
Open End

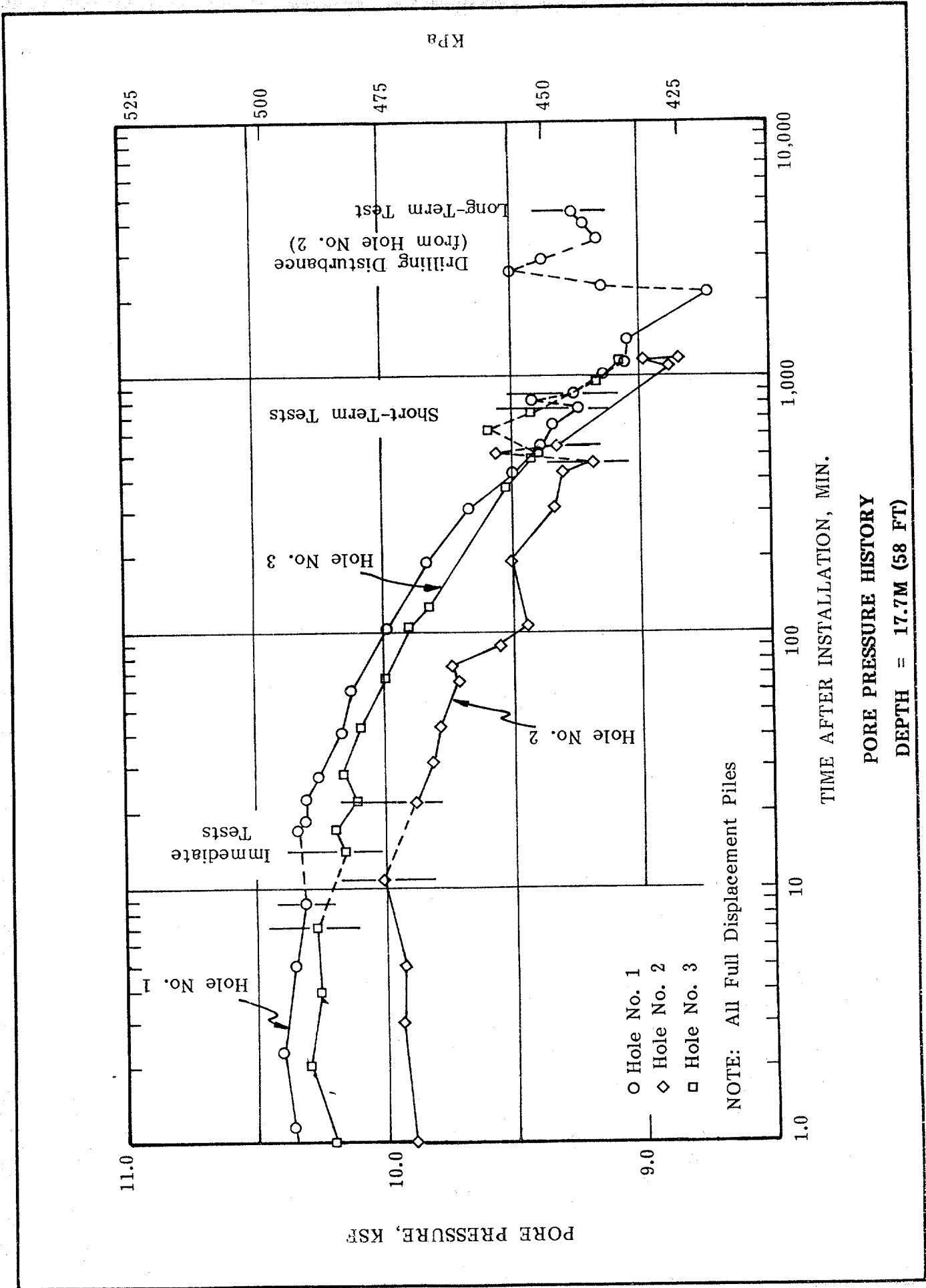
Load/
Small Displ - Short Time
Open End

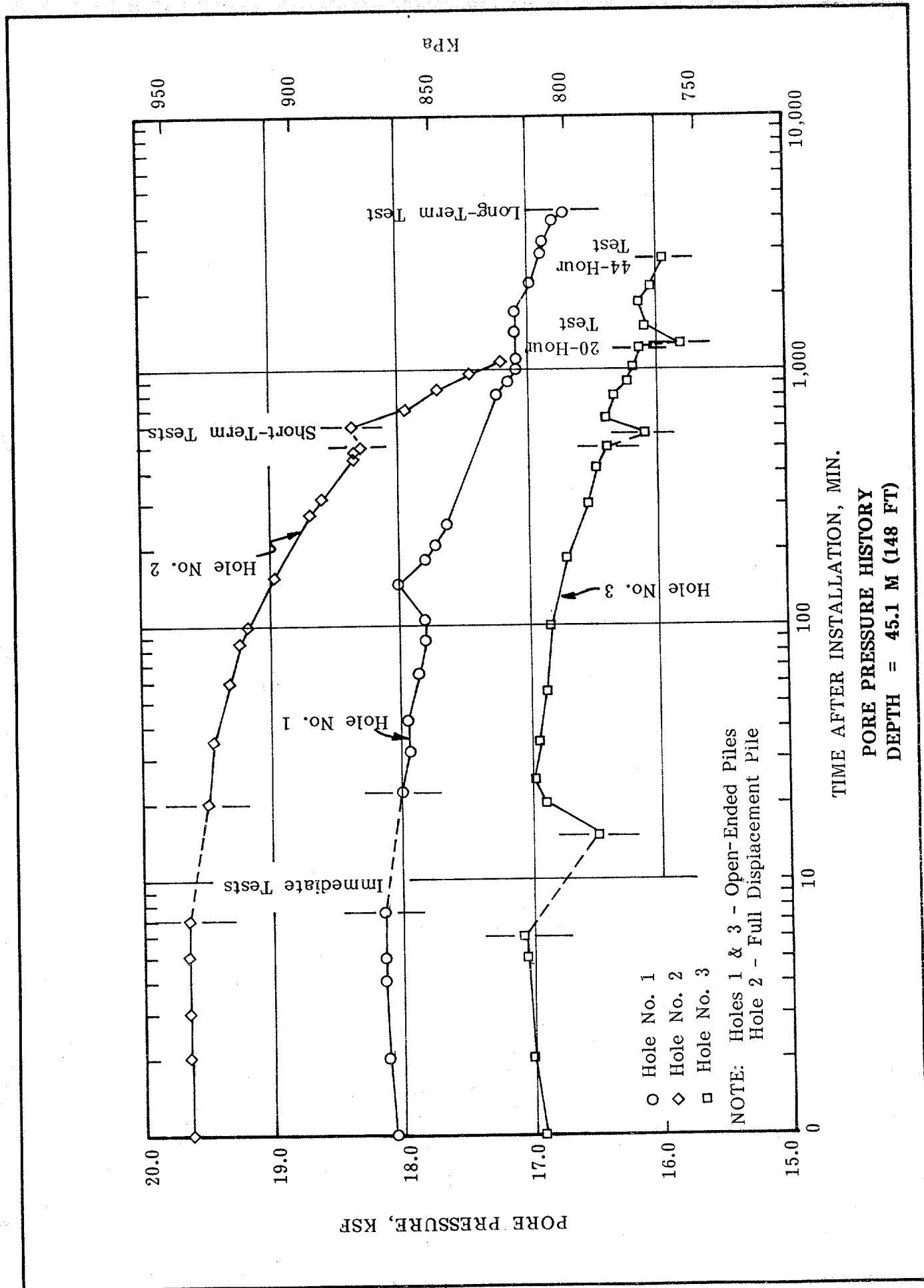
Short Time Approx. 8 Hours
Long Time Approx. 72 Hours

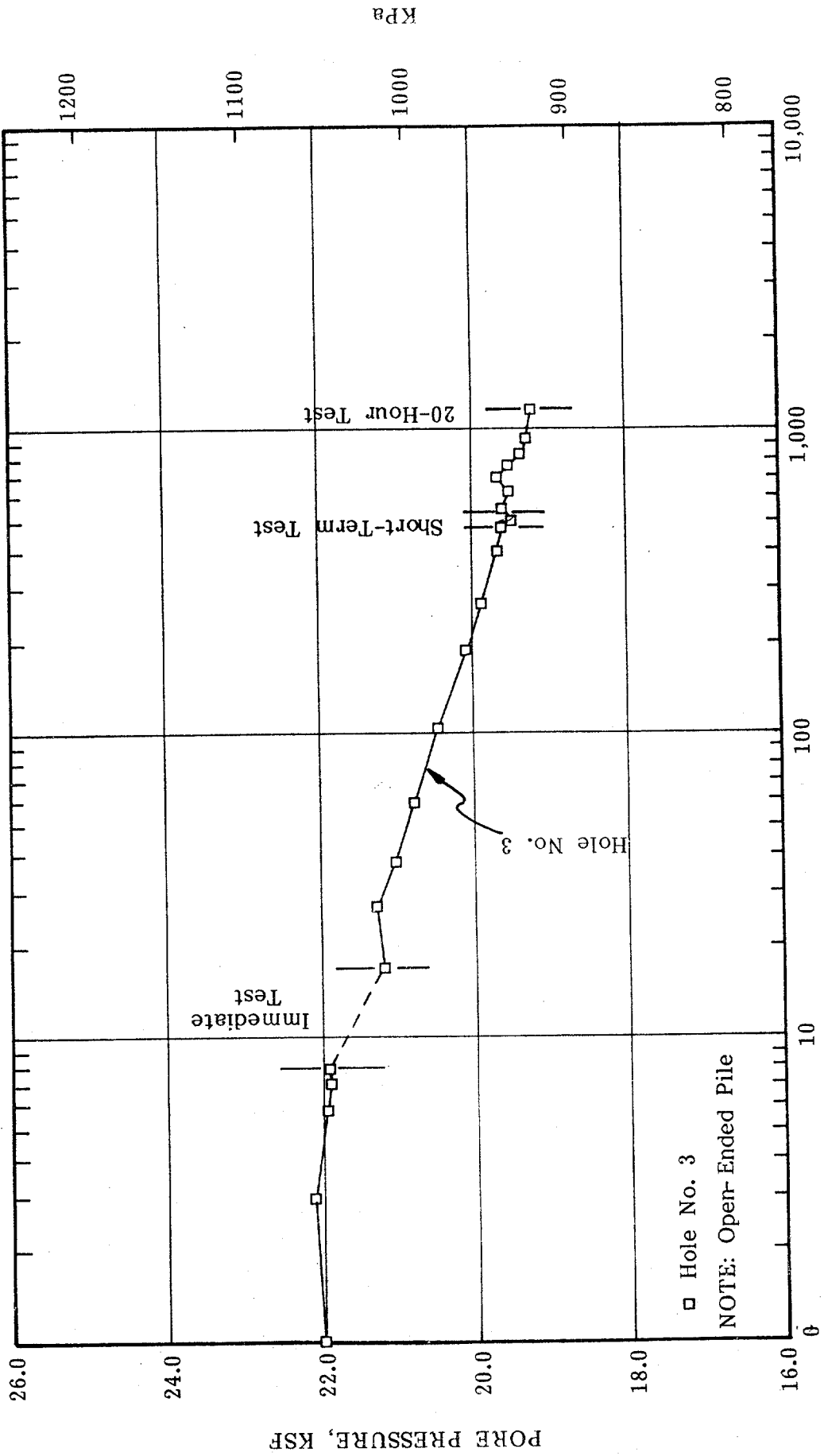
CONOCO SMALL TOOL PROGRAM

SUMMARY OF TESTS PERFORMED

Depth m (ft)	Type Test	Hole 1		Hole 2		Hole 3	
		f_{max}	f_{min}	f_{max}	f_{min}	f_{max}	f_{min}
17.7 (58)	Immediate	X		X		X	
	8-hour			X	X	X	X
	72-hour	X	X				
	Pull-out	X		X		X	
45.1 (148)	Immediate	X		X		X	
	8-hour			X	X	X	X
	20-hour					X	X
	44-hour					X	X
	72-hour	X	X				
	Pull-out	X		X		X	
54.3 (178)	Immediate					X	
	8-hour					X	X
	20-hour					X	X
	Pull-out					X	
63.4 (208)	Immediate	X		X		X	
	8-hour			X	X	X	X
	20-hour						
	72-hour	X	X	X	X		
	144-hour			X	X		
	Pull-out	X		X		X	





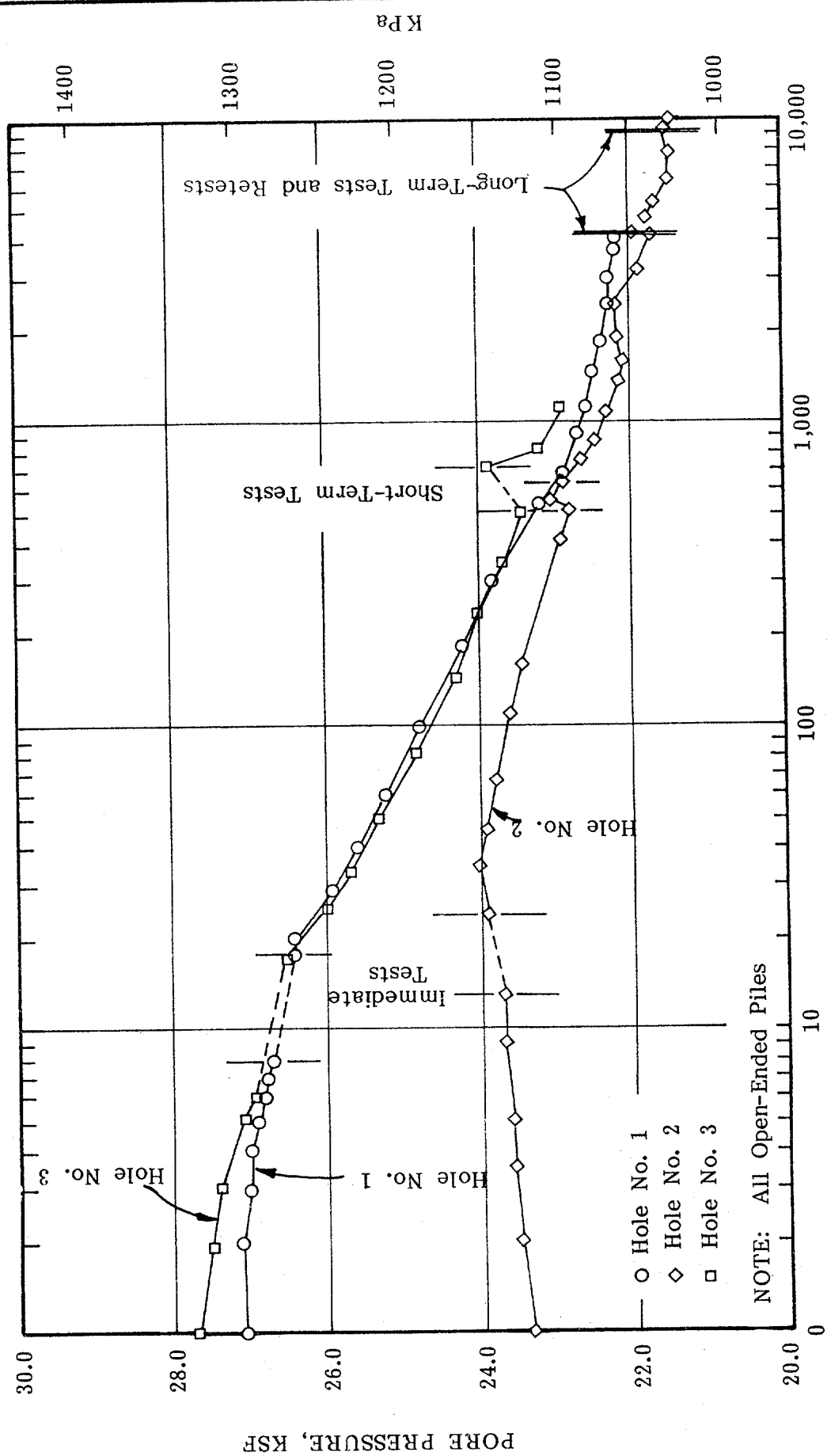


TIME AFTER INSTALLATION, MIN.

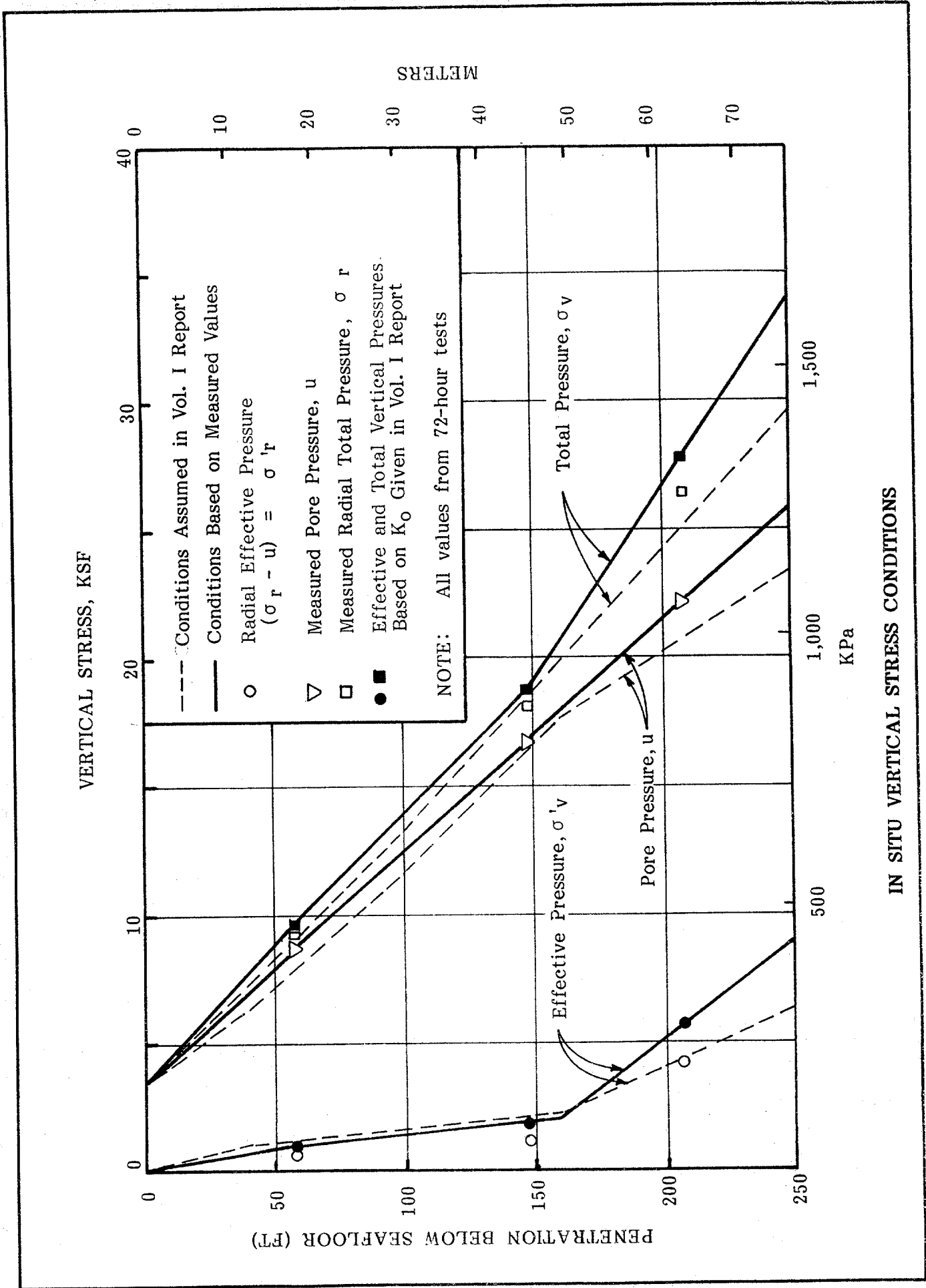
PORE PRESSURE HISTORY
DEPTH = 54.3M (178 FT)

□ Hole No. 3

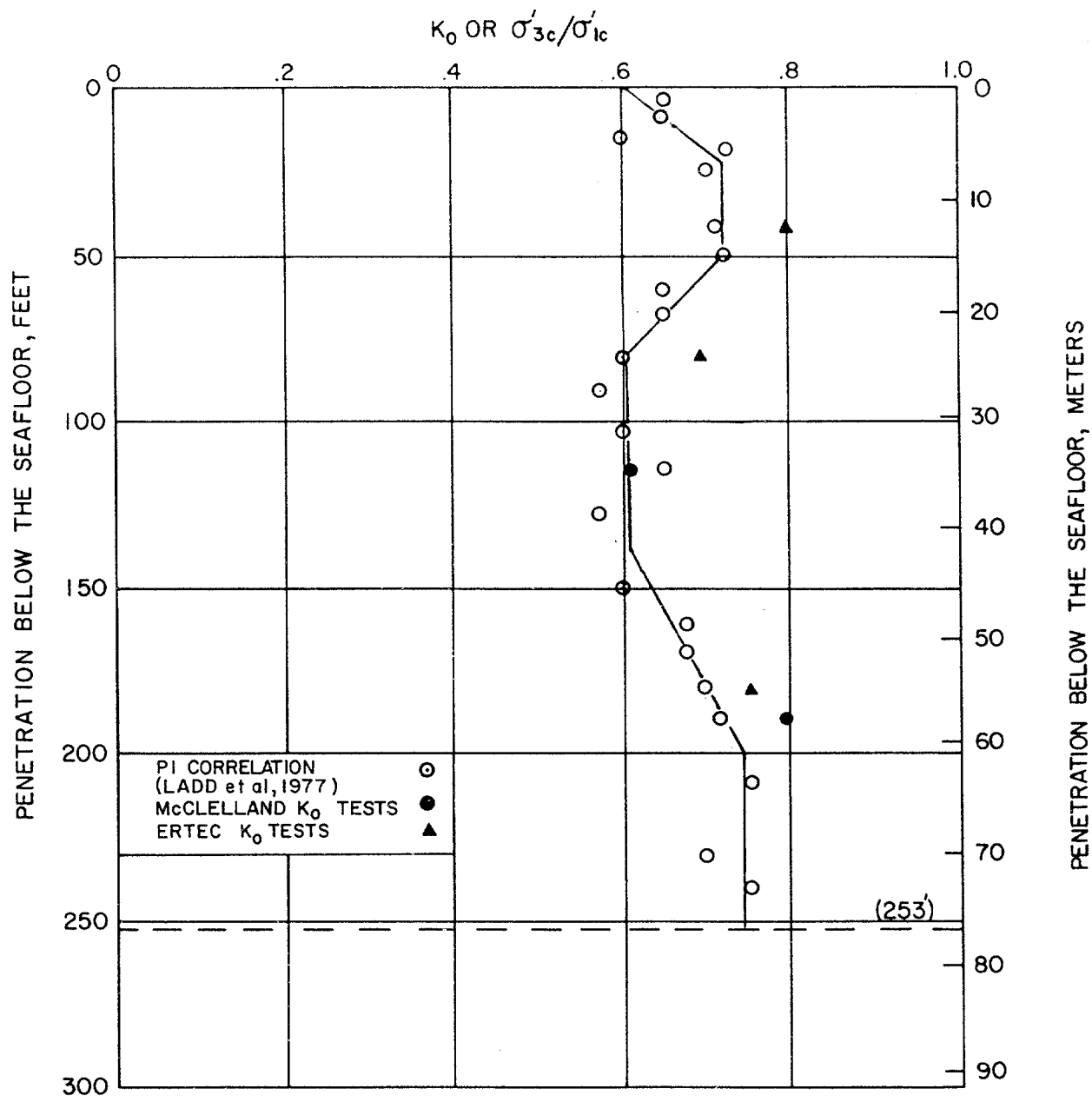
NOTE: Open-Ended Pile



JOB NO.

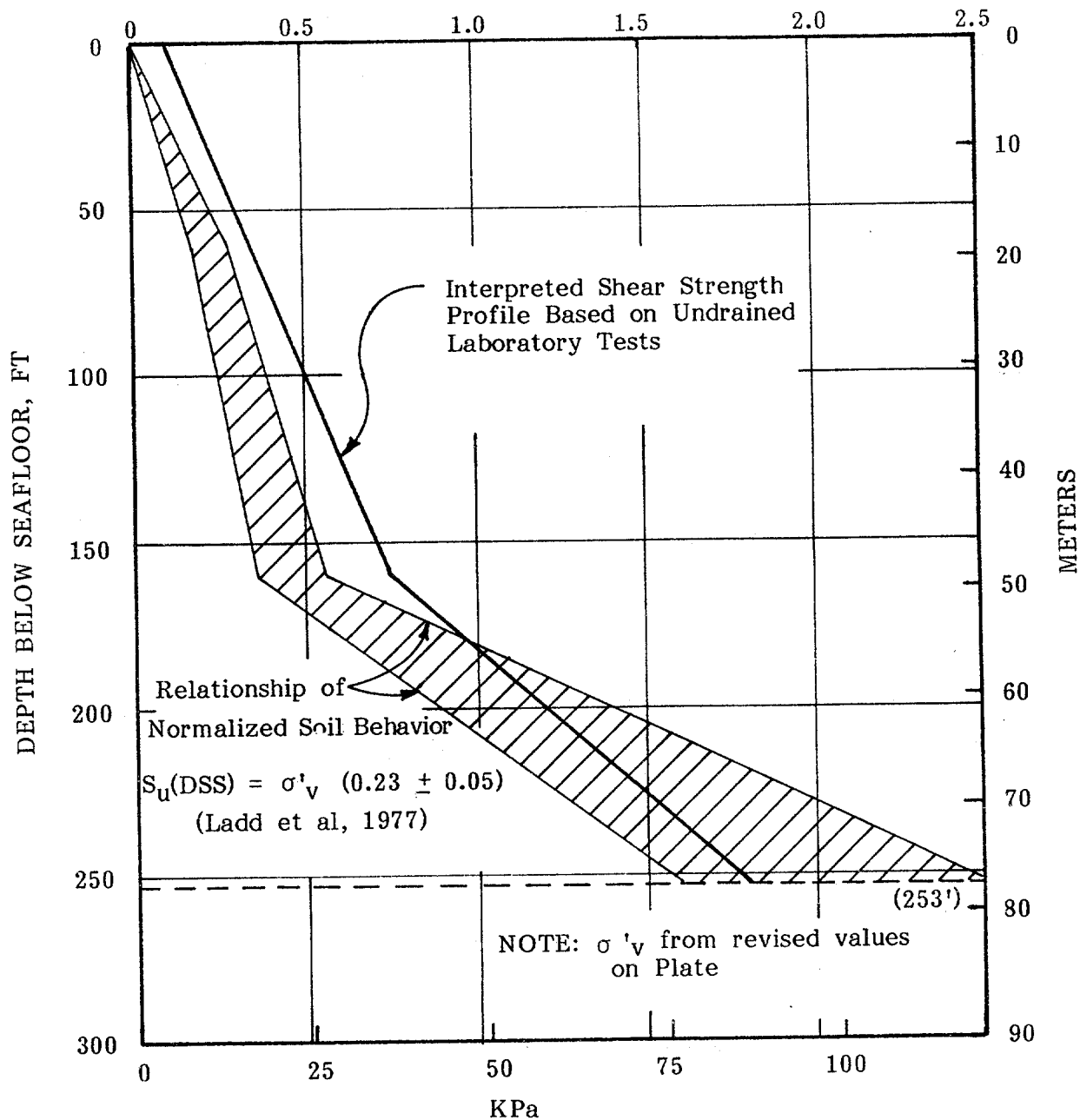


IN SITU VERTICAL STRESS CONDITIONS



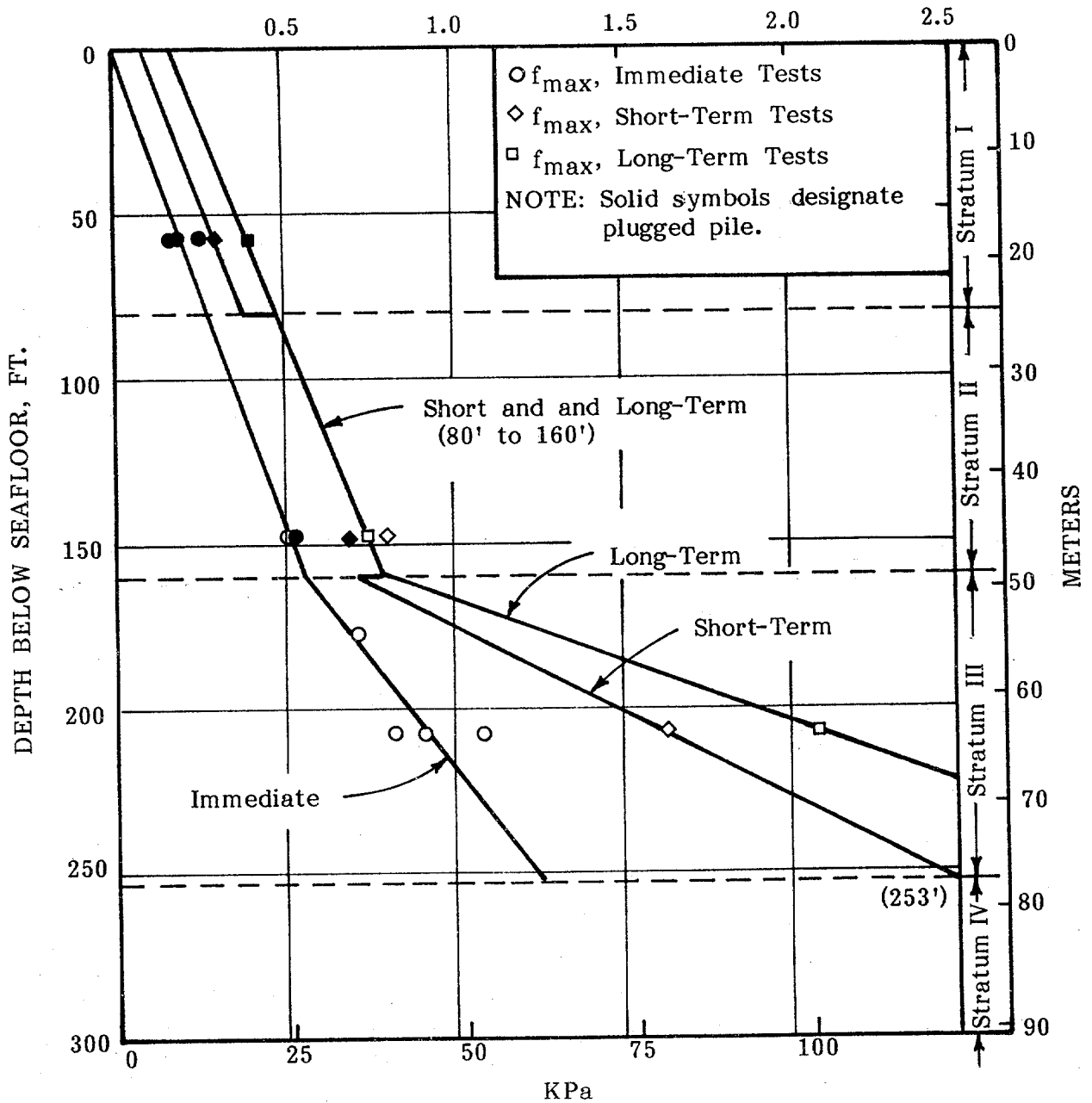
K_0 VERSUS PENETRATION
BLOCK 58, WEST DELTA AREA
GULF OF MEXICO

UNDRAINED SHEAR STRENGTH, KSF



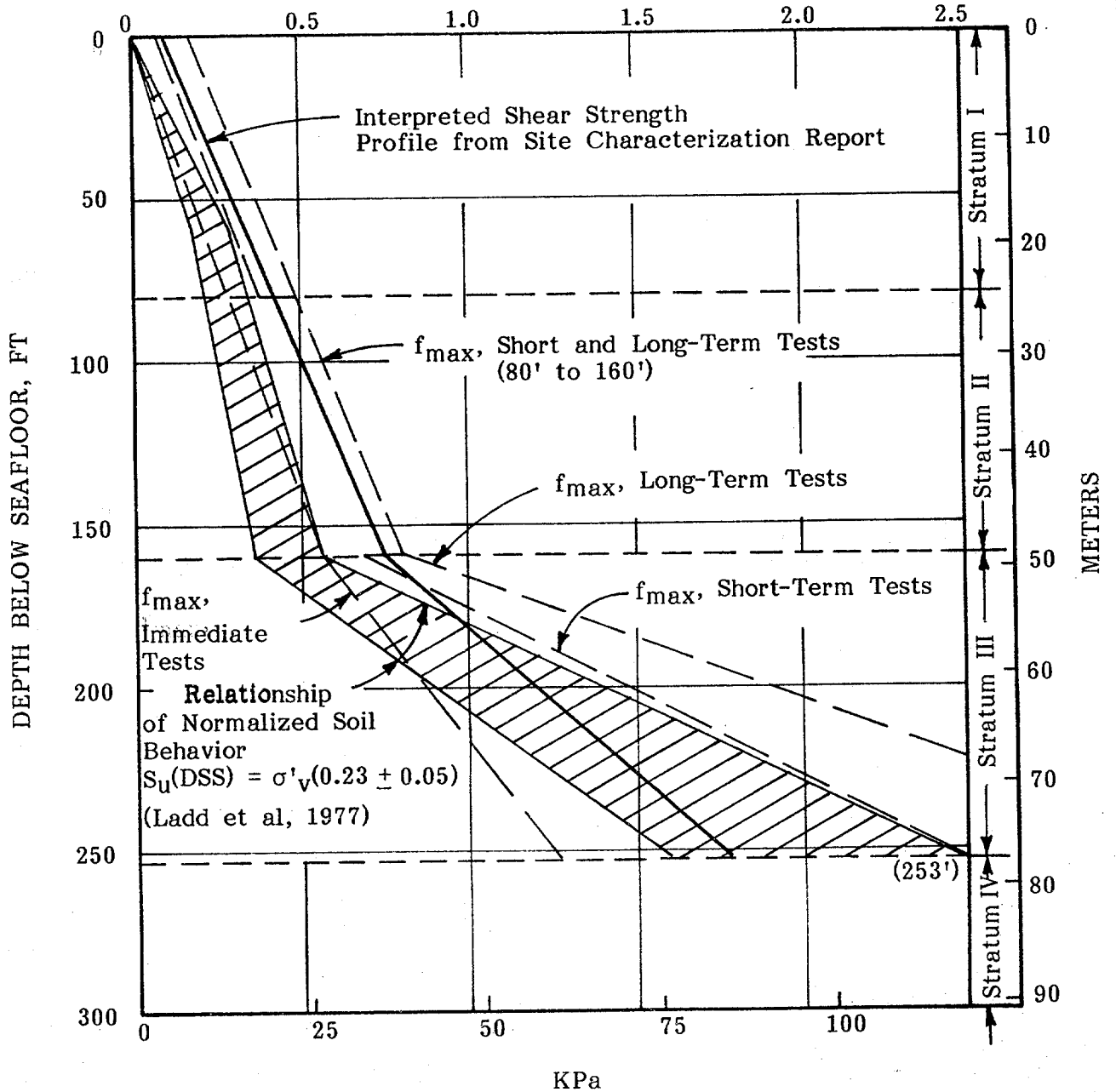
REVISED ESTIMATES FOR
UNDRAINED SHEAR STRENGTH

PEAK FRICTION, f_{max} , KSF



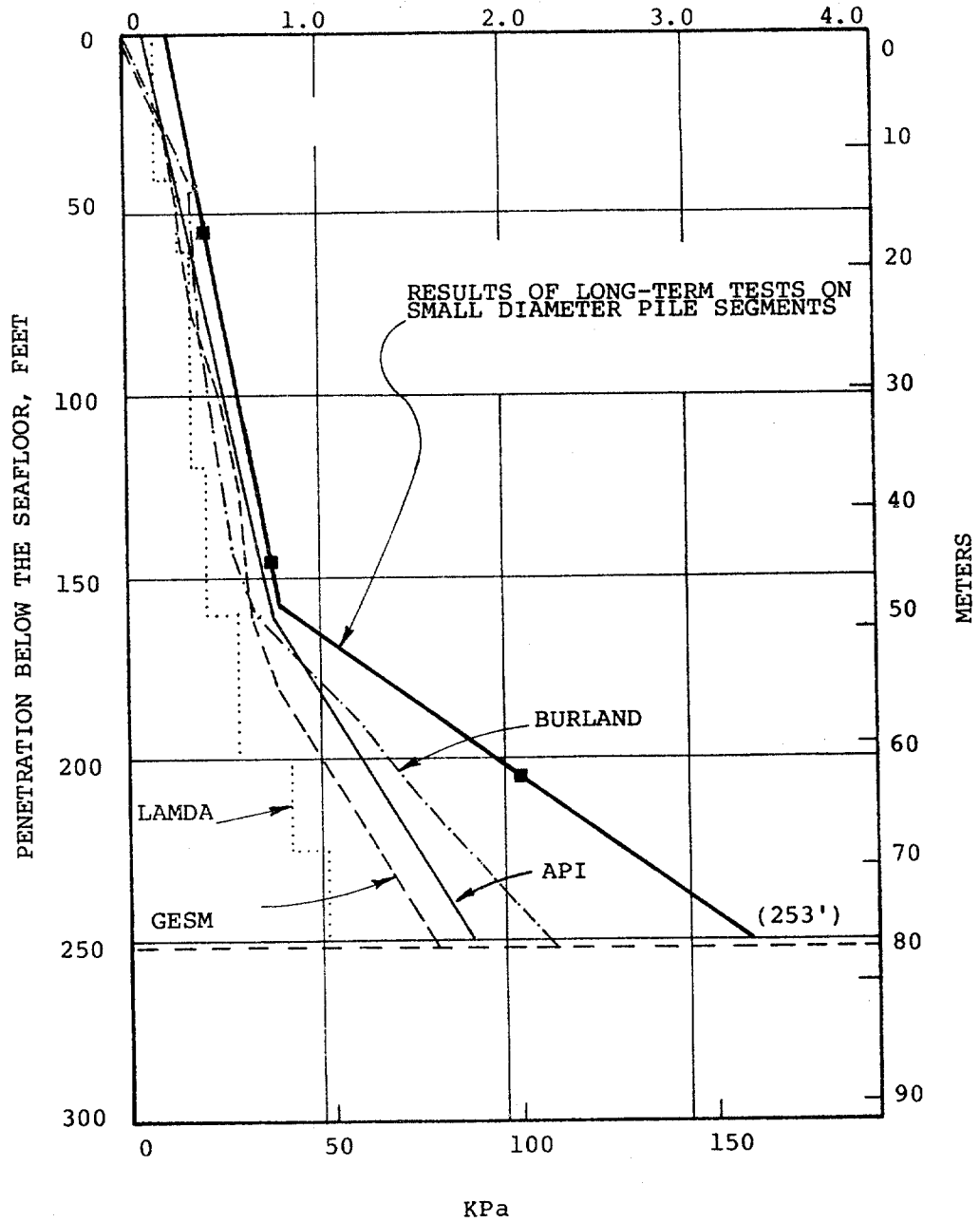
PEAK FRICTION (f_{max}) VERSUS DEPTH
FOR TYPE I TESTS

UNDRAINED SHEAR STRENGTH (S_u) OR PEAK FRICTION (f_{max}), KSF



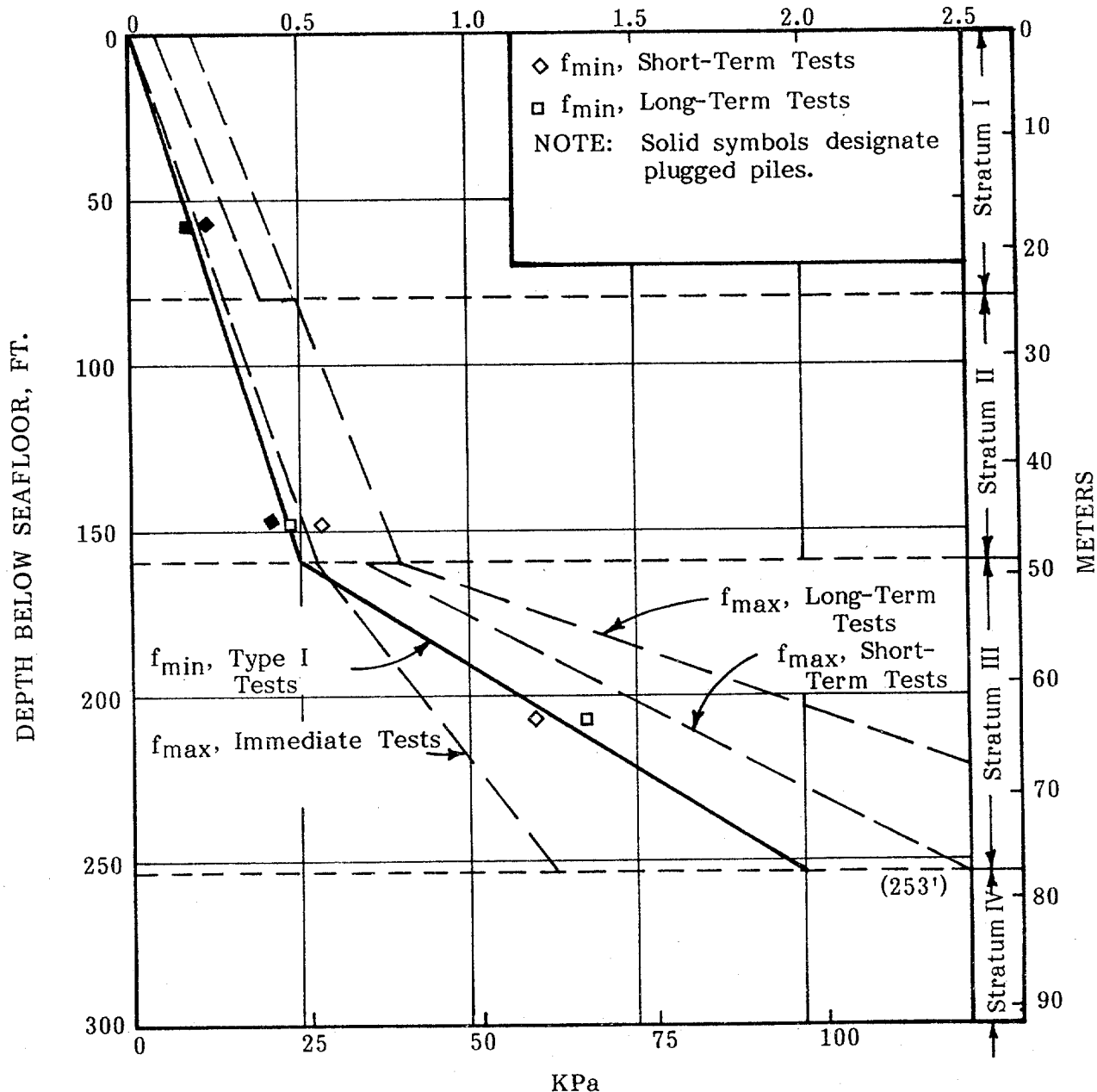
COMPARISON OF ESTIMATED UNDRAINED SHEAR STRENGTH TO PEAK FRICTION FROM TYPE I TESTS

UNIT SKIN FRICTION, KIPS PER SQ. FT.



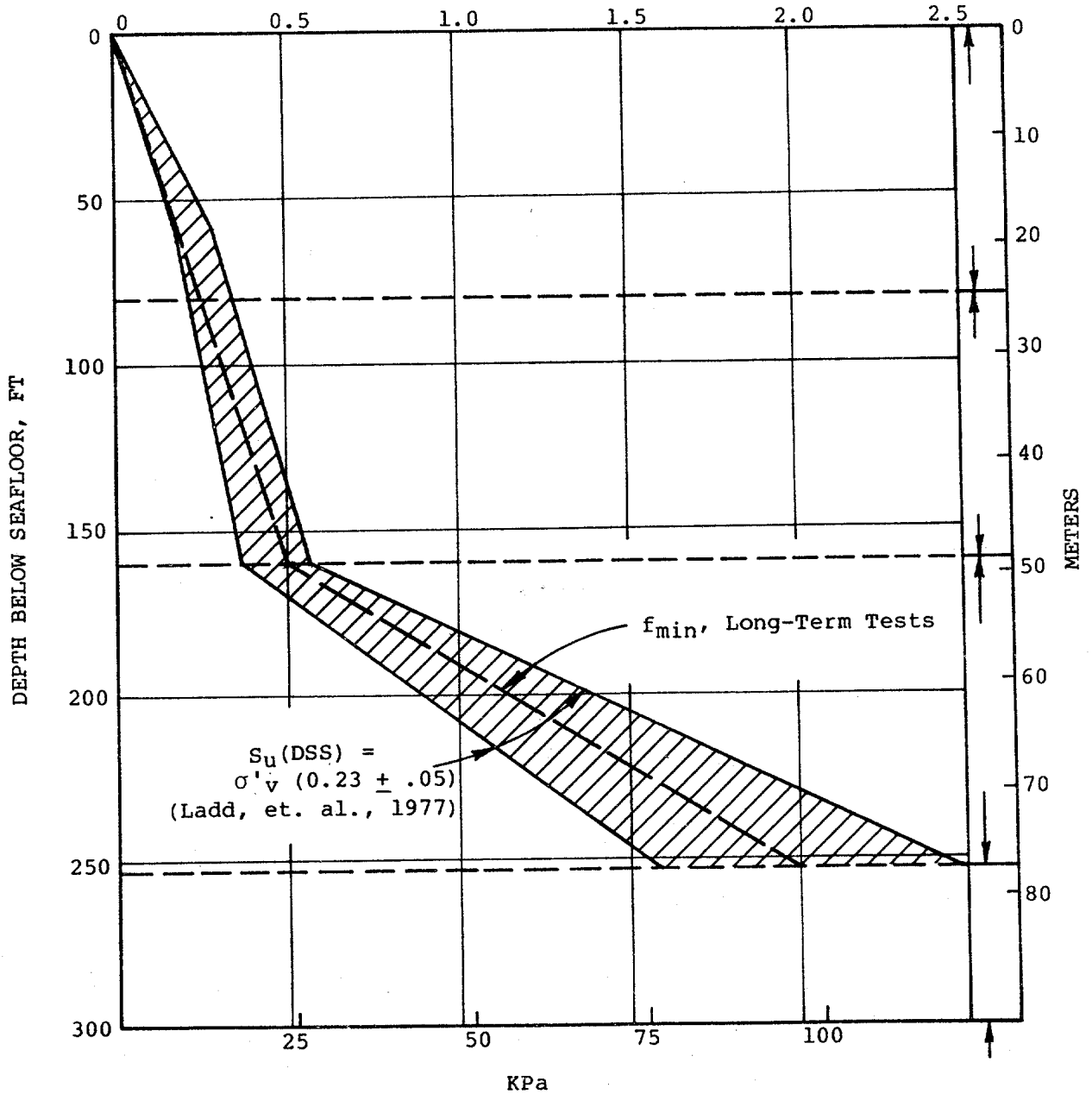
COMPARISON OF LONG-TERM TEST RESULTS AND ANALYTICAL PILE CAPACITY PREDICTIONS

PILE FRICTION, KSF



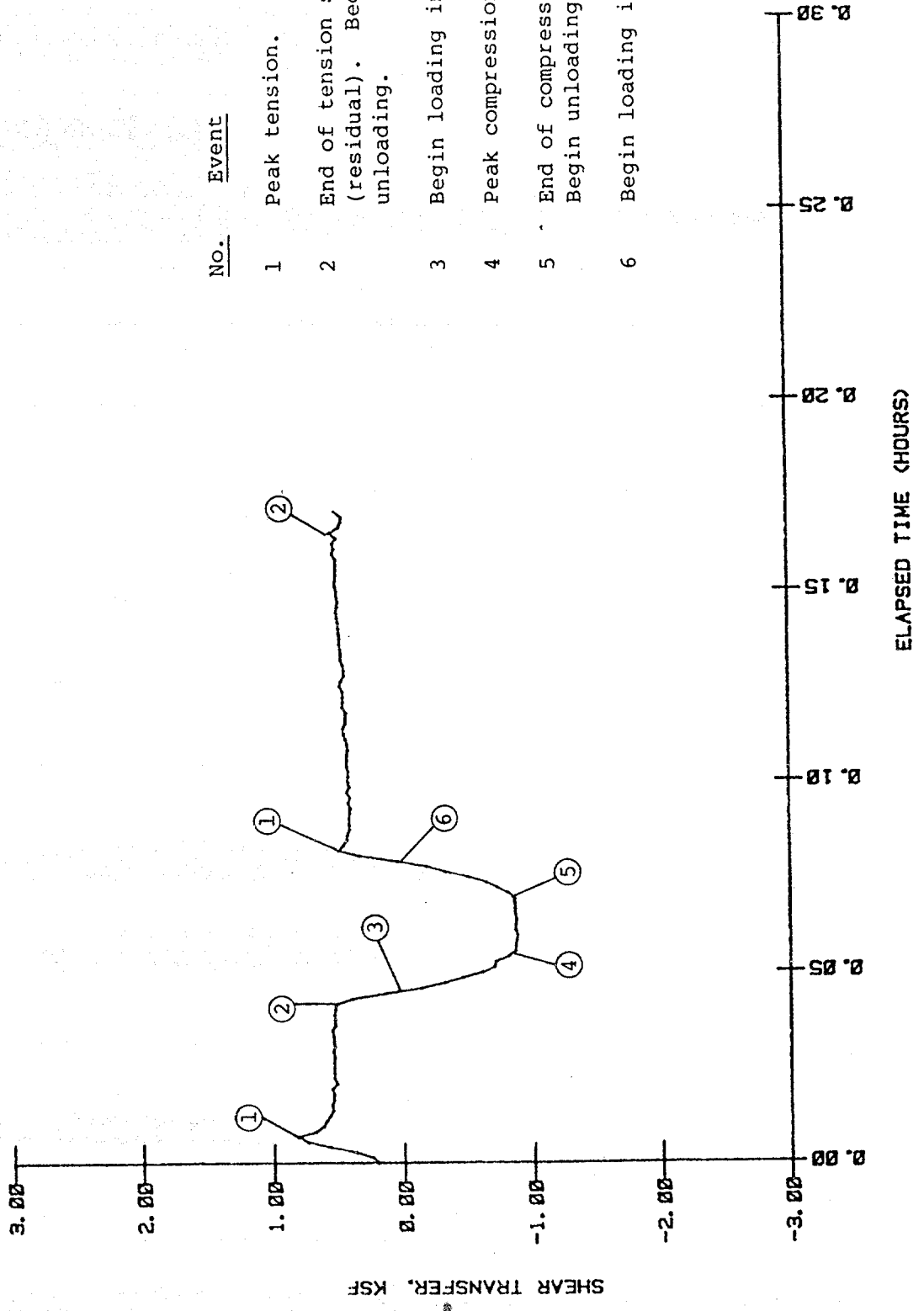
COMPARISON OF MINIMUM AND MAXIMUM FRICTION, TYPE I TESTS

UNDRAINED SHEAR STRENGTH (S_u) OR MINIMUM FRICTION (f_{min}), KSF

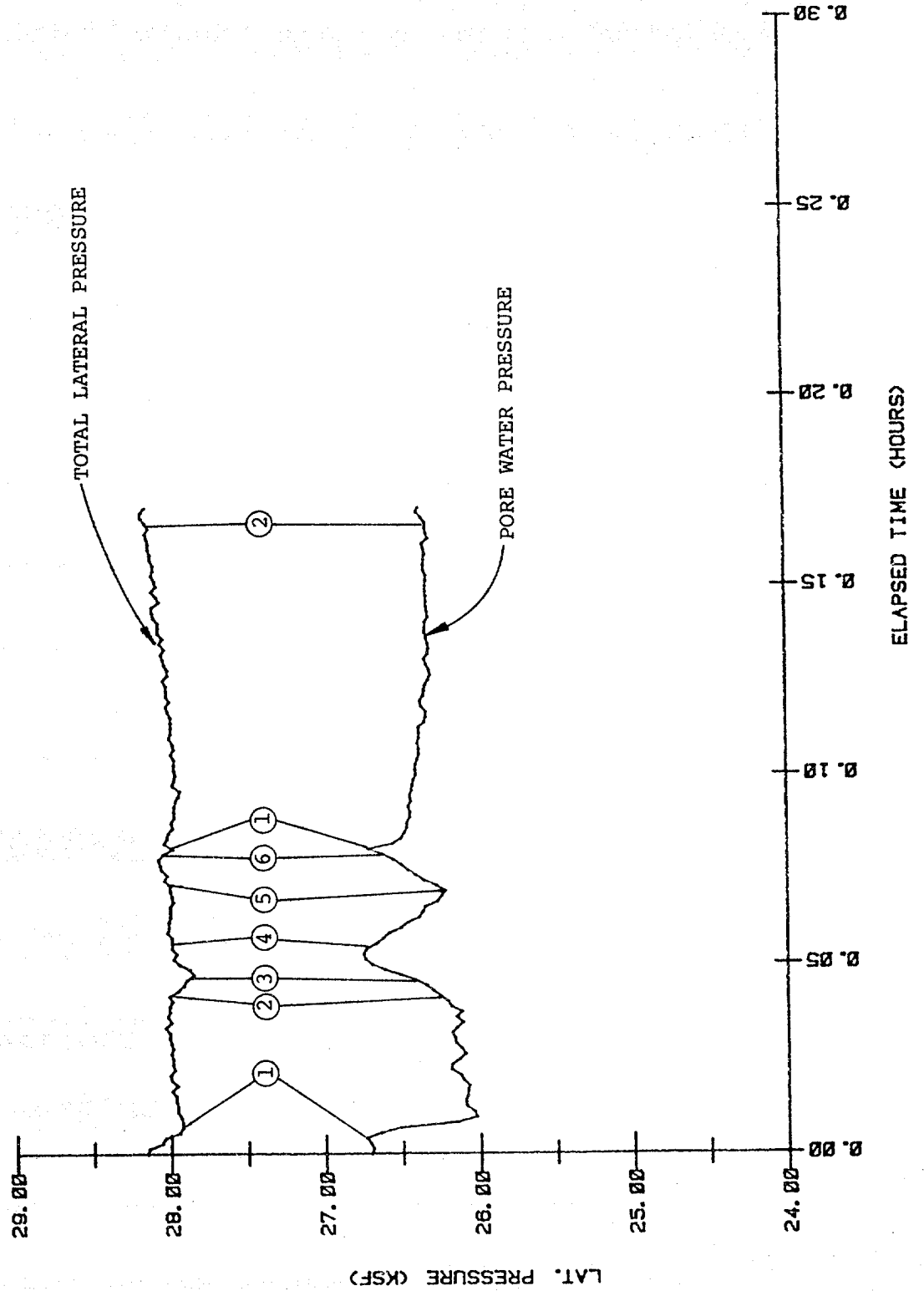


COMPARISON OF MINIMUM (DEGRADED) FRICTION TO UNDRAINED SHEAR STRENGTH ESTIMATED USING SHANSEP PROCEDURES

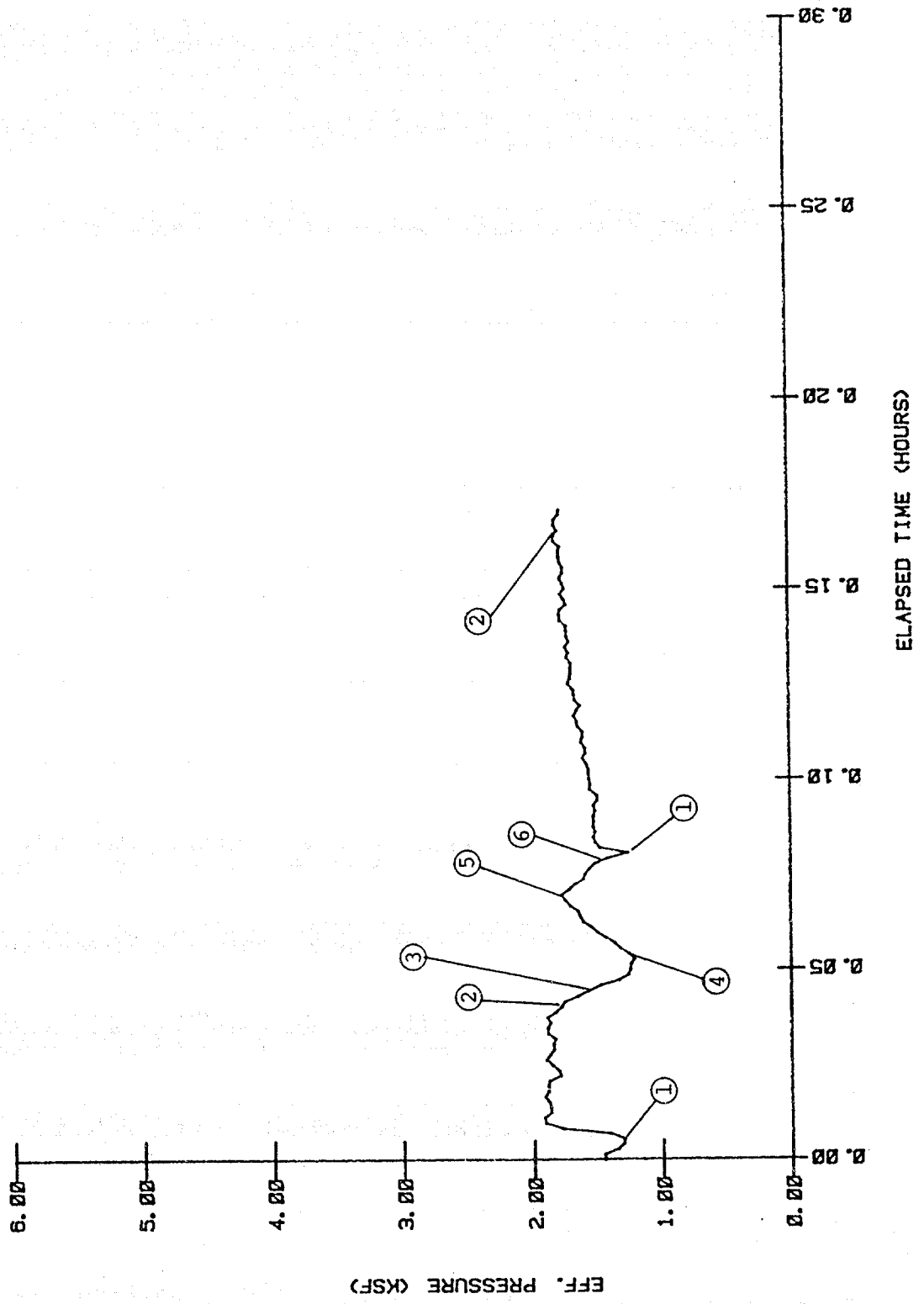
SHEAR DURING TEST
 WEST DELTA BLOCK 58A
 HOLE 1 AT 208 FT (I)



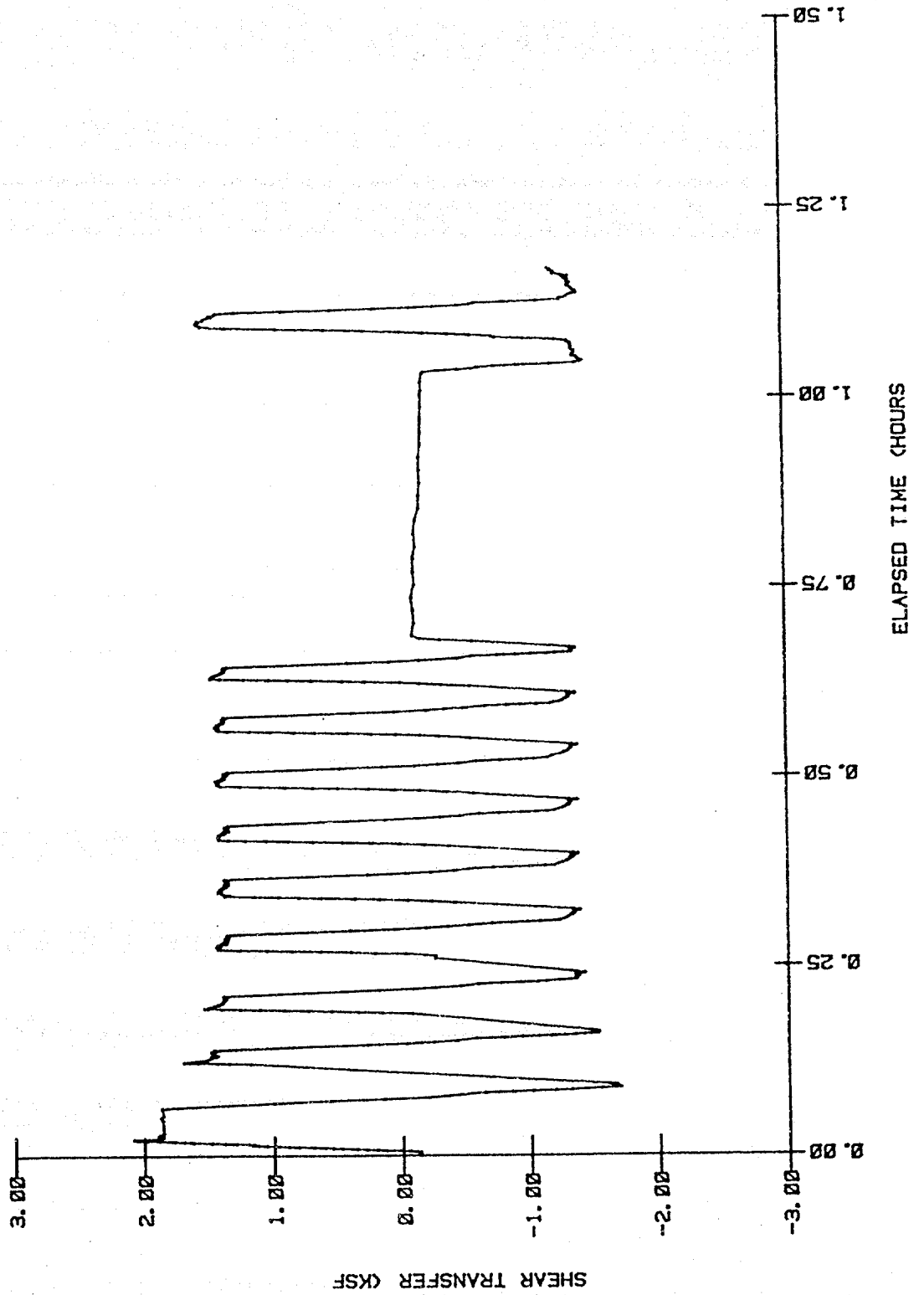
PRESSURE DURING TEST
WEST DELTA BLOCK 58A
HOLE 1 AT 208 FT (I)



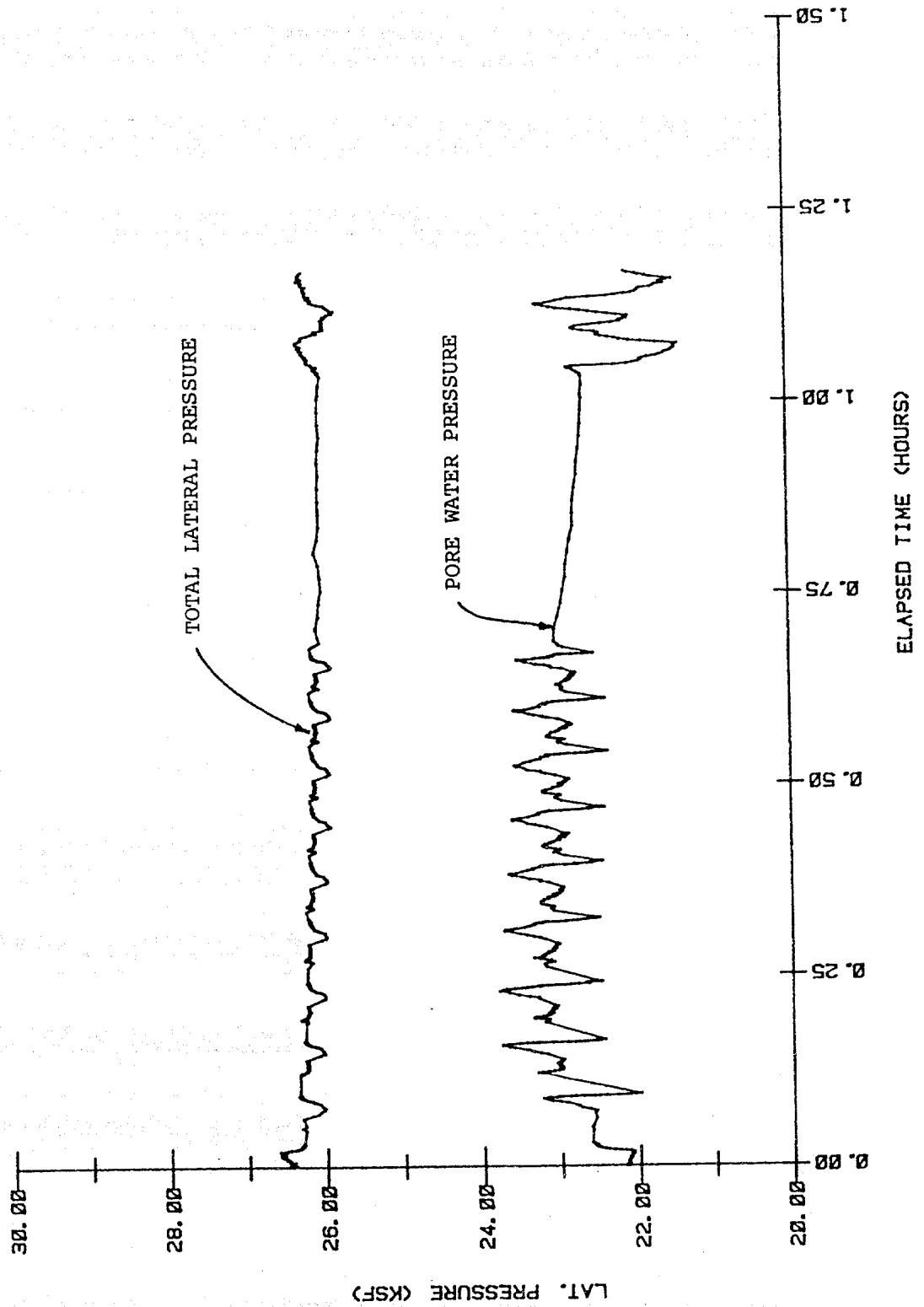
PRESSURE DURING TEST
WEST DELTA BLOCK 58A
HOLE 1 AT 208 FT (I)



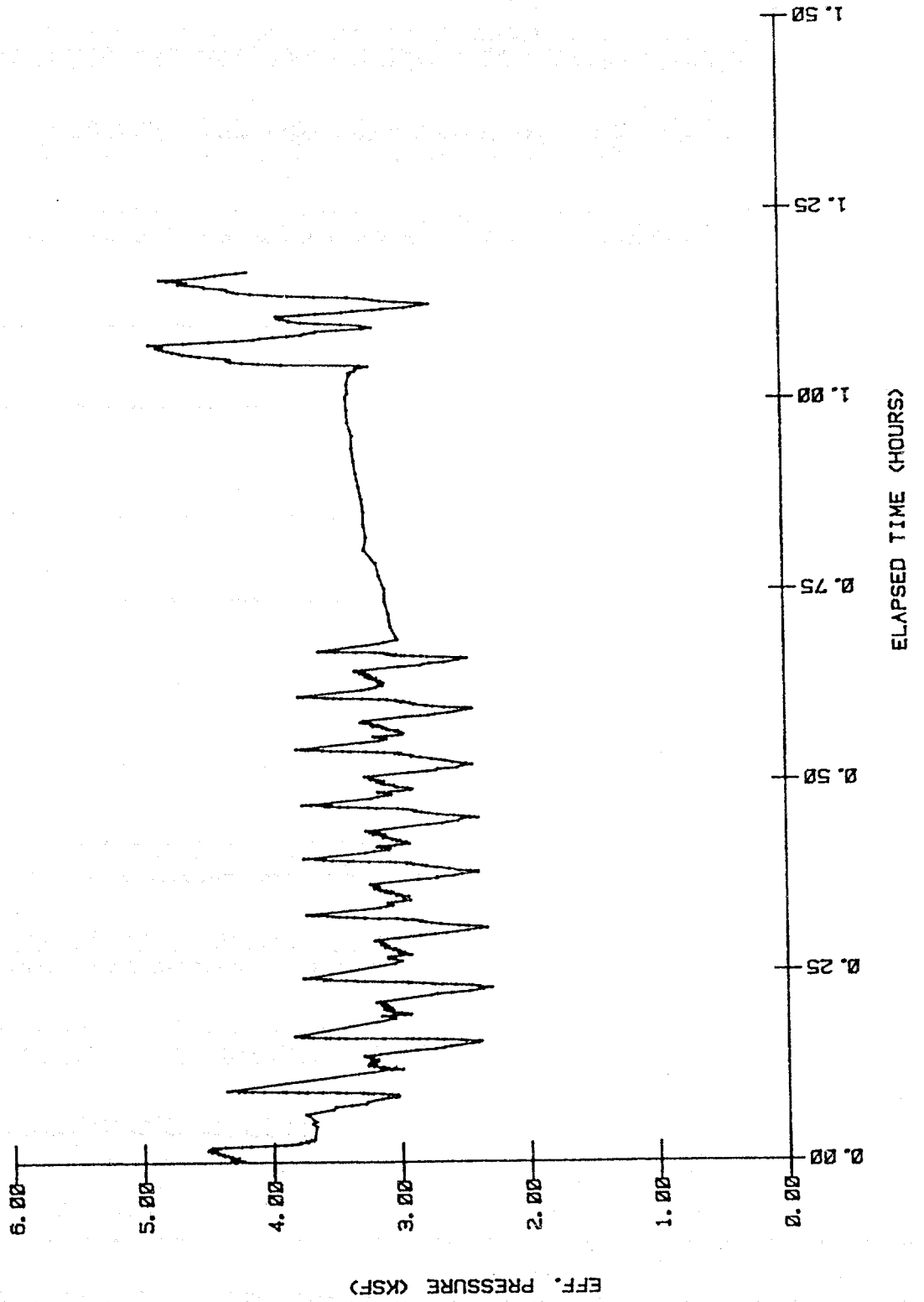
SHEAR DURING TEST
WEST DELTA BLOCK 58A
HOLE 1 AT 208 FEET



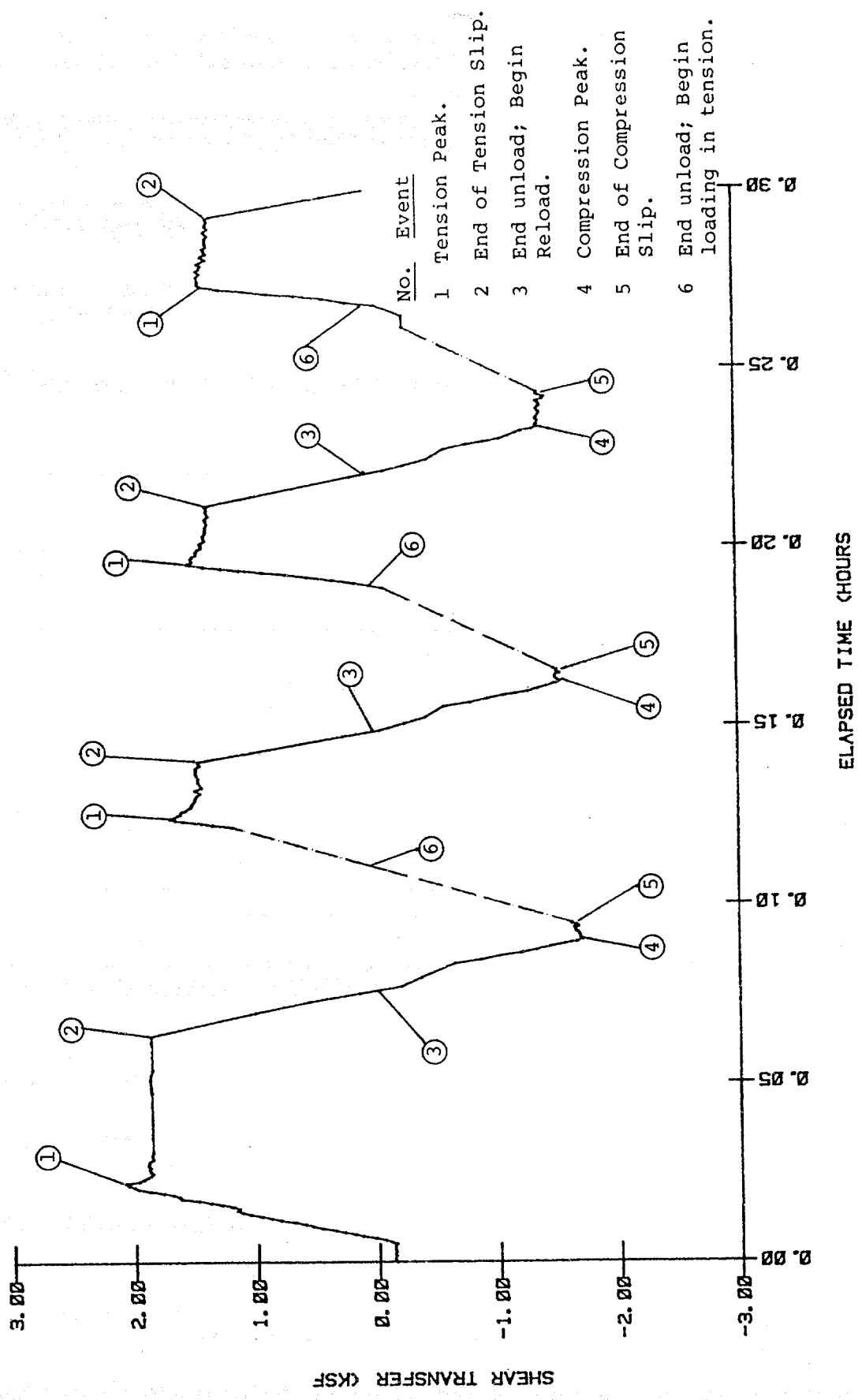
PRESSURE DURING TEST
WEST DELTA BLOCK 58A
HOLE 1 AT 208 FT



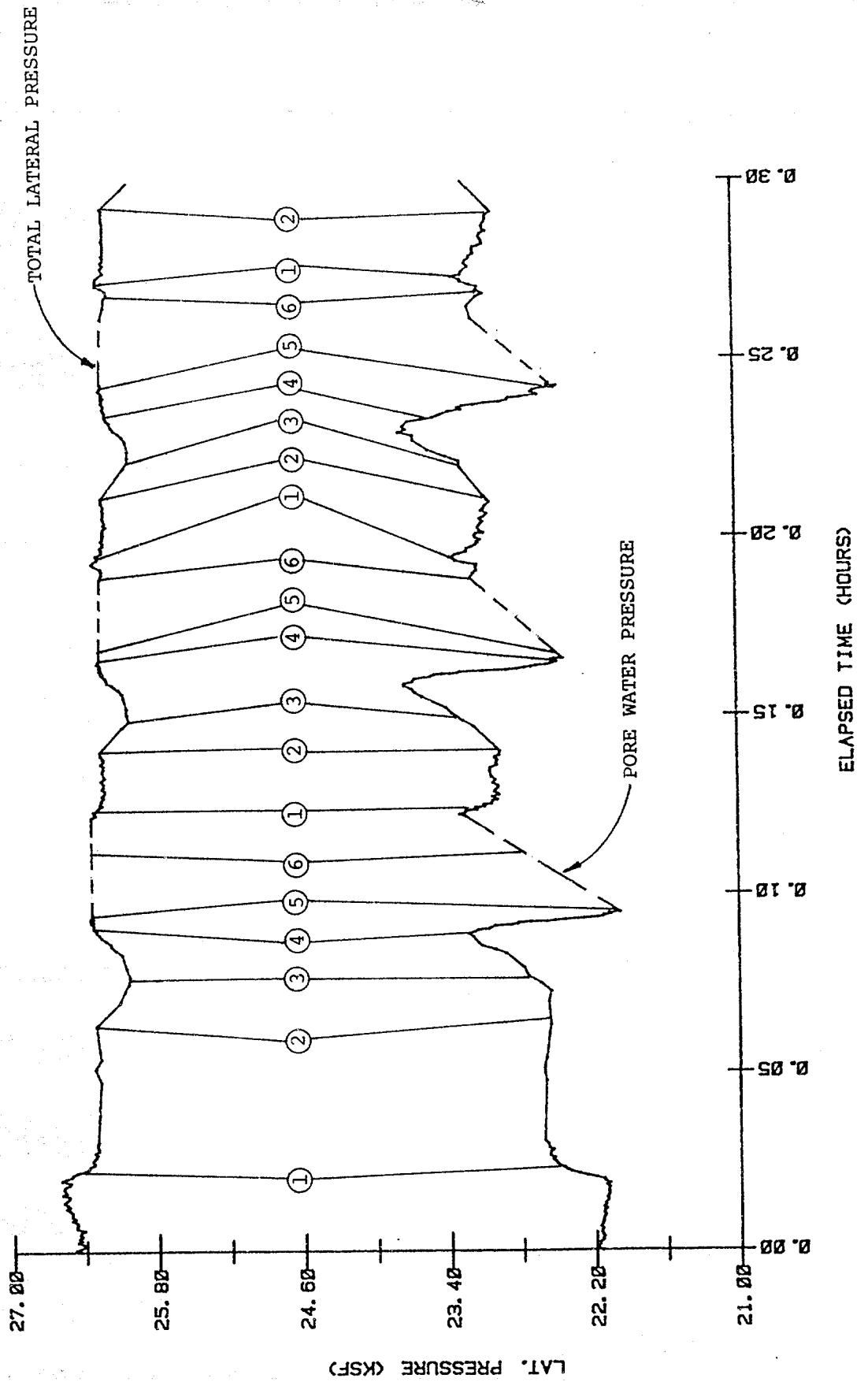
PRESSURE DURING TEST
WEST DELTA BLOCK 58A
HOLE 1 AT 208 FT



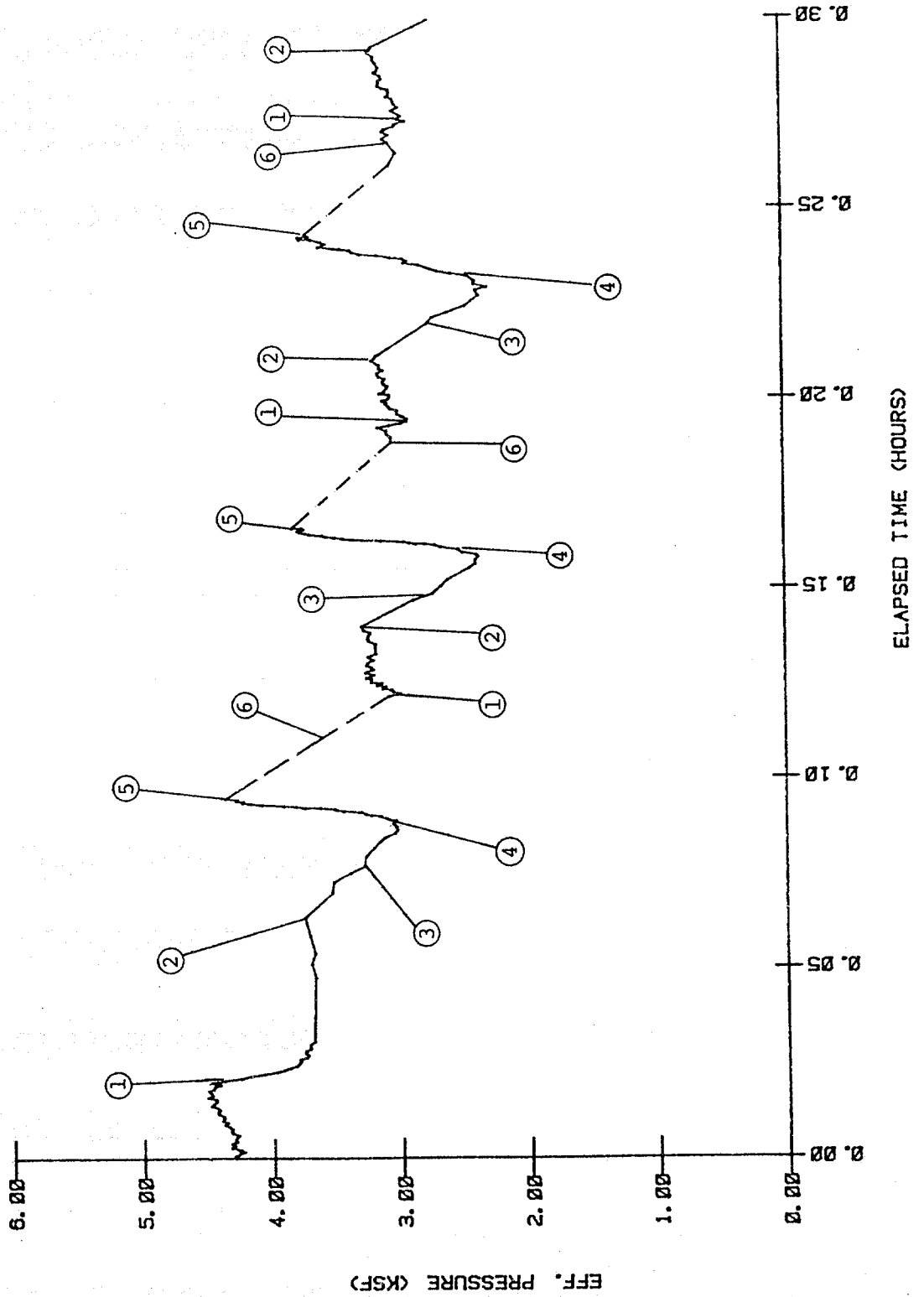
SHEAR DURING TEST
WEST DELTA BLOCK 58A
HOLE 1 AT 208 FEET



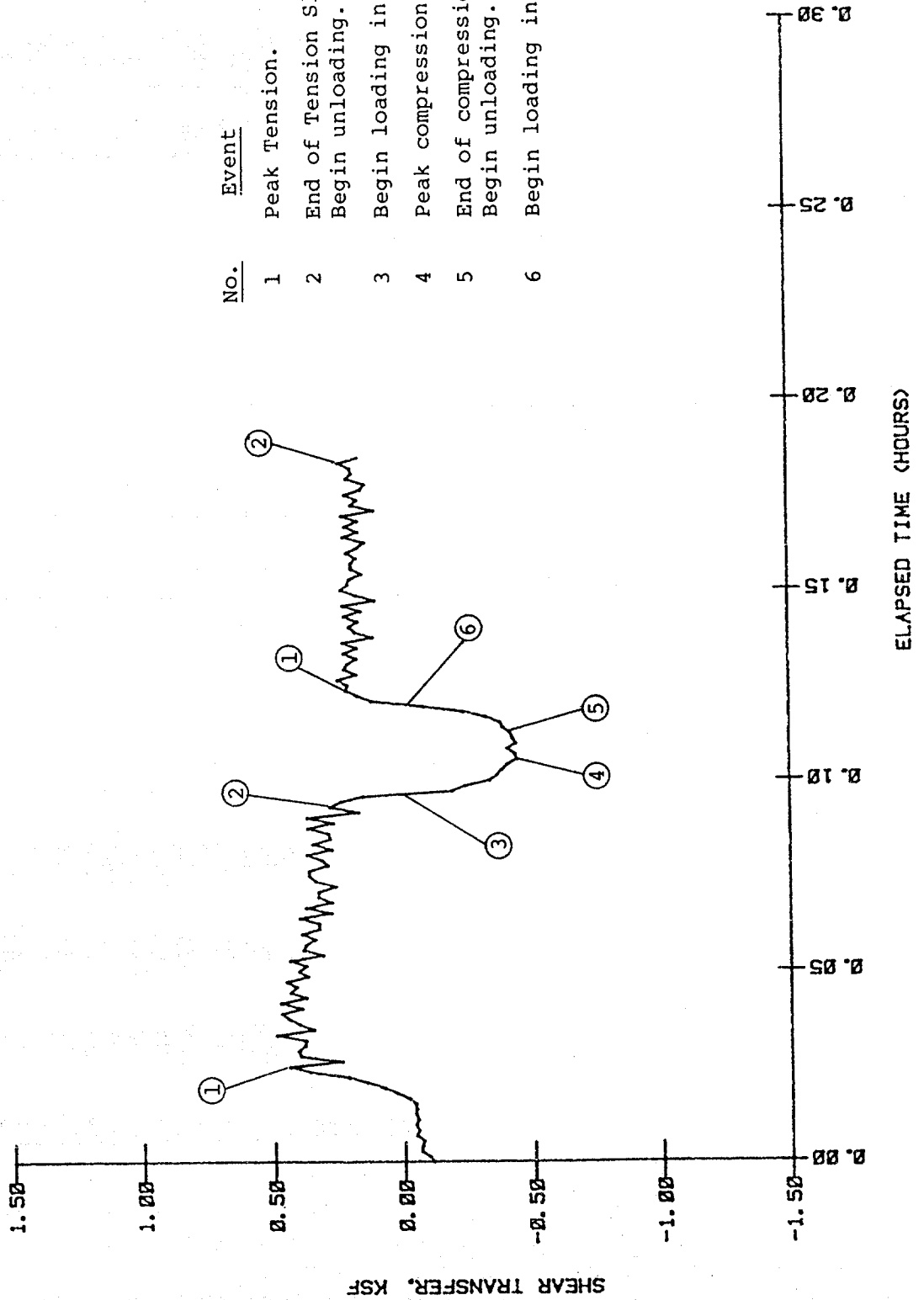
PRESSURE DURING TEST
 WEST DELTA BLOCK 58A
 HOLE 1 AT 208 FEET



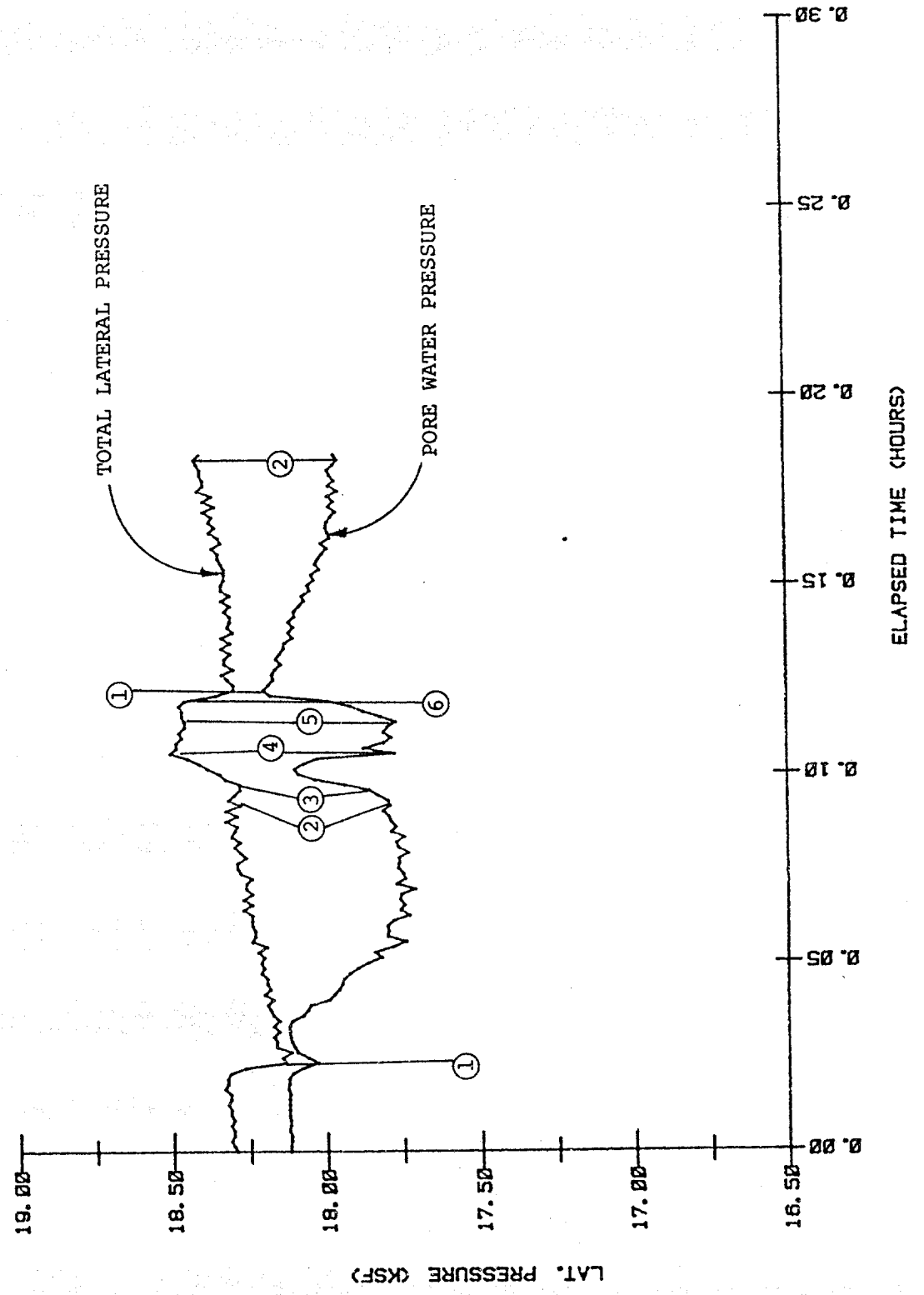
PRESSURE DURING TEST
WEST DELTA BLOCK 58A
HOLE 1 AT 208 FEET



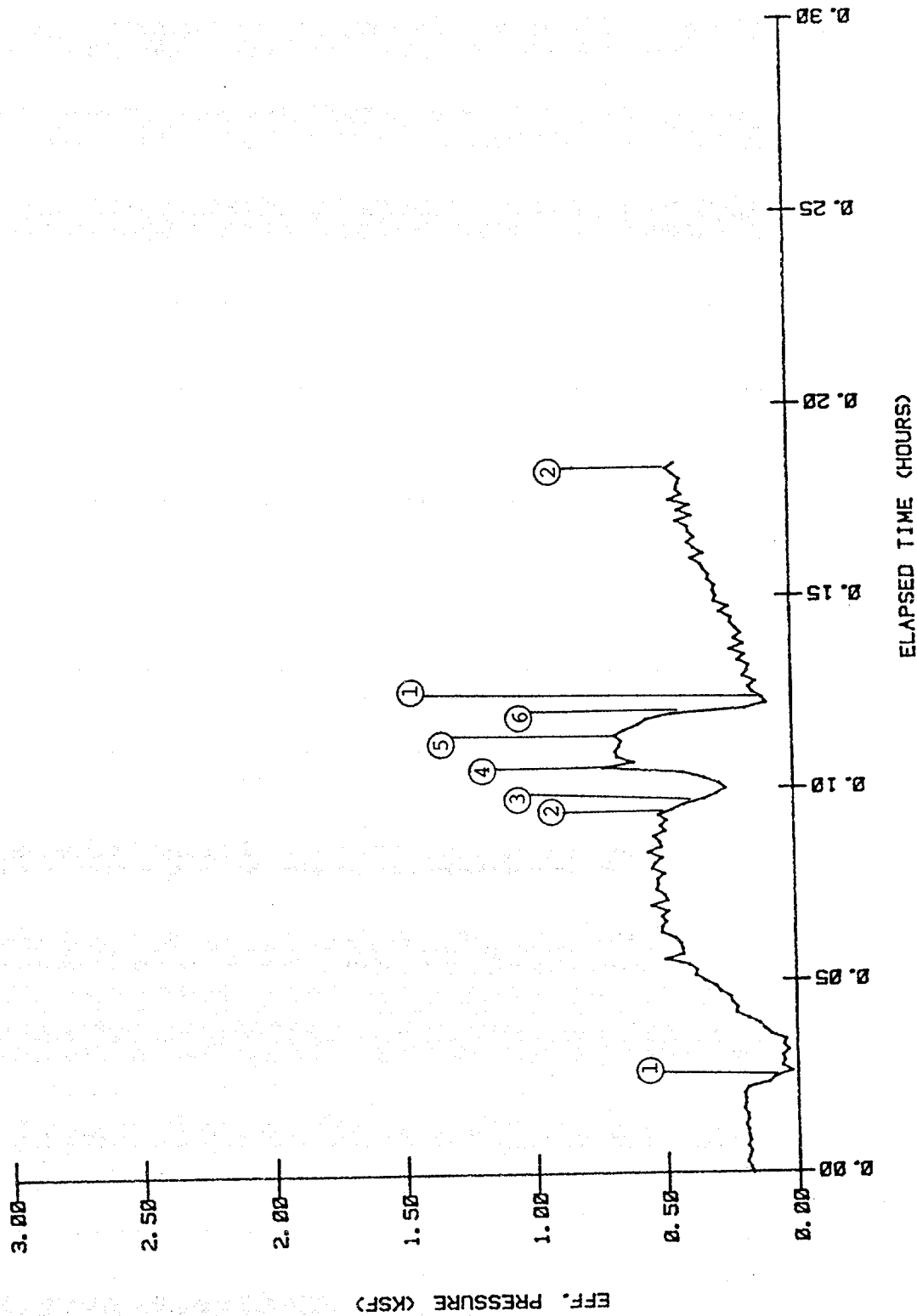
SHEAR DURING TEST
 WEST DELTA BLOCK 58A
 HOLE 1 AT 148 FEET (I)



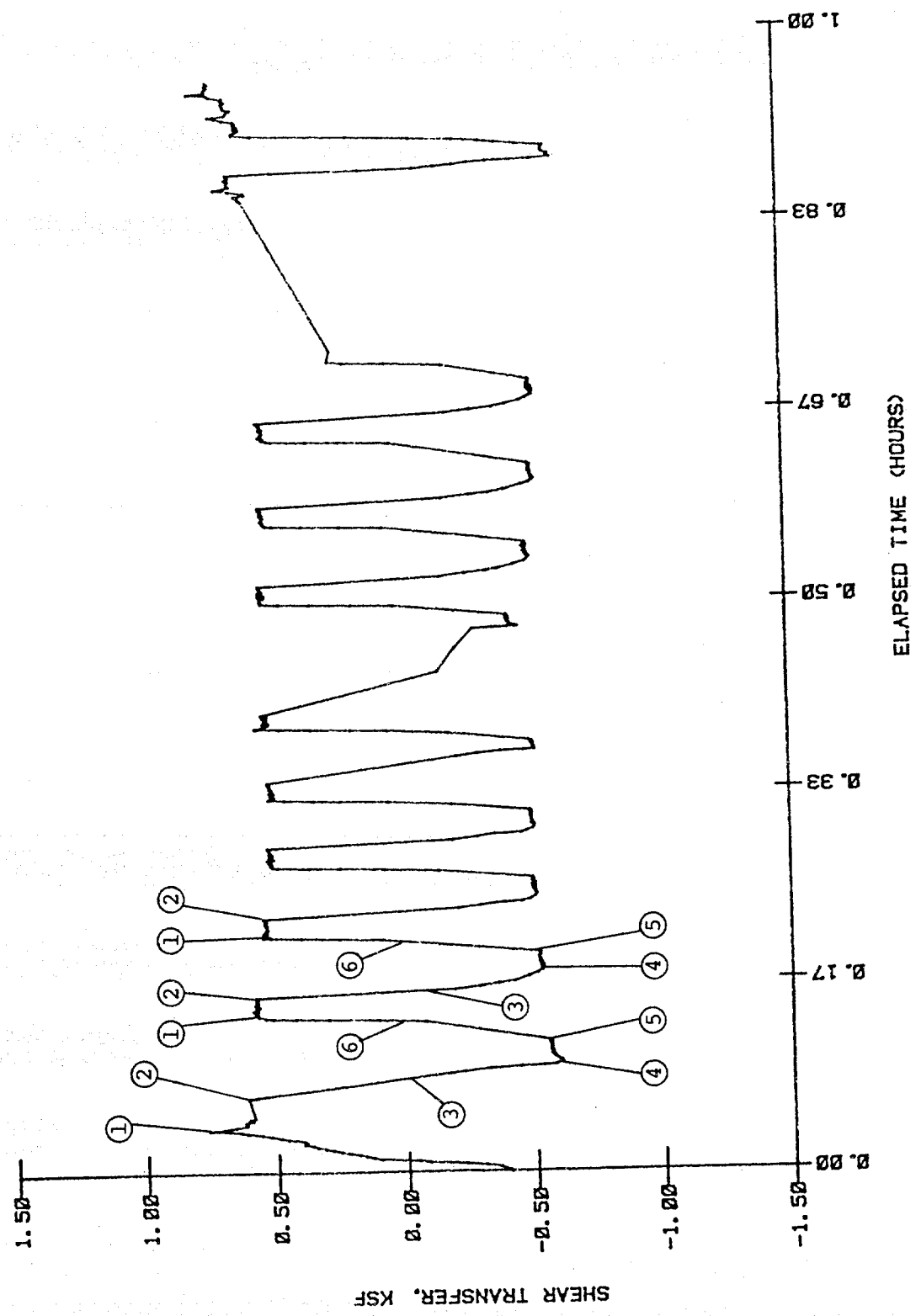
PRESSURE DURING TEST
WEST DELTA BLOCK 58A
HOLE 1 AT 148 FT (I)



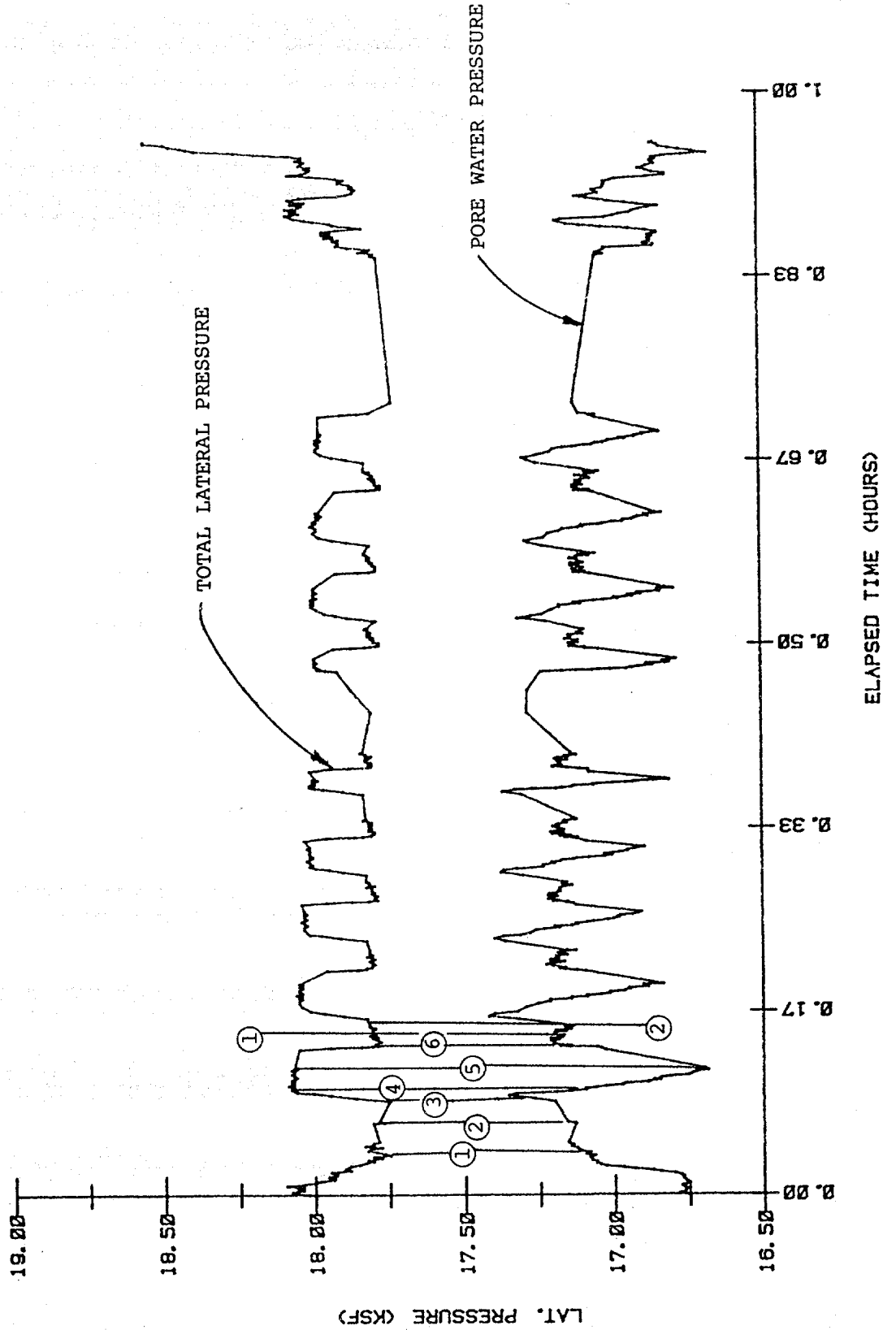
PRESSURE DURING TEST
WEST DELTA BLOCK 58A
HOLE 1 AT 148 FT (I)



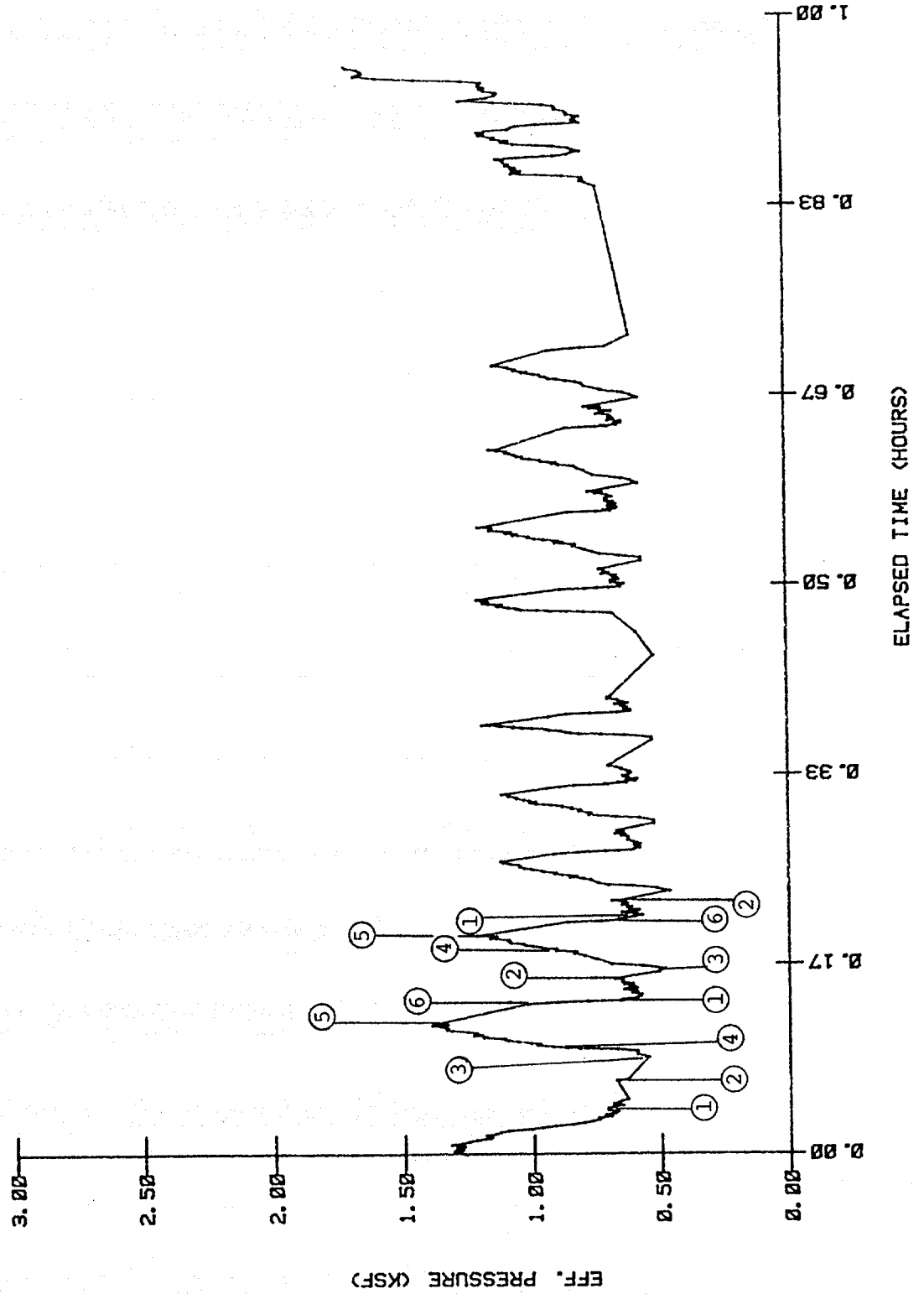
SHEAR DURING TEST
 WEST DELTA BLOCK 58A
 HOLE 1 AT 148 FEET



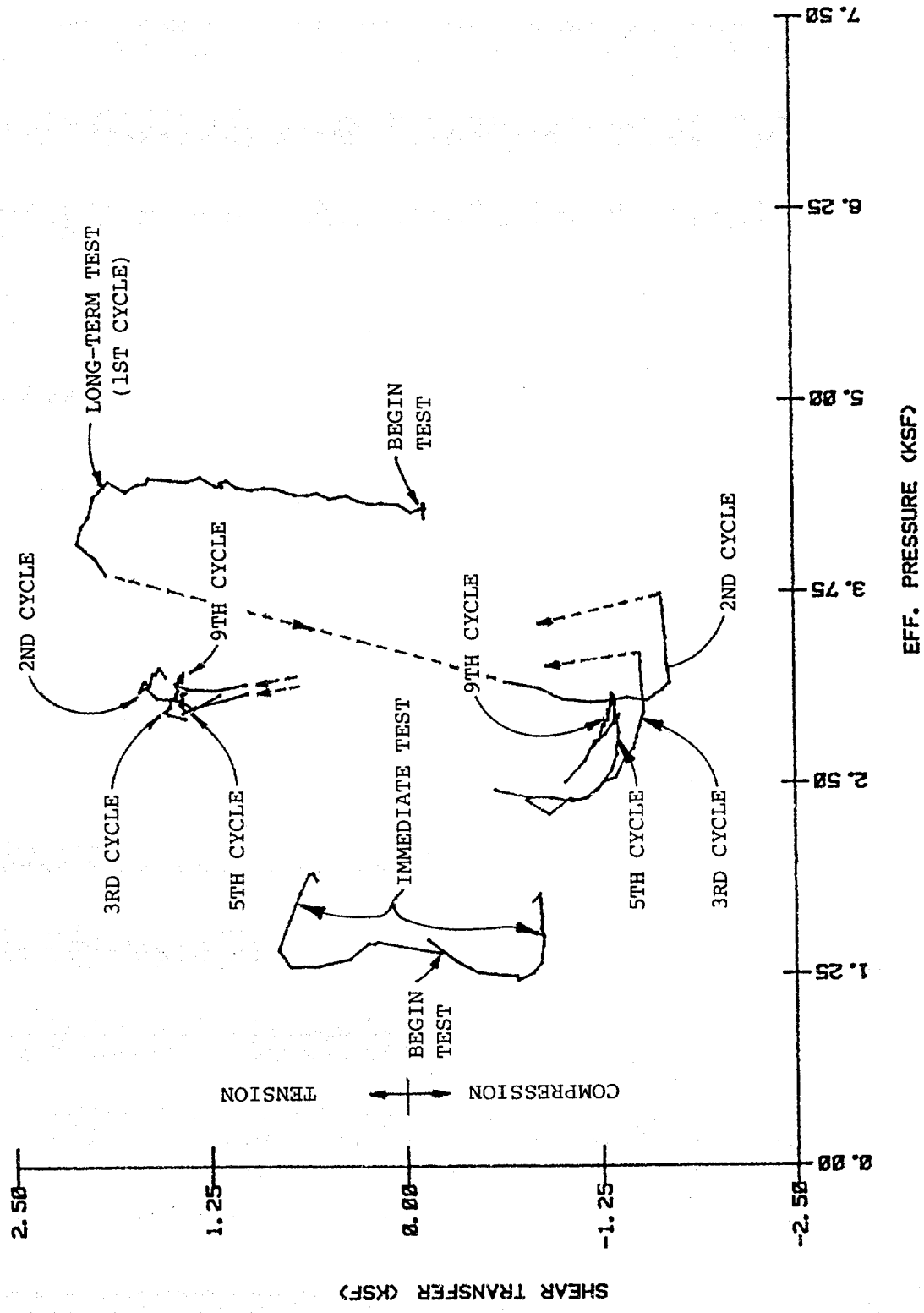
PRESSURE DURING TEST
WEST DELTA BLOCK 58A
HOLE 1 AT 148 FEET



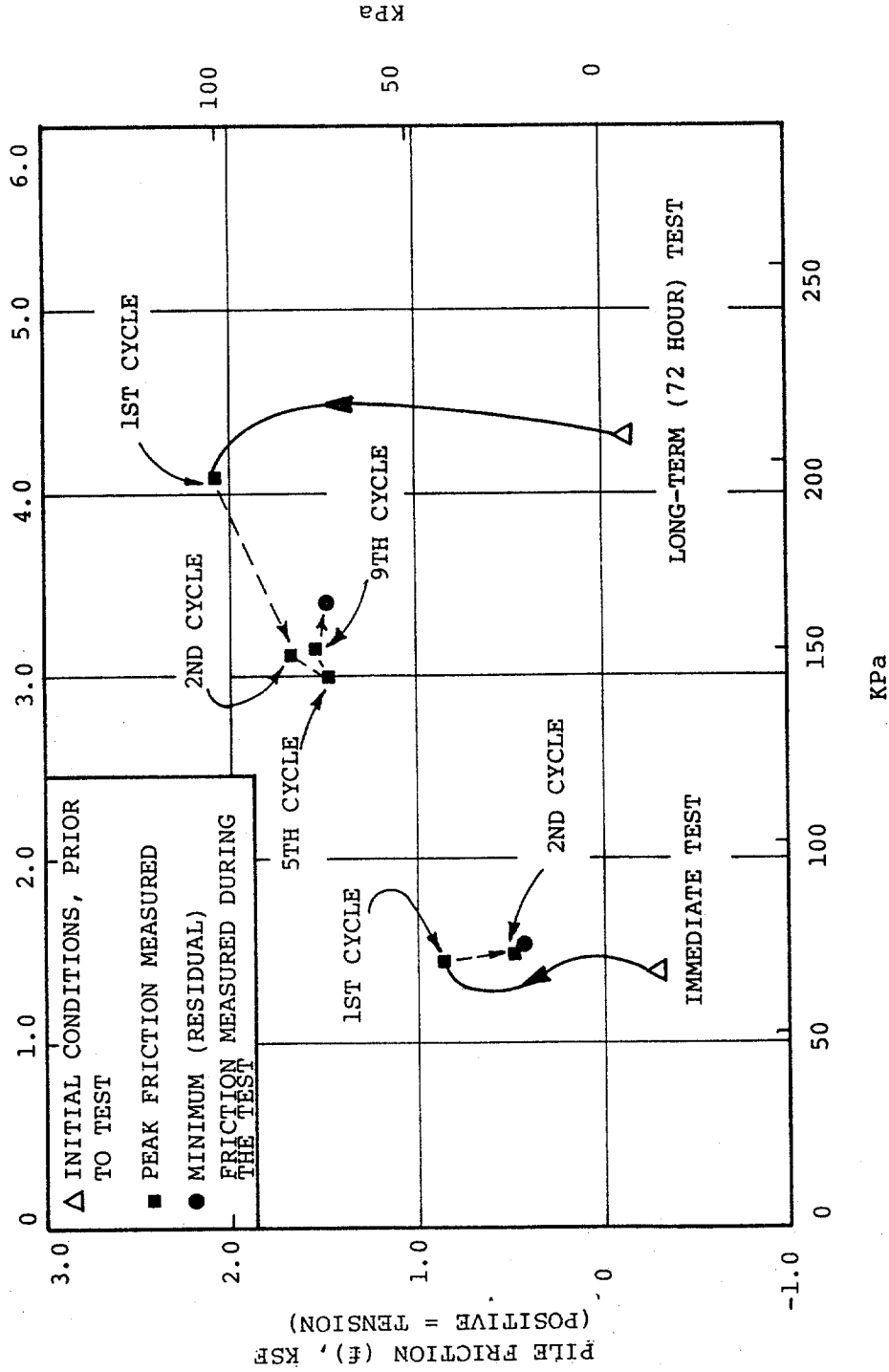
PRESSURE DURING TEST
 WEST DELTA BLOCK 58A
 HOLE 1 AT 148 FEET



STRESS PATHS
 208 FT. DEPTH
 WEST DELTA BLK 58A

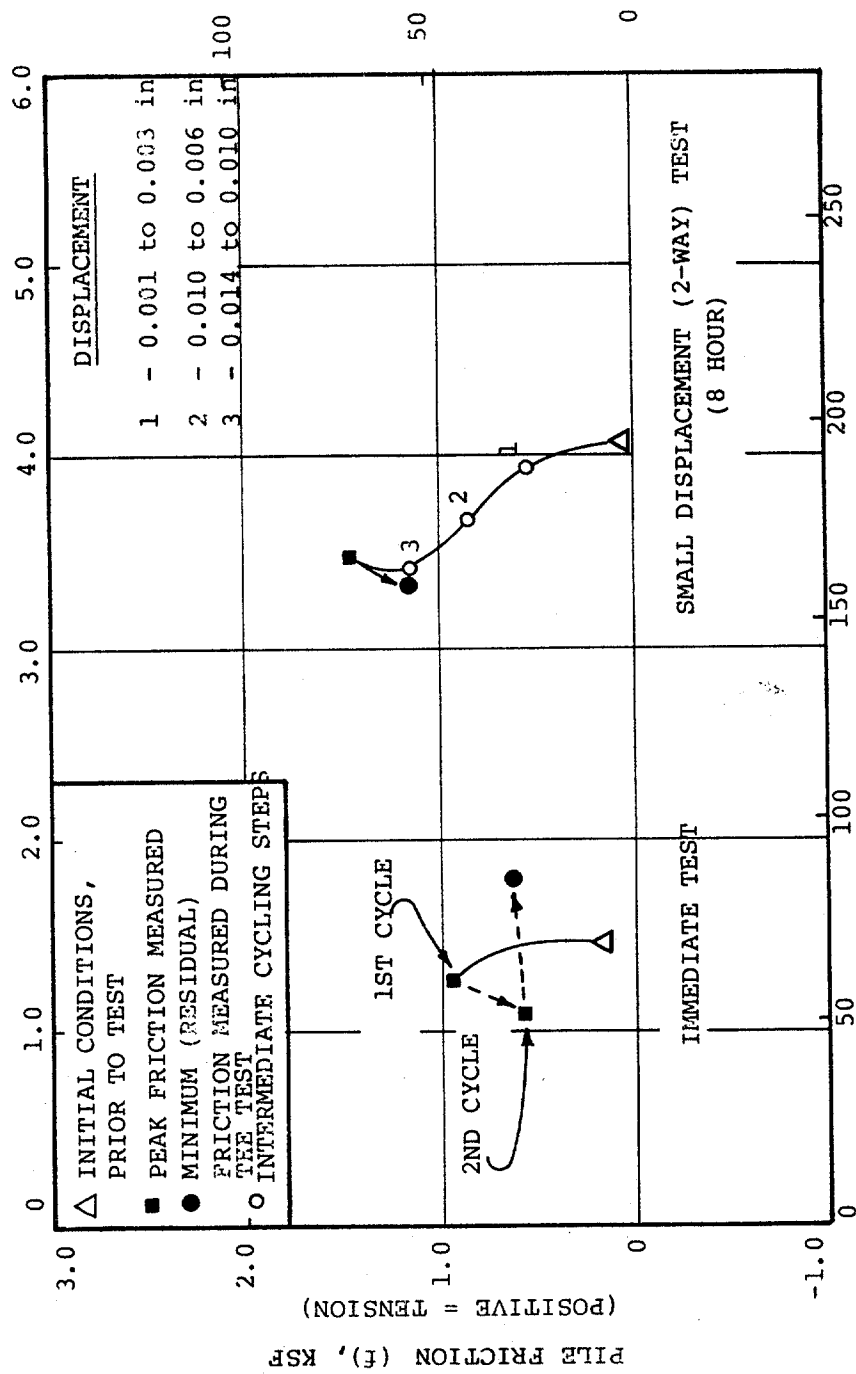


RADIAL EFFECTIVE STRESS ($\sigma' r$), KSF



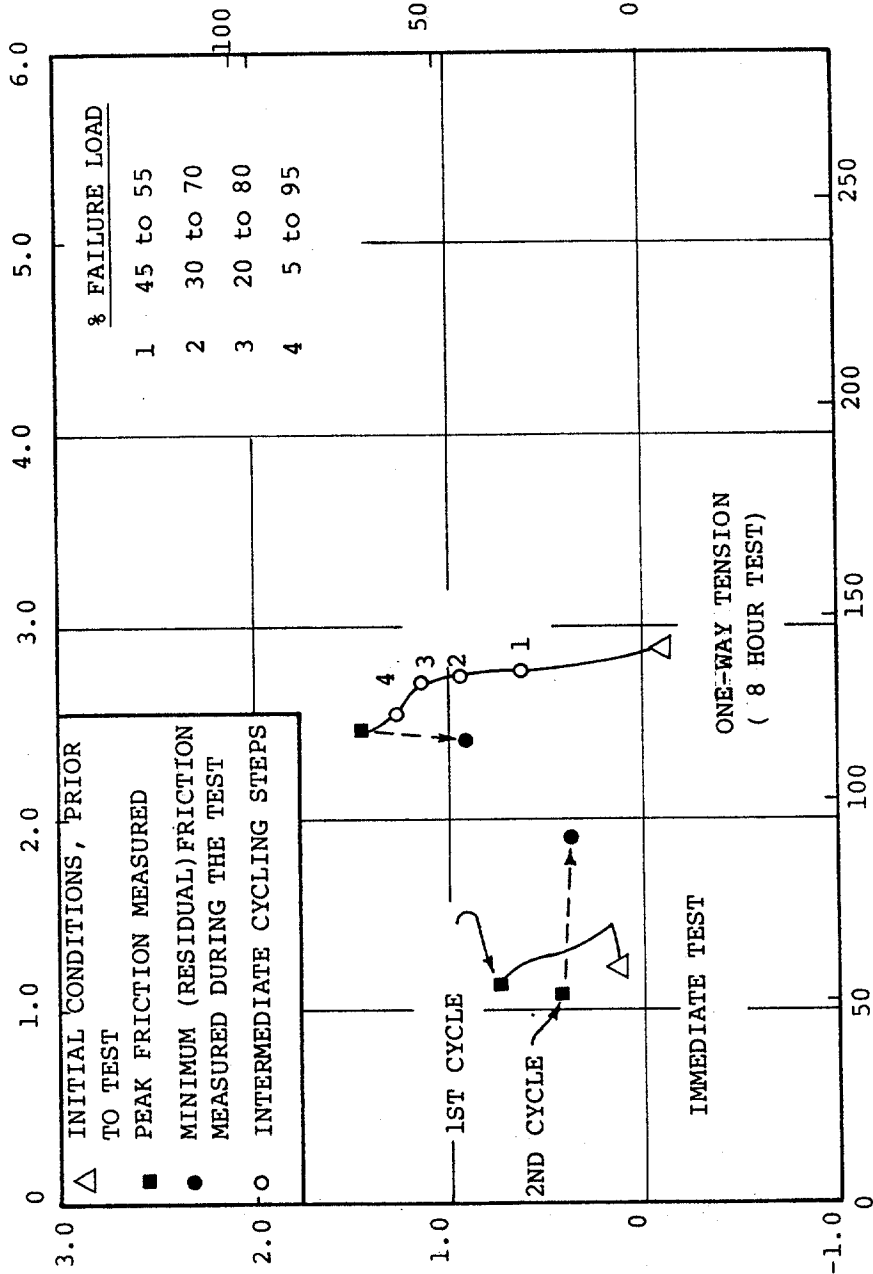
STRESS PATHS - HOLE 1, 63.4 M (208 FT)
IMMEDIATE TEST AND LONG-TERM (TYPE I) TEST

RADIAL EFFECTIVE STRESS (σ'_r), KSF



STRESS PATHS - HOLE 3, 63.4 M (208 FT)
 IMMEDIATE TEST AND SHORT-TERM SMALL-DISPLACEMENT (TYPE II) TEST

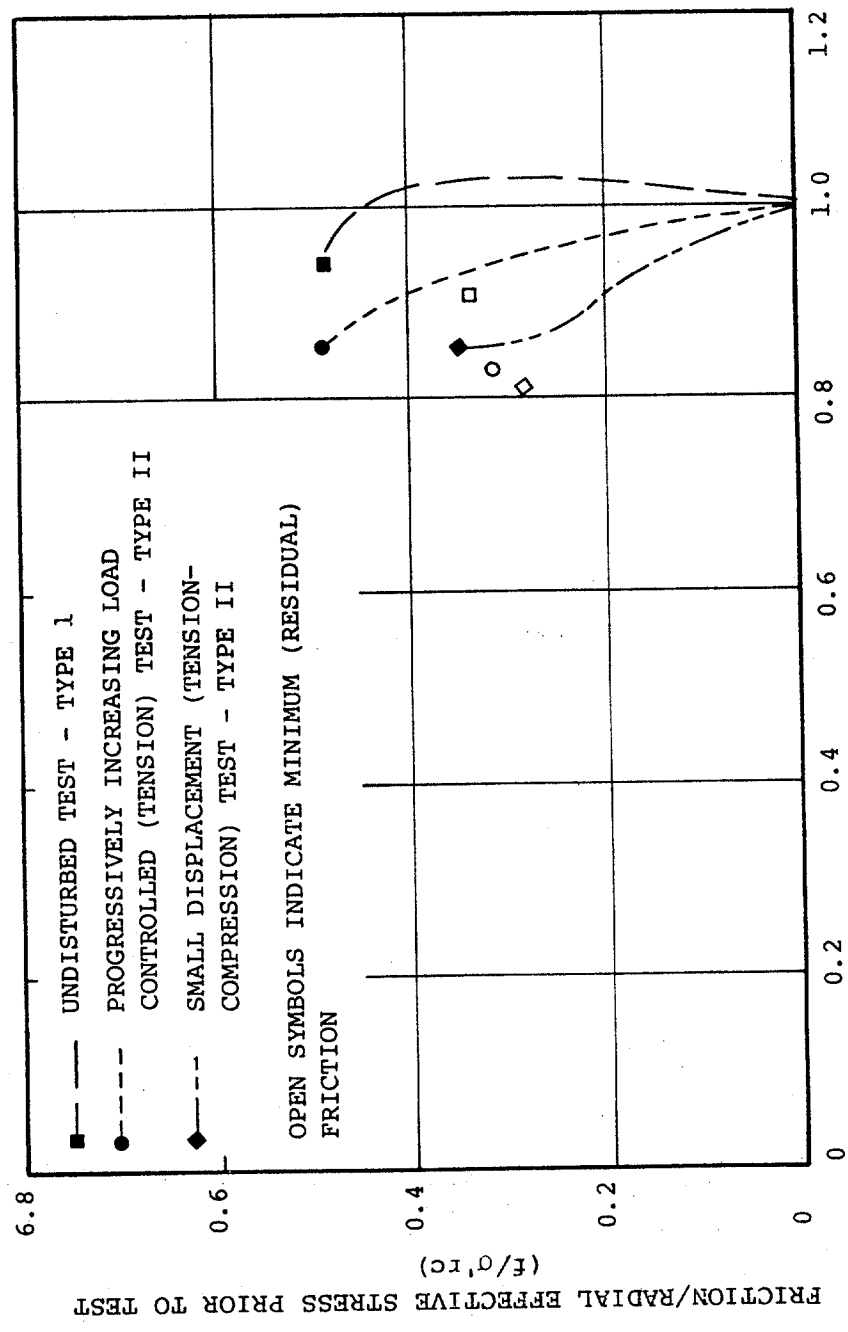
RADIAL EFFECTIVE STRESS (σ'_r), KSF



PILE FRICTION (f), KSF
(POSITIVE = TENSION)

KPa

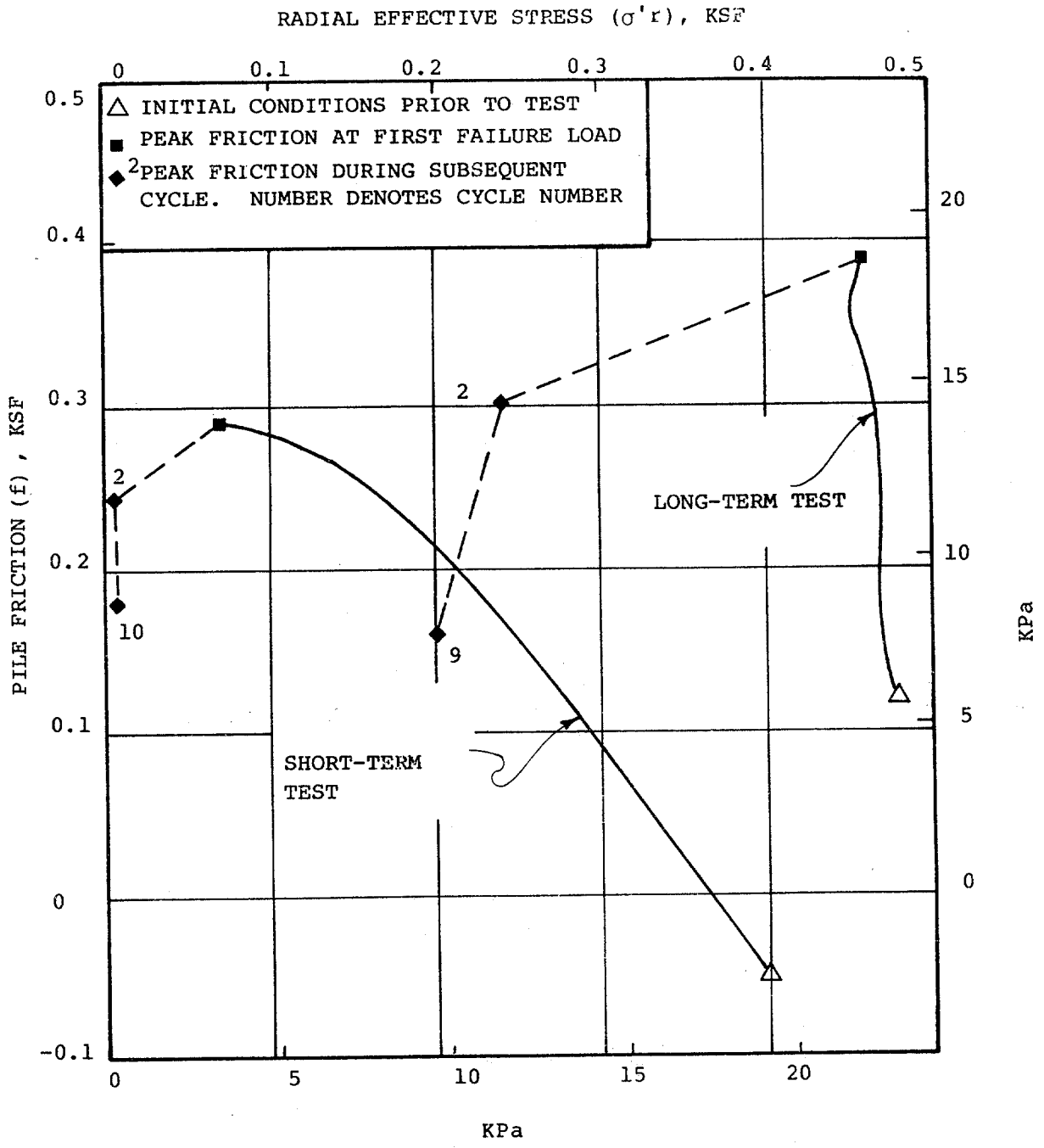
STRESS PATHS - HOLE 3, 54.3 M (178 FT)
IMMEDIATE TEST AND SHORT TERM PROGRESSIVELY INCREASING
LOAD CONTROLLED (TYPE II) TEST



EFFECTIVE RADIAL STRESS/EFFECTIVE RADIAL STRESS PRIOR TO TEST
 (σ'_r / σ'_{rc})

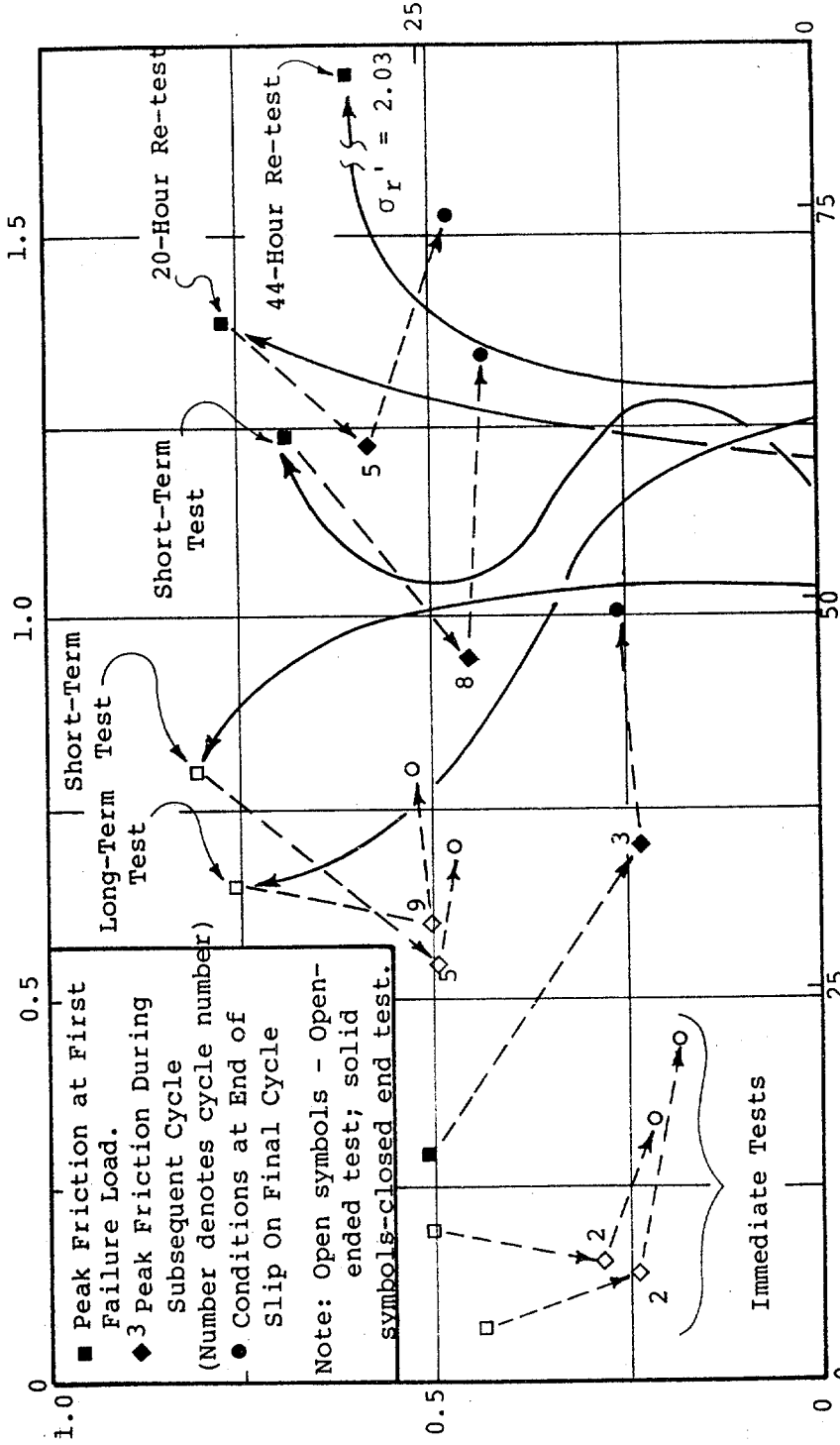
FRICTION/RADIAL EFFECTIVE STRESS PRIOR TO TEST
 (f / σ'_{rc})

STRESS PATH COMPARISON OF UNDISTURBED, LOAD CONTROLLED AND DISPLACEMENT CONTROLLED TESTS (STRATUM III)



STRESS PATHS - COMPOSITE OF TESTS
 PERFORMED IN STRATUM I, 17.7 M (58 FT)

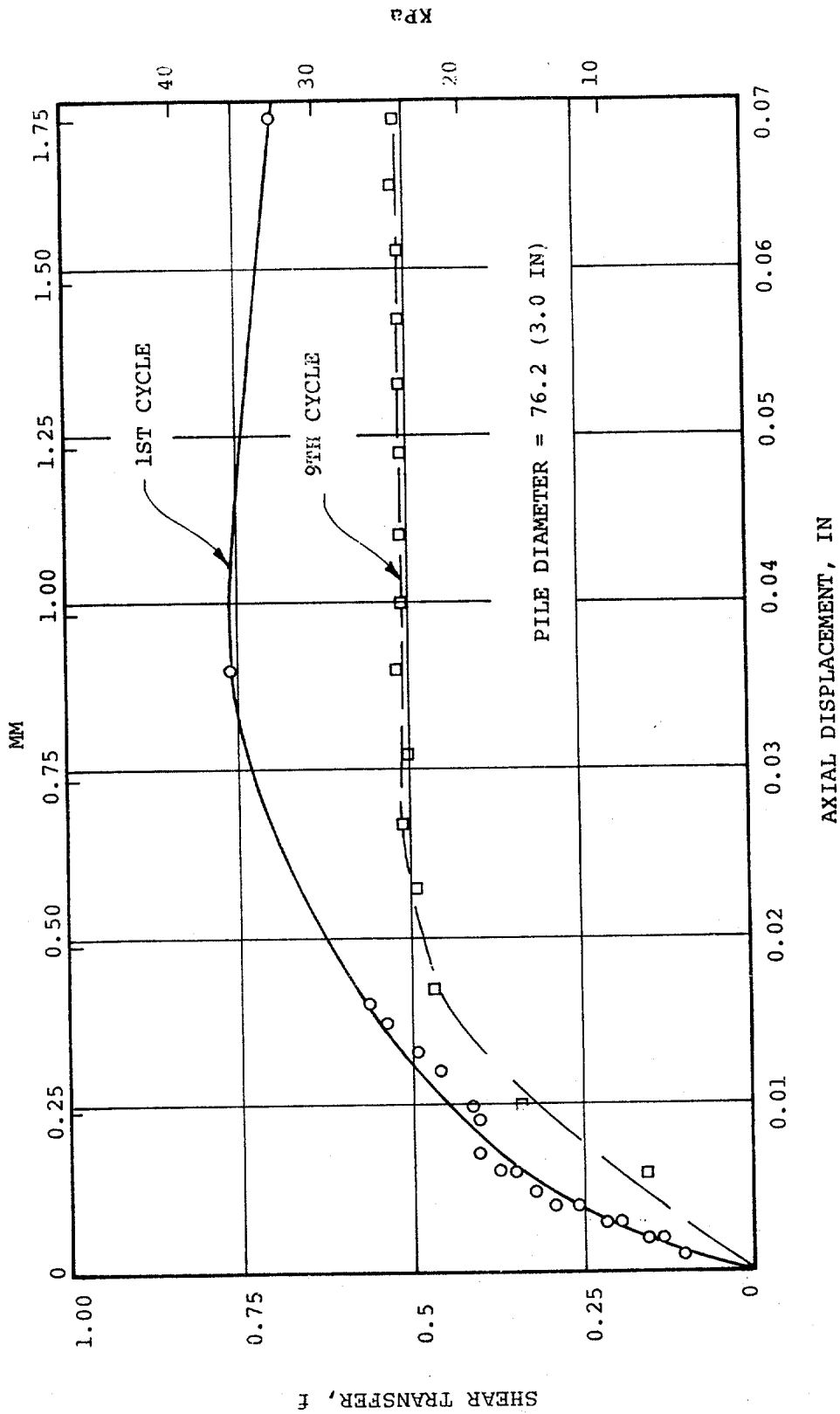
RADIAL EFFECTIVE STRESS (σ'_r), KSF



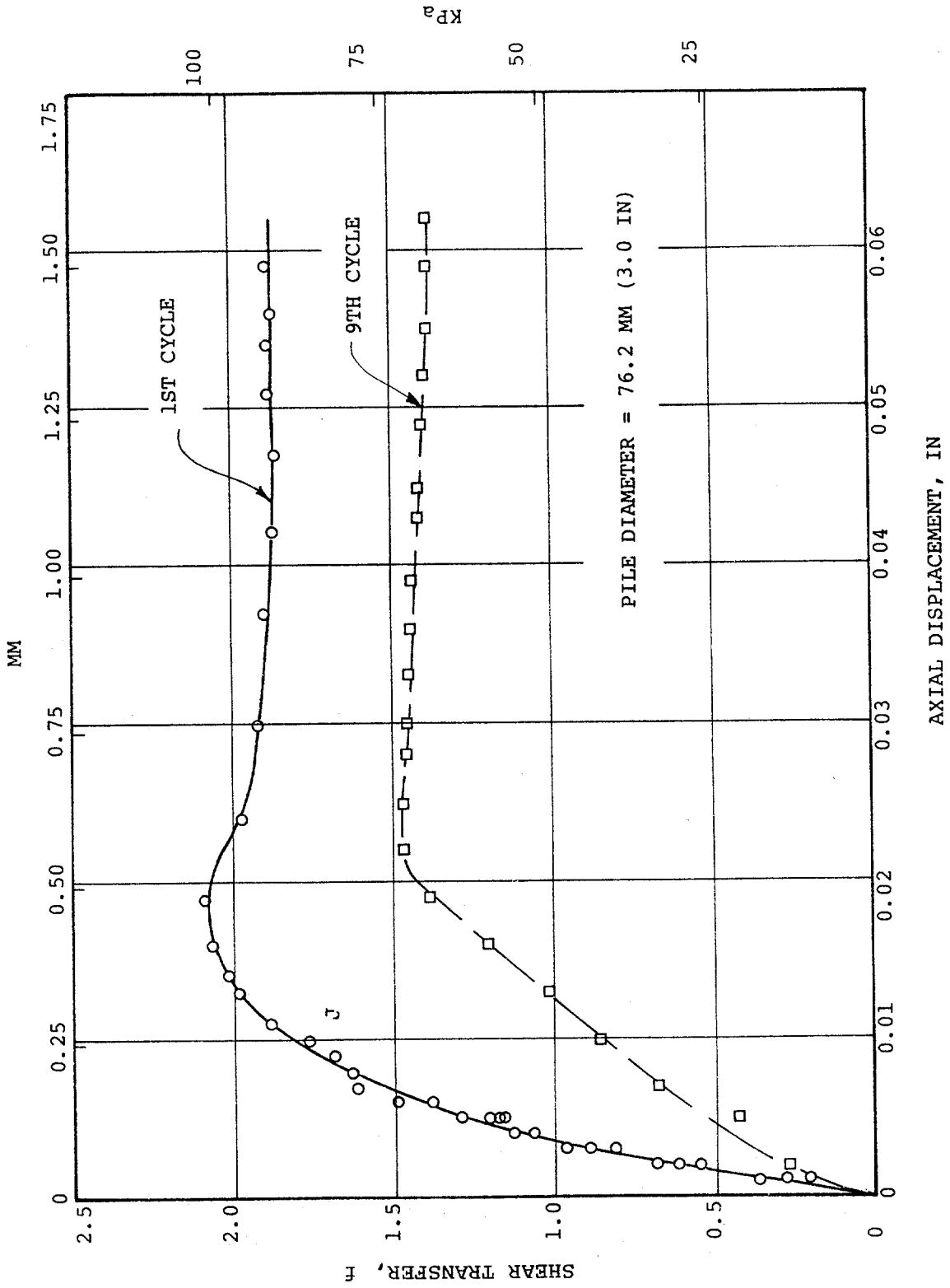
PILE FRICTION (F), KSF

Kpa

STRESS PATHS - COMPOSITE OF TESTS PERFORMED IN STRATUM II, 45.1 M (148 FT)



T-Z CURVES FOR LONG-TERM TEST AT 45.1 M (148 FT)



T-Z CURVES FOR LONG-TERM TEST AT 63.4 M (208 FT)

APPENDIX

TEST RESULTS

TEST HOLE 1

TEST HOLE 2

TEST HOLE 3

TEST HOLE 1

DEPTH 1 = 17.7 meters (58 ft)

Immediate Test

Shear vs Displacement

Page

A-1

Long-Term test - Type I

Shear vs Displacement

A-2

DEPTH 2 = 45.1 meters (148 feet)

Long-Term Test - Type I

Shear vs Displacement

A-3

Total Pressure vs Displacement

A-4

Pore Pressure vs Displacement

A-5

Effective Pressure vs Displacement

A-6

DEPTH 3 = 63.4 meters (208 feet)

Immediate Test

Shear vs Displacement

A-7

Total Pressure vs Displacement

A-8

Pore Pressure vs Displacement

A-9

Effective Pressure vs Displacement

A-10

Long-Term Test - Type I

Shear vs Displacement

A-11

Total Pressure vs Displacement

A-12

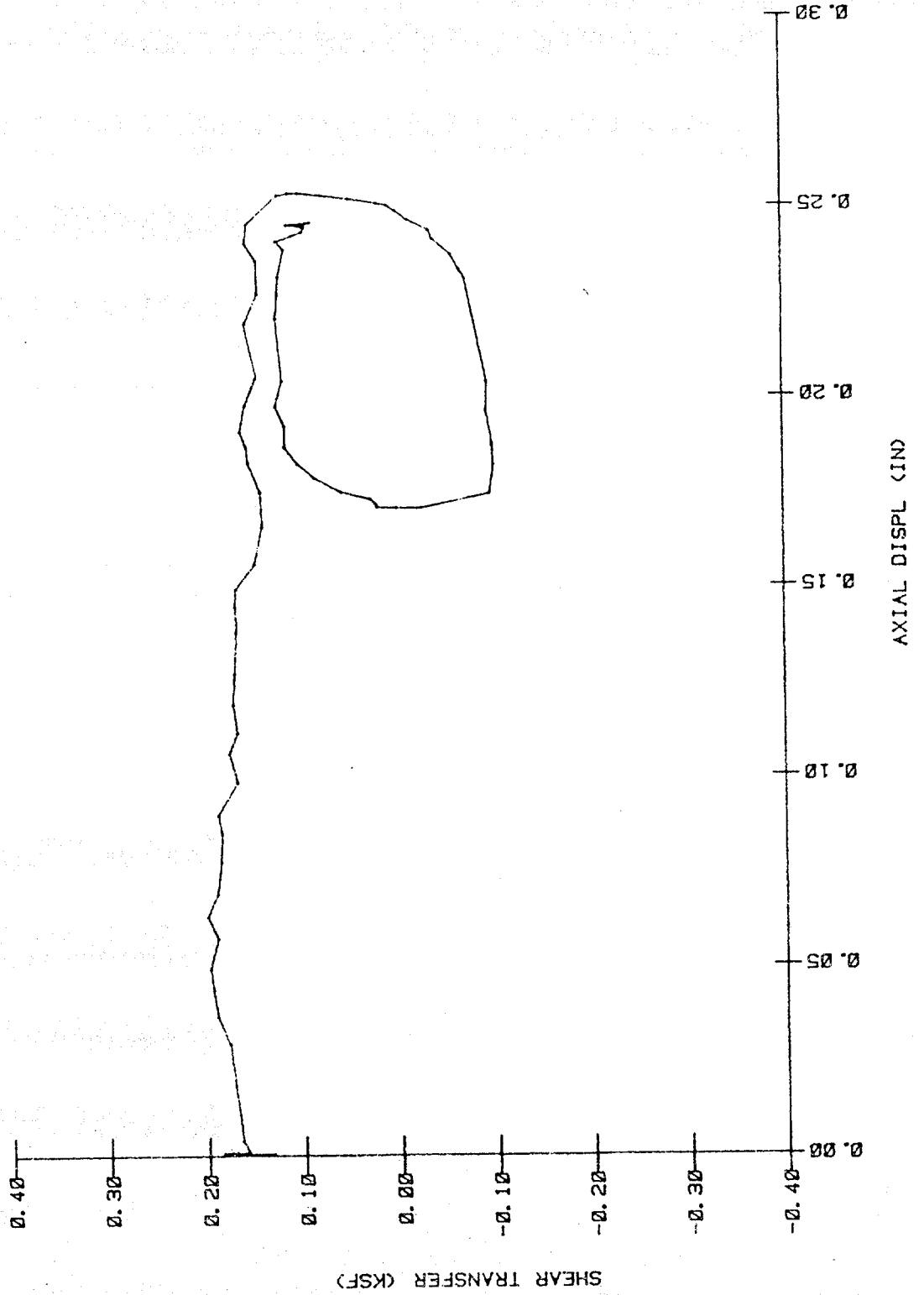
Pore Pressure vs Displacement

A-13

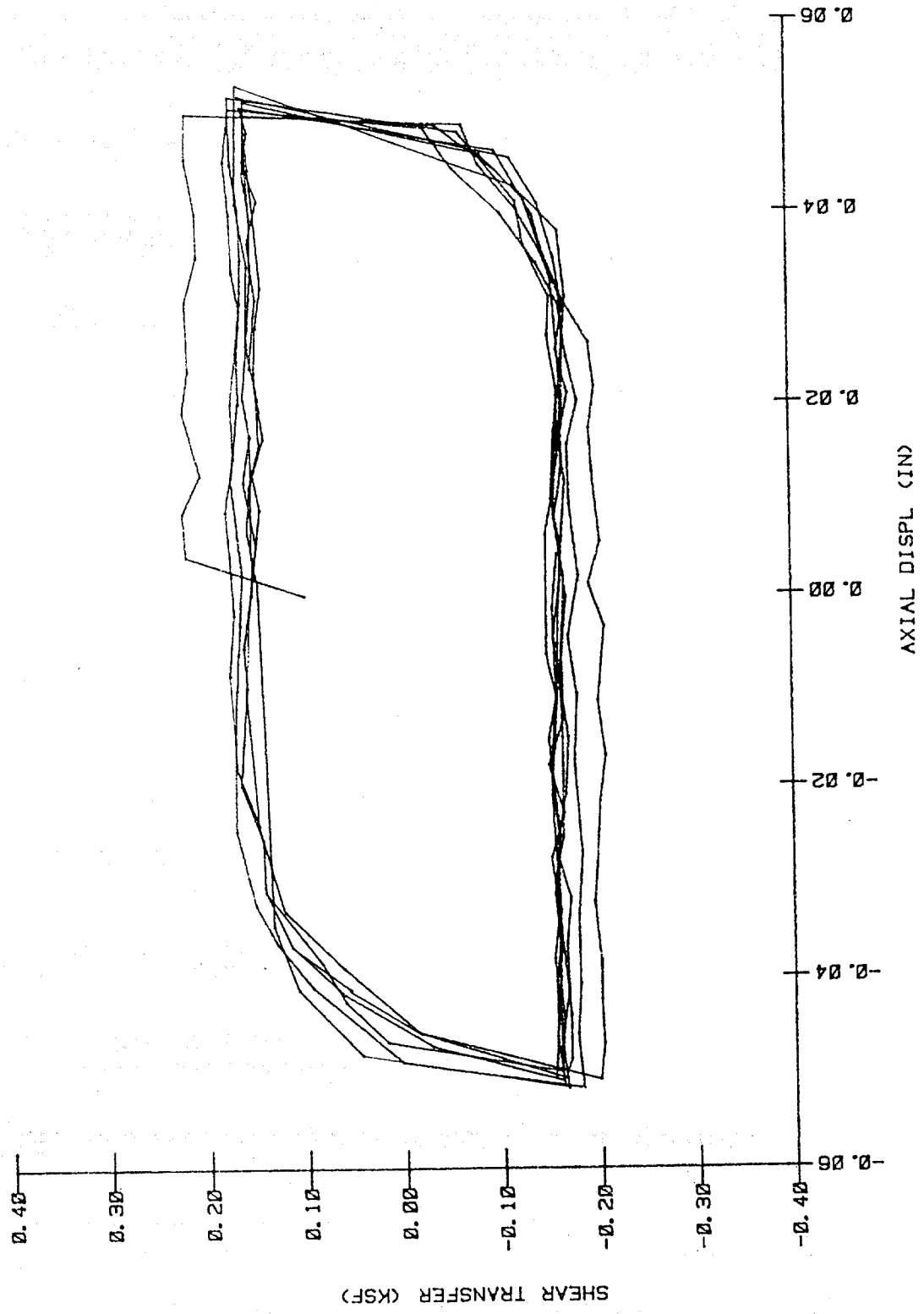
Effective Pressure vs Displacement

A-14

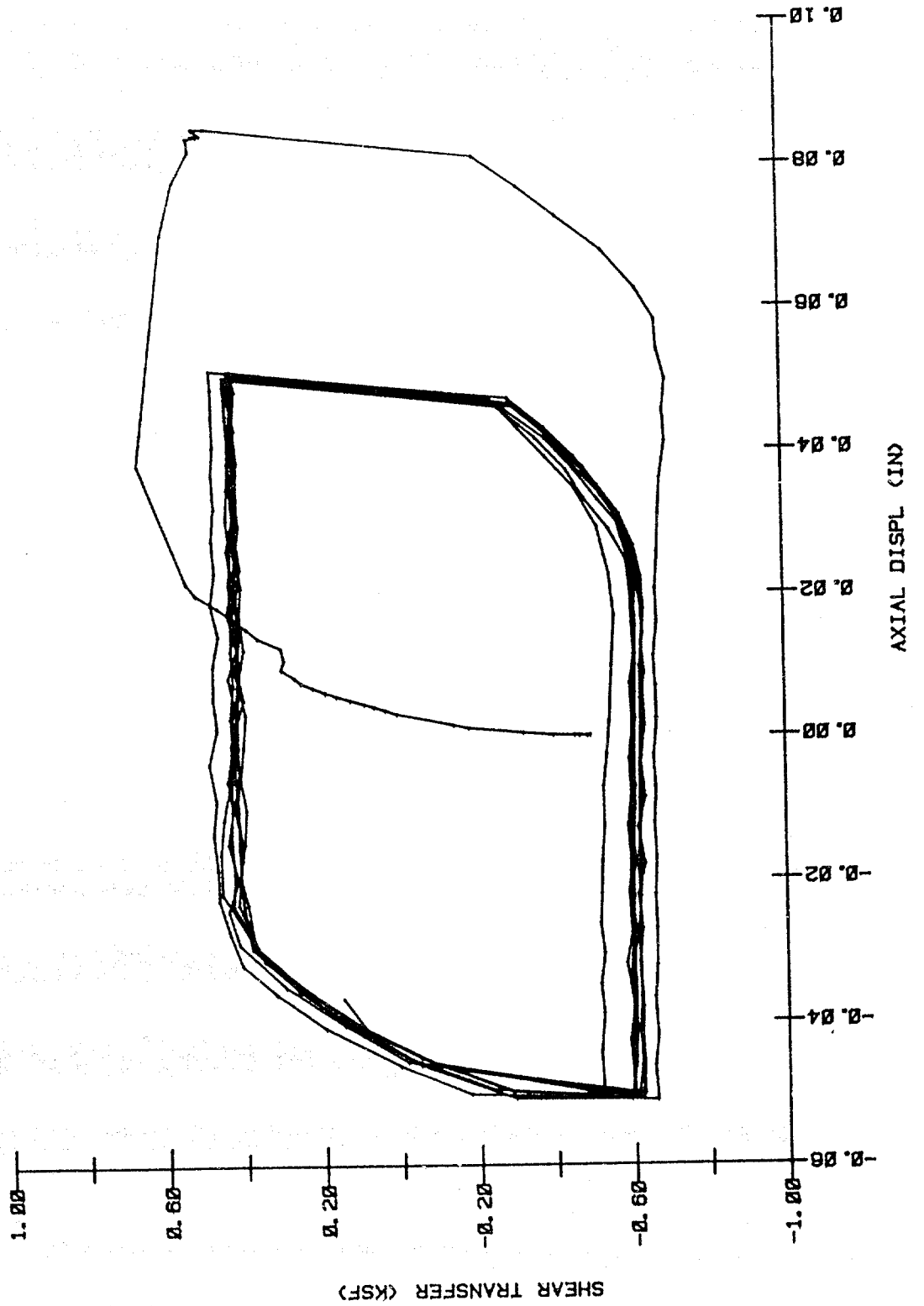
IMMEDIATE TEST
HOLE 1 - DEPTH 1
30 NOV 1982 19:50



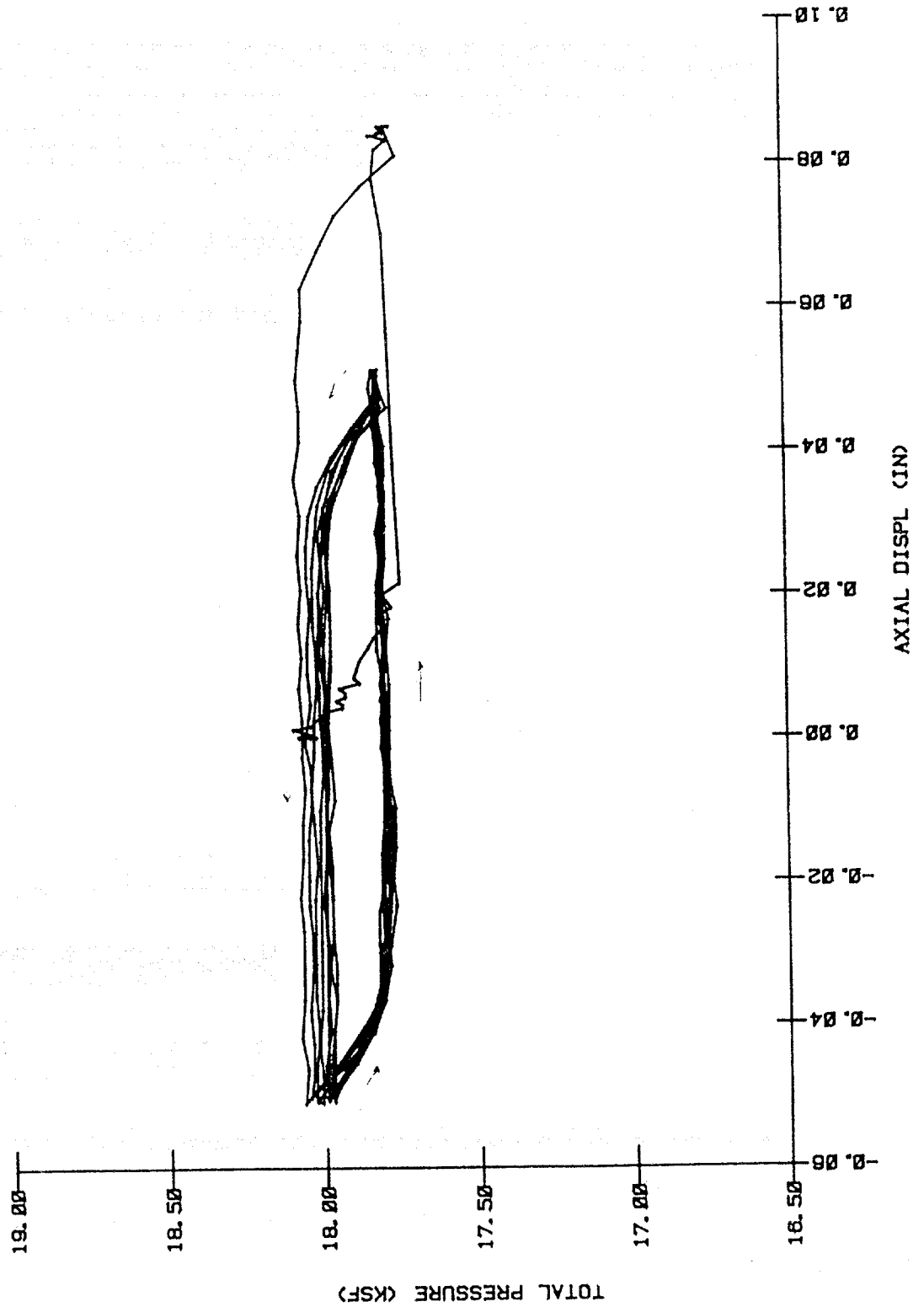
LONG-TERM TEST
HOLE 1 - DEPTH 1
03 DEC 1982 19:44



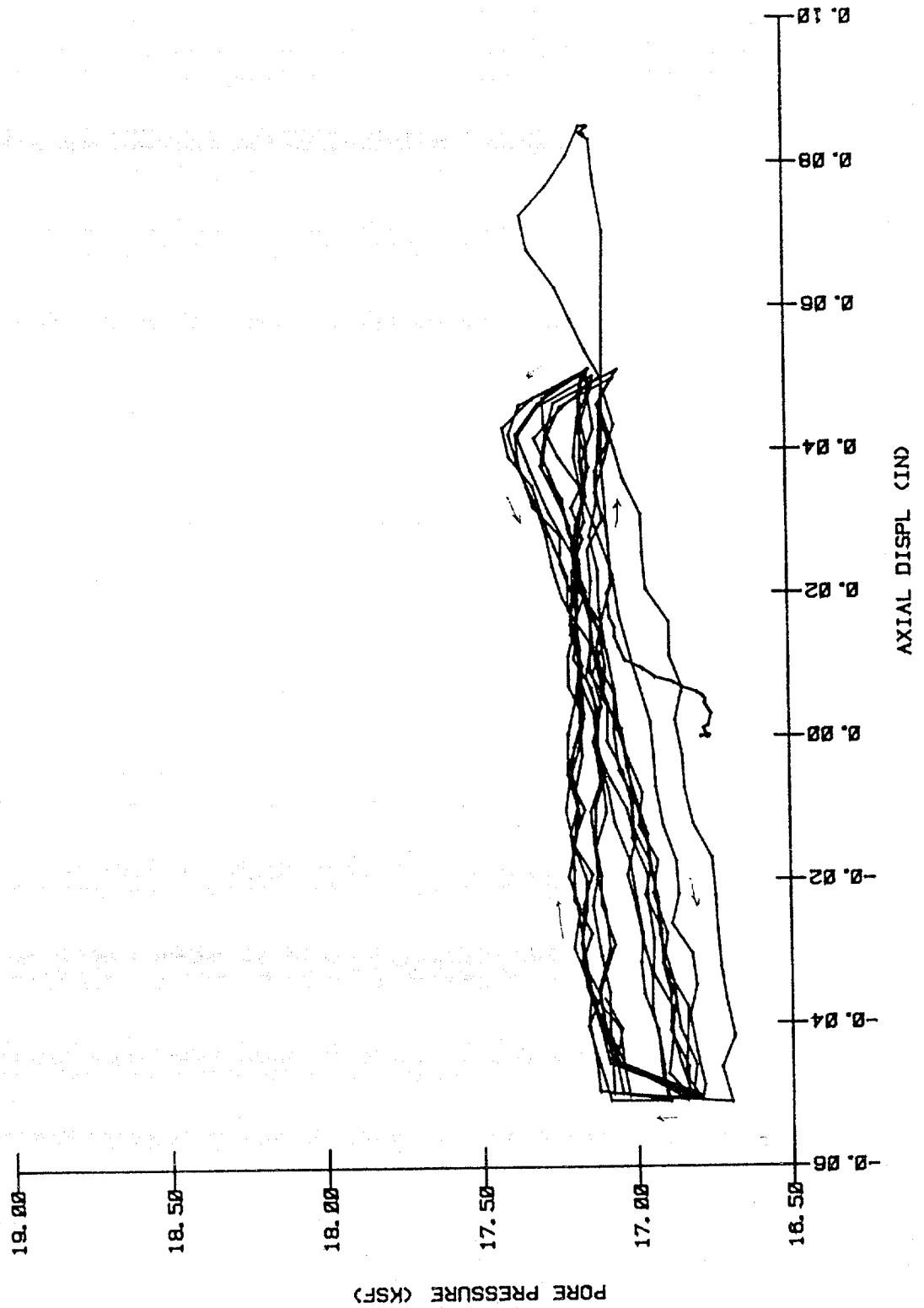
LONG-TERM TEST
HOLE 1 - DEPTH 2
07 DEC 1982 13:19



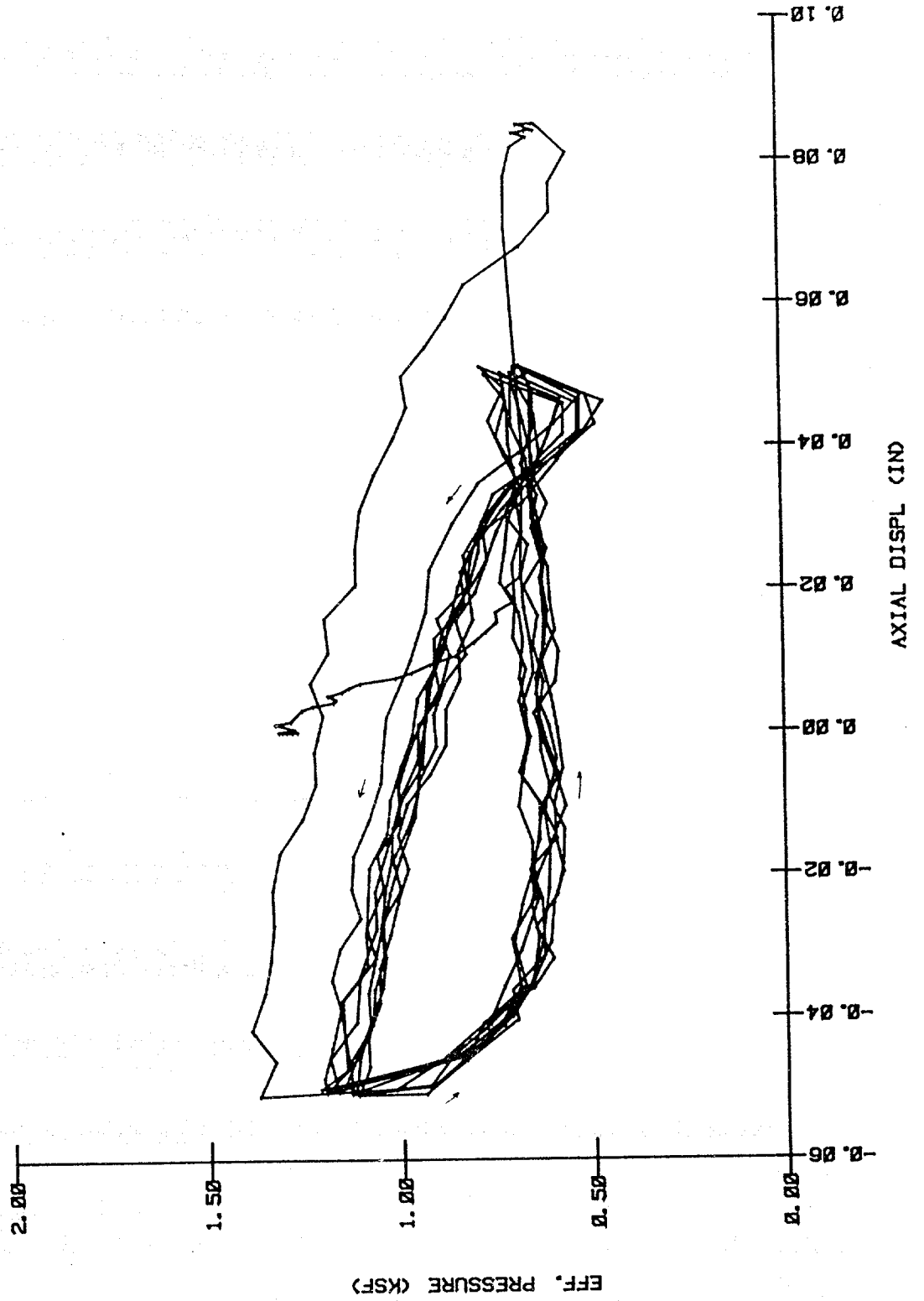
LONG-TERM TEST
HOLE 1 - DEPTH 2
07 DEC 1982 13:19



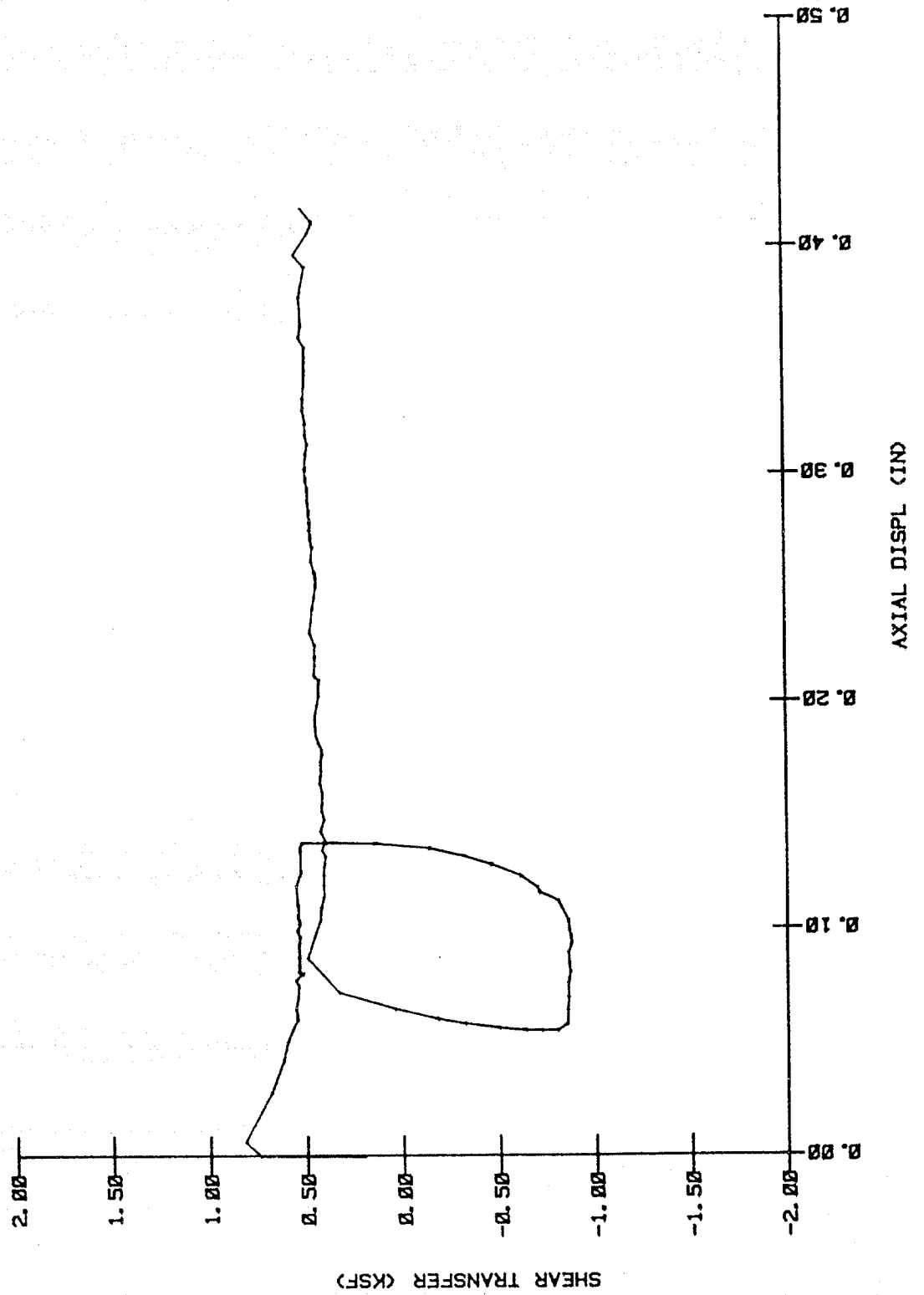
LONG-TERM TEST
HOLE 1 - DEPTH 2
07 DEC 1982 13:19



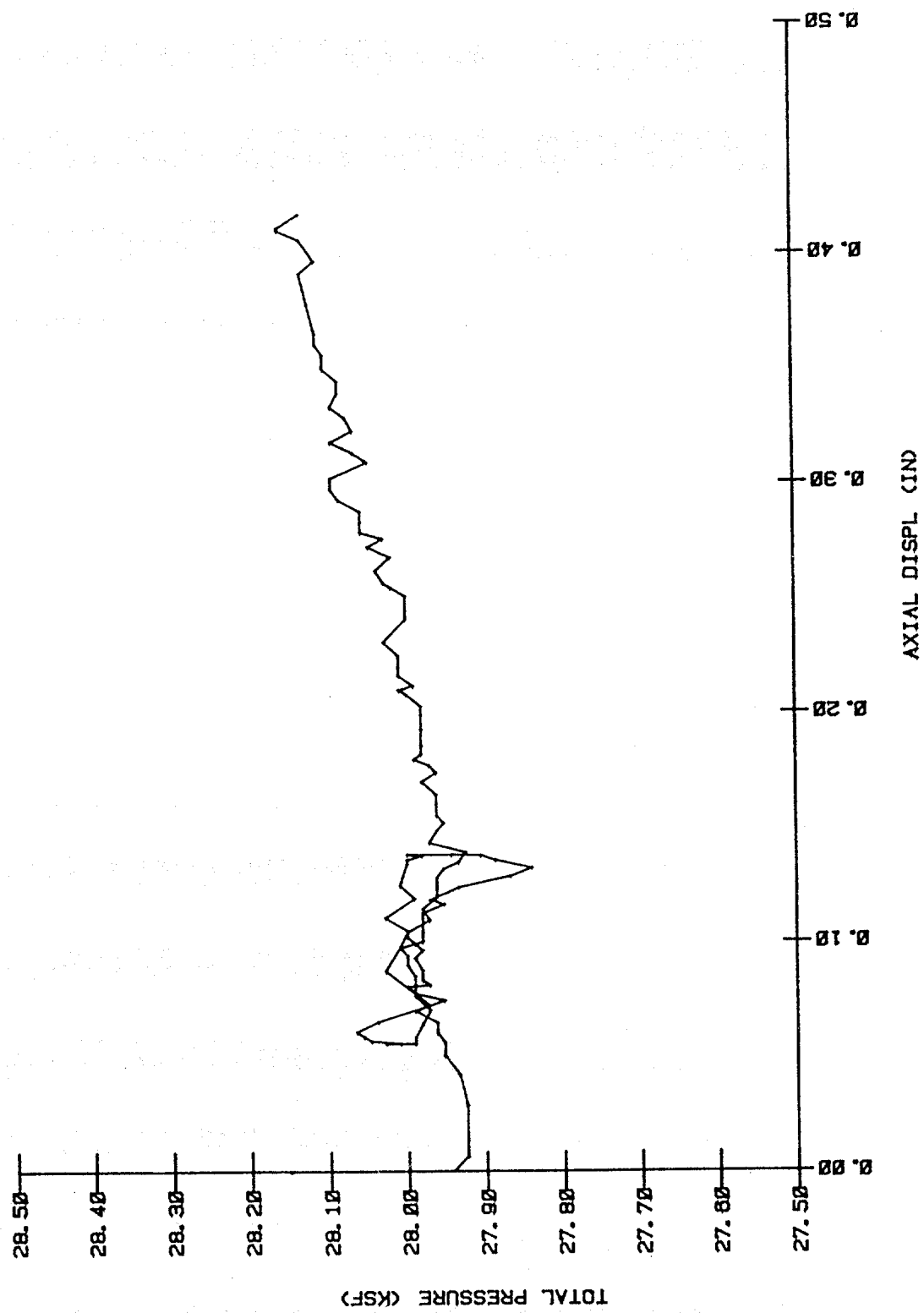
LONG-TERM TEST
HOLE 1 - DEPTH 2
Ø7 DEC 1982 13:19



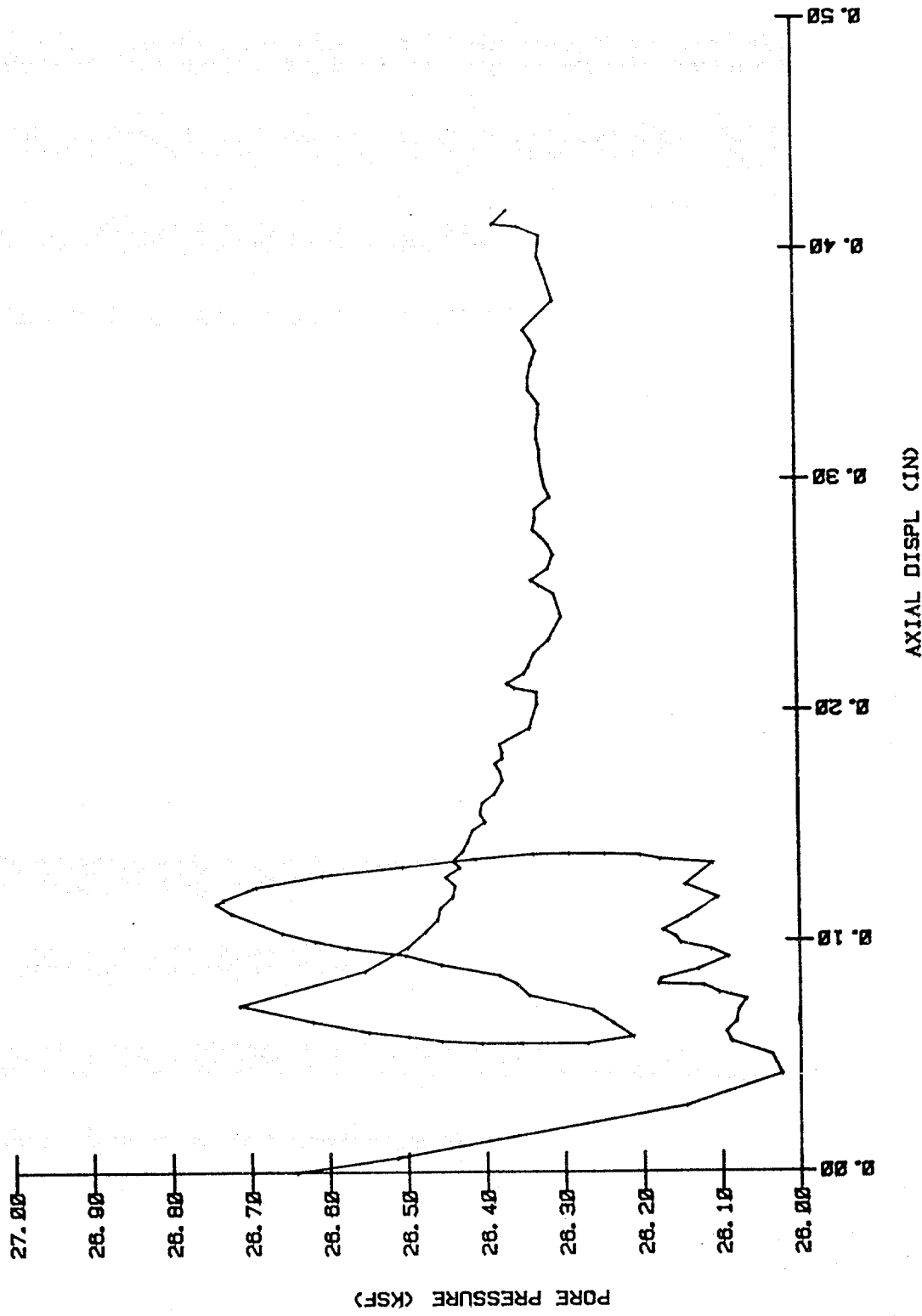
IMMEDIATE TEST
HOLE 1 - DEPTH 3
Ø7 DEC 1982 19:28



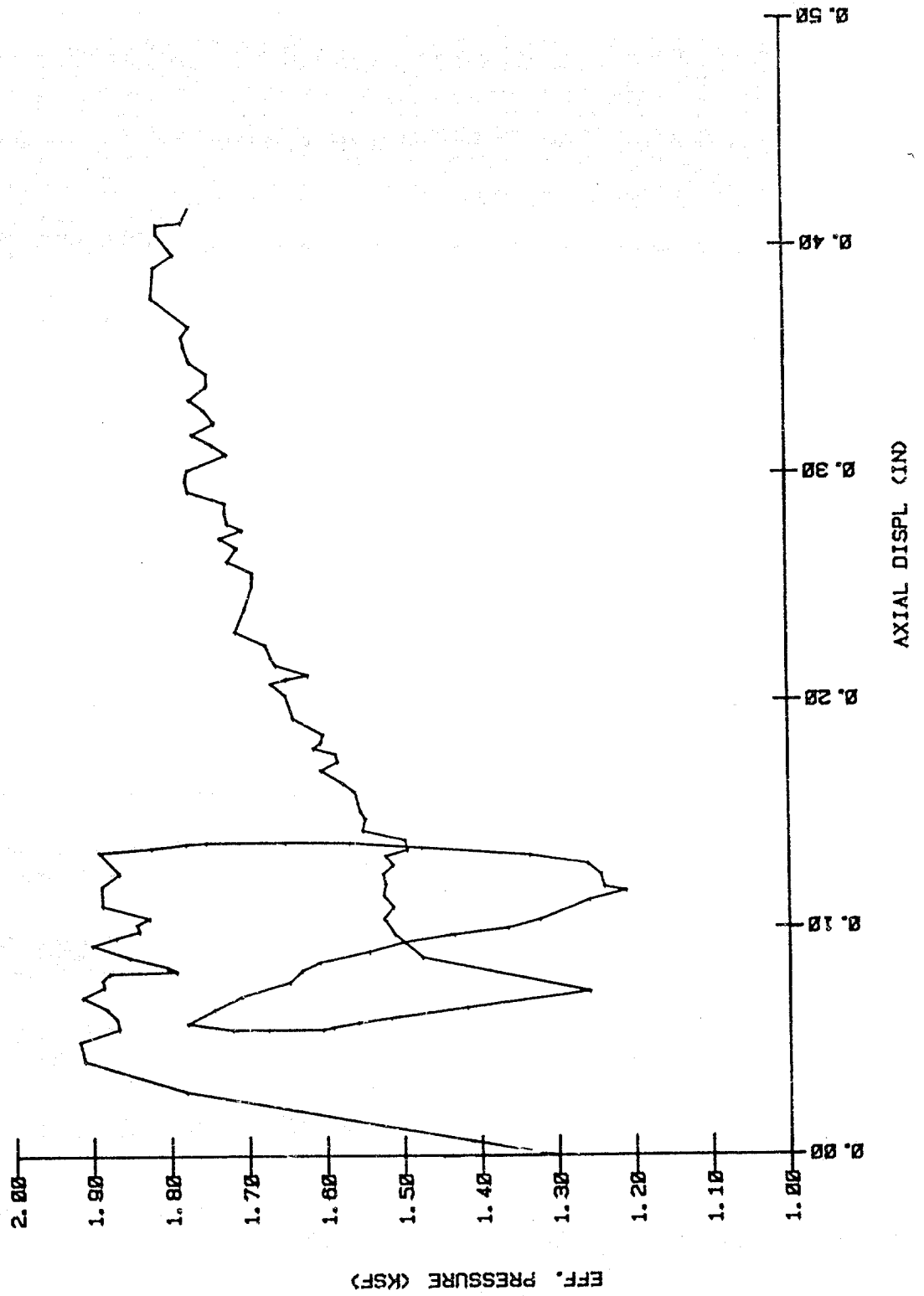
**IMMEDIATE TEST
HOLE 1 - DEPTH 3
07 DEC 1982 19:28**



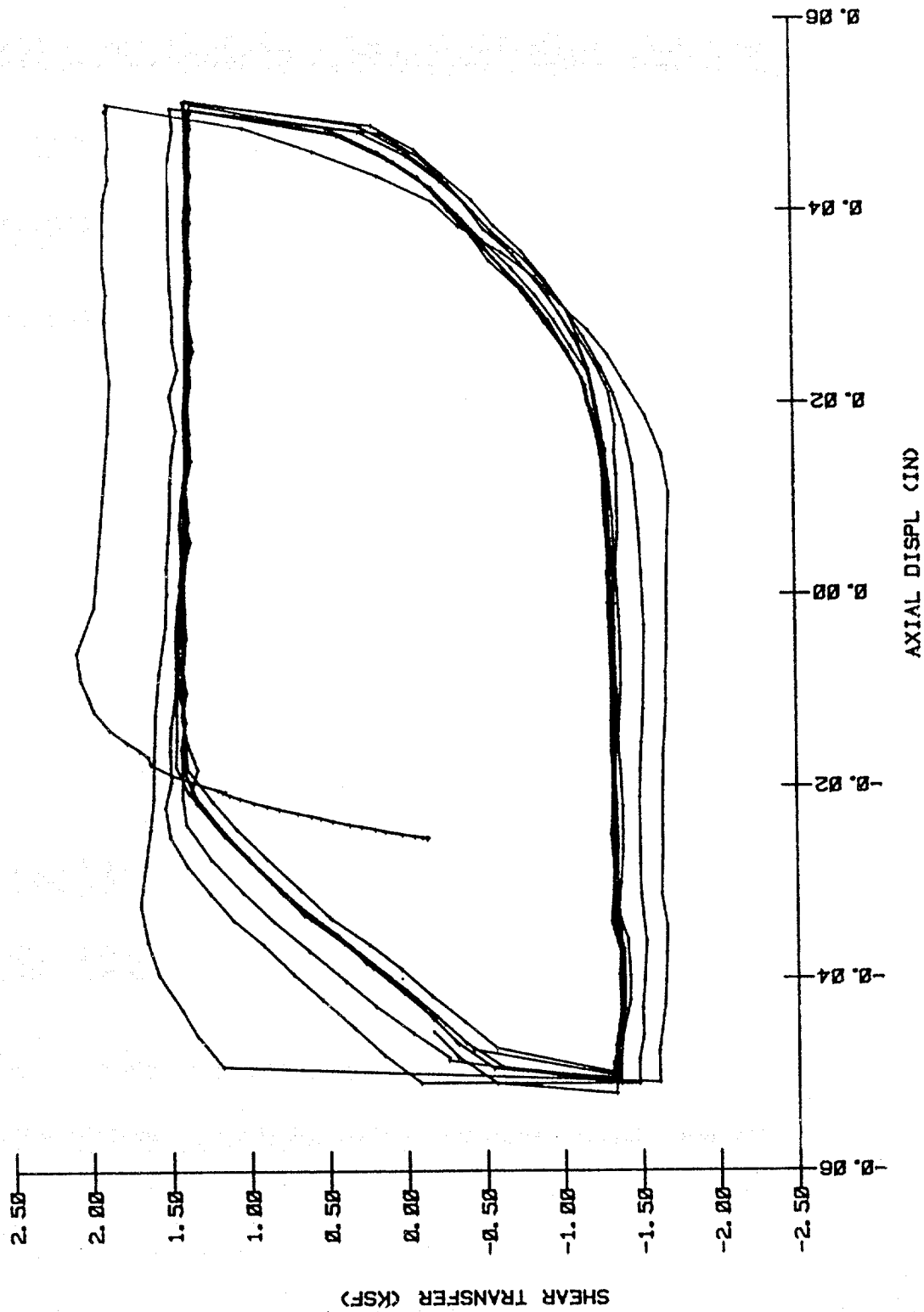
IMMEDIATE TEST
HOLE 1 - DEPTH 3
07 DEC 1982 19:28



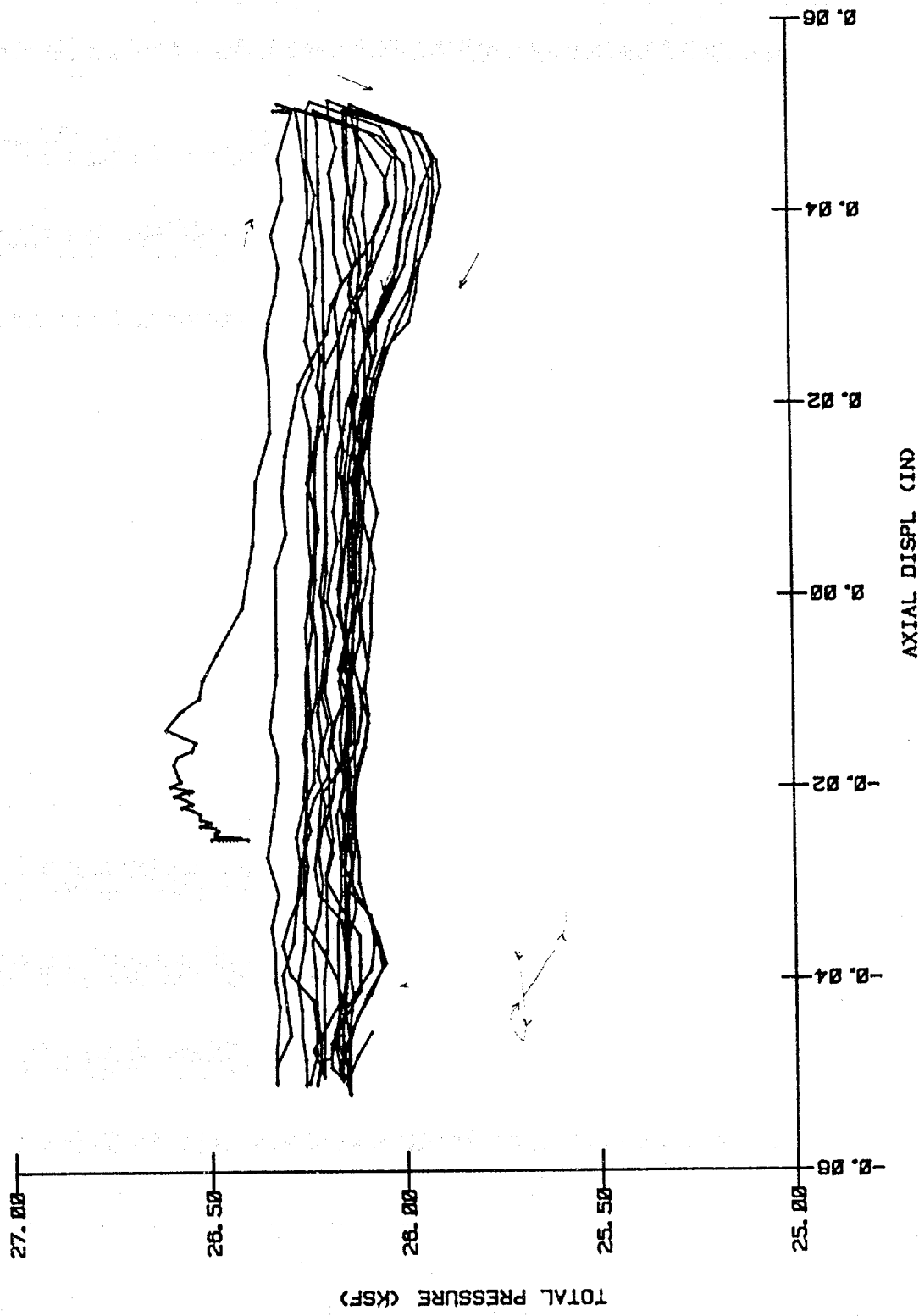
**IMMEDIATE TEST
HOLE 1 - DEPTH 3
07 DEC 1982 19:28**



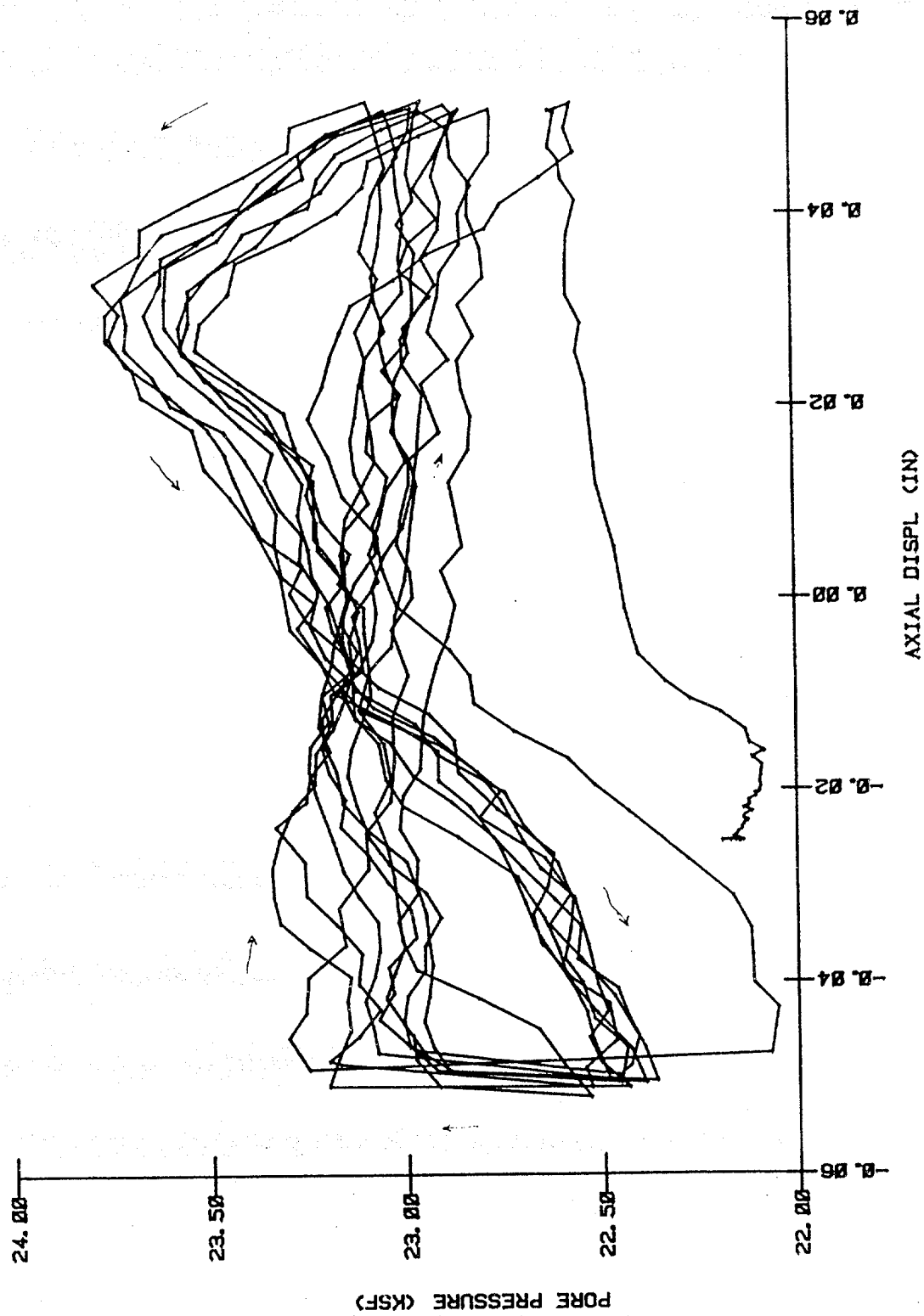
LONG-TERM TEST
HOLE 1 - DEPTH 3
10 DEC 1982 16:40



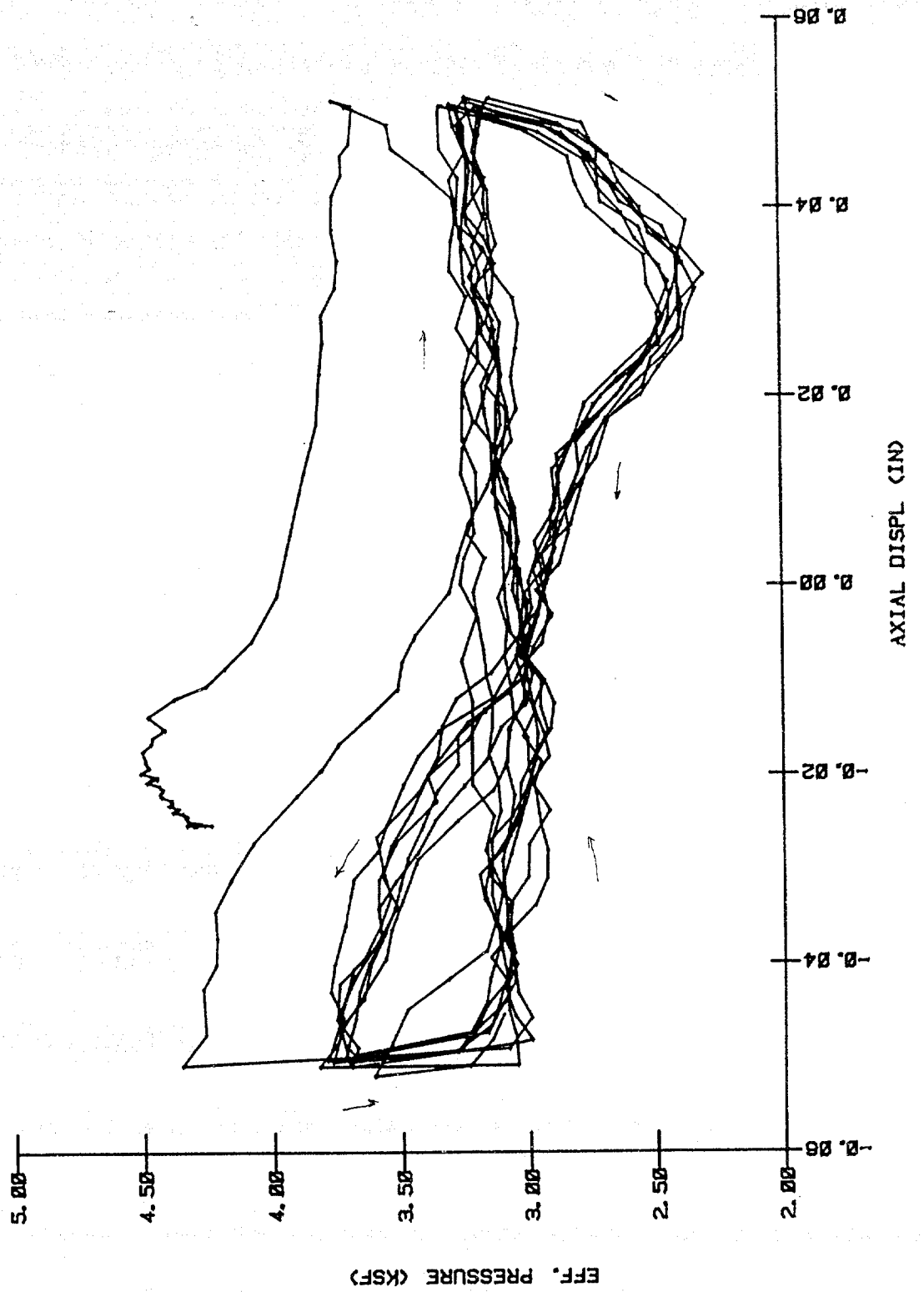
LONG-TERM TEST
HOLE 1 - DEPTH 3
10 DEC 1982 16: 40



**LONG-TERM TEST
HOLE 1 - DEPTH 3
10 DEC 1982 16:40**



LONG-TERM TEST
HOLE 1 - DEPTH 3
10 DEC 1982 16:40



TEST HOLE 2

Page

DEPTH 1 = 17.7 meters (58 feet)

Immediate Test

Shear vs Displacement

A-15

Short-Term Test - Type I

Shear vs Displacement

A-16

DEPTH 2 = 45.1 meters (148 feet)

Immediate Test

Shear vs Displacement

A-17

Short-Term Test - Type I

Shear vs Displacement

A-18

DEPTH 3 = 63.4 meters (208 feet)

Immediate Test

Shear vs Displacement

A-19

Short-Term Test - Type I

Shear vs Displacement

A-20

Long-Term Test - Type II (70-hour)

Shear vs Displacement

A-21

Long-Term Test - Type II (144-hour)

Shear vs Displacement

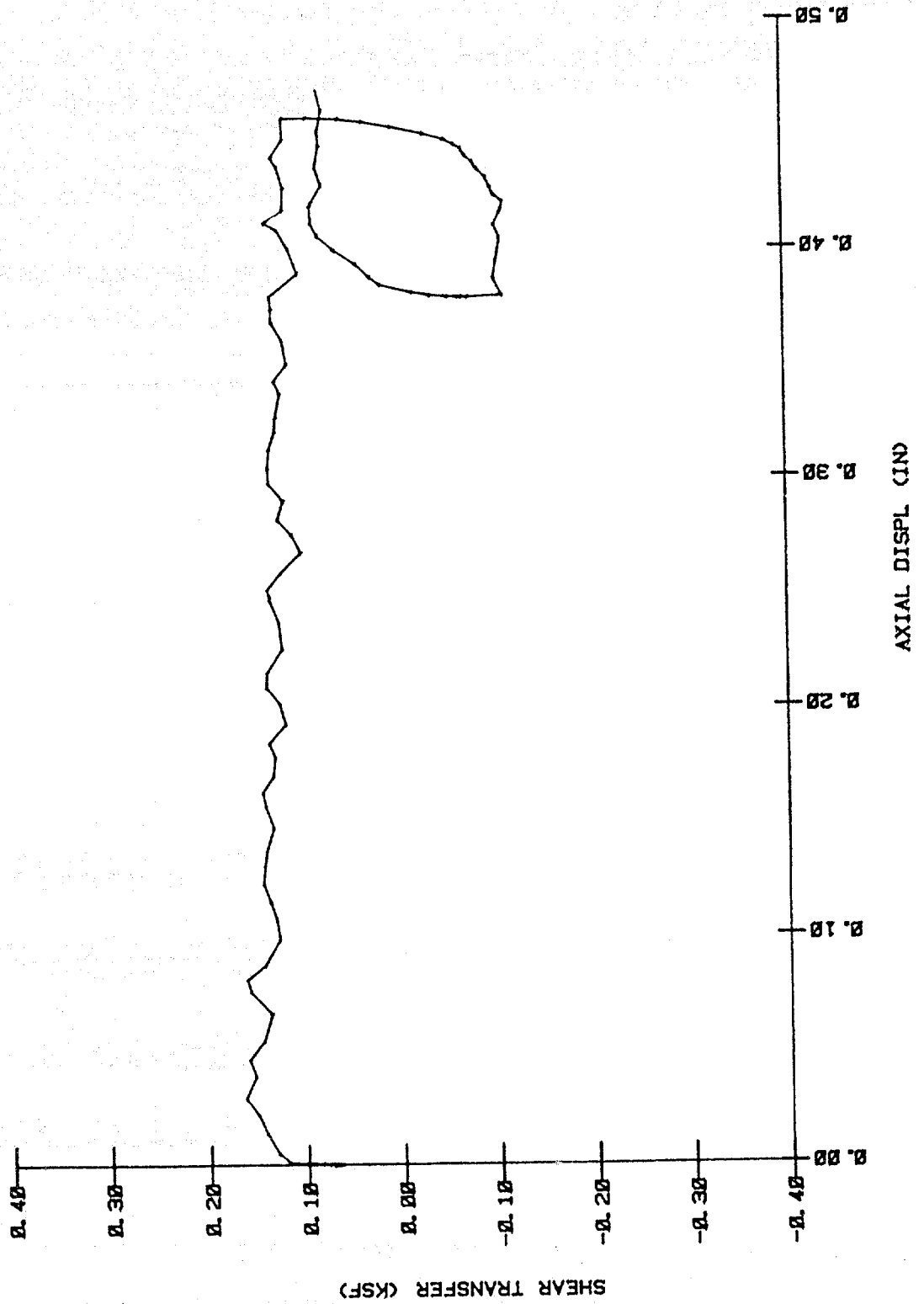
A-22

Pull-Out Test

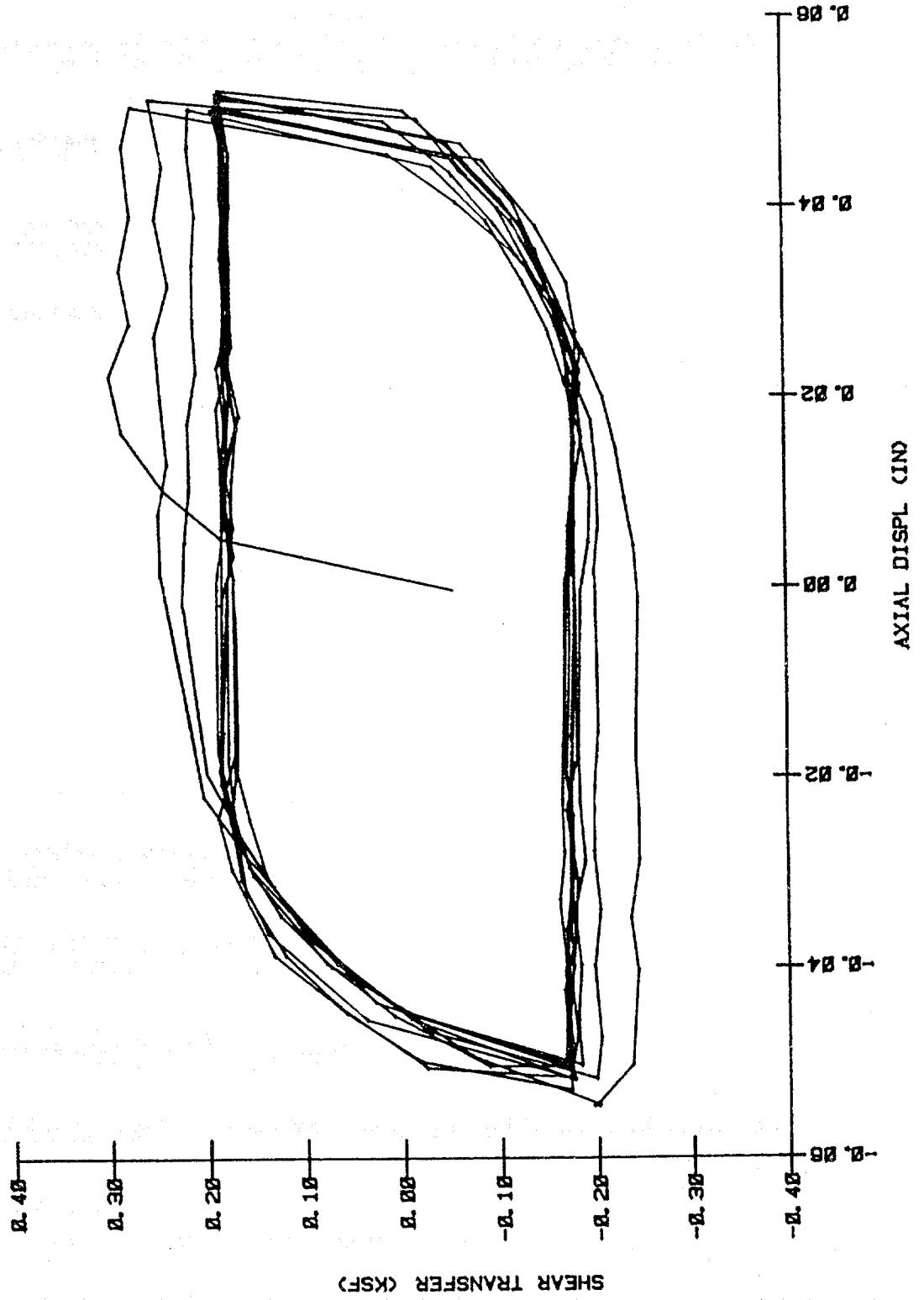
Shear vs Displacement

A-23

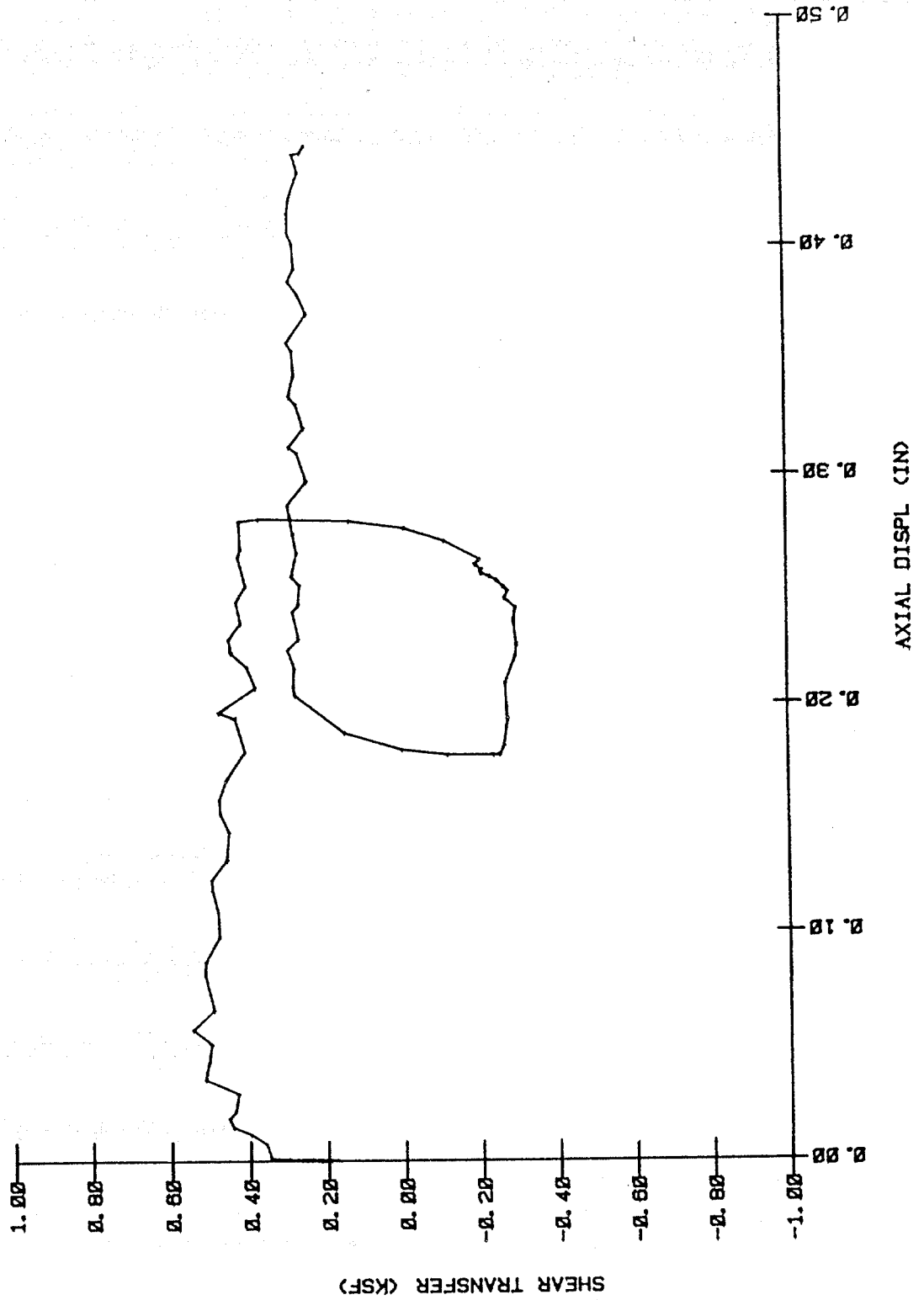
IMMEDIATE TEST
HOLE 2 - DEPTH 1
01 DEC 1982 11:48



SHORT-TERM TEST
HOLE 2 - DEPTH 1
01 DEC 1982 19:34



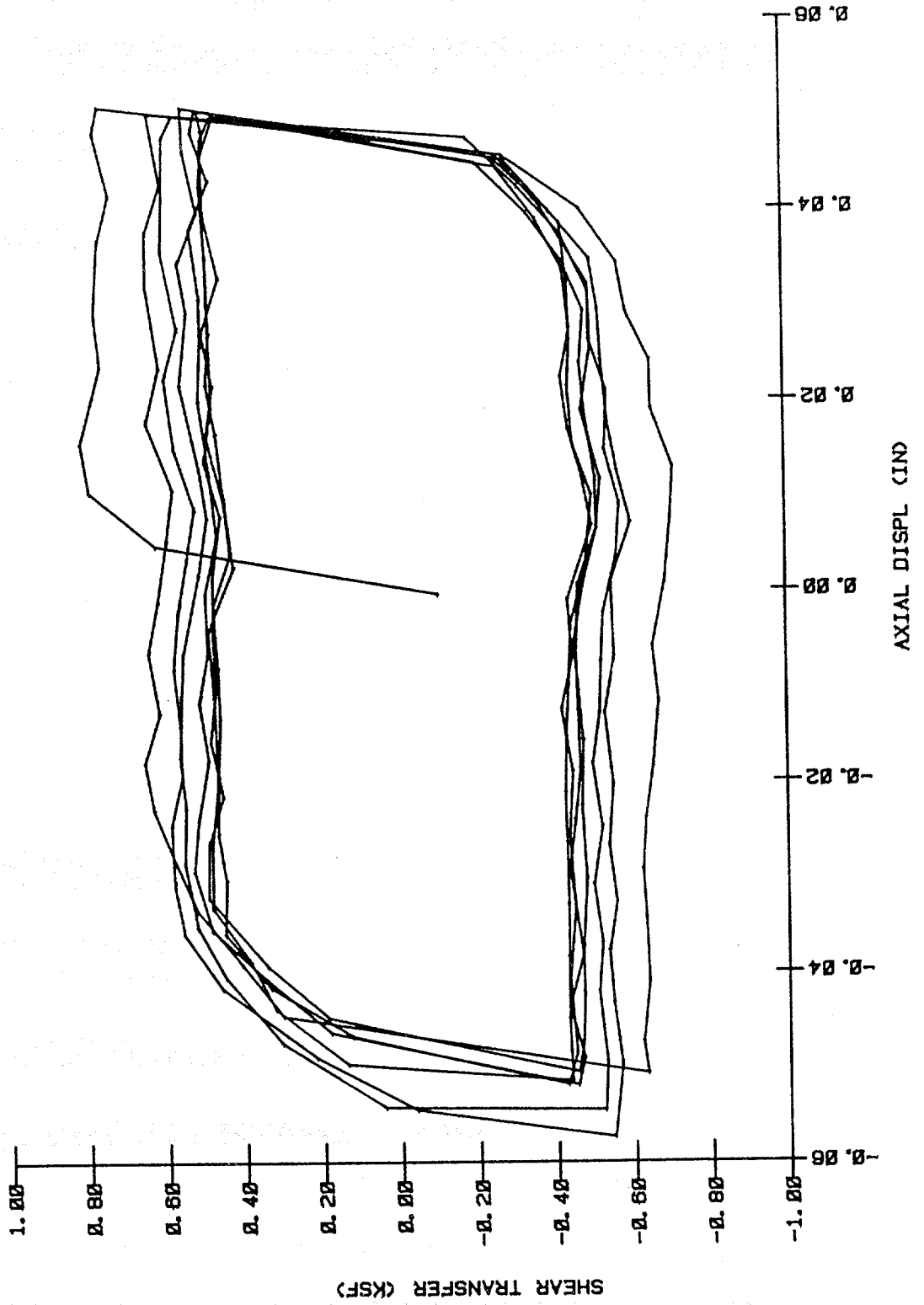
IMMEDIATE TEST
HOLE 2 - DEPTH 2
02 DEC 1982 14:18



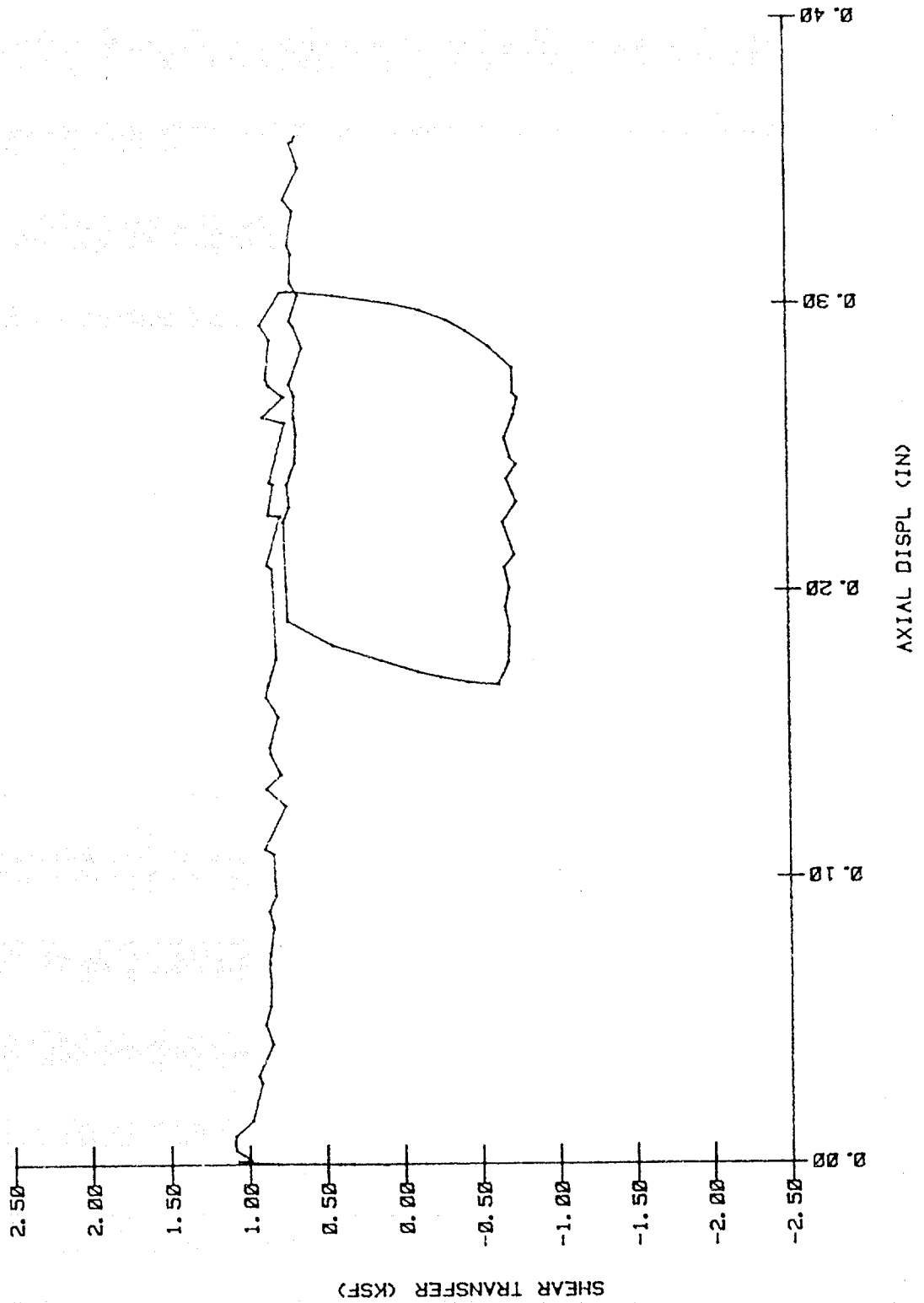
SHORT-TERM TEST

HOLE 2- DEPTH 2

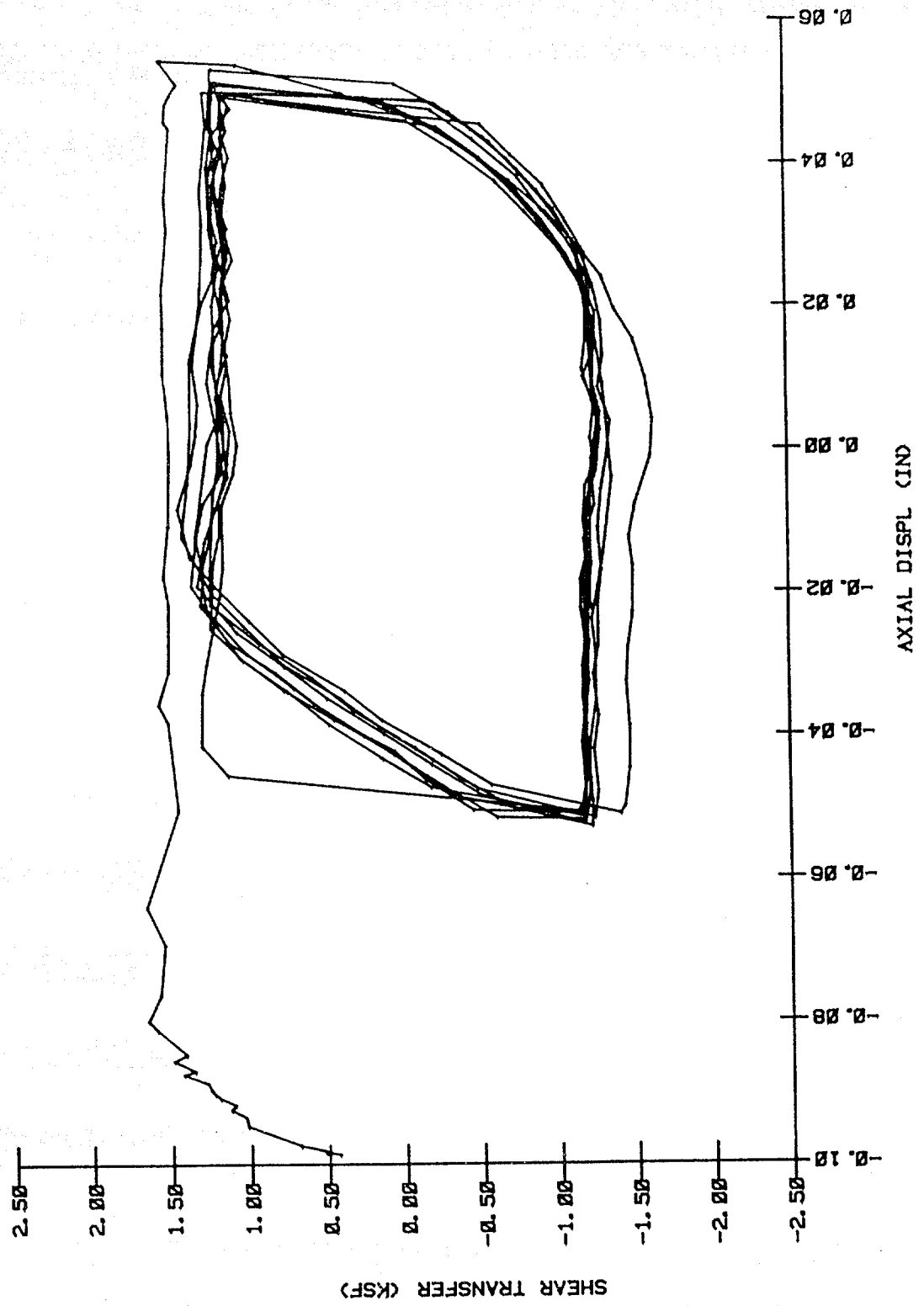
02 DEC 1982 22: 44



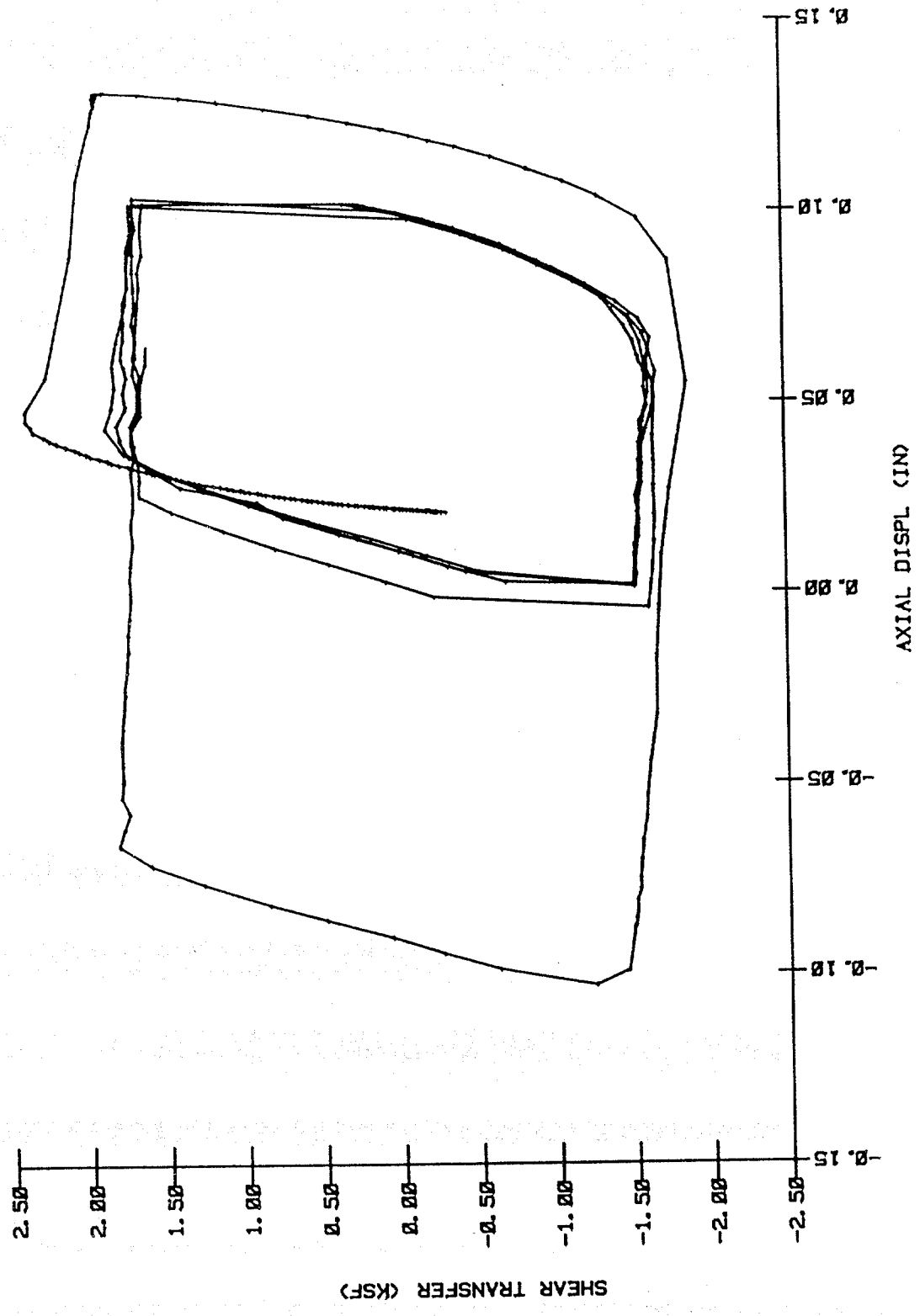
IMMEDIATE TEST
HOLE 2 - DEPTH 3
03 DEC 1982 12:51



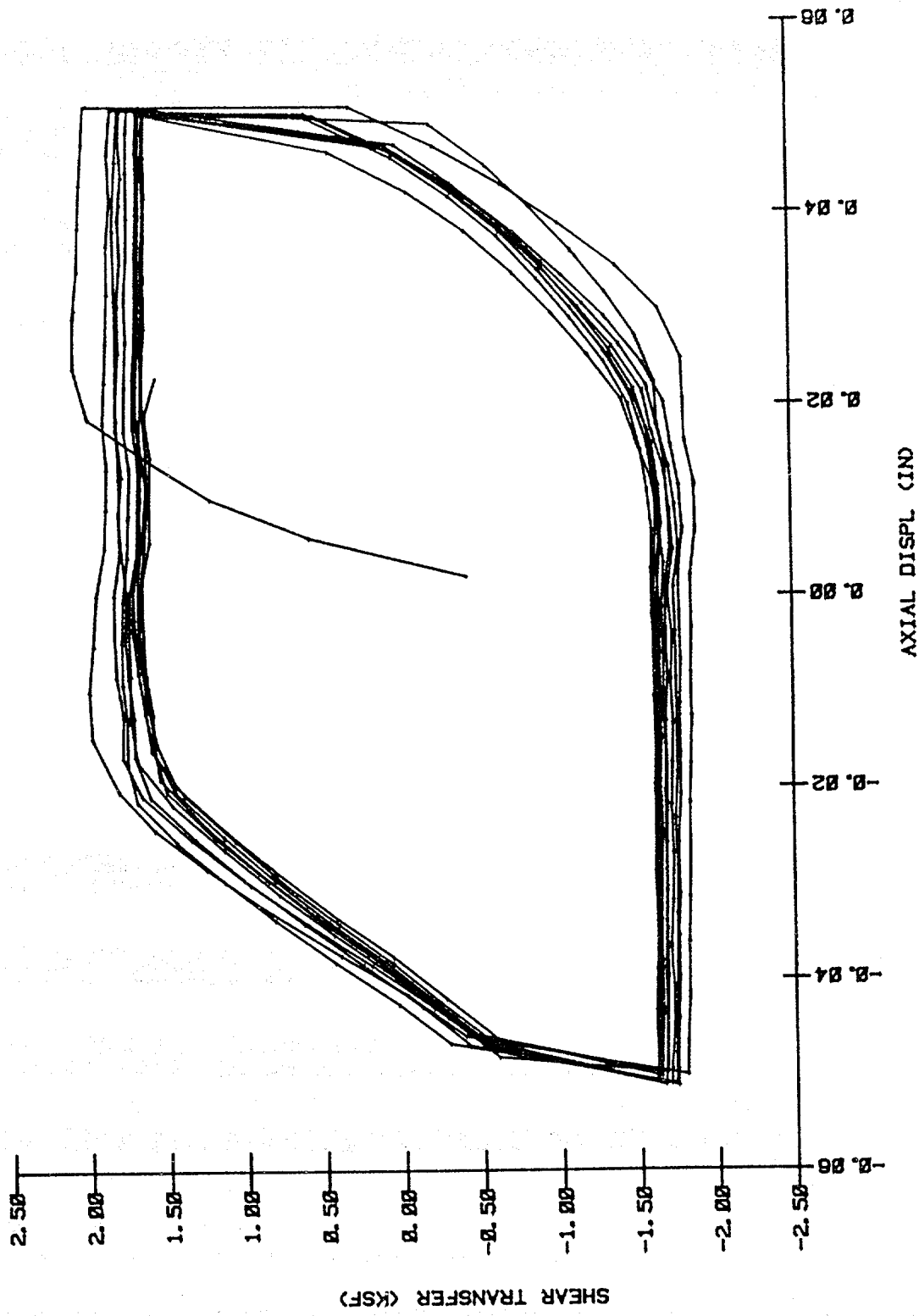
SHORT-TERM TEST
HOLE 2 - DEPTH 3
03 DEC 1982 21:08



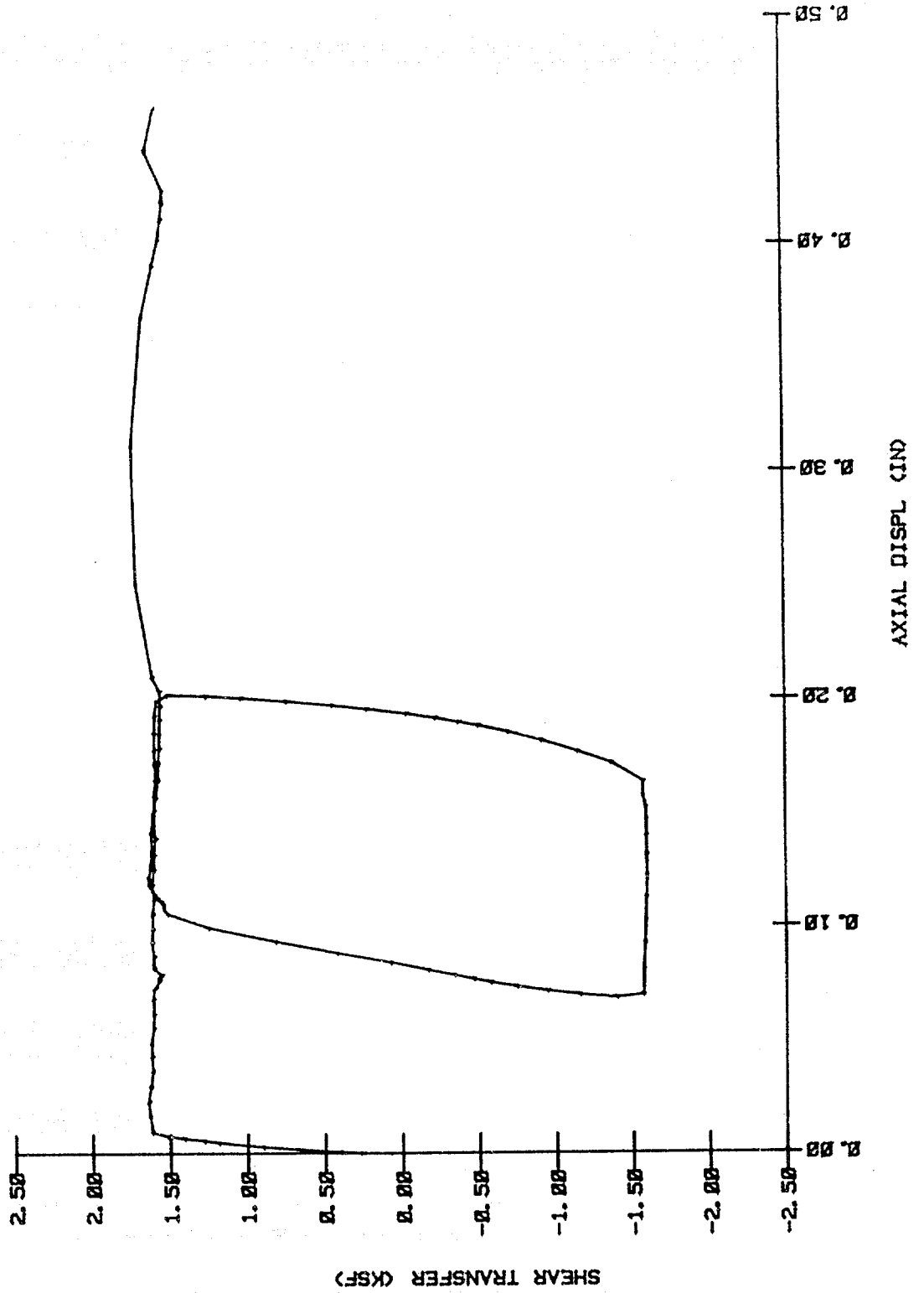
70-HOUR TEST
HOLE 2 - DEPTH 3
06 DEC 1982 10:27



144-HOUR TEST
HOLE 2 - DEPTH 3
09 DEC 1982 11:52



PULL-OUT TEST
HOLE 2 - DEPTH 3
09 DEC 1982 12:42



TEST HOLE 3

Page

DEPTH 1 = 17.7 meters (58 feet)

Immediate Test

Shear vs Displacement A-24

Short-Term Test - Type II - Small Displacement

Shear vs Displacement (+0.005 in) A-25

Shear vs Displacement (+0.010 in) A-26

Shear vs Displacement (+0.015 in) A-27

Shear vs Displacement (+0.020 in) A-28

Shear vs Displacement (+0.025 in) A-29

Shear vs Displacement (+0.030 in) A-30

Shear vs Displacement (+0.50 in) A-31

Shear vs Displacement (Composite) A-32

DEPTH 2 = 45.1 meters (148 feet)

Immediate Test

Shear vs Displacement A-33

Short-Term Test - Type I

Shear vs Displacement A-34

Long-Term Test - Type II (20-hour)

Shear vs Displacement A-35

Long-Term Test - Type II (44-hour)

Shear vs Displacement A-36

Pull-Out Test

Shear vs Displacement A-37

TEST HOLE 3 (cont.)

Page

DEPTH 3 = 54.3 meters (178 feet)

Immediate Test

Shear vs Displacement

A-38

Short-Term Test - Type II - One Way

Load Controlled Test

Shear vs Displacement,

Bias = 50% Estimated Failure Load

45% to 55%

A-39

40% to 60%

A-40

30% to 70%

A-41

20% to 80%

A-42

14% to 86%

A-43

5% to 95%

A-44

-5% to 105%

A-45

Composite Plus Large-Displacement Cycling

A-46

Lateral Pressure During the Test

A-47

Effective Pressure During the Test

A-48

Long-Term Test - Type II (20-hour)

Shear vs Displacement

A-49

DEPTH 4 - 63.4 meters (208 feet)

Immediate Test

Shear vs Displacement

A-50

Short-Term test - Type II - Small displacement

Shear vs Displacement (-.001 to .003 in)

A-51

Shear vs Displacement (-.008 to .004 in)

A-52

Shear vs Displacement (-.012 to .008 in)

A-53

Shear vs Displacement (-.018 to .014 in)

A-54

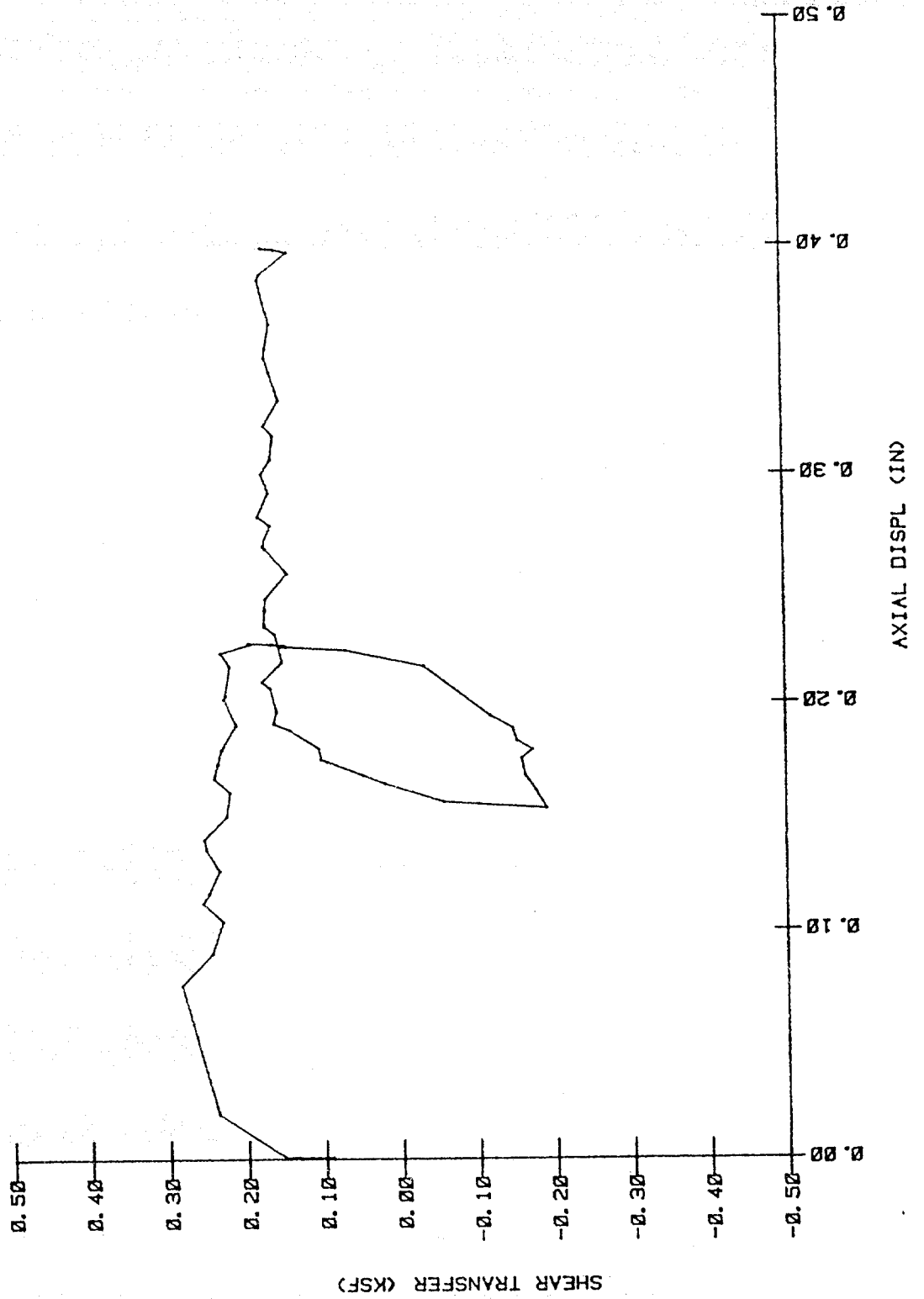
Shear vs Displacement (-.022 to .018 in)

A-55

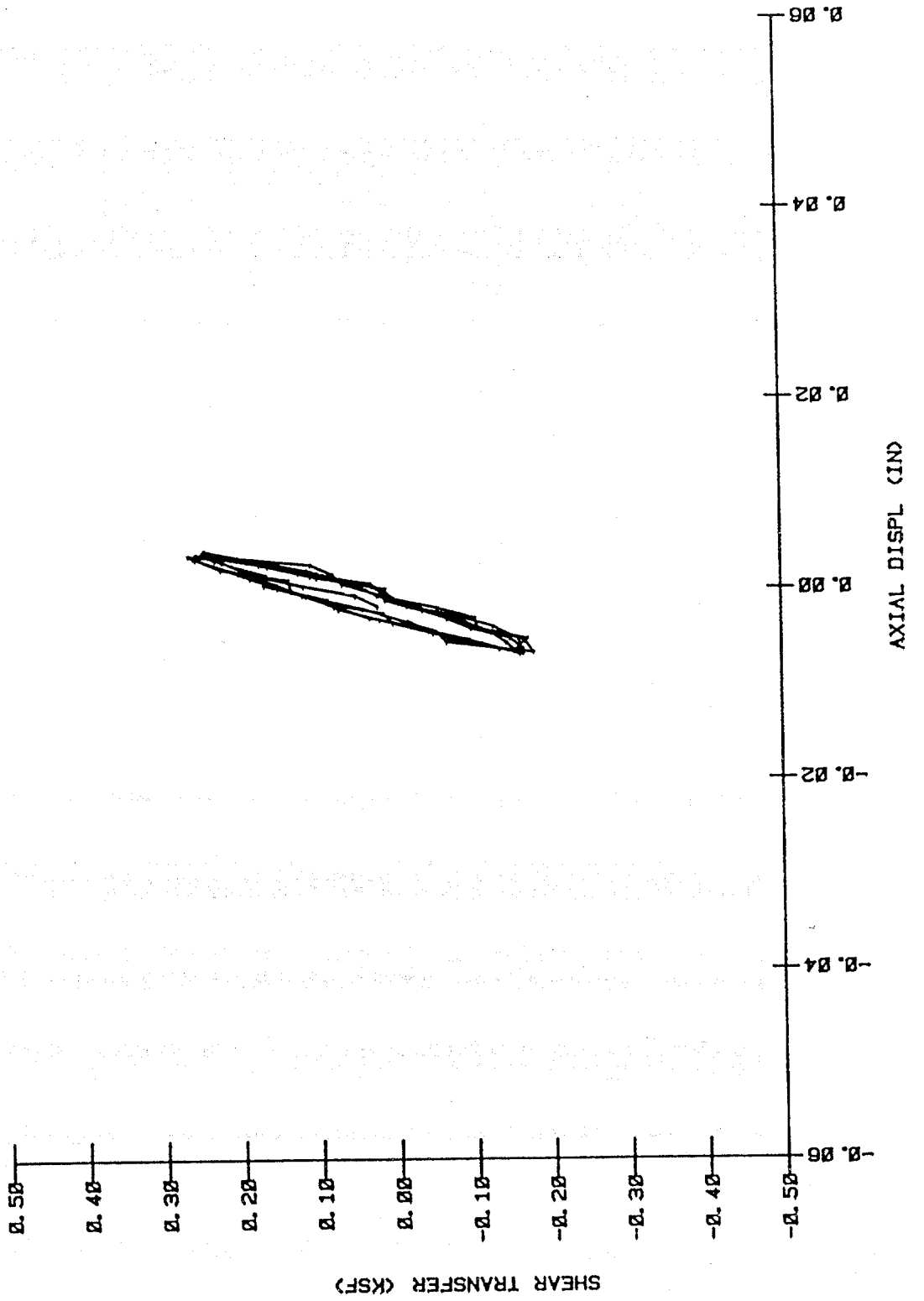
TEST HOLE 3 (cont.)

	<u>Page</u>
Shear vs Displacement (-.050 to .050 in)	A-56
Shear vs Displacement (Composite)	A-57
Pull-Out Test	
Shear vs Displacement	A-58

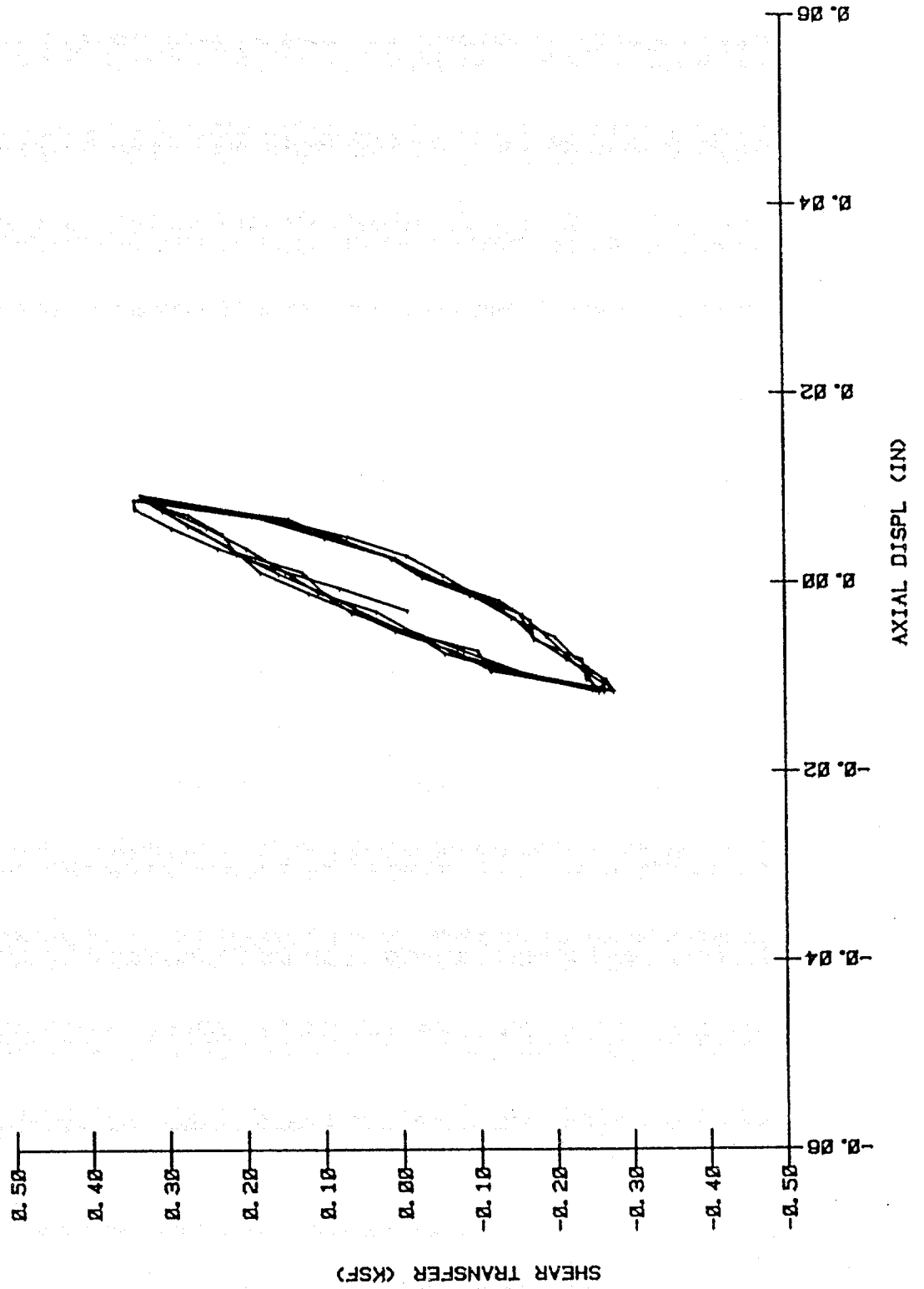
IMMEDIATE TEST
HOLE 3 - DEPTH 1
05 DEC 1982 11:32



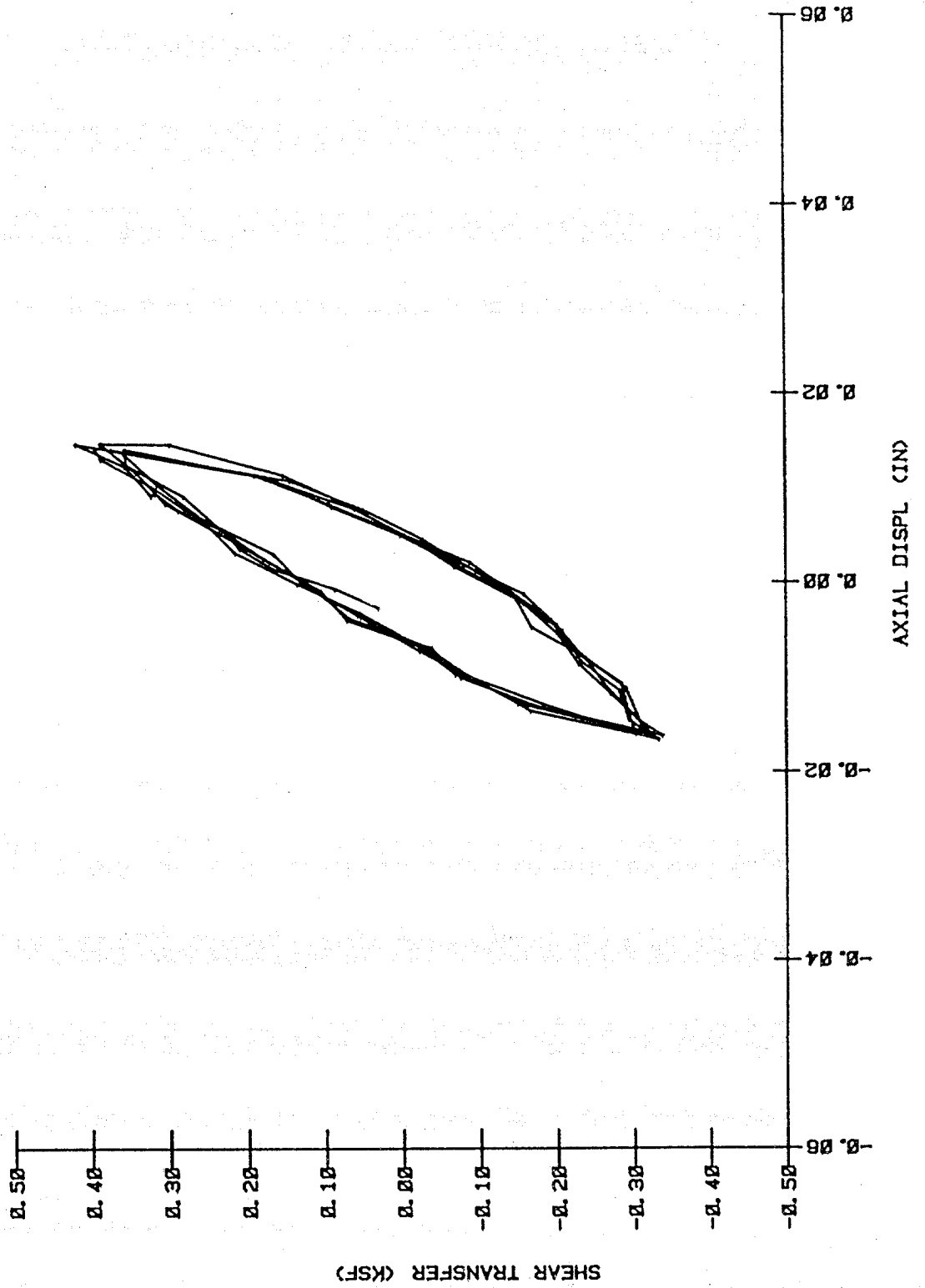
SHORT-TERM TEST
HOLE 3 - DEPTH 1
05 DEC 1982 19:53



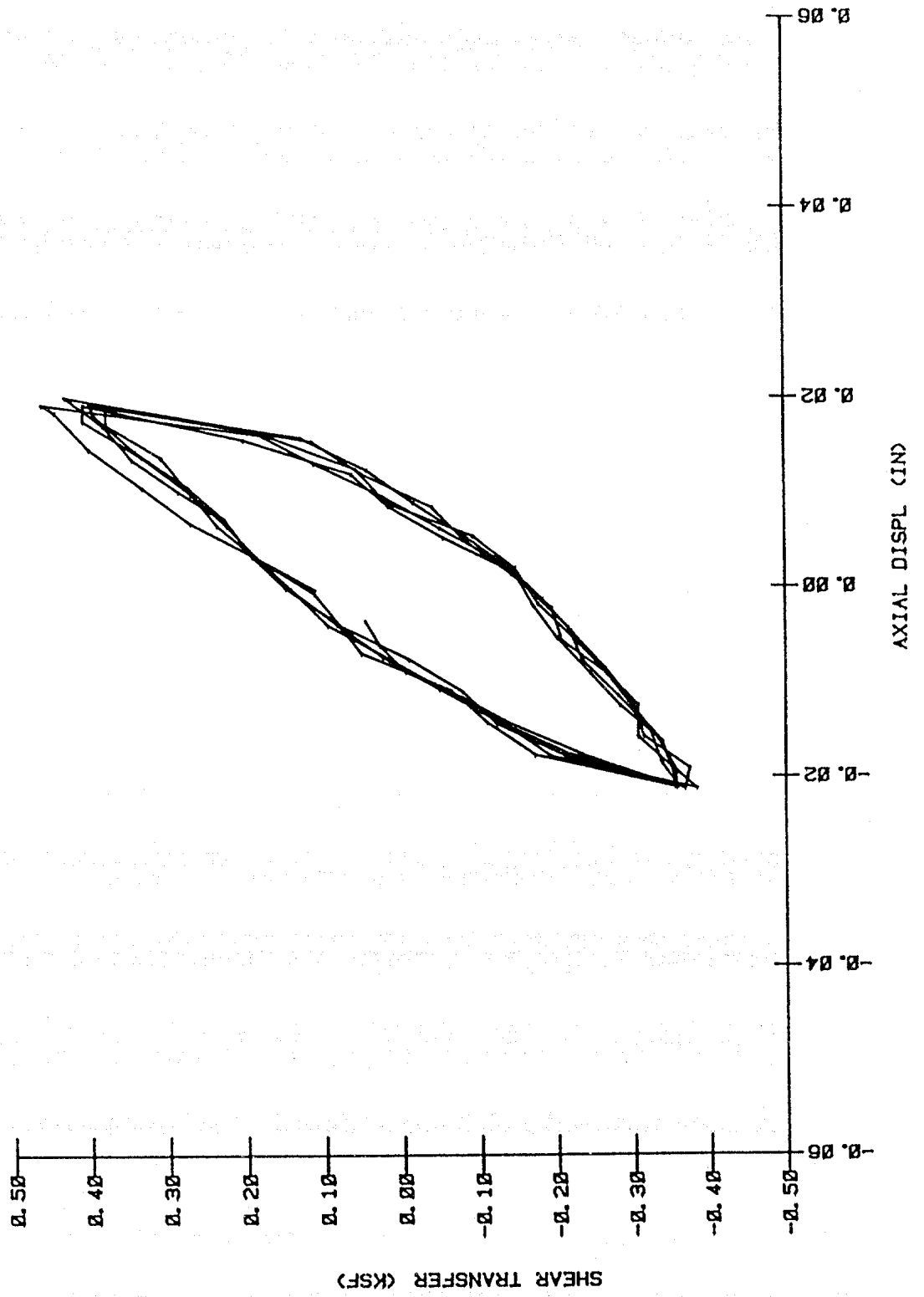
SHORT-TERM TEST
HOLE 3 - DEPTH 1
05 DEC 1982 19:53



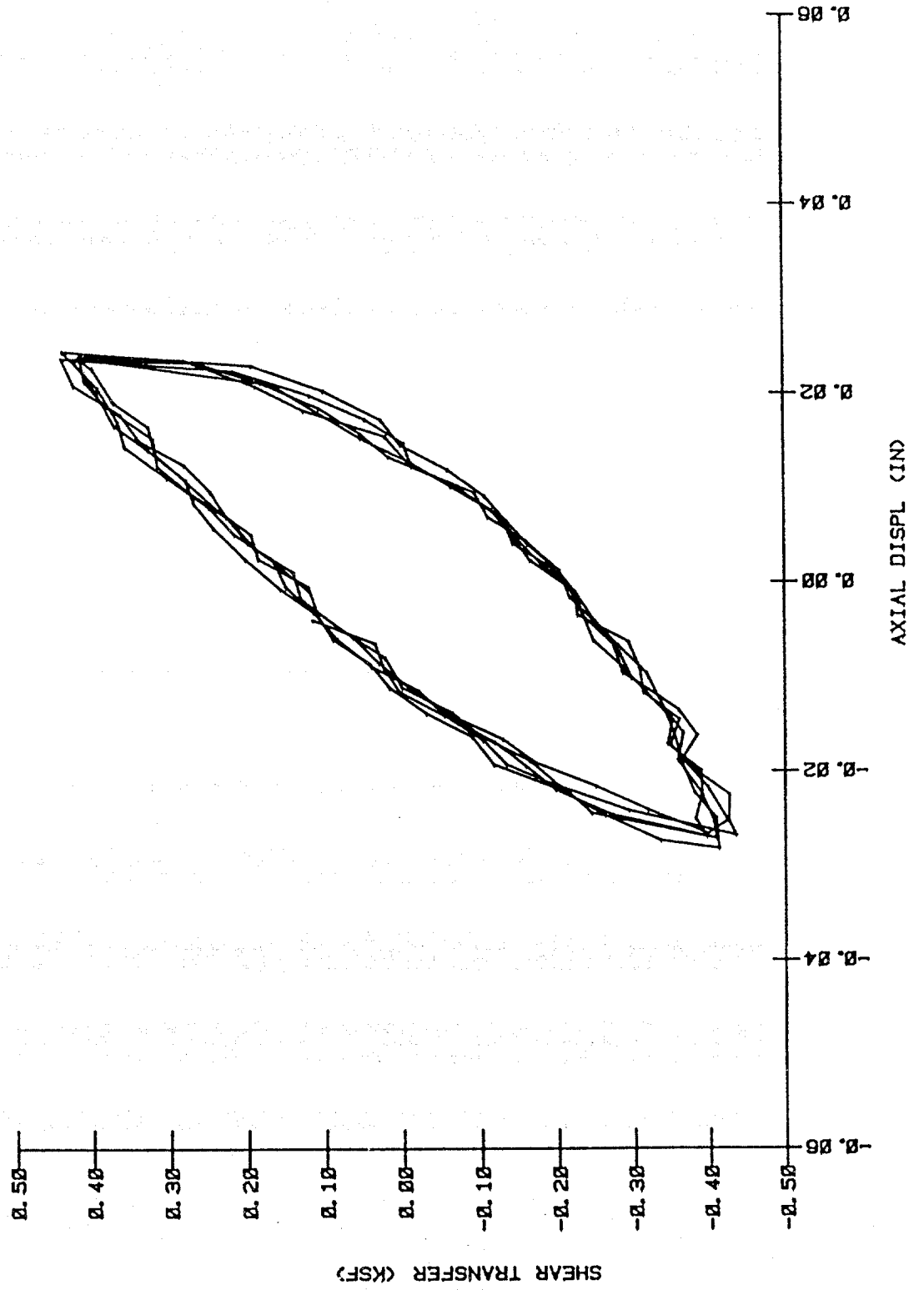
SHORT-TERM TEST
HOLE 3 - DEPTH 1
05 DEC 1982 19:53



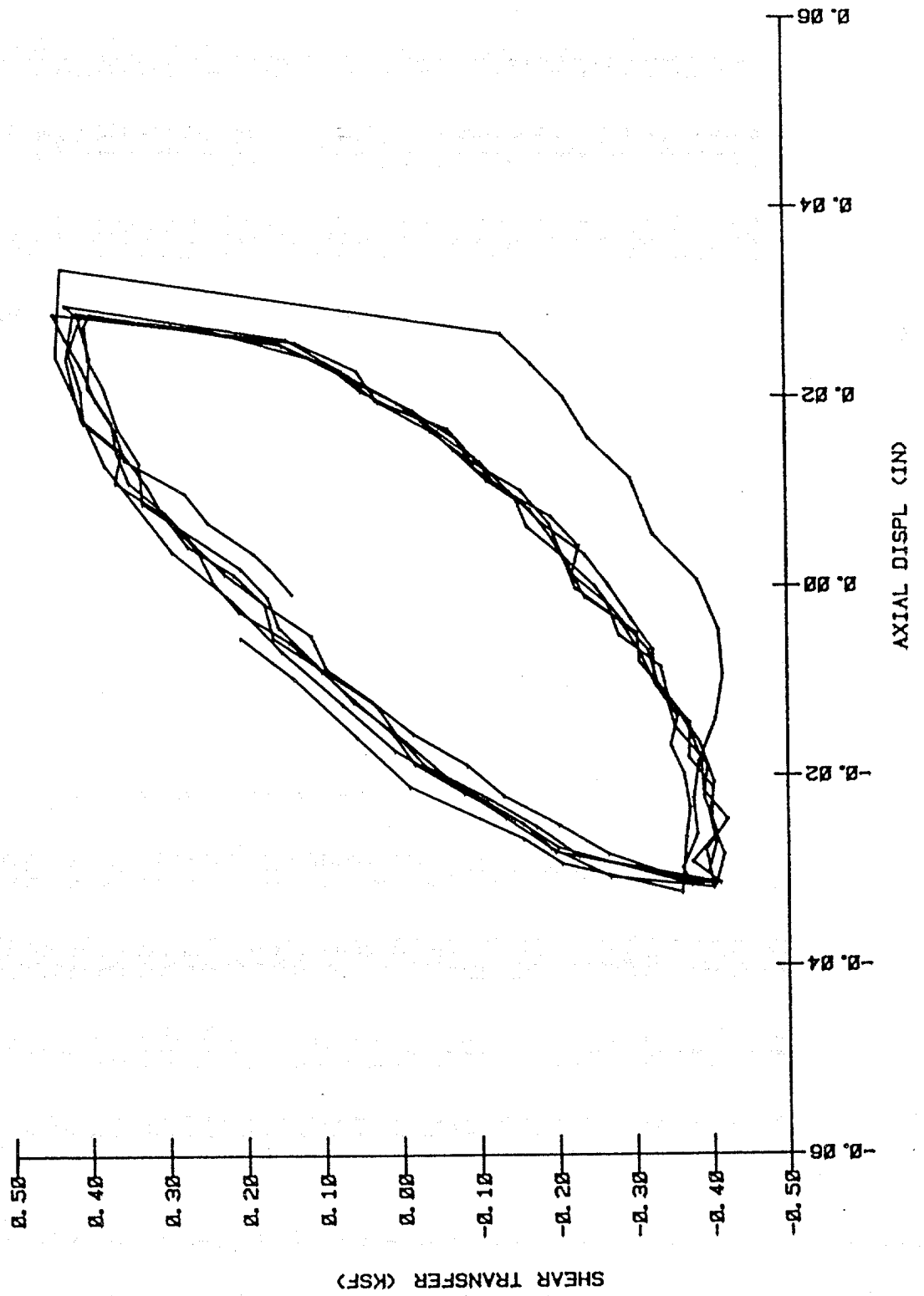
SHORT-TERM TEST
 HOLE 3 - DEPTH 1
 05 DEC 1982 19:53



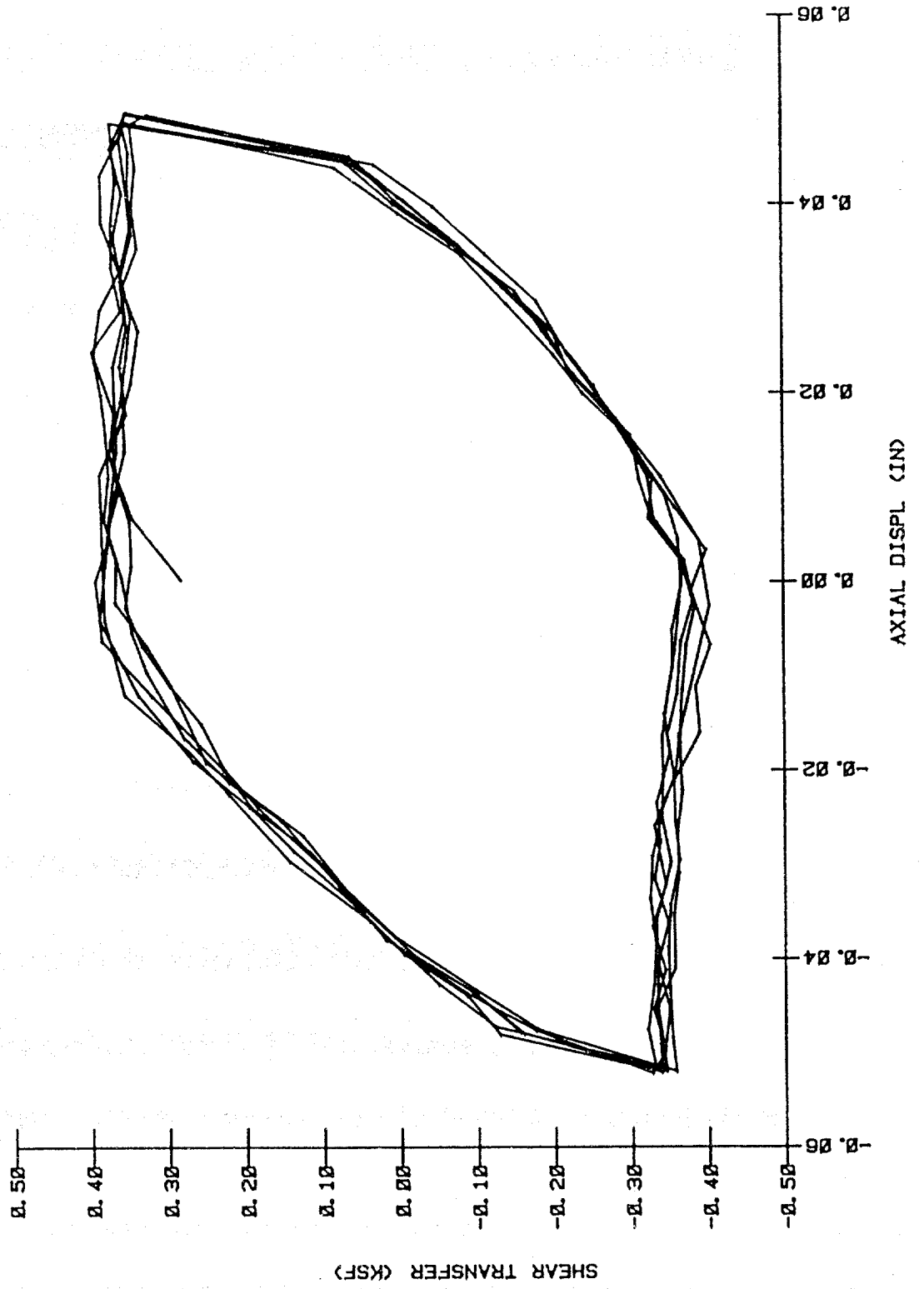
SHORT-TERM TEST
HOLE 3 - DEPTH 1
05 DEC 1982 19:53



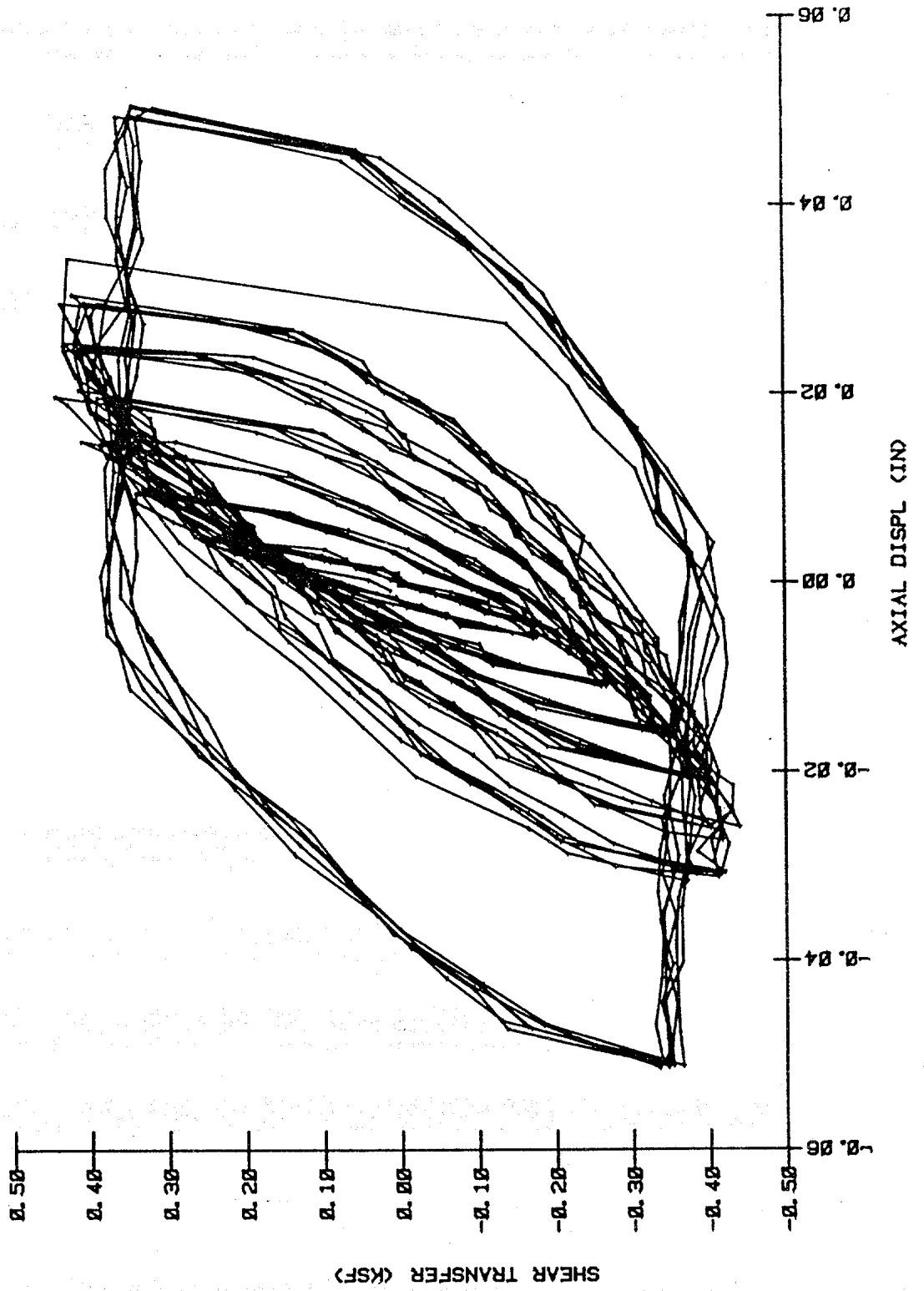
SHORT-TERM TEST
HOLE 3 - DEPTH 1
05 DEC 1982 19:53



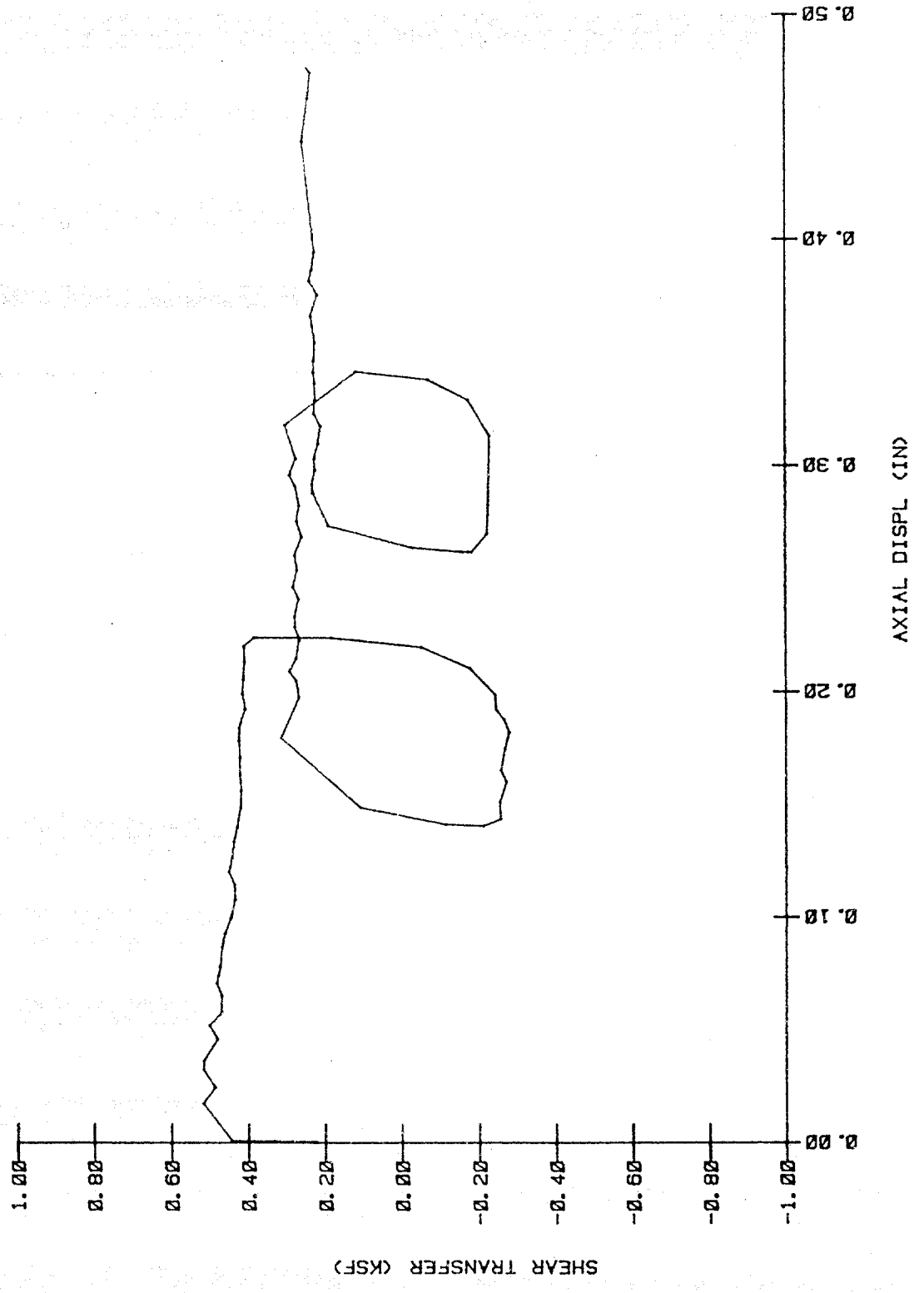
SHORT-TERM TEST
HOLE 3 - DEPTH 1
05 DEC 1982 19:53



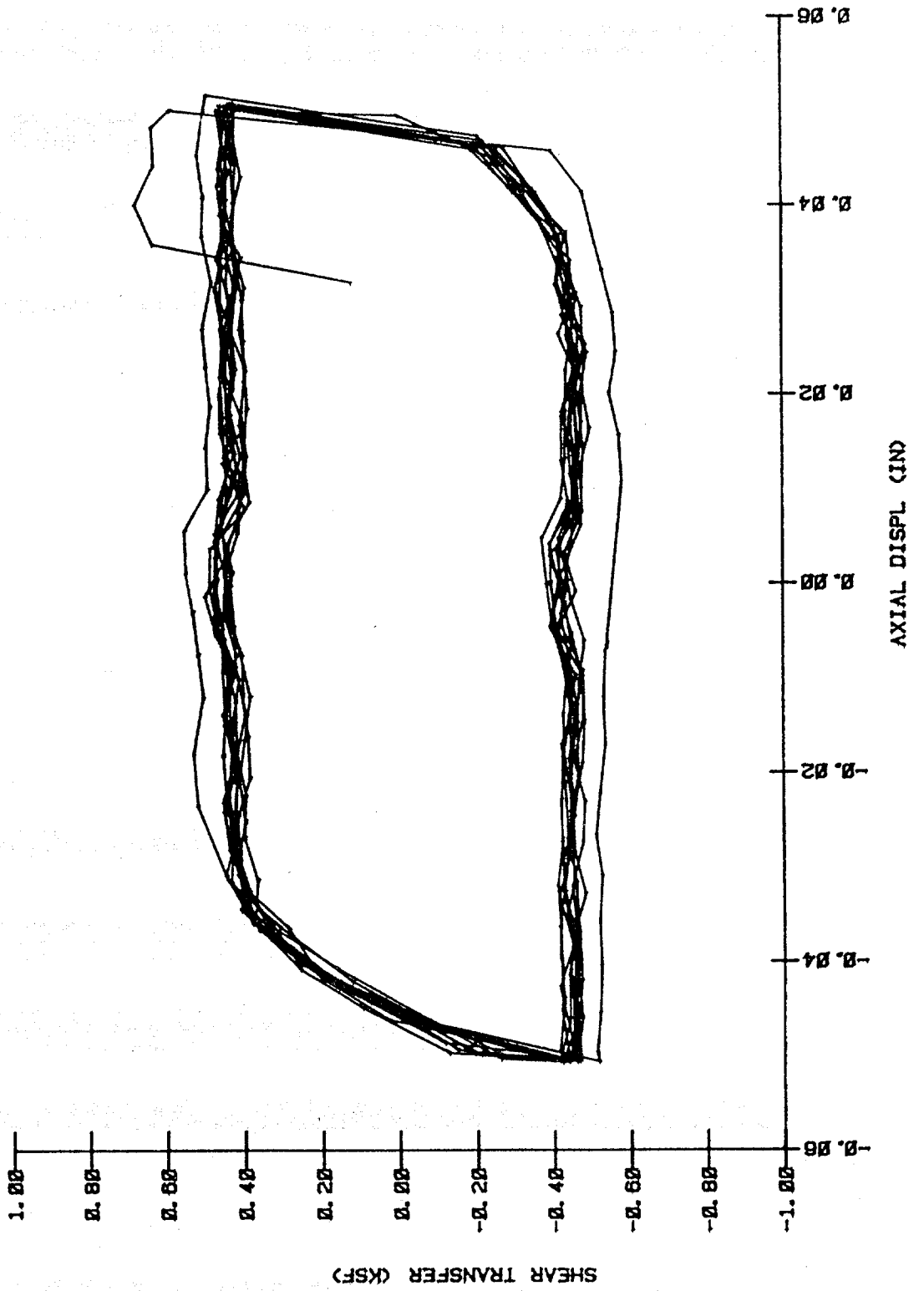
SHORT-TERM TEST
HOLE 3 - DEPTH 1
05 DEC 1982 19:53



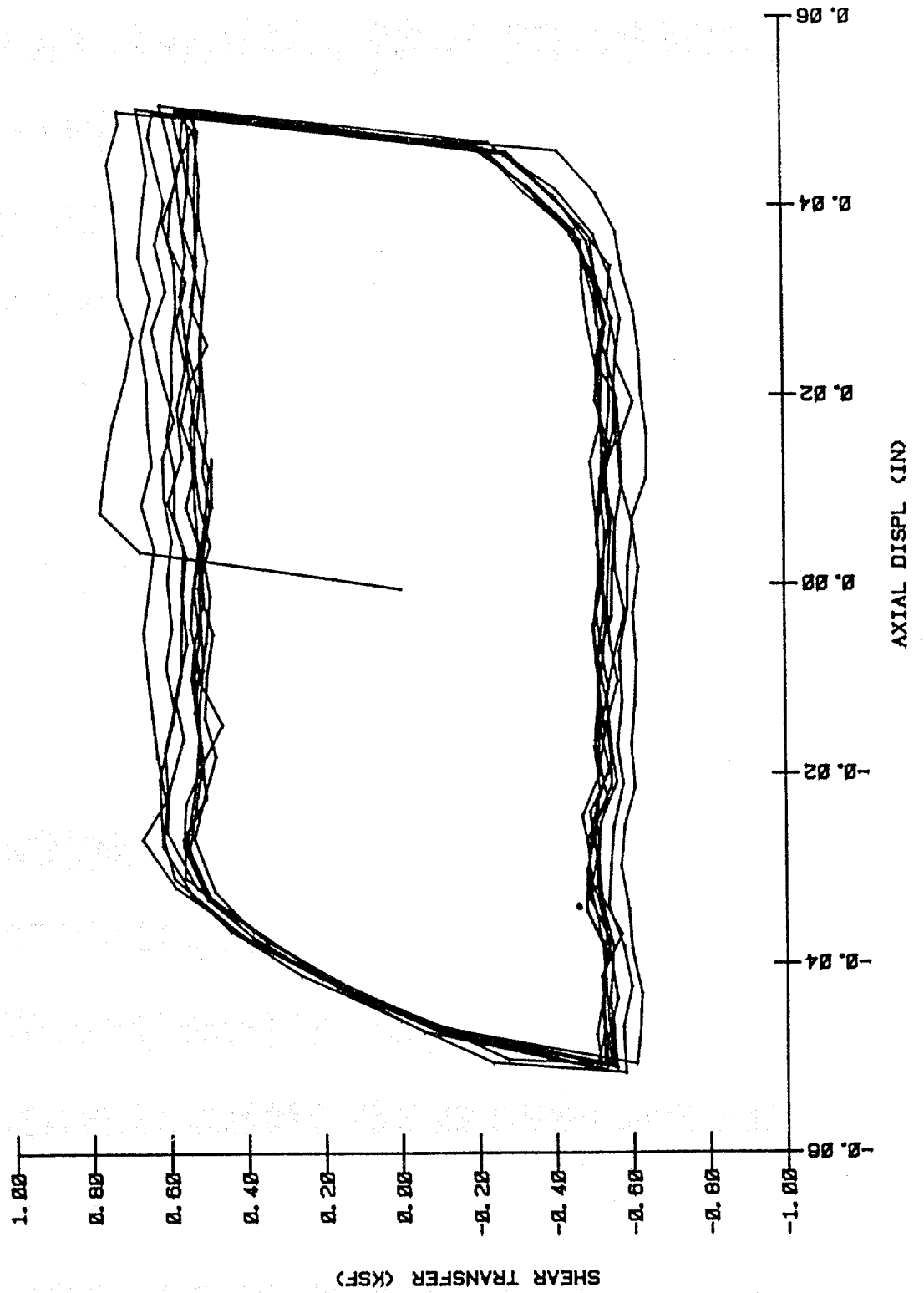
IMMEDIATE TEST
HOLE 3 - DEPTH 2
06 DEC 1982 11:52



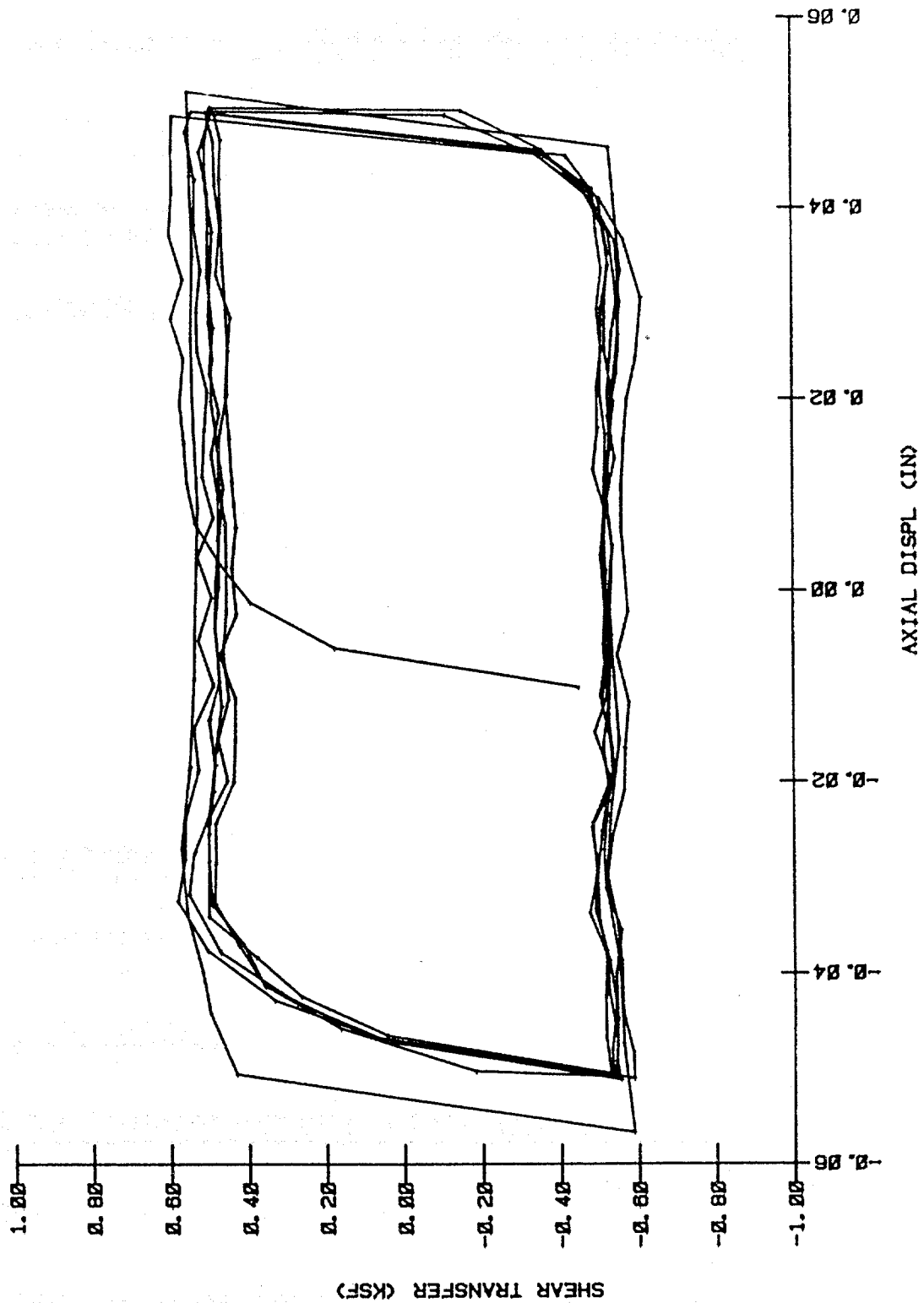
SHORT-TERM TEST
HOLE 3 - DEPTH 2
06 DEC 1982 20:07



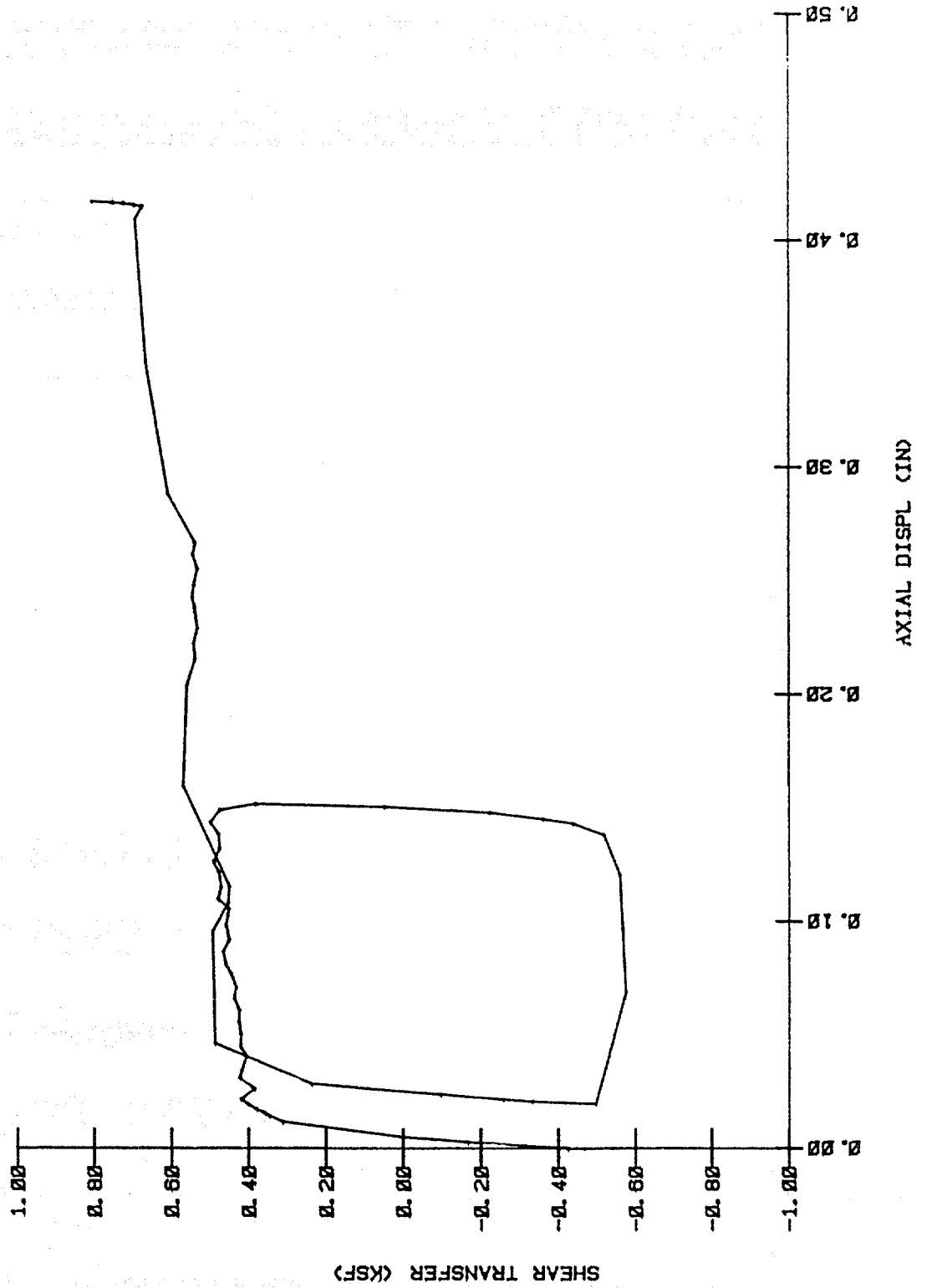
20-HOUR TEST
HOLE 3 - DEPTH 2
07 DEC 1982 08:15



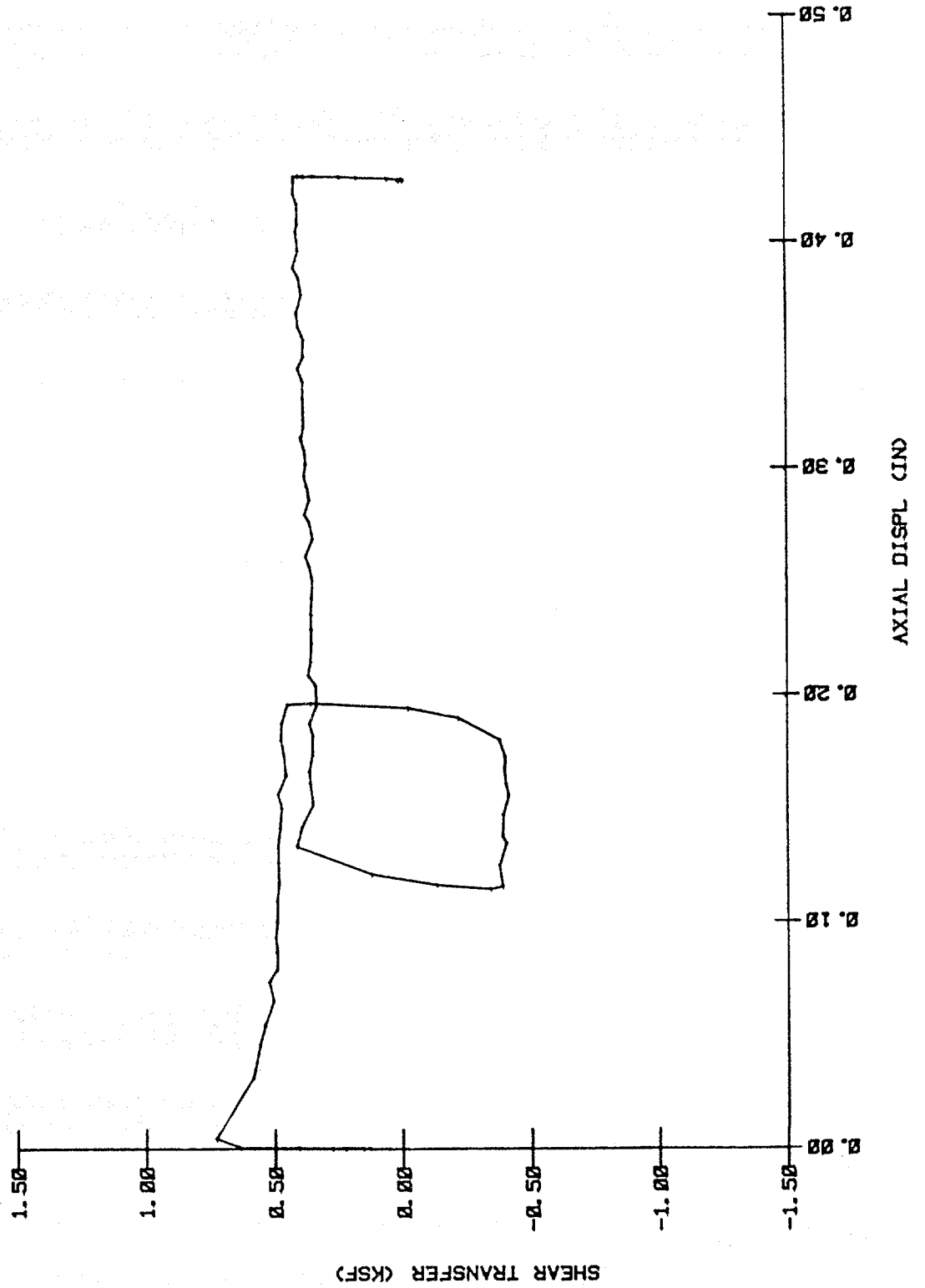
44-HOUR TEST
HOLE 3 - DEPTH 2
08 DEC 1982 07:44



PULL-OUT TEST
HOLE 3 - DEPTH 2
08 DEC 1982 08:12



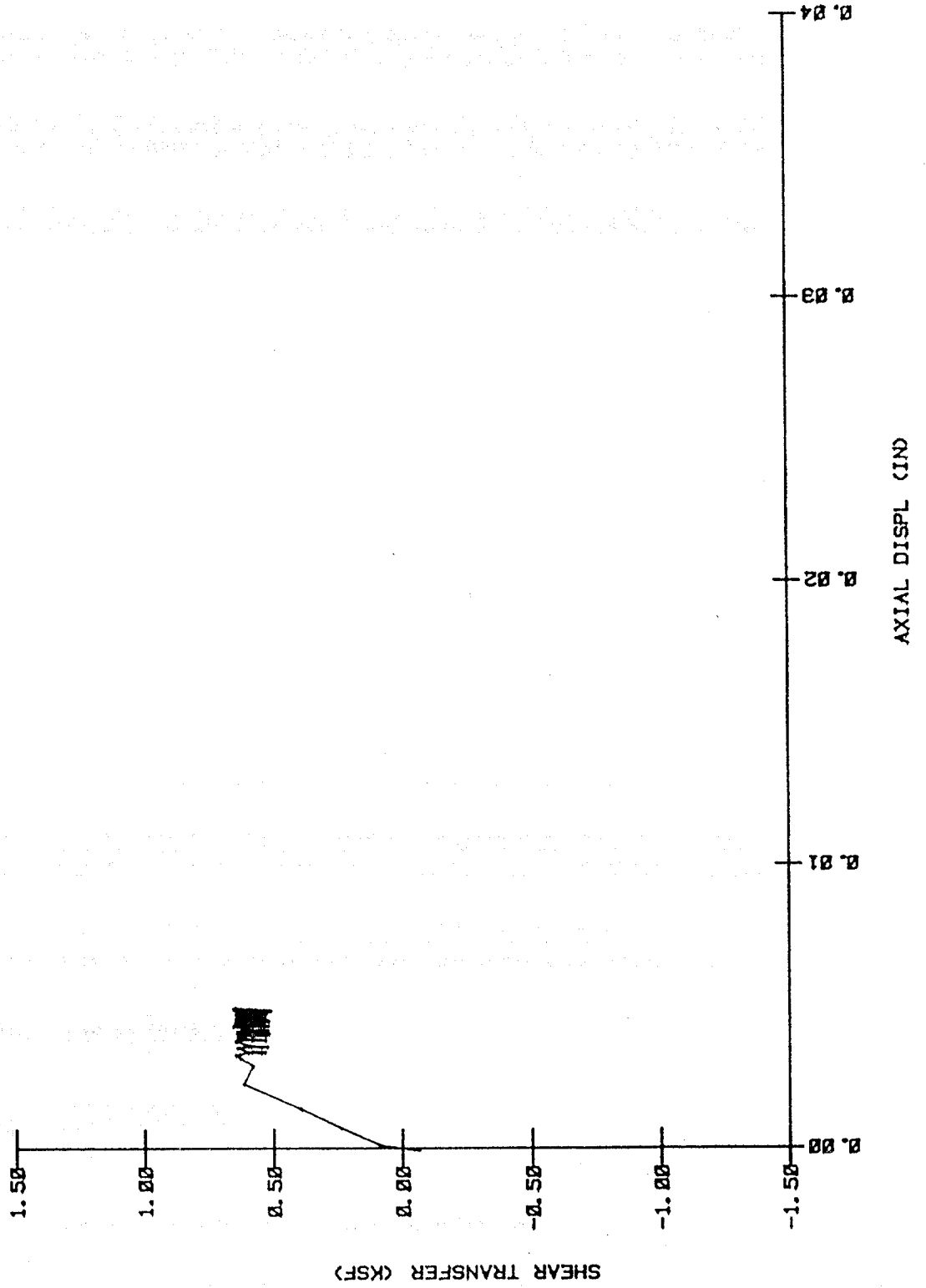
IMMEDIATE TEST
HOLE 3 - DEPTH 3
08 DEC 1982 11:51



ONE-WAY TENSION TEST

HOLE 3 - DEPTH 3

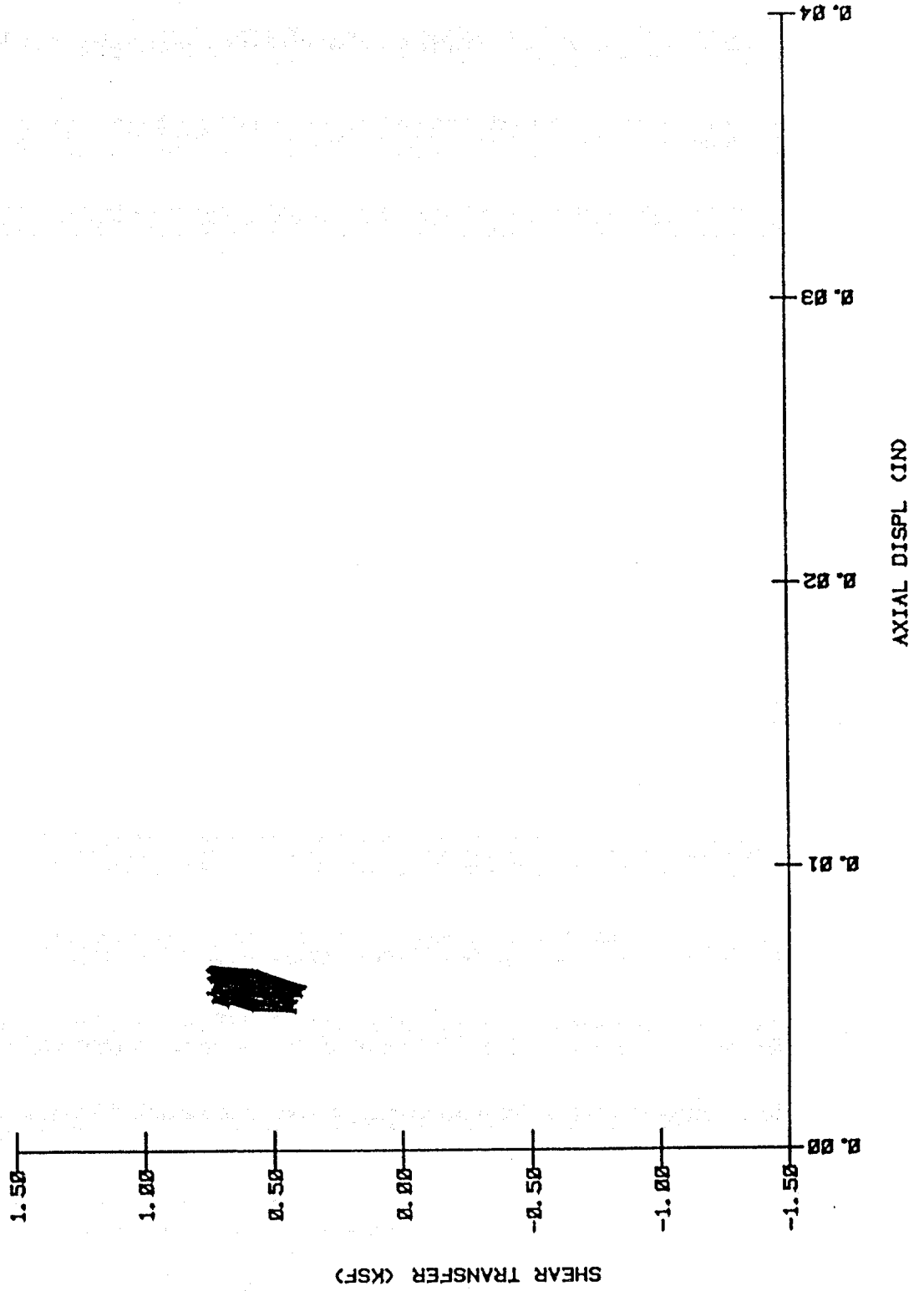
08 DEC 1982 20:08



ONE-WAY TENSION TEST

HOLE 3 - DEPTH 3

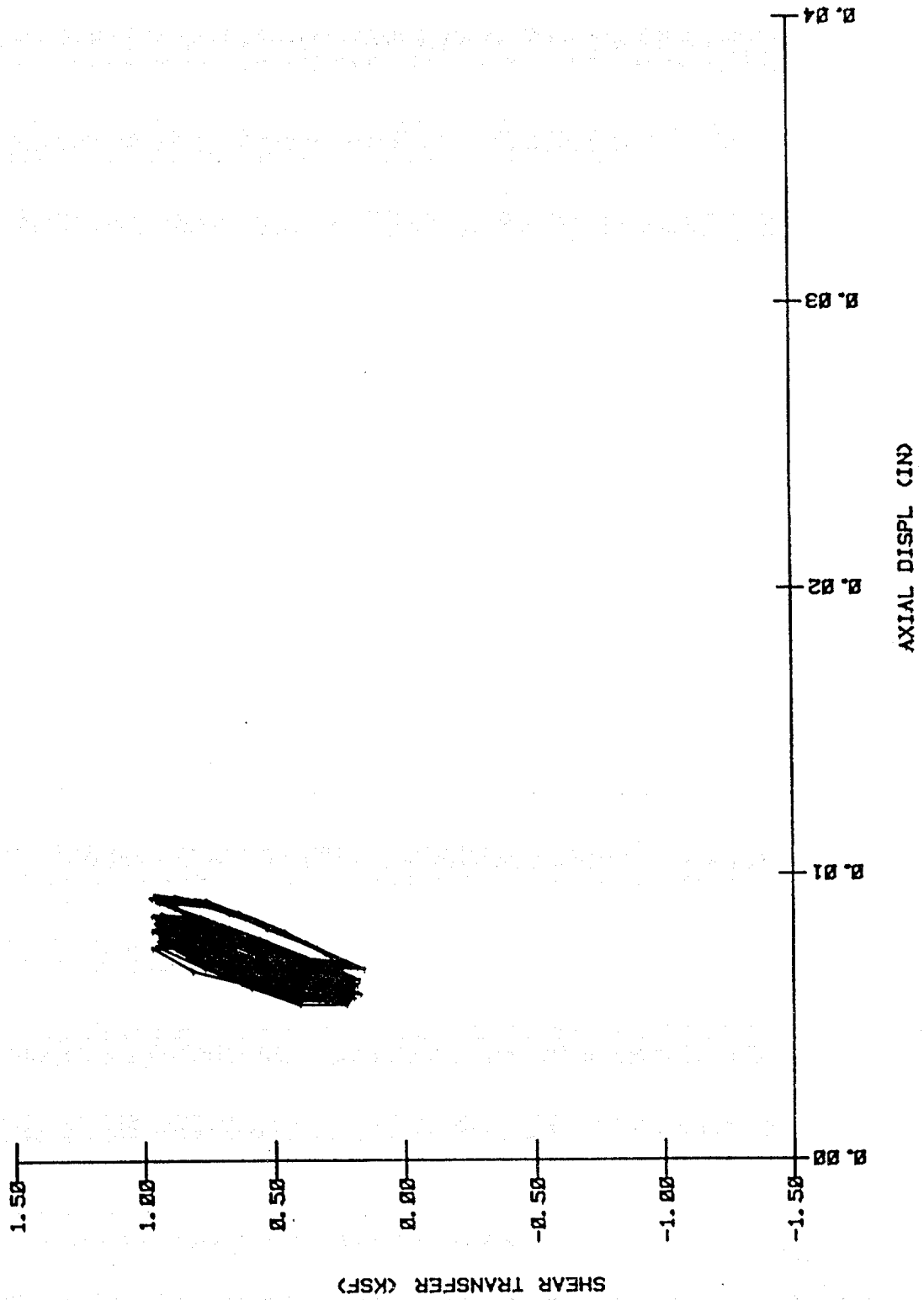
08 DEC 1982 20:08



ONE-WAY TENSION TEST

HOLE 3 - DEPTH 3

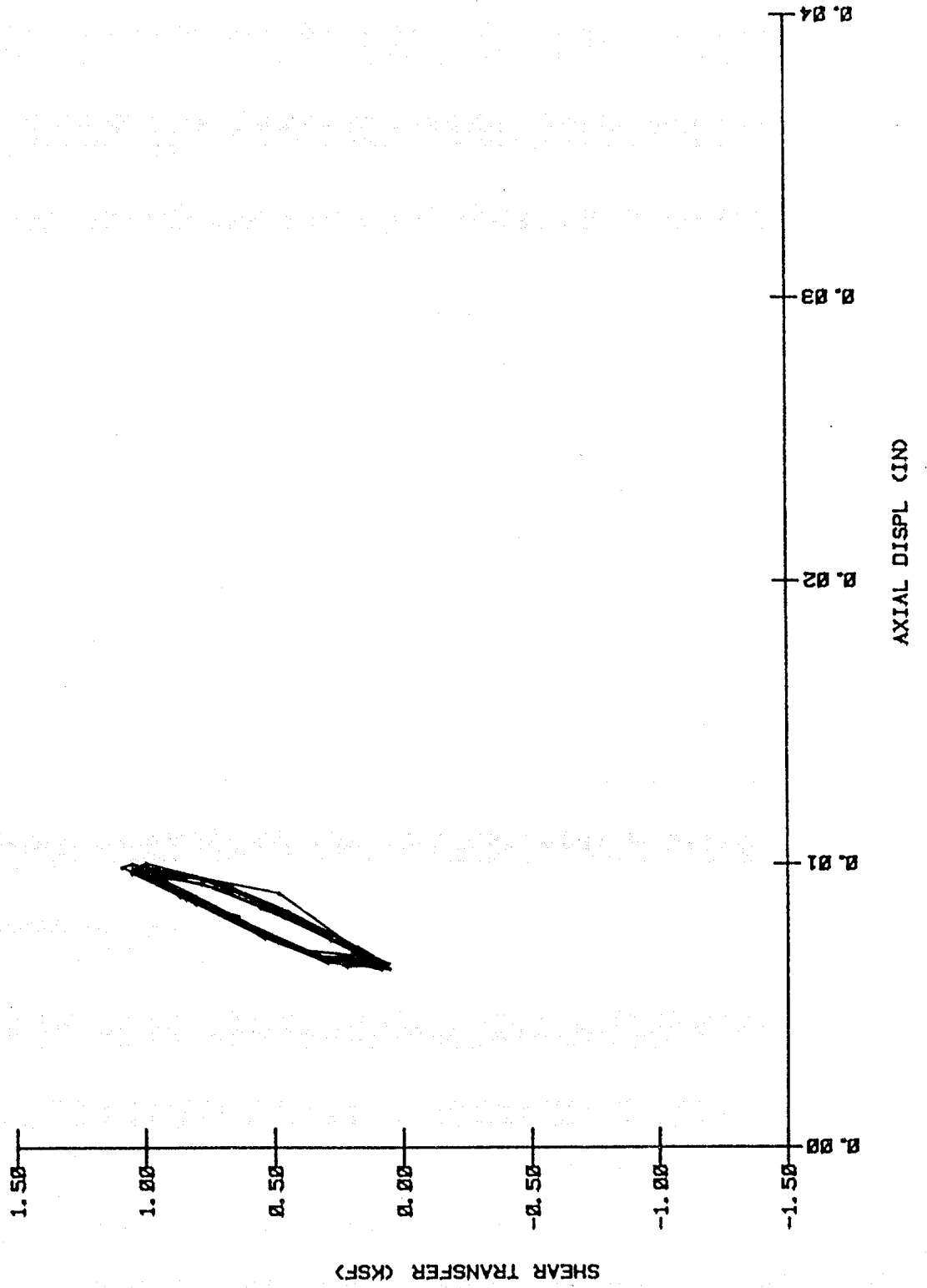
08 DEC 1982 20:08



ONE-WAY TENSION TEST

HOLE 3 - DEPTH 3

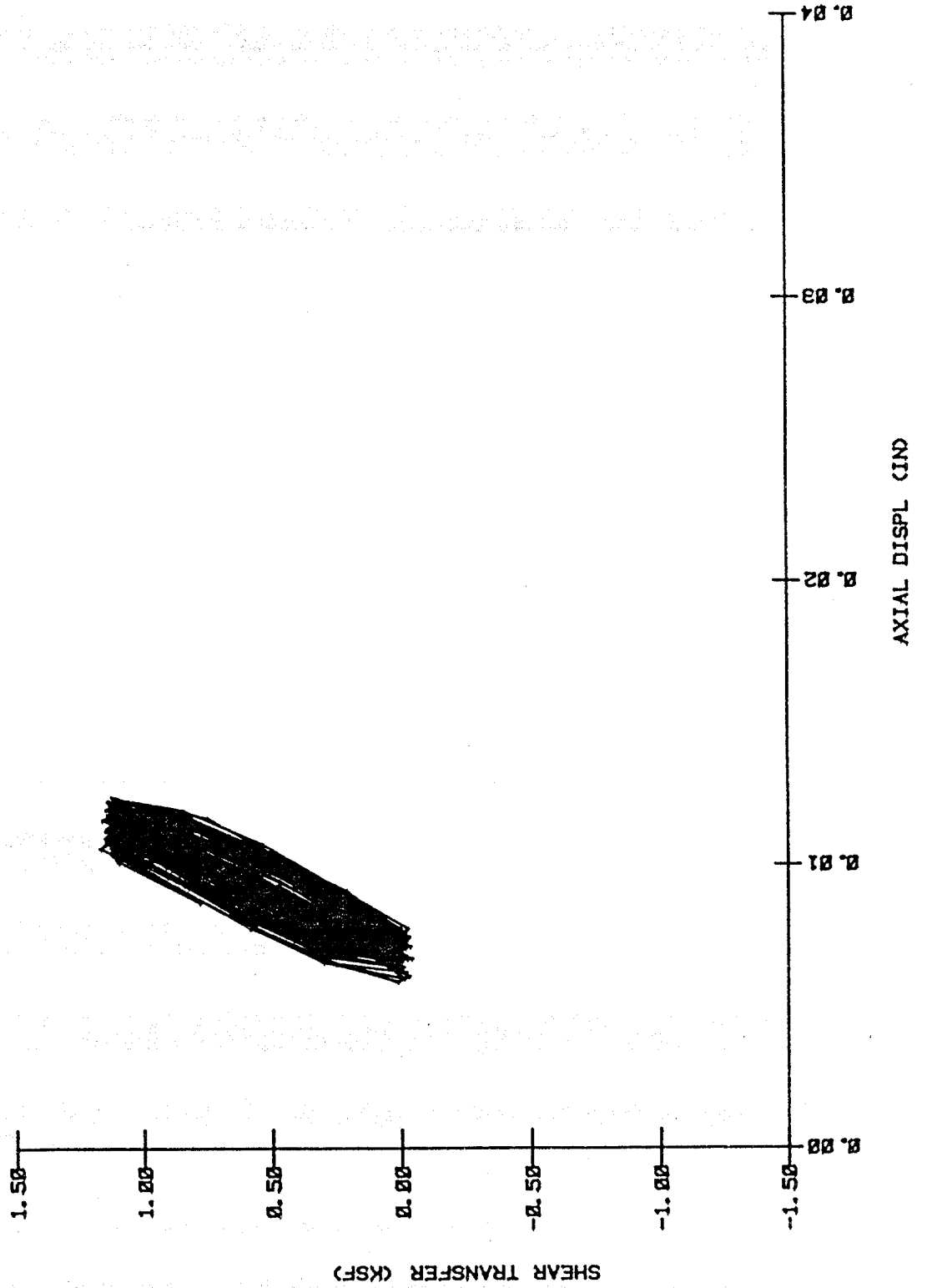
08 DEC 1982 20:08



ONE-WAY TENSION TEST

HOLE 3 - DEPTH 3

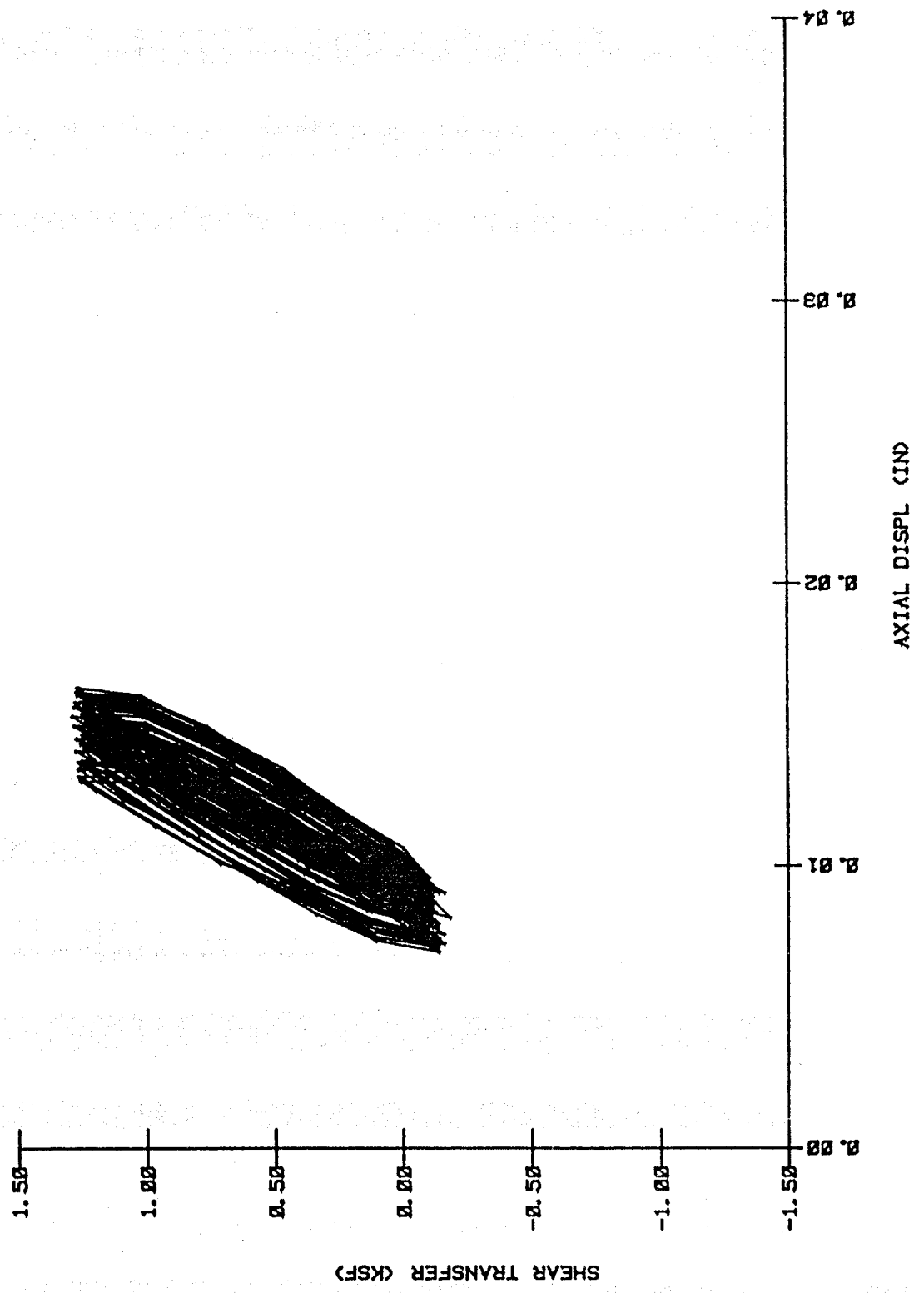
08 DEC 1982 20:08



ONE-WAY TENSION TEST

HOLE 3 - DEPTH 3

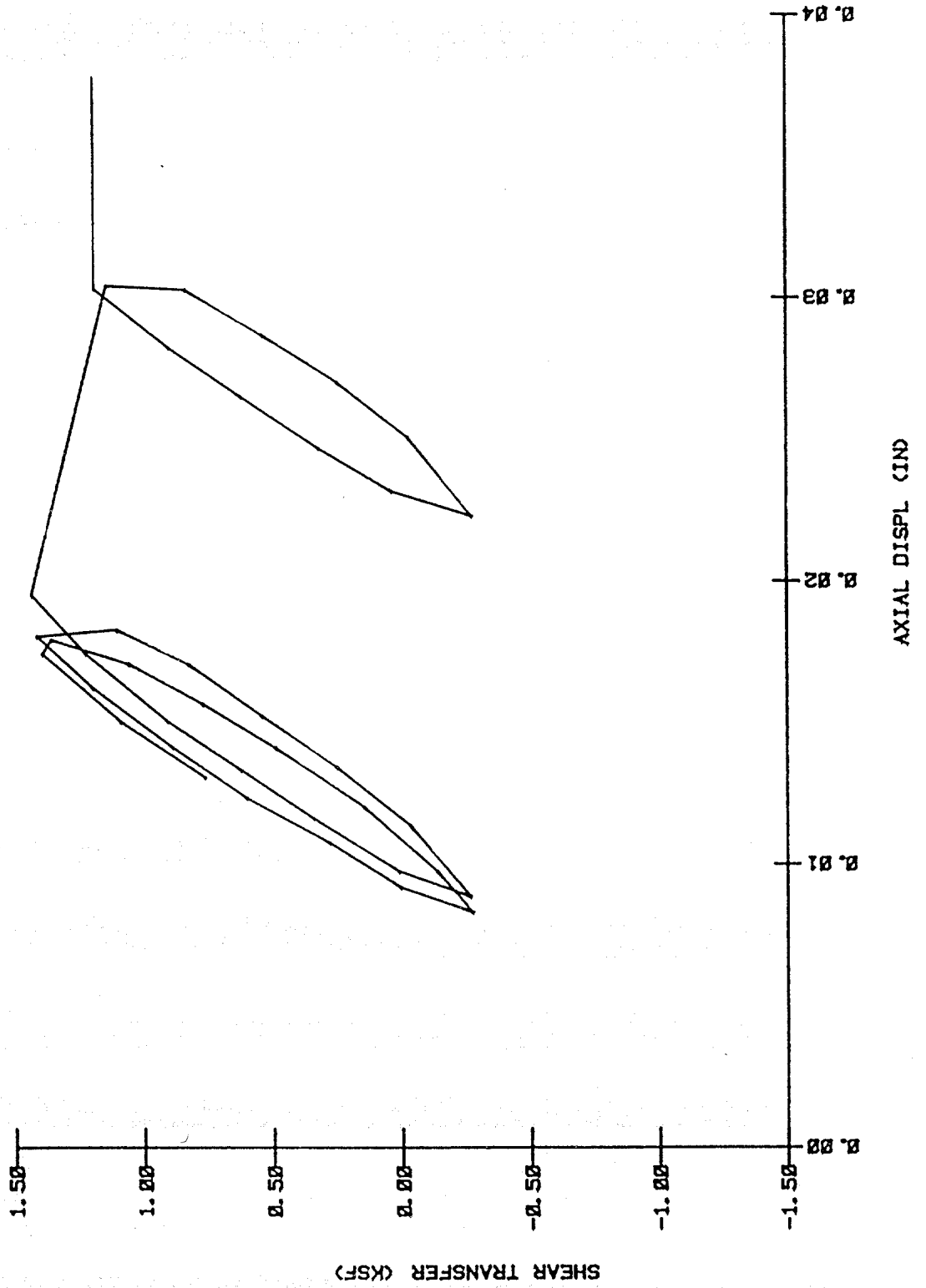
08 DEC 1982 20:08



ONE-WAY TENSION TEST

HOLE 3 - DEPTH 3

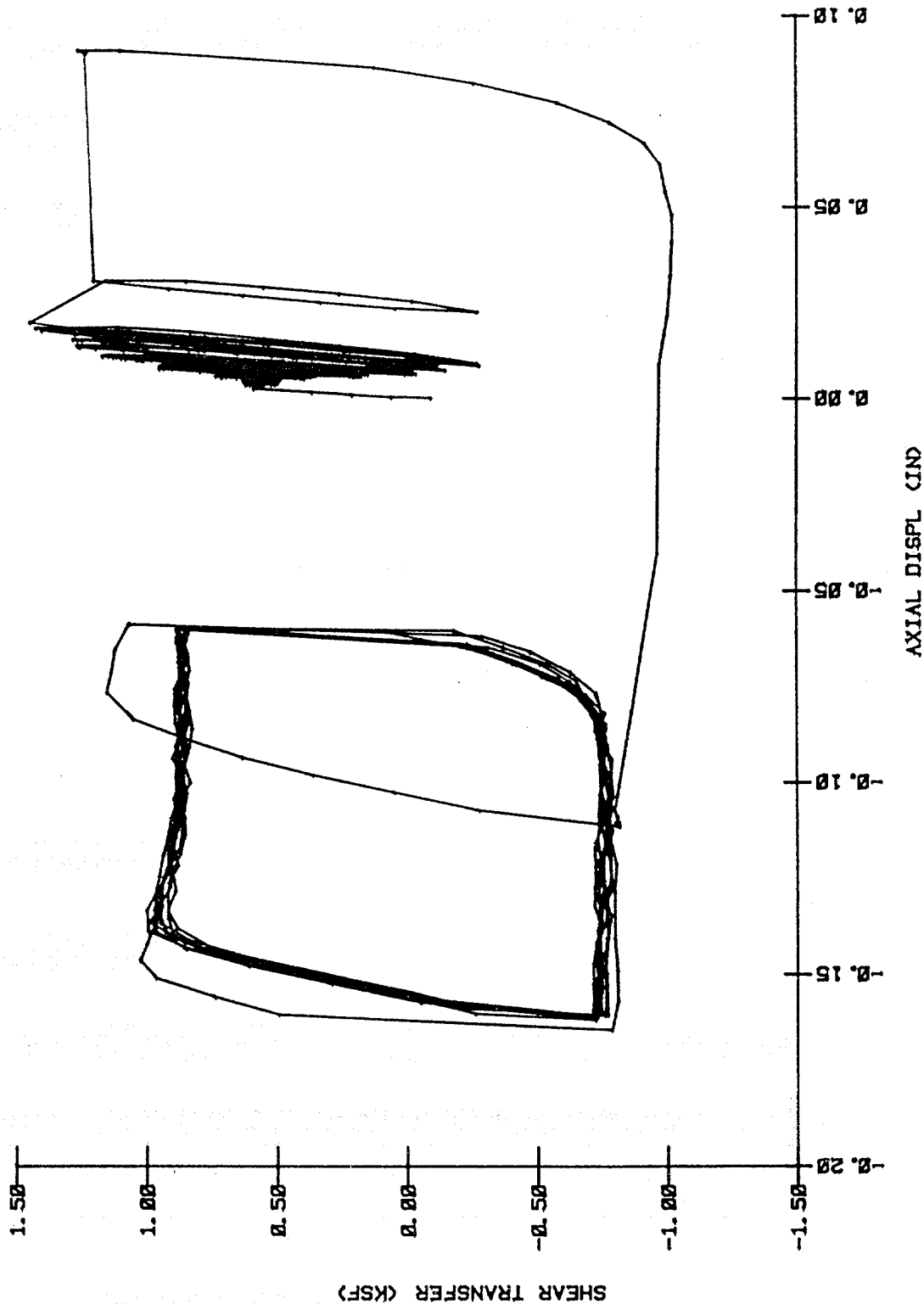
08 DEC 1982 20:08



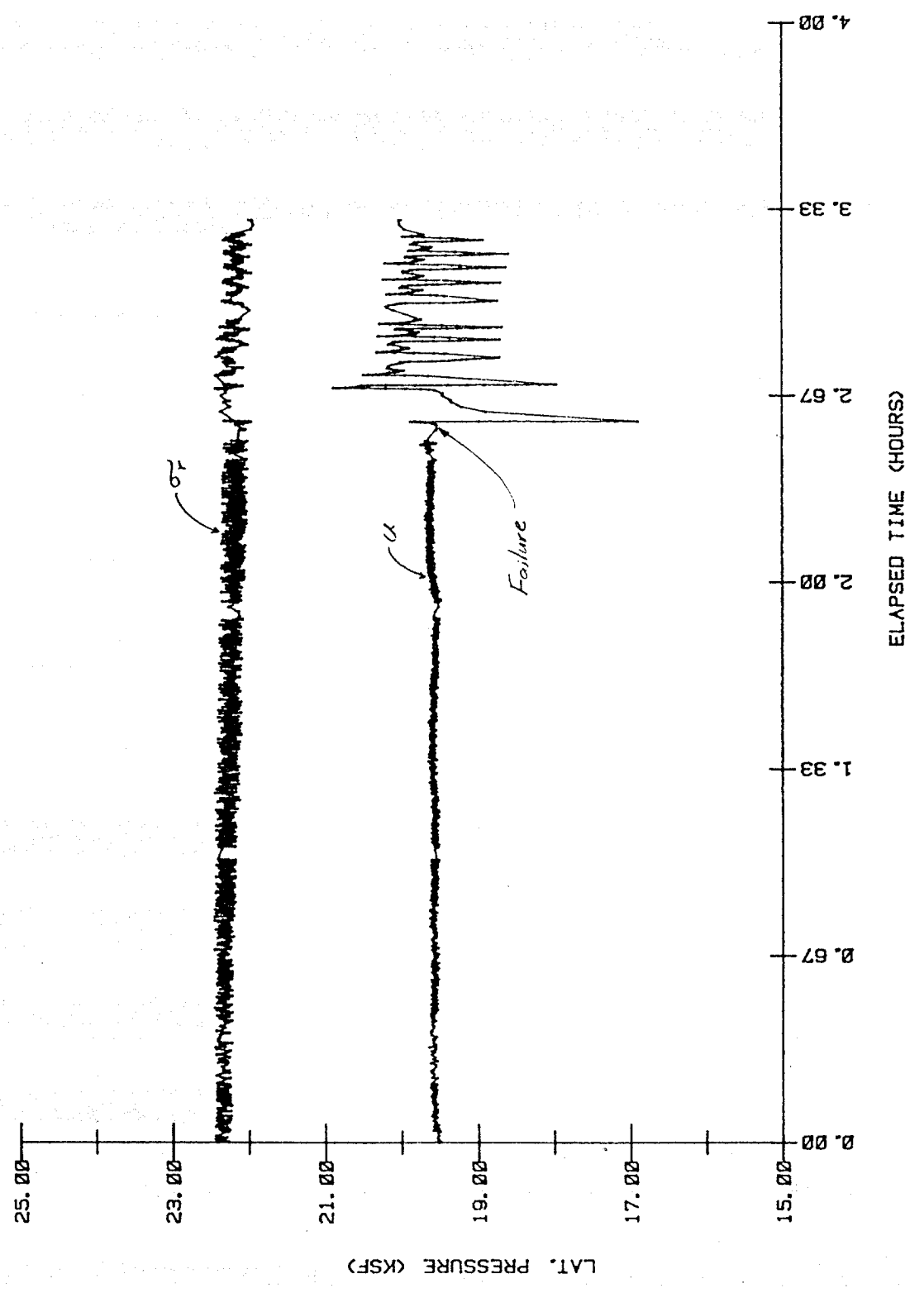
ONE-WAY TENSION TEST

HOLE 3 - DEPTH 3

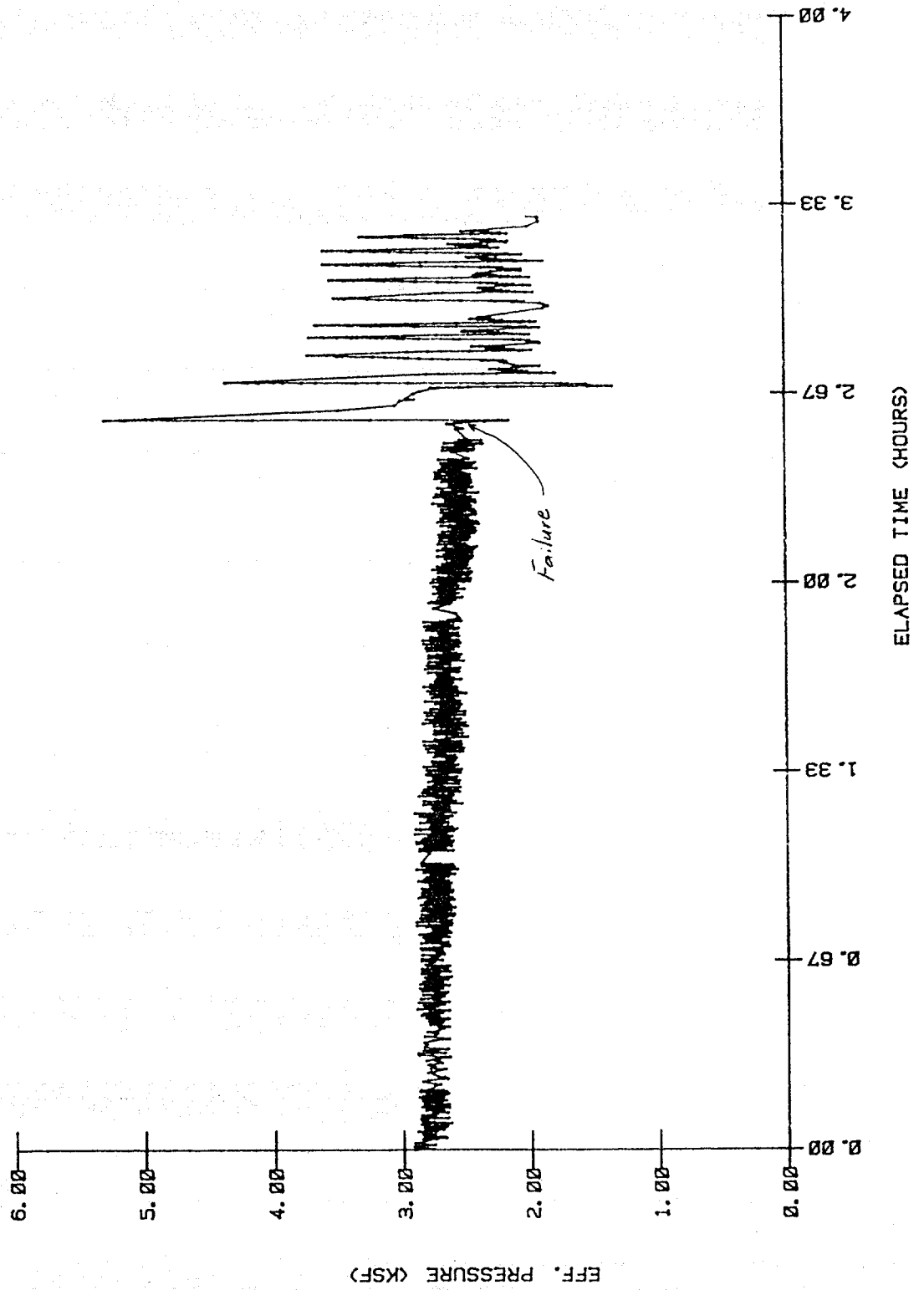
08 DEC 1982 20:08



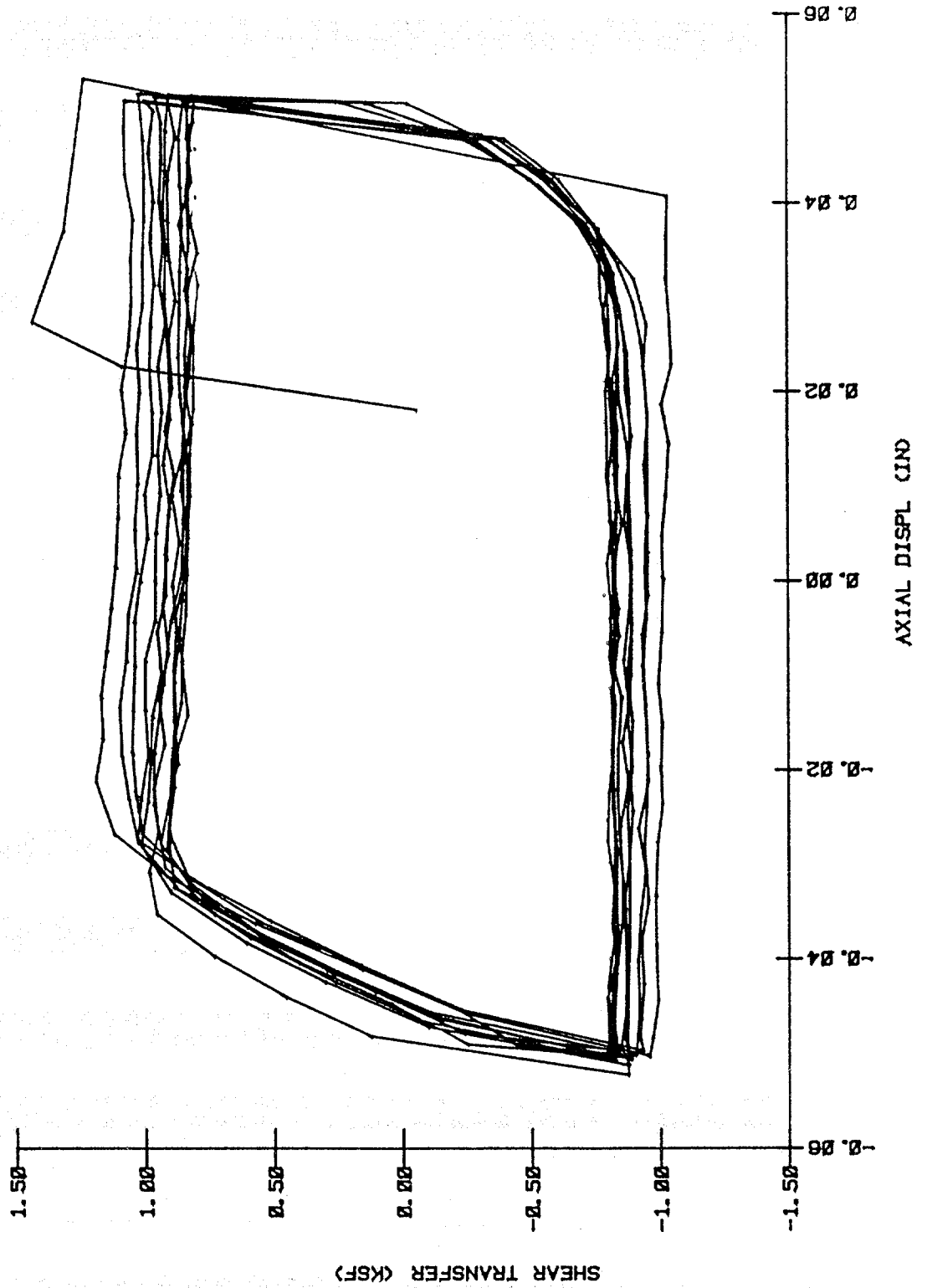
PRESSURE DURING TEST
WEST DELTA BLOCK 58A
HOLE 3 AT 178 FT



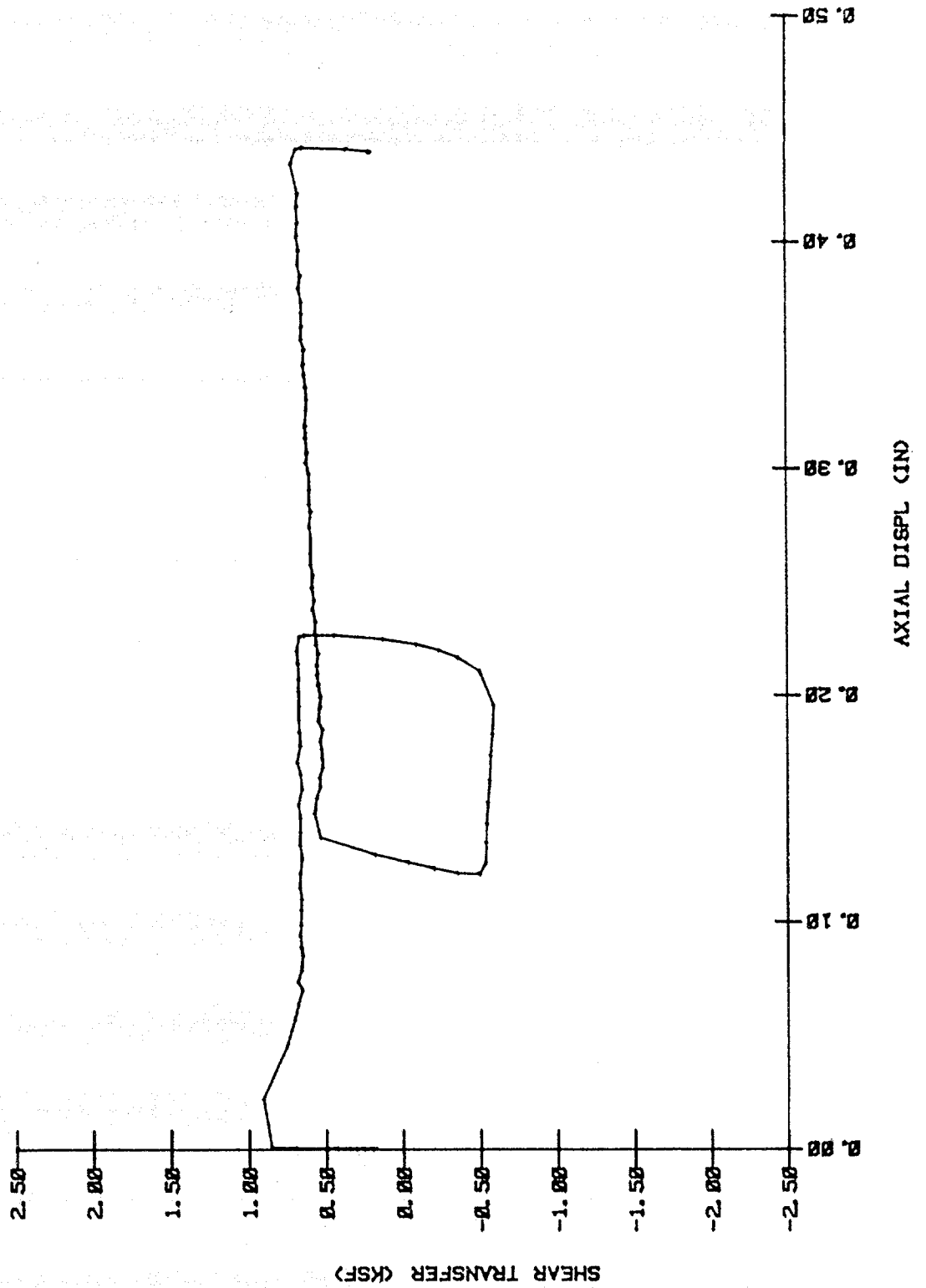
PRESSURE DURING TEST
WEST DELTA BLOCK 58A
HOLE 3 AT 178 FT



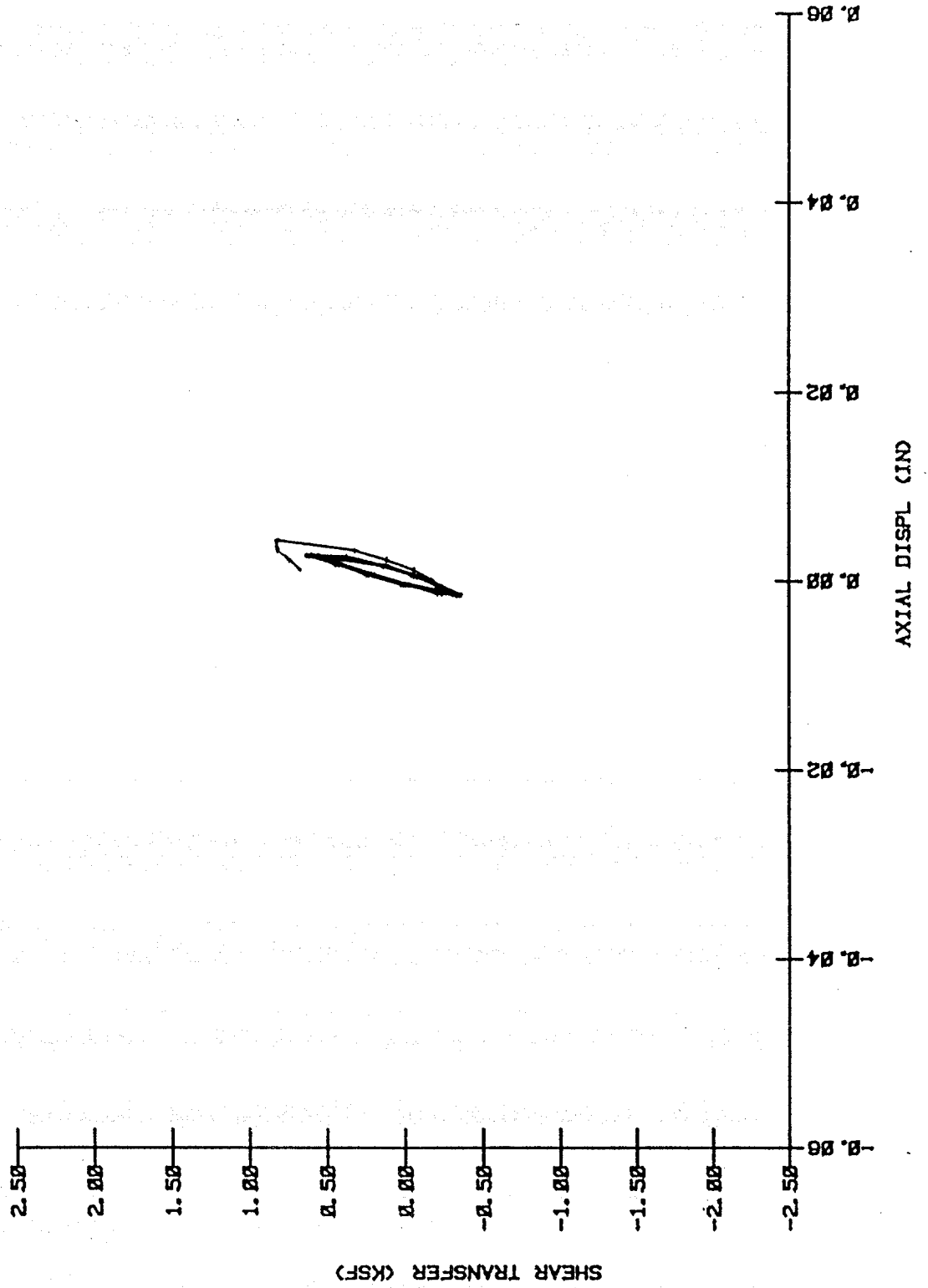
20-HOUR TEST
HOLE 3 - DEPTH 3
09 DEC 1982 07:18



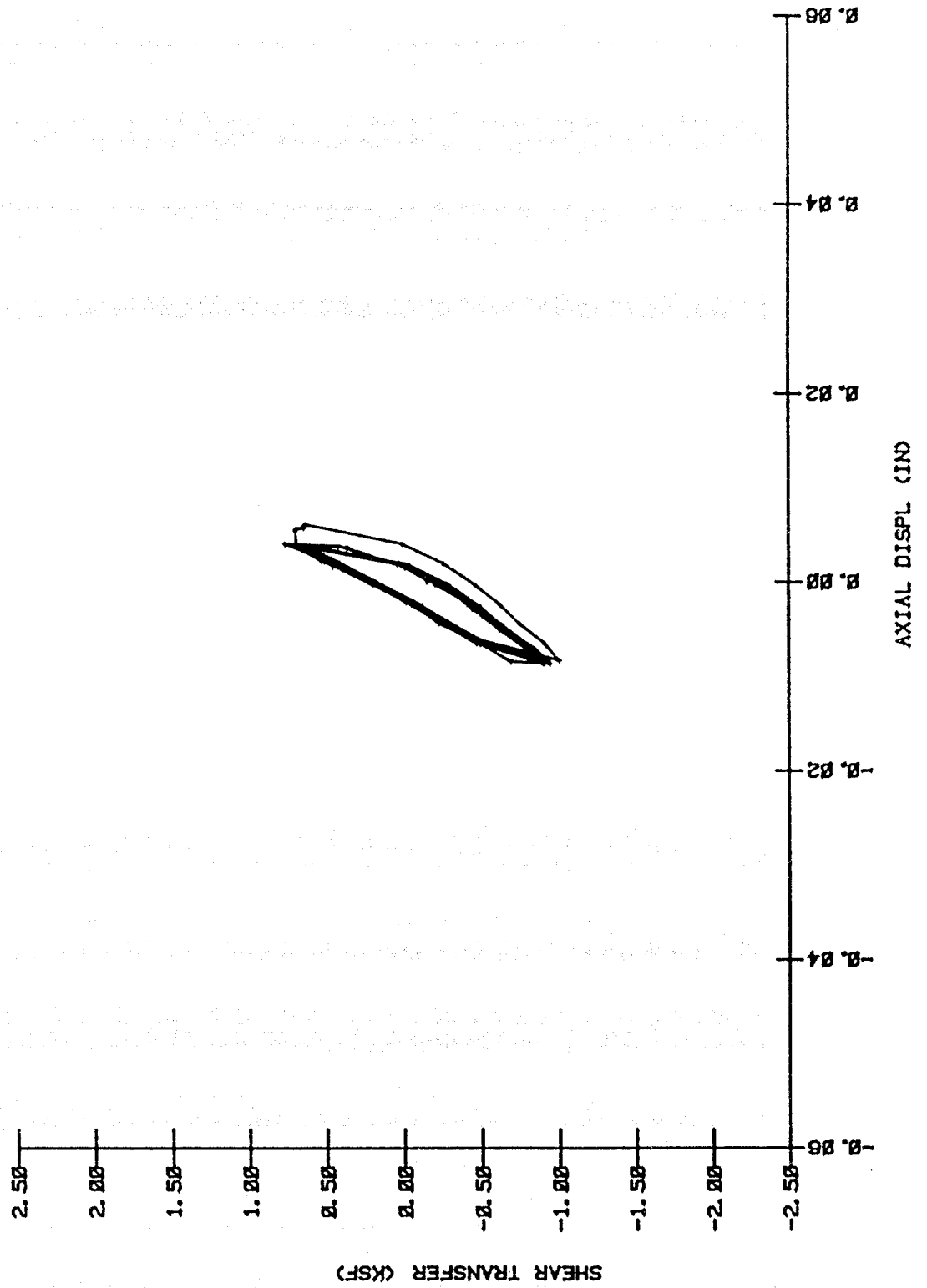
IMMEDIATE TEST
HOLE 3 - DEPTH 4
09 DEC 1982 13:30



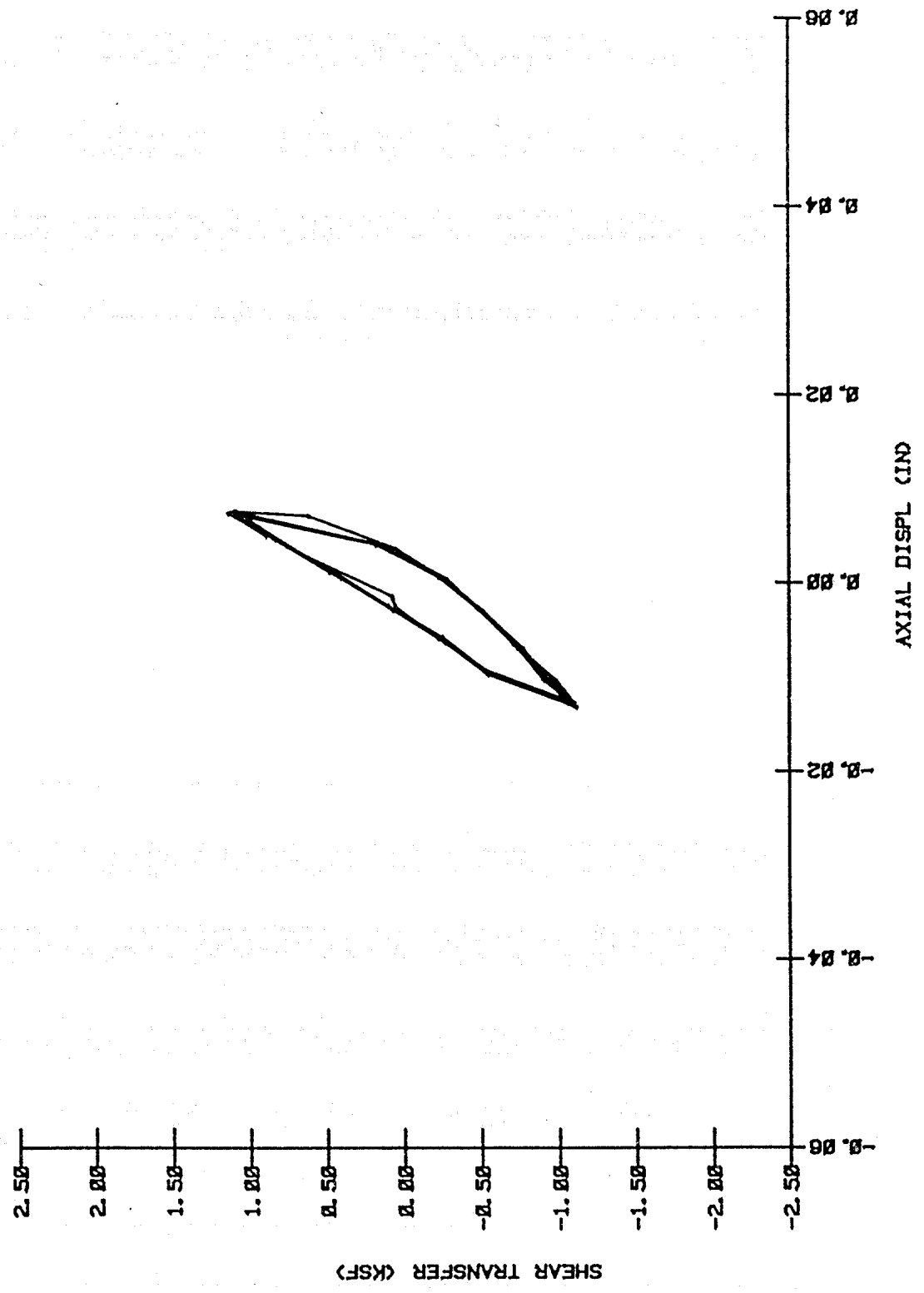
SHORT-TERM TEST
HOLE 3 - DEPTH 4
09 DEC 1982 21:21



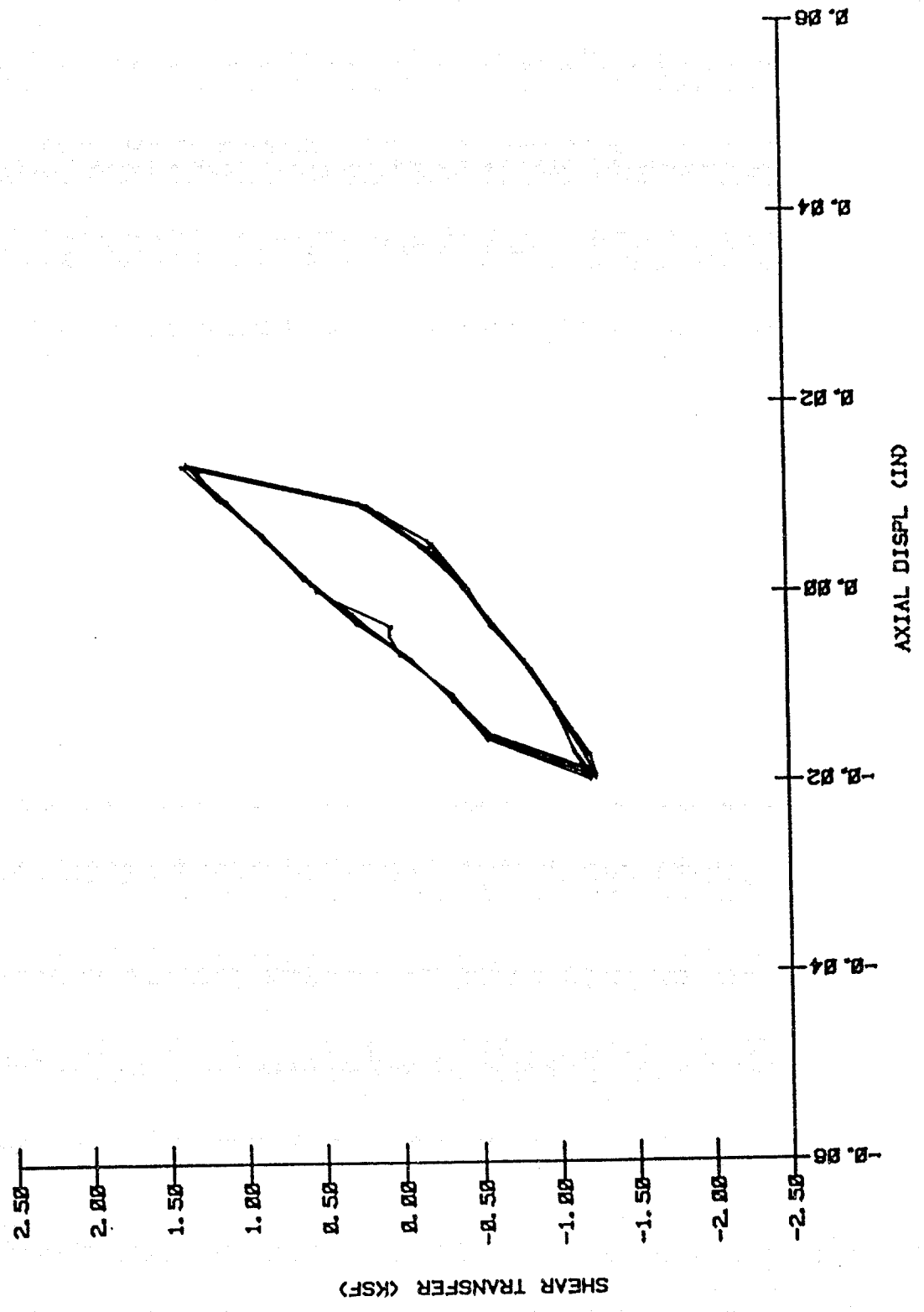
SHORT-TERM TEST
HOLE 3 - DEPTH 4
09 DEC 1982 21:21



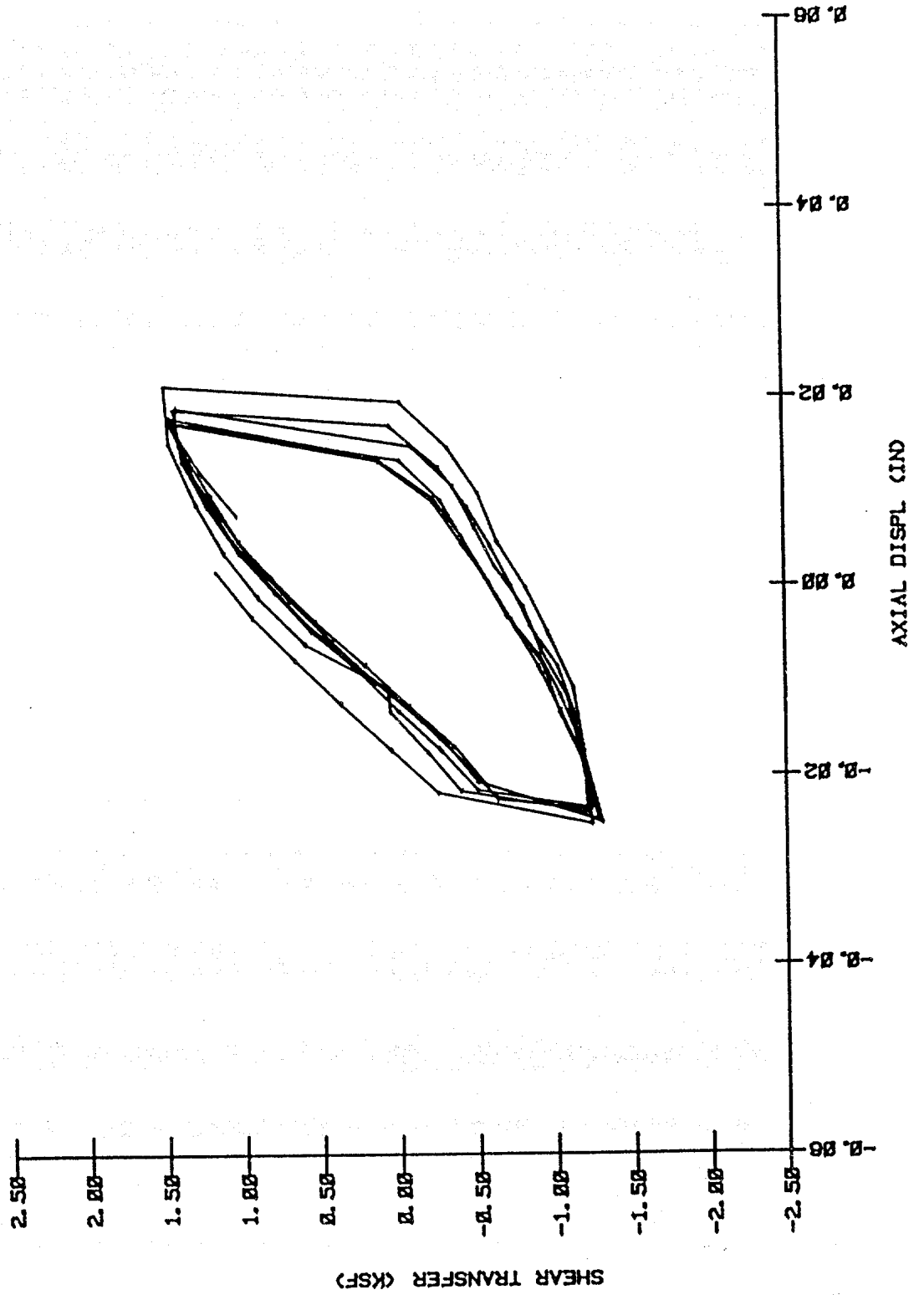
SHORT-TERM TEST
HOLE 3 - DEPTH 4
09 DEC 1982 21:21



SHORT-TERM TEST
HOLE 3 - DEPTH 4
09 DEC 1982 21:21



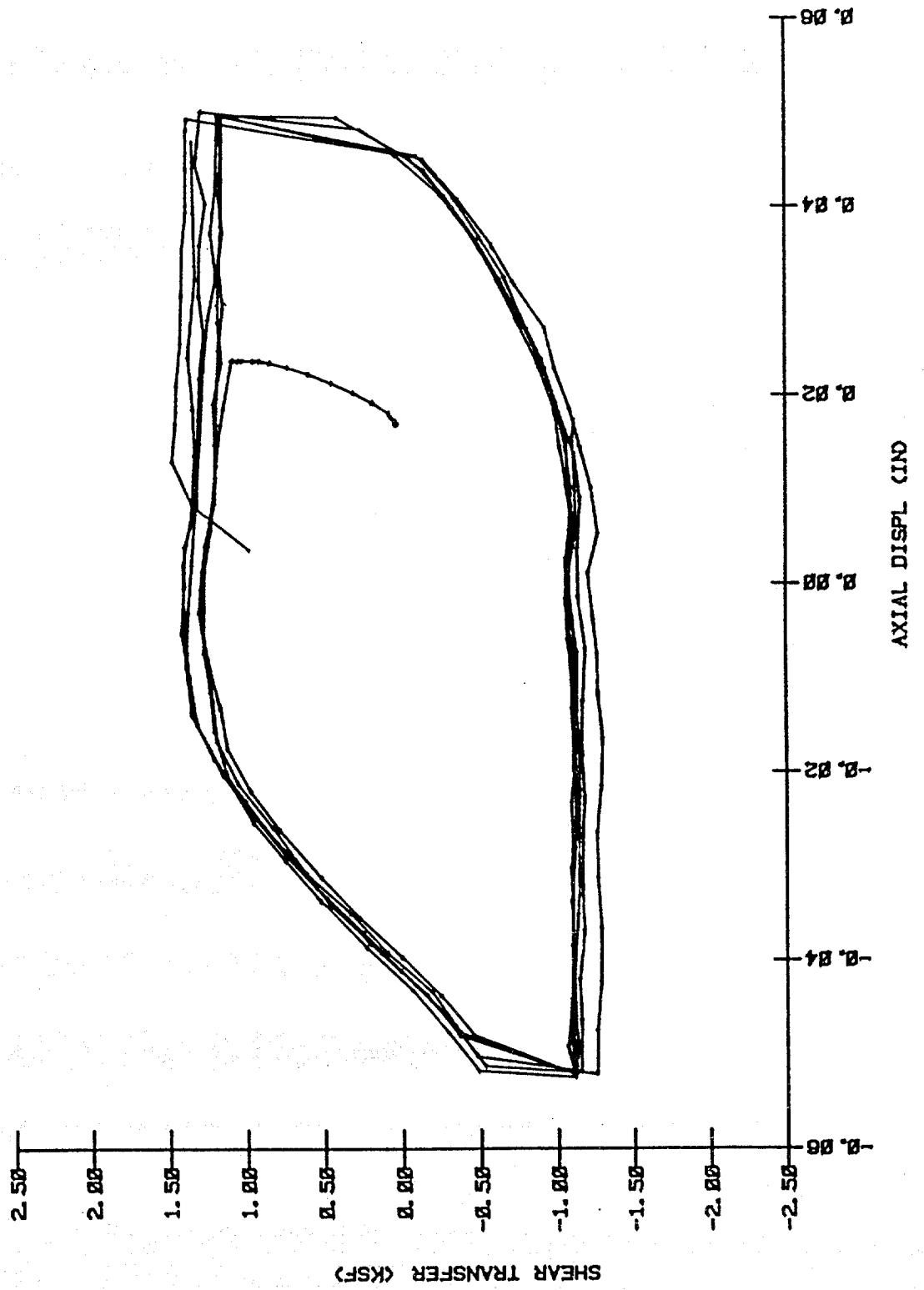
SHORT-TERM TEST
HOLE 3 - DEPTH 4
09 DEC 1982 21:21



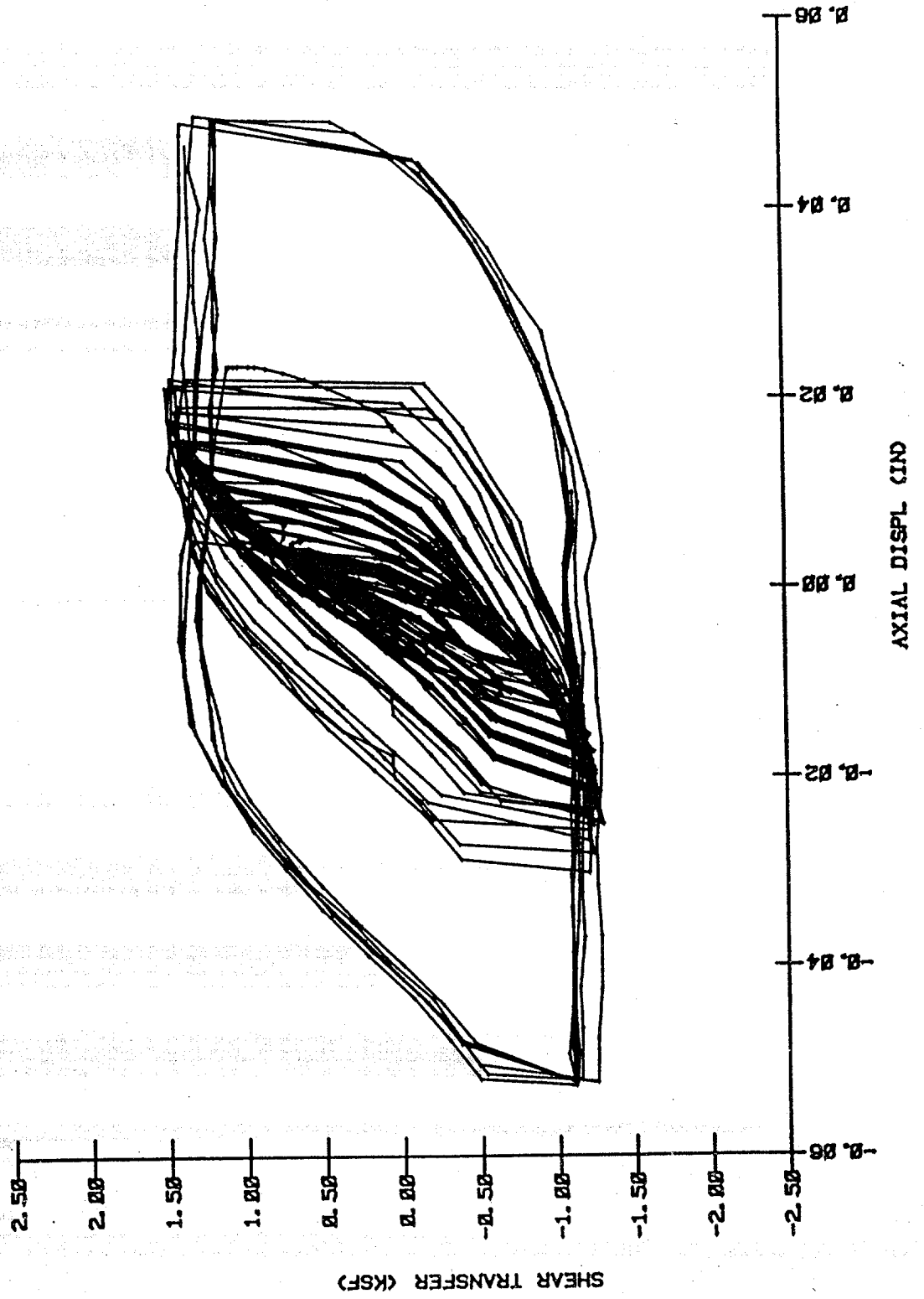
SHORT-TERM TEST

HOLE 3 - DEPTH 4

09 DEC 1982 21: 21



SHORT-TERM TEST
HOLE 3 - DEPTH 4
09 DEC 1982 21:21



PULL-OUT TEST
HOLE 3 - DEPTH 4
10 DEC 1982 07:56

